

**Isolation of secondary fungal metabolites  
and their influence on sphingolipid metabolism**

**Dissertation**

zur

Erlangung des Doktorgrades (Dr. rer. nat.)

der

Mathematisch-Naturwissenschaftlichen Fakultät

der

Rheinischen Friedrich-Wilhelms-Universität Bonn

vorgelegt von

**Ana Kralj**

aus

Zagreb, Kroatien

Bonn 2007

Angefertigt mit Genehmigung der Mathematisch-Naturwissenschaftlichen Fakultät  
der Rheinischen Friedrich-Wilhelms-Universität Bonn

1. Referentin : PD Dr. Gerhild van Echten-Deckert

2. Referentin : Prof. Dr. Gabriele M. König

Tag der Promotion : 04.12.2007.

## **Vorveröffentlichungen der Dissertation**

### **In Advance Publications of the Dissertation**

Teilergebnisse aus dieser Arbeit wurden mit Genehmigung der Mathematisch-Naturwissenschaftlichen Fakultät, vertreten durch die Mentorin/Betreuerin der Arbeit, in folgenden Beiträgen vorab veröffentlicht:

Parts of the results of this study have been published in advance by permission of the Mathematisch-Naturwissenschaftliche Fakultät, represented by the supervisor of this study:

#### **Publikationen / Research Papers**

A. Kralj, S. Kehraus, A. Krick, E. Eguereva, G. Kelter, M. Maurer, A. Wortmann, H. H. Fiebig, G. M. König; Arugosins G and H: Prenylated polyketides from the marine-derived fungus *Emericella nidulans* var. *acristata*. *J. Nat. Prod.* **2006**, *69*, 995-1000.

A. Kralj, S. Kehraus, A. Krick, G. van Echten-Deckert, G. M. König; Two new depsipeptides from the marine fungus *Spicellum roseum*. *Planta Med.* **2007**, *73*, 366-371.

A. Kralj, M. Gurgui, G. M. König, G. van Echten-Deckert; Trichothecenes induce accumulation of glucosylceramide in neural cells by interfering with lactosylceramide synthase activit. *Toxicol. Appl. Pharmacol.* doi:10.1016/j.taap.2007.08.005.

#### **Tagungsbeiträge / Research Presentations**

A. Kralj, S. Kehraus, A. Krick, G. M. König; Two new arugosin derivatives from the marine fungus *Emericella* sp. Poster presented at the 4<sup>th</sup> European Conference on Marine Natural Products, Paris, France, September 12-16, 2005, *Book of Abstracts*, Abstract P27.

**To Marko**

## **Acknowledgements**

I wish to express my cordial gratitude to my supervisor Prof. Dr. G. M. König for the expert guidance, encouragement and kind support during the course of this project. I would like to thank her for introducing me into the important aspects of my work and for providing excellent scientific working facilities and friendly atmosphere.

My sincere gratitude also goes to PD Dr. G. van Echten-Deckert, my co-supervisor. I would like to thank her for introducing me to the sphingolipid world, encouragement, support and constructive criticism in demanding phases of this study. I am particularly grateful for careful revisions of the PhD thesis and for sincere help with many issues which made my research much easier.

My appreciation goes to Prof. Dr. C. E. Müller and Prof. Dr. M. Höfer for participating in the examination committee.

A part of this research involved collaborations with other research groups. For this work thanks go to:

Prof. Dr. H. H. Fiebig, Dr. G. Kelter and Dr. A. Maier, Oncotest GmbH, Institute of Experimental Oncology, Freiburg, for providing cytotoxicity data of extracts and pure compounds.

Dr. M. Maurer, Oncotest GmbH, Institute of Experimental Oncology, Freiburg, for performing immunostimulating assays of pure compounds.

C. Sondag, Department of Chemistry, Bonn, for (HR)EI MS measurements.

Ekaterina Eguereva for the isolation of fungal strains and screening of fungal extracts, for excellent technical assistance in all aspects of laboratory work and for helpful discussions concerning fungal collection. But even more than this, a tremendous thank for support and help, especially in early months in the laboratory, for learning and practicing of German, for being a friend, a colleague and a teacher.

Dr. Stefan Kehraus for performing special NMR experiments and for help in analyses of NMR spectra. Special thanks for proofreading of manuscripts, for help, support and encouragement during this study.

Dr. Anja Krick for numerous LC-MS measurements, for proofreading of manuscripts, for encouragement and discussions during this project.

Edith Neu for performing agar diffusion assays and for friendly assistance in administrative issues.

A part of this work dealing with biochemistry was performed in a research group of PD Dr. van Echten-Deckert, Kekulé Institute for Organic Chemistry and Biochemistry, Bonn. I would like to thank to all its members for friendly working atmosphere and for a kind assistance in the laboratory. A big thank to Andrea Raths for the assistance in the cell culture laboratory, and Roland Broere for the help with molecular biology techniques.

Particular thanks go to Dr. Mihaela Gurgui for an enormous help in the laboratory, for support, discussions and suggestions concerning sphingolipid analyses, and for proofreading of manuscripts and thesis. Moreover, I thank her for being a great friend, for listening and comforting me during the hard times, for endless discussions of all kind and for being always an excellent host.

Additionally, warm thanks to the all members of the Institute for Pharmaceutical Biology, Bonn, for a wonderful working atmosphere, help and support in the laboratory, scientific discussions, and, especially, for encouragement and patience with my German difficulties. Special thanks to the girls in the group for funny and interesting cocktail meetings.

I would like to express my deepest gratitude to my parents for daily e-mails, telephone calls and support during the years of this study. Many thanks go to my sisters and all friends from Croatia for patience and support, especially at the beginning of this study.

At the end, I would like to thank my husband Marko for an enormous encouragement, help, love and support in all phases of my stay in Germany, without whom I would not even start this study nor would I finish it. Special thanks for learning me the basics of scientific thinking and for believing in me constantly.

<b>Table of contents</b>	<b>Page</b>
<b>1 Introduction</b>	<b>1</b>
1.1 Fungi as a source of biologically active metabolites	1
1.1.1 Cytotoxic fungal metabolites	1
1.2 Sphingolipids	7
1.2.1 Sphingolipid metabolism and function. General remarks	7
1.2.2 Sphingolipids in cancer	11
1.2.2.1 Ceramide	12
1.2.2.2 Glucosylceramide and other glycosphingolipids	13
1.3 Influence of fungal metabolites on sphingolipid metabolism	15
1.3.1 Inhibitors of serine palmitoyltransferase	15
1.3.2 Inhibitors of ceramide formation	17
<b>2 Scope of the present study</b>	<b>21</b>
2.1 Biological and chemical screening of fungal extracts	21
2.2 Chemical investigation of selected fungal strains	21
2.3 Biological evaluation of isolated pure compounds	21
<b>3 Materials and methods</b>	<b>22</b>
3.1 Fungal strains	22
3.1.1 Isolation of the fungal strains	22
3.1.1.1 Isolation from algal material	22
3.1.1.2 Isolation from the sponge	22
3.1.2 Fungal strains for chemical investigation	22
3.1.3 Cultivation of fungal strains	23
3.2 Chromatography	23
3.2.1 Thin layer chromatography (TLC)	23
3.2.2 Vacuum liquid chromatography (VLC)	24
3.2.3 Size exclusion chromatography (SEC)	24
3.2.4 High performance liquid chromatography (HPLC)	24

3.3	Structure elucidation	25
3.3.1	NMR spectroscopy	25
3.3.2	Mass spectrometry	25
3.3.3	UV measurements	26
3.3.4	IR spectroscopy	26
3.3.5	Optical rotation	26
3.3.6	Molecular modeling	27
3.4	Amino acids analysis	27
3.4.1	Marfey`s method	27
3.5	Cell culture	29
3.5.1	Primary cultured neurons	29
3.5.2	Neuroblastoma B104 cell line	29
3.5.3	Sphingolipid labeling in cultured cells	29
3.5.4	Cell viability assay	30
3.5.5	Cell harvesting	30
3.5.6	Protein determination	30
3.6	Sphingolipid analysis	31
3.6.1	Extraction of lipids	31
3.6.2	Removal of lipid contaminants	31
3.6.3	Removal of salts by reversed-phase chromatography	31
3.6.4	Separation of sphingolipids by thin-layer chromatography	32
3.6.5	Lactosylceramide synthase (LacCer) assay	33
3.7	Reverse transcription-polymerase chain reaction (RT-PCR)	33
3.7.1	RT-PCR protocols	34
3.8	MRP1- and Pgp-related transport activities	36
3.8.1	MRP1- and Pgp-mediated accumulation assay	36
3.8.2	MRP1- and Pgp-mediated efflux assay	36
3.9	Biological tests	38
3.9.1	Agar diffusion assay	38
3.9.2	Cytotoxicity test against human cancer cell lines	38
3.9.3	Immunostimulating activity	39
3.10	Chemicals and other materials	40
3.10.1	Apparatus and expendable materials	40
3.10.2	Cell culture media	42



3.10.3	Chemicals and solvents	42
3.10.4	Kits	44
3.10.5	Lipids	45
3.10.6	Primers	45
3.10.7	Radioactivity	45
3.10.8	Solutions and buffers	46
<b>4</b>	<b>Results</b>	<b>47</b>
4.1	Screening of fungal extracts for biologically active metabolites	47
4.1.1	Screening of fungal extracts for cytotoxic activity	47
4.1.2	Antimicrobial and antialgal activities of fungal extracts	49
4.1.3	Influence of fungal extracts on sphingolipid metabolism	49
4.2	Arugosins G and H: Prenylated polyketides from the marine-derived fungus <i>Emericella nidulans</i> var. <i>acristata</i> (Strain number 652)	52
4.2.1	Introduction	52
4.2.2	Cultivation, extraction and isolation	54
4.2.3	Results and discussion	54
4.3	Two New Depsipeptides from the Marine Fungus <i>Spicellum roseum</i> (Strain number 74)	65
4.3.1	Introduction	65
4.3.2	Cultivation, extraction and isolation	66
4.3.3	Absolute configuration of spicellamide A (11) and spicellamide B (12)	66
4.3.4	Results and discussion	67
4.4	Lipopeptides from the strain <i>Fusarium dimerum</i> complex (Strain number 18)	73
4.4.1	Introduction	73
4.4.2	Cultivation, extraction and isolation	73
4.4.3	Results and discussion	74
4.5	Secondary metabolites from selected marine fungi	78
4.5.1	<i>Arthrinium sacchari</i>	78
4.5.2	<i>Aspergillus terreus</i>	81
4.5.3	<i>Fusarium oxysporum</i>	83
4.5.4	<i>Paecilomyces lilacinus</i>	86

4.6	Influence of fungal metabolites from the strain <i>Spicellum roseum</i> on sphingolipid metabolism	88
4.6.1	Alterations of glycosphingolipid profile by the extract of <i>Spicellum roseum</i>	88
4.6.2	Cultivation, extraction and bioassay-guided isolation	89
4.6.3	Brefeldin A – uncoupling of ganglioside biosynthesis	94
4.6.4	Effect of trichothecene derivatives on glycosphingolipid metabolism	96
4.6.4.1	Influence of trichothecenes on lactosylceramide synthase in neural cells	98
4.6.4.2	Influence of trichothecenes on galactosyltransferase II	100
4.6.4.3	Influence of trichothecenes on the translocation of glucosylceramide	102
4.6.4.4	Influence of trichothecenes on ceramide level in neural cells	104
<b>5</b>	<b>Discussion</b>	<b>106</b>
5.1	Selection of fungal strains	106
5.2	Isolated natural products	107
5.3	Interference of fungal metabolites with sphingolipid metabolism	108
5.3.1	Trichothecenes – alterations of glycosphingolipid profiles	109
5.4	General discussion	111
<b>6</b>	<b>Summary</b>	<b>113</b>
<b>7</b>	<b>References</b>	<b>115</b>
<b>8</b>	<b>Appendix</b>	<b>130</b>
8.1	Results of the cytotoxicity assay	130
8.1.1	Cytotoxicity of extracts and VLC fractions	131
8.1.2	Cytotoxicity of isolated compounds	137
8.2	<sup>1</sup> H and <sup>13</sup> C NMR spectra of isolated compounds	139

## Abbreviations

°C	Degrees Celsius
1D	One Dimensional
2D	Two Dimensional
$[\alpha]_D^T$	Specific rotatory power; Sodium D-line (589 nm); T: Temperature
$\delta$	NMR chemical shift [ppm]
$\lambda$	Wavelength [nm]
$\mu\text{Ci}$	$10^{-6}$ curie
$\mu\text{g}$	$10^{-6}$ gram
$\mu\text{L}$	$10^{-6}$ litre
$\mu\text{m}$	$10^{-6}$ metre
$\mu\text{M}$	micromolar
$\nu$	Wave number [ $\text{cm}^{-1}$ ]
8-dT	8-deoxy trichothecin
ACN	Acetonitrile
ASW	Artificial Sea Water
BFA	Brefeldin A
BMS	Biomalt Salt Medium
BSA	Bovine Serum Albumin
br	Broad
c	concentration
$\text{CaCl}_2$	Calcium chloride
CDP-choline	Cytidine-5-diphosphate choline
CFDA	5-carboxyfluorescein diacetate
$\text{CH}_2\text{Cl}_2$	Dichloromethane (see DCM)
cm	$10^{-2}$ metre
CMF	$\text{Ca}^{2+}/\text{Mg}^{2+}$ -free isotonic solution
$\text{CO}_2$	Carbon dioxide
COSY	Correlated Spectroscopy
CsA	Cyclosporine A
$\text{CuSO}_4$	Copper sulphate
CZ	Czapek Medium
d	doublet

DAD	Diode Array Detector
DCM	Dichloromethane
DEPT	Distortionless Enhancement by Polarisation Transfer
dest.	Distilled
DMEM	Dulbecco's Modified Eagle Medium
DMSO	Dimethyl sulfoxide
DNA	Deoxyribonucleic acid
EDTA	Ethylenediamine-tetra-acetic acid
e.g.	example given
EI	Electro Ionisation
ER	Endoplasmic Reticulum
ESI	Electro Spray Ionisation
EtOAc	Ethyl Acetate
EtOH	Ethanol
FDAA	1-Fluoro-2,4-dinitrophenyl-5-L-alaninamide
g	grams
GC	Gas-Chromatography
GlcCer	Glucosylceramide
GSL	Glycosphingolipid
h	hour
H <sub>3</sub> BO <sub>3</sub>	Boric acid
HBSS	Hank's Balanced Salt Solution
HCl	Hydrochloric acid
HMBC	Heteronuclear Multiple-Bond Correlation
HMQC	Heteronuclear Multiple Quantum Correlation
HPLC	High Performance or High Pressure Liquid Chromatography
H <sub>2</sub> O	Water
H <sub>2</sub> SO <sub>4</sub>	Sulphuric acid
HSQC	Heteronuclear Single Quantum Correlation
Hz	Hertz
IC <sub>50</sub>	Inhibition Concentration (drug concentration causing 50 % growth inhibition)
IL	Interleukine
IR	Infrared
<i>J</i>	Spin-spin coupling constant [Hz]

KBr	Potassium bromide
KCl	Potassium chloride
KH <sub>2</sub> PO <sub>4</sub>	Potassium dihydrogen phosphate
L	Liter
LacCer	Lacrosylceramide
LC	Liquid Chromatography
LC <sub>50</sub>	Lethal Concentration (drug concentration, causing 50 % reduction of the initial existent cell quantity)
m	Multiplet (in connection with NMR data)
M	Molarity
MDR	Multidrug Resistance
MEM	Minimum Essential Medium
MeOH	Methanol
mg	10 <sup>-3</sup> gram
MgCl <sub>2</sub>	Magnesium chloride
MHz	Megahertz
min	minute
mL	10 <sup>-3</sup> litre
mM	10 <sup>-3</sup> Mol
MnCl <sub>2</sub>	Manganese chloride
MRP1	Multidrug Resistance Protein 1
MS	Mass Spectrometry
MTT	(3-[4,5-dimethylthiazol-2-yl]-2,5-diphenyltetrazolium bromide)
MYA	Malt-yeast agar Medium
NaCl	Sodium chloride
NaHCO <sub>3</sub>	Sodium hydrogen carbonate
NaOH	Sodium hydroxide
Na <sub>2</sub> SO <sub>4</sub>	Sodium sulphate
NH <sub>4</sub> Ac	Ammonium acetate
nm	nanometer
NMR	Nuclear Magnetic Resonance
NOE	Nuclear Overhauser Effect
NOESY	Nuclear Overhauser Effect Spectroscopy
NP	Normal Phase Silica gel

PBS	Phosphate Buffered Saline
PE	Petroleum ether
Pgp	P-glycoprotein
ppm	parts per million
q	Quartet
R <sub>f</sub>	Retention Factor (defined as the distance traveled by the compound divided by the distance traveled by the solvent)
Rh123	Rhodamine 123
RI	Refractive Index
RNA	Ribonucleic acid
ROESY	Rotating Frame Overhauser Effect Spectroscopy
RP	Reversed Phase
R <sub>T</sub>	Retention Time
RT-PCR	Reverse transcription-polymerase chain reaction
s	Singlet
Sa	Sphinganine
SCUBA	Self Contained Underwater Breathing Apparatus
SEC	Size Exclusion Chromatography
SL	Sphingolipid
SM	Sphingomyelin
So	Sphingosine
sp.	Species
SPT	Serine palmitoyltransferase
SrCl <sub>2</sub>	Strontium chloride
t	Triplet
Td-ol	Trichodermol
THF	Tetrahydrofuran
TLC	Thin Layer Chromatography
UV	Ultraviolet
VLC	Vacuum-liquid Chromatography

## Abstract

Development of new drugs, especially in the area of oncological and infectious diseases, represents today one of the most important research fields. The marine environment is a tremendous source of natural products. Drug development is now turning toward potentially more selective ways (e.g. inducement of certain signaling molecules) in disease treatments, especially when concerning cancer. Sphingolipids (SLs) are ubiquitous constituents of eukaryotic cellular membranes that are involved in cell growth, proliferation, differentiation and apoptosis. These sphingolipid-regulated processes are crucial in cancer development and progression. Pharmacological or molecular manipulations of any of the enzymes involved in SL metabolism have been proposed as new strategies in the treatment of cancer or diseases caused by disrupted sphingolipid balance. The toxic effects of some fungal metabolites were related to their ability to interfere with SL metabolism. The aim of this study was the investigation of secondary metabolites produced by marine-derived fungi with cytotoxic properties and the isolation of new compounds with potent biological activity, preferably with the potential to influence sphingolipid metabolism.

Extracts of seven fungal strains, including five algal-derived and two sponge-derived strains, were chemically investigated. This investigation resulted in the isolation and structure elucidation of 29 pure compounds. Four compounds, arugosin G and H, spicellamide A and B, proved to be new. Arugosins G and H, together with arugosins A and B, were isolated from algicolous fungus *Emericella nidulans* var. *acristata*. They are benzophenone derivatives, biosynthetically related to xanthenes, which showed moderate antitumor activity toward individual tumor cell lines. Cyclohexadepsipeptides spicellamide A and B, isolated from sponge-derived fungus *Spicellum roseum*, exhibited moderate cytotoxicity in neuroblastoma cells. Bioassay-guided isolation of cytotoxic compounds revealed the presence of cytochalasins from an *Arthrimum sacchari* extract, of aflatoxins from an *Emericella nidulans* var. *acristata* extract and of trichothecenes from a *Spicellum roseum* extract.

Trichothecenes are cytotoxic compounds that have several inhibitory effects on eukaryotic cells. Tests on sphingolipid metabolism exhibited alterations in the expression of glycosphingolipids by two compounds from trichothecene family, 8-deoxy-trichothecin and trichodermol. In cerebellar neurons and neuroblastoma cells both compounds inhibit lactosylceramide synthase activity and induce an accumulation of glucosylceramide. These data describe a new effect of trichothecenes. However, further studies have to clarify the fate and physiological consequence of accumulated glucosylceramide and also its correlations with known effects of trichothecenes.

## **1 Introduction**

### **1.1 Fungi as a source of biologically active metabolites**

Since the discovery of penicillin, a potent antibiotic produced by *Penicillium notatum*, (Fleming, 1929), a new area in natural product research has started. Fungi were noticed as a source of chemically new compounds with various biological activities. The isolation from soil was a common method to get fungal isolates. However, fungal strains from terrestrial sources yielded often already described secondary metabolites. Thus, fungi from new origins were needed. The marine environment offers a wide array of potential fungal sources including sediment, sand, driftwood, mangrove wood, sea water, algae, sponges and other invertebrates (Jensen and Fenical, 2000). Fungi obtained either from sponges, algae, or wooden substrates account for about 70 % of chemistry described from marine-derived fungi. Sponge-derived fungi comprise about 33 % of the total compounds in the literature and have the highest number of novel metabolites. Algicolous fungi take the second place accounting for 24 % of the total number of compounds with 27 % of them being new metabolites (Bugni and Ireland, 2004). Fungal strains, residing inside sponge or algal tissue, can be isolated by placing algal thalli or tissues of the sponge, after surface sterilization to remove unwanted epibionts, on suitable agar media. Interestingly, most of the isolated endophytic fungi are not obligate marine fungi. However, they are a tremendous source of natural products, which is not surprising if considering the complex ecological situation of the endophyte within the host plant (König *et al.*, 2006).

The present work thus deals with the investigation of marine fungal strains, derived from algae or sponges, aiming at finding new bioactive natural products.

#### **1.1.1 Cytotoxic fungal metabolites**

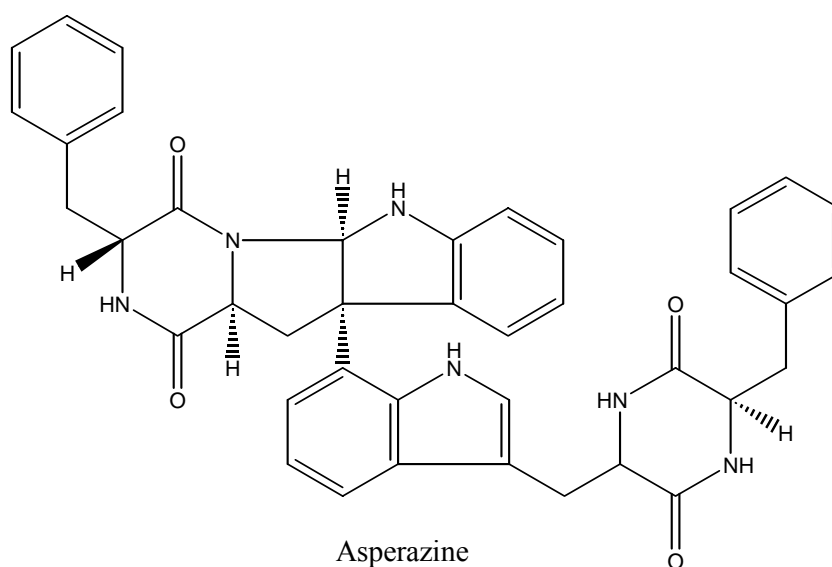
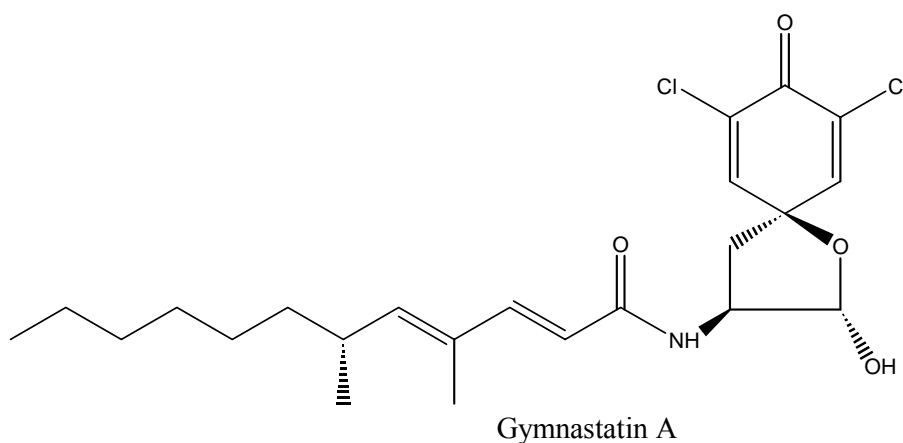
Marine-derived fungi are an extremely interesting and valuable source of novel natural products (Bhadury *et al.*, 2006). Biological activities are mainly focused in the areas of antibiotic and anticancer properties (Donia and Hamann, 2003; Simmons *et al.*, 2005), but other selective activities include antiviral, antiparasitic, neuritogenic activity, phosphatase and kinase inhibition (Butler, 2005). Development of new anticancer drugs represents today one of the most important research areas. An analysis of the number of chemotherapeutic agents and their sources indicates that over 60 % of the approved drugs are derived from natural



compounds (da Rocha *et al.*, 2001). The present study is thus devoted to the investigation of cytotoxic properties of fungal extracts.

First report of novel cytotoxic metabolites from a sponge-derived fungus describes gymnastatins that are obtained from a strain *Gymnascella dankaliensis* derived from the sponge *Halichondria japonica* (Numata *et al.*, 1997). Gymnastatins A, B and C exhibited potent cytotoxicity in a P388 lymphocytic leukemia test system with LC<sub>50</sub> values of 18, 108, and 106 ng mL<sup>-1</sup>, respectively.

Asperazine, isolated from a *Hyrtios proteus* sponge-derived *Aspergillus niger* showed selective cytotoxicity against leukemia cells while exhibiting no antimicrobial activity, suggesting asperazine has a specific mammalian target (Varoglu and Crews, 2000).

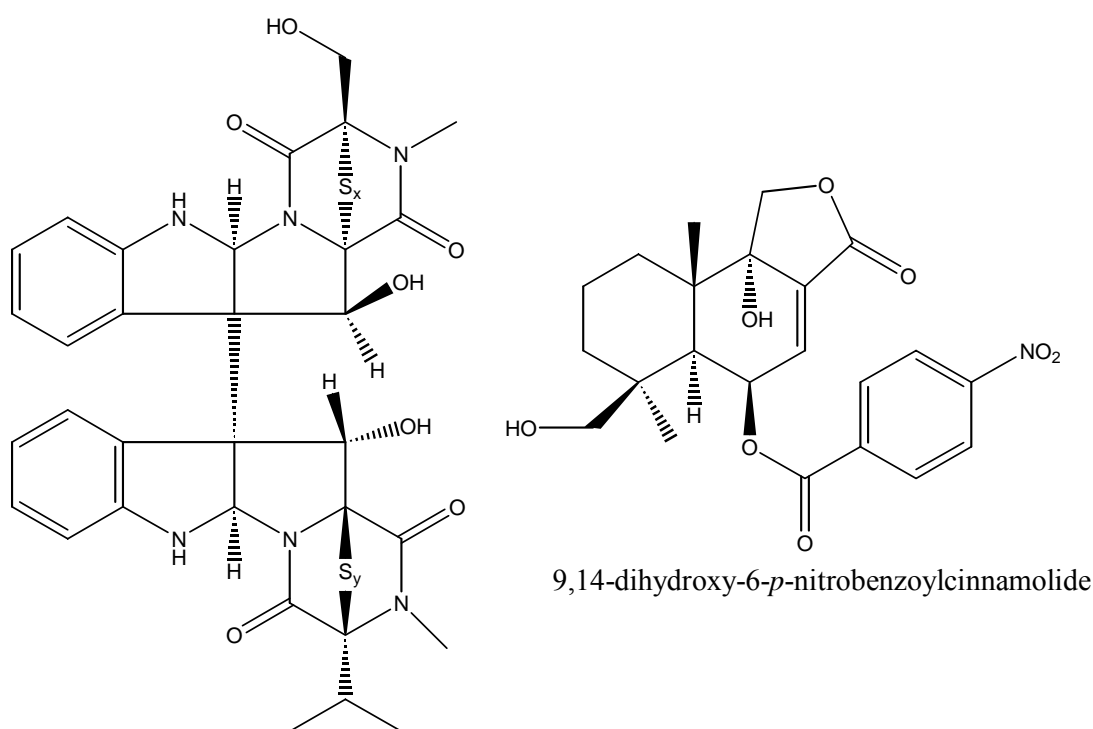


One of the largest classes of cytotoxic metabolites from algicolous fungi is the leptosin family of dimeric diketopiperazines (Takahashi *et al.*, 1994; Takahashi *et al.*, 1995). The compounds

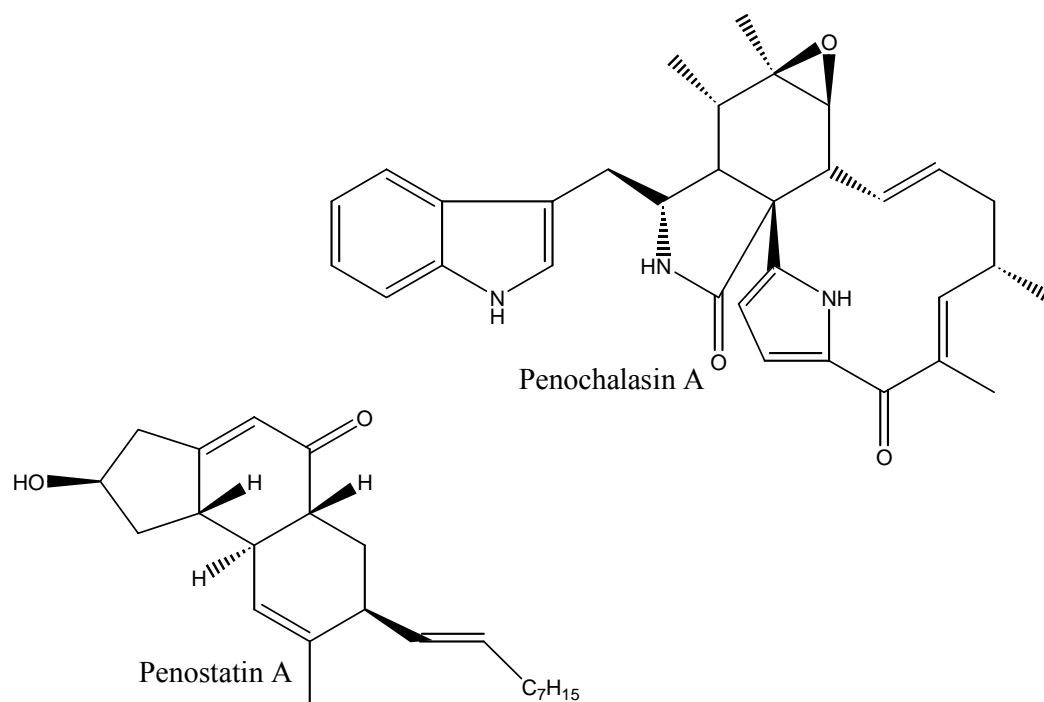
were isolated from algicolous fungus *Leptosphaeria* sp. Leptosins A and C exhibited cytotoxic activity against a P388 leukemia cell line with a mean  $LC_{50}$  of 1.85 and 1.75  $\text{ng mL}^{-1}$ , respectively (Pettit *et al.*, 2002).

Studies on *Penicillium* isolate OUPS-79 (obtained from the marine alga *Enteromorpha intestinalis*) resulted in the isolation of two unrelated classes of cytotoxic compounds, penochalasin (Iwamoto *et al.*, 2001) and penostatins (Iwamoto *et al.*, 1999). Penochalasin and penostatins have various effects on cells mainly due to their ability to cap F-actin, and have been useful tools for cytoskeletal research. They showed potent cytotoxic activity against P388 leukemia cells exhibiting an  $LC_{50}$  of 0.4  $\text{ng mL}^{-1}$ , (penochalasin A), 0.3  $\text{ng mL}^{-1}$ , (penochalasin B) and 0.5  $\text{ng mL}^{-1}$ , (penostatin A) (Maruta *et al.*, 1999).

Cytotoxic sesquiterpenoid nitrobenzoyl esters, isolated from *Aspergillus versicolor*, showed a mean  $LC_{50}$  of 1.1  $\mu\text{g mL}^{-1}$  in 60 cell-line panel (Belofsky *et al.*, 1998).

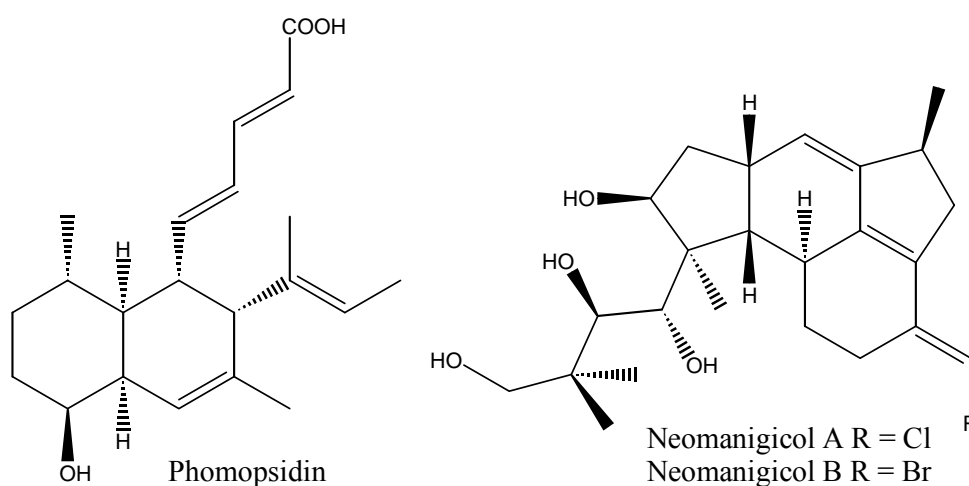


Leptosin A  $x = 4$ ;  $y = 2$   
 Leptosin B  $x = 3$ ;  $y = 2$   
 Leptosin C  $x = 2$ ;  $y = 2$   
 Leptosin G  $x = 4$ ;  $y = 3$

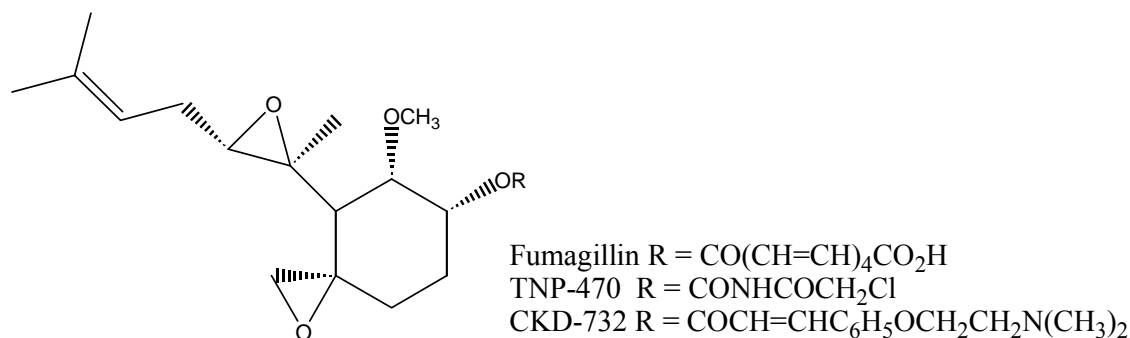


Cytotoxic metabolites obtained from fungi isolated from other sources are compounds like phomopsidin. Phomopsidin is isolated from *Phomopsis* sp., obtained from a submerged mangrove branch, which exhibited an inhibition of microtubule assembly with an LC<sub>50</sub> 5.7  $\mu$ M (Kobayashi *et al.*, 2003).

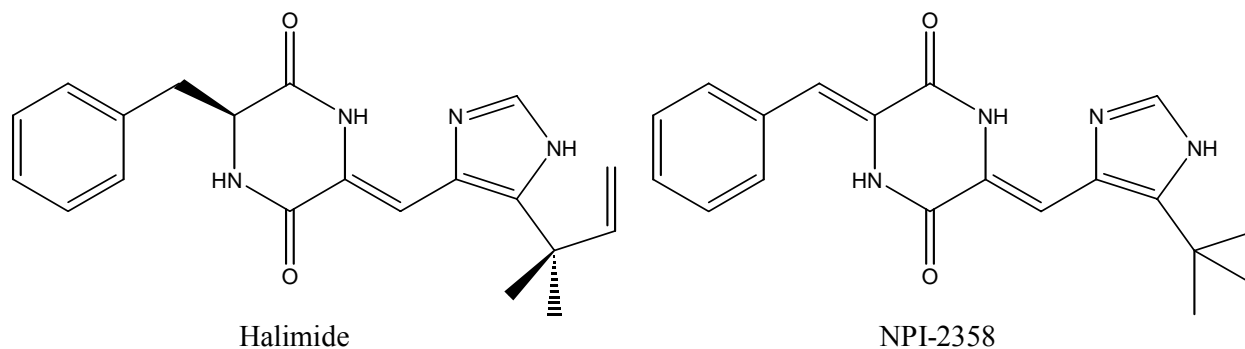
Neomanigicols were isolated from *Fusarium* sp. which was obtained from a driftwood sample in a mangrove habitat. Neomanigicols A and B showed cytotoxic activity against an MCF-7 human breast carcinoma with an LC<sub>50</sub> value of 4.9  $\mu$ M and 27  $\mu$ M, respectively (Renner *et al.*, 1998).



One of the best evaluated fungal metabolite in oncological research is fumagillin. Fumagillin was first isolated from *Aspergillus fumigatus* and it was used for treatment of intestinal amoebiasis (Killough *et al.*, 1952; Griffith *et al.*, 1998). It was later found to inhibit angiogenesis through binding to methionine aminopeptidase 2 (Liu *et al.*, 1998; Kim *et al.*, 2004). A number of fumagillin analogues were prepared (Marui *et al.*, 1992; Lee *et al.*, 2007) including TNP-470, which was found to have higher potency and lower toxicity than fumagillin (Ingber *et al.*, 1990), and is one of the first inhibitors of angiogenesis to reach clinical trials (Kruger and Figg, 2000). CKD-732 (Han *et al.*, 2000) is currently undergoing clinical trial and exhibited better potency and less cytotoxicity compared with TNP-470 (Lee *et al.*, 2004; Kim *et al.*, 2007).



Halimide was discovered concurrently from a marine and a terrestrial fungus, *Aspergillus* sp., and is produced as a mixture of (+) and (-) enantiomers (Kanoh *et al.*, 1997; Fairchild *et al.*, 1998). Early studies showed that the (-) enantiomer inhibited cell proliferation by binding at the colchicine-binding site of tubulin and disrupting the microtubule network, which resulted in G<sub>2</sub>/M cell cycle arrest (Kanoh *et al.*, 1999a; Kanoh *et al.*, 1999b). Additionally, the (-) enantiomer exhibited elevated cytotoxic activity against various tumor cells including lung, colon, breast and leukemia with IC<sub>50</sub> values in the low to submicromolar range (Kanoh *et al.*, 1999a). To remove chirality and optimize biological activity, a series of synthetic analogs was generated, including NPI-2358. Nereus Pharmaceuticals has initiated a Phase I clinical trial to evaluate the safety of tumor vascular disrupting agent NPI-2358 for the treatment of patients with solid tumors (Spear, 2007).



From the literature review it can be concluded that most of the cytotoxic metabolites are produced by genus of *Aspergillus* or *Penicillium*. One explanation for the high number of compounds reported from these two genera is that are both of them salt tolerant, fast growing species and are easily obtained from many substrates. Additionally, *Aspergillus* and *Penicillium* spp. are known to produce extracts with a wide variety of activities. Thus, decreasing the isolation number of ubiquitous species could represent a valid method to increase the probability of the isolation of novel chemical structures.

## 1.2 Sphingolipids

### 1.2.1 Sphingolipid metabolism and function. General remarks

In 1884 J. L. W. Thudichum discovered a new class of lipids while studying the chemical composition of the brain. He named them sphingolipids after the sphinx of Greek mythology because of the riddle of their structure (Thudichum, 1884). Sphingolipids (SLs) are ubiquitous constituents of eukaryotic cellular membranes. Although sphingolipids have been considered for many years only as structural components of membranes, it is now acknowledged that they are also involved in controlling cellular processes such as proliferation, growth, migration, differentiation, senescence, and apoptosis (Cuvillier, 2002; Hannun and Obeid, 2002; Malisan and Testi, 2002; Spiegel and Milstien, 2003). Hence, they are currently recognized as signaling molecules capable of determining cellular fate.

The basic building block of all sphingolipids is sphingosine (4E-(2-amino-1,3-dihydroxy)-octadecene) having the *D-erythro* (or *2S*, *3R*) configuration, or sphinganine (dihydrosphingosine). A fatty acid is attached to carbon-2 of the sphingoid base via an amide bond, yielding ceramide, and attachment of hydrophilic head groups to the OH-group at C-1 yields complex SLs.

The metabolic pathways of simple and complex SLs are shown in Figure 1-2-1. It is clear from that figure that the metabolites are interconvertible which complicates determination concerning the specific role of each one of them. *De novo* synthesis of sphingolipids occurs at the cytosolic face of the endoplasmic reticulum (ER), and starts by the condensation of serine and palmitoyl-CoA catalyzed by serine palmitoyltransferase (SPT), which is a pyridoxal phosphate dependent enzyme (Mandon *et al.*, 1992). Its product, 3-ketosphinganine, is immediately reduced by the NADPH dependent 3-ketosphinganine reductase yielding *D-erythro*-sphinganine. After acylation of sphinganine to dihydroceramide by the enzyme (dihydro)ceramide synthase, ceramide is subsequently formed by introduction of a 4,5-*trans* double bond by dihydroceramide desaturase (Rother *et al.*, 1992; Michel *et al.*, 1997). Ceramide is the central lipid in the metabolism of sphingolipids (van Echten-Deckert and Herget, 2006). Once formed, it is subsequently transported from the ER to the Golgi complex where it serves as a substrate for the synthesis of sphingomyelin and more complex glycosphingolipids (GSLs). Sphingomyelin biosynthesis requires the transfer of phosphorylcholine headgroup from phosphatidylcholine to ceramide, liberating diacylglycerol through the action of sphingomyelin synthase (Ramstedt and Slotte, 2002).

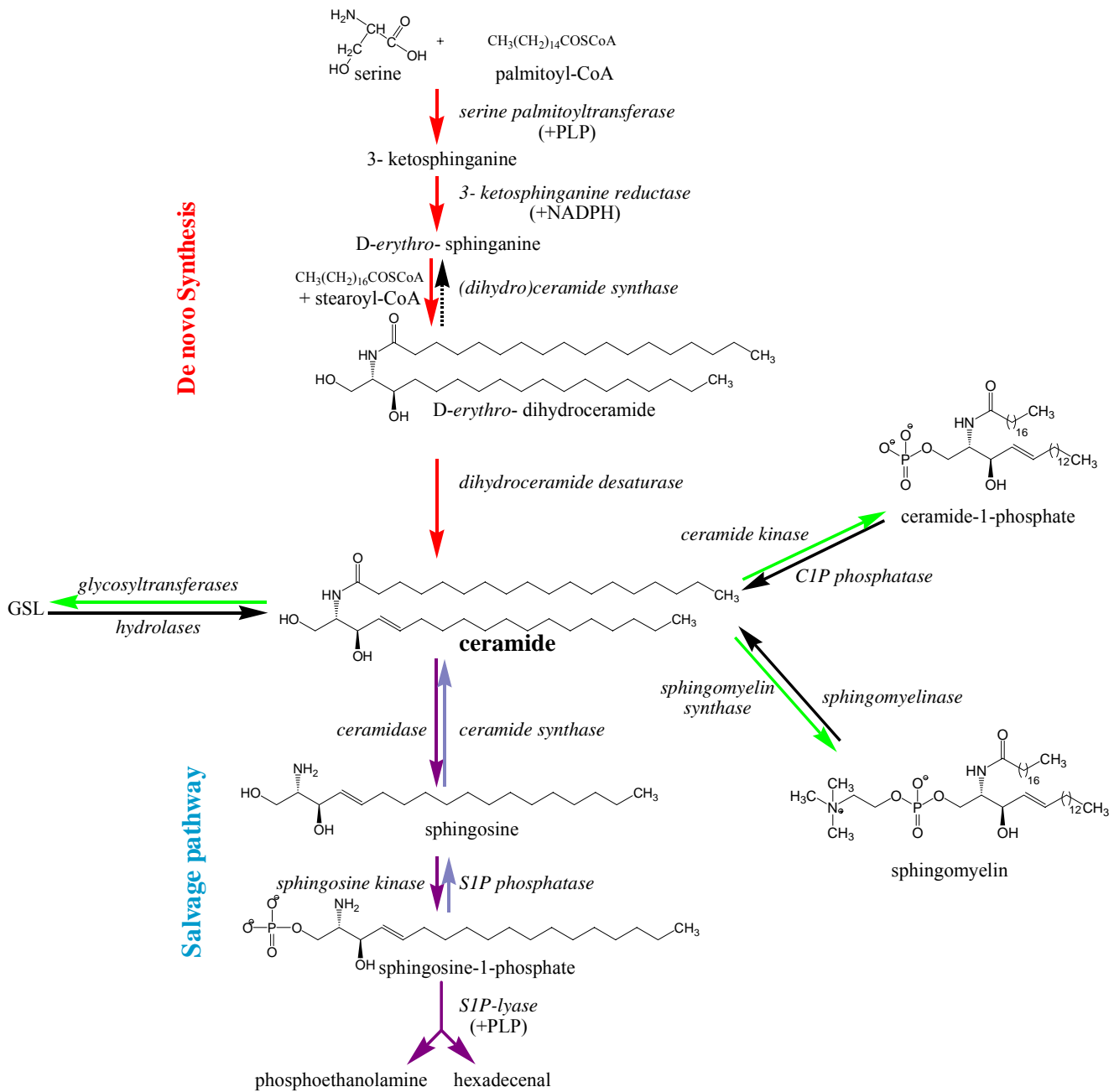


**Figure 1-2-1.** Scheme of sphingolipid metabolism.

Ceramide is the central molecule in the metabolism of sphingolipids. It can be formed *de novo* (red arrows), from hydrolysis of sphingomyelin or glycosphingolipids, or from dephosphorylation of ceramide-1-phosphate (C1P) (black arrows) or recycling of sphingosine (salvage pathway). Ceramide can serve as a precursor in many biosynthetic pathways (green arrows). The major pathway for catabolism of ceramide is its deacylation by ceramidases to sphingosine, which in turn is phosphorylated to generate sphingosine-1-phosphate (S1P) (dark blue arrows). S1P can be irreversibly cleaved by lyase to phosphoethanolamine and hexadecenal (dark blue arrows) or it can be dephosphorylated by phosphatases that regenerate sphingosine in the ceramide salvage pathway (light blue arrows). GSL, glycosphingolipids; PLP, pyridoxal phosphate; NADPH, nicotine adenine dinucleotide phosphate (Wedeking and van Echten-Deckert, 2006).

The biosynthesis of most GSLs requires the glucosylation of ceramide which is catalyzed by glucosylceramide (GlcCer) synthase on the cytosolic surface of the Golgi apparatus (Futerman and Pagano, 1991). Almost all gangliosides are derived from lactosylceramide (LacCer), which is formed by the transfer of galactose to GlcCer (van Echten-Deckert and Herget, 2006). This reaction is catalyzed by the enzyme lactosylceramide synthase which is found on the luminal leaflet of Golgi membranes (Lannert *et al.*, 1998; Giraudo and Maccioni, 2003). Addition of one or two sialic acid molecules to LacCer results in formation of GM3 and GD3 (Figure 1-2-2), respectively, which represent precursors of more complex gangliosides that are particularly enriched in brain (van Echten-Deckert and Herget, 2006).

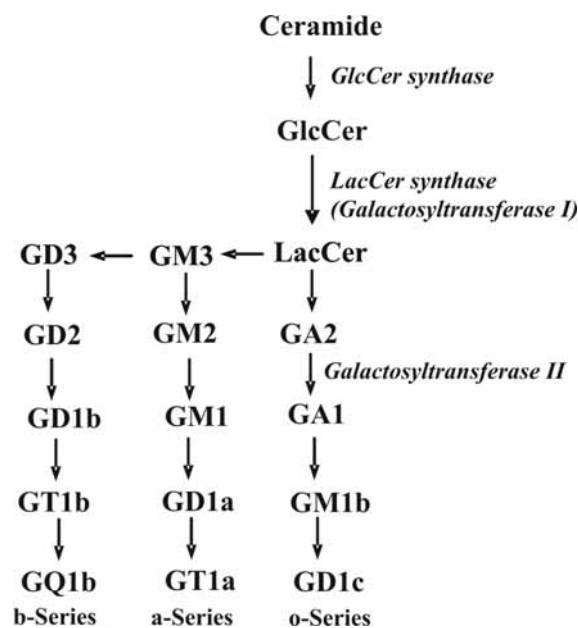


**Figure 1-2-2.** Biosynthesis of glycosphingolipids.

GlcCer, glucosylceramide; LacCer, lactosylceramide. Modified from (van Echten and Sandhoff, 1993). The terminology of gangliosides (GM3, GD3, GA2, GM2, GD2, GA1, GM1, GD1b, GM1b, GD1a, GT1b, Gd1c, GT1a, GQ1b) is according to Svennerholm (Svennerholm, 1963).

Interestingly, the topology of GlcCer biosynthesis differs from that of LacCer formation. Thus, GlcCer synthesized at the cytosolic face of the Golgi apparatus (Coste *et al.*, 1986; Lannert *et al.*, 1998) or a pre-Golgi compartment (van Echten and Sandhoff, 1989) must be translocated across the Golgi membrane to be accessible for the enzyme LacCer synthase, which is active at the luminal face of Golgi membranes. It has been suggested that multidrug resistance (MDR) proteins (MDR1 P-glycoprotein (Pgp) and multidrug resistance protein1



(MRP1)) can act as GlcCer flippases in Golgi membranes in several cell lines (Raggers *et al.*, 1999; De Rosa *et al.*, 2004).

Another important metabolite that can be generated from ceramide is ceramide-1-phosphate, which is formed by the action of ceramide kinase (Bajjalieh *et al.*, 1989).

Catabolism of sphingolipids occurs after endocytosis primarily in the lysosomes by the stepwise action of specific hydrolases that remove the headgroups of complex SLs, resulting in the formation of ceramide (Hannun *et al.*, 2001) (Figure 1-2-1). Other subcellular compartments, including Golgi apparatus and plasma membranes, contain hydrolases and contribute in degradation of SLs (Goni and Alonso, 2002). Sphingomyelin and glycosphingolipids are degraded to ceramide through the action of sphingomyelinases and exoglycosidases, respectively (Hannun, 1994; van Echten-Deckert and Herget, 2006). Ceramide is then deacylated by ceramidases to sphingosine (Hassler and Bell, 1993). Sphingosine may be phosphorylated into sphingosine-1-phosphate, or it can enter the salvage pathway to form ceramide (Hannun *et al.*, 2001). Sphingosine-1-phosphate can also enter the salvage pathway by the action of phosphatases that regenerate sphingosine, or it can be irreversibly cleaved to phosphoethanolamine and hexadecenal by a pyridoxal 5'-phosphate (PLP)-dependent lyase (Van Veldhoven, 2000; Ikeda *et al.*, 2004). The aldehyde intermediate is oxidized to fatty acid whereas phosphoethanolamine can be utilized for the synthesis of phosphatidylethanolamine. Thus, both of SL-breakdown products may enter glycerolipid metabolic pathway (Hannun *et al.*, 2001).

Sphingolipids are essential for the growth of not only mammalian cells but also invertebrate and fungal cells (Hanada *et al.*, 1992; Dickson, 1998; Adachi-Yamada *et al.*, 1999), and modulate various cellular events including proliferation, differentiation, and apoptosis (Pettus *et al.*, 2002; Proia, 2003; Watterson *et al.*, 2005). In addition, sphingolipids, along with cholesterol, form detergent-resistant membrane microdomains, so called "lipid rafts", which are implicated in signal transduction and membrane trafficking (Barenholz, 2004; Lucero and Robbins, 2004). The pathological aspects of SLs have also been receiving attention. Inborn dysfunctions of enzymes or accessory factors involved in the degradation of sphingolipids often cause infant lethality, suggesting that the abnormal accumulation of SLs is toxic to cells or tissues (Futerman and van Meer, 2004; Kolter and Sandhoff, 2006). Also, various types of pathogens exploit sphingolipids of host cells as membrane receptors (Wedeking and van

Echten-Deckert, 2006). In addition, lipid-rafts of host cells can be platforms for infection signaling and entry of intracellular parasites (Hanada, 2005).

### 1.2.2 Sphingolipids in cancer

As already mentioned above, sphingolipids generate biologically active signals that affect cell proliferation, differentiation and apoptosis. These sphingolipid-regulated processes are crucial in cancer development and progression, and influence the efficacy of anti-cancer therapeutics (Kok and Sietsma, 2004; Fox *et al.*, 2006; Ogretmen, 2006). A dynamic sphingolipid equilibrium has been described where pro-apoptotic SLs exist in a balance with pro-survival SLs (Cuvillier *et al.*, 1996).

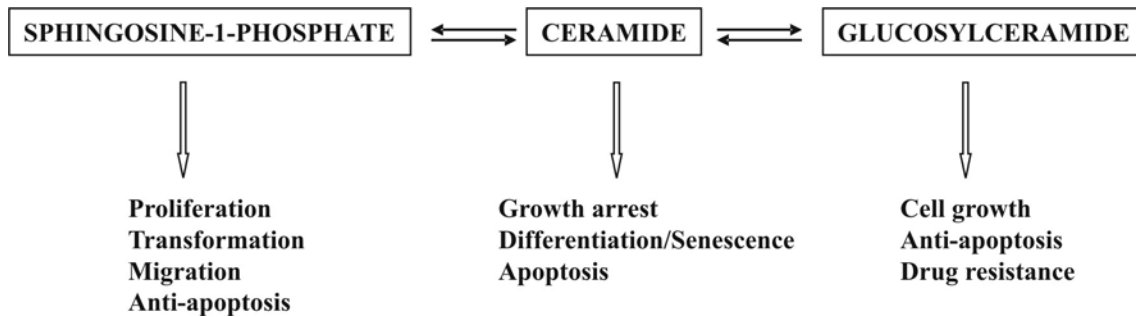


**Figure 1-2-3.** The biological roles of sphingolipids.

The most common example of this equilibrium is the balance between ceramide and sphingosine-1-phosphate (Figure 1-2-3). When this balance shifts either way, it can lead to cellular death or growth arrest in the case of ceramide accumulation or alternatively to proliferative disorders (i.e. cancer, angiogenesis) in the case of formation of sphingosine-1-phosphate. In addition, other sphingolipid-based second messengers, including ceramide-1-phosphate and glycosphingolipids are also in dynamic flux with ceramide. Thus, pharmacological or molecular manipulations of any of the enzymes involved in SL metabolism have been proposed as a tool to increase the sensitivity of tumors to various therapeutic agents (Modrak *et al.*, 2006). Sphingosine kinase, sphingomyelinase, ceramidase, and glucosylceramide synthase, among other enzymes important to SL metabolism, are being studied as potential new drug targets.

### 1.2.2.1 Ceramide

The function of ceramide as a mediator of apoptosis suggests novel therapeutic approaches based on elevating levels of endogenous ceramide and/or mimicking its actions. A number of clinically important cytotoxic agents appear to be effective because of their ability to activate ceramide-mediated pathways in cancer cells (Figure 1-2-4). Drugs can impact ceramide metabolism by promoting ceramide synthesis *de novo*, by activating sphingomyelinase, and/or by blocking glucosylceramide formation. Targeting enzymes of ceramide formation appears to elevate endogenous levels of ceramide, leading to increased cytotoxic responses in various cancer cells (Ogretmen and Hannun, 2004; Reynolds *et al.*, 2004).

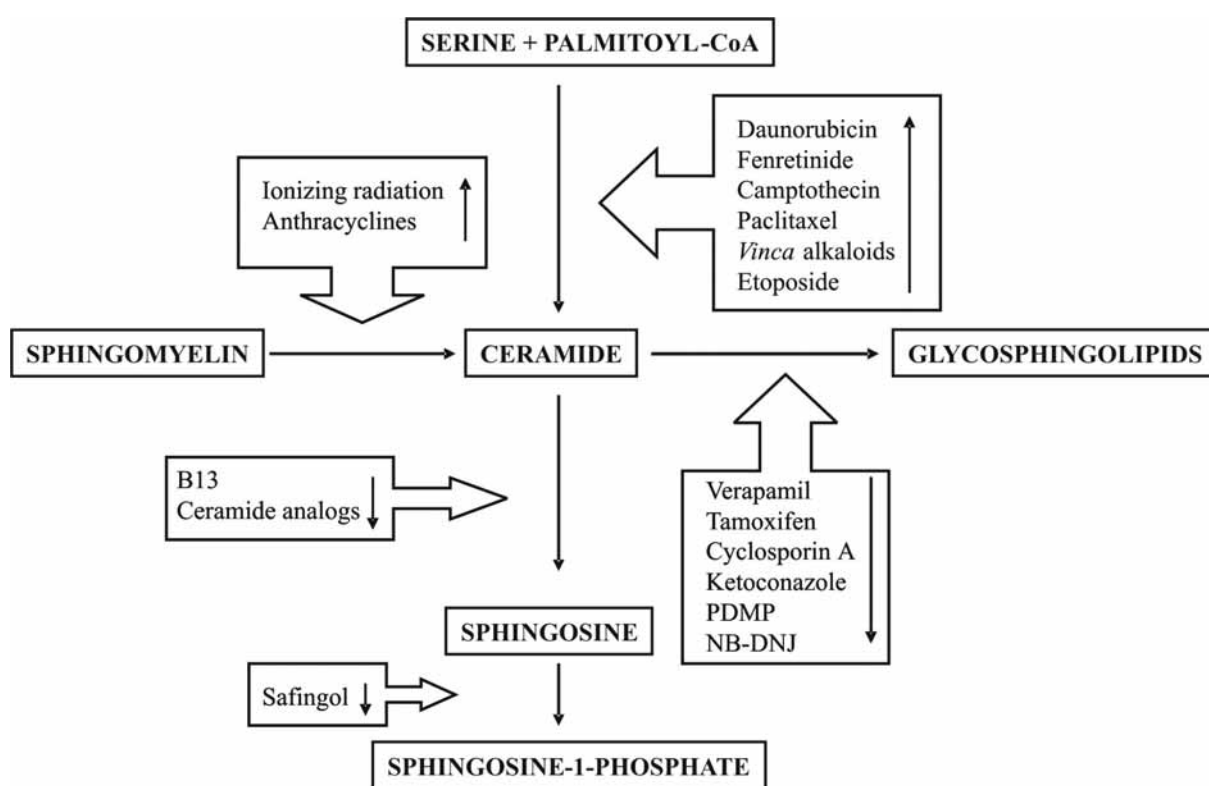


**Figure 1-2-4.** Compounds that contribute to increased levels of cellular ceramide.

↑, stimulation; ↓, inhibition. Modified from Duan, 2005; (Duan, 2005).

Both of the anthracyclines doxorubicin and daunorubicin effectively elevate ceramide levels in several cell types. It is reported that daunorubicin promotes ceramide formation and apoptosis by stimulating ceramide synthase activity (Bose *et al.*, 1995) or via hydrolysis of sphingomyelin (Jaffrezou *et al.*, 1996). Some of the cytotoxic properties of vinca alkaloids (vincristine and vinblastine), widely used in the treatment of leukemia patients, may be due to increase *de novo* formation of cellular ceramide (Zhang *et al.*, 1996). The effects of paclitaxel inhibited microtubule depolymerization in different solid tumors were also linked to *de novo*

synthesis of ceramide (McCloskey *et al.*, 1996; Charles *et al.*, 2001). On the other hand, triphenylethylene antiestrogens, such as tamoxifen, block conversion of ceramide to glucosylceramide (Cabot *et al.*, 1996) and, thereby, promote increases in cellular ceramide. Multidrug treatments, such as a combination of tamoxifen with agents that elevate *de novo* ceramide formation like doxorubicin, increase the anti-tumor effect of a single drug (Lucci *et al.*, 1999).

Until recently, cancer chemotherapy has focused primarily on targeting DNA, critical cellular proteins or metabolites involved in DNA synthesis and repair, or on targeting microtubule disruption. Cancer drug development is now turning toward potentially more selective ways to inducing tumor cell death or cytostasis (Reynolds *et al.*, 2004). The ability of ceramide and ceramide-generating drugs to induce cytotoxicity in cancer cells via few apoptotic signaling pathways provides new approaches in cancer therapy.

#### **1.2.2.2 Glucosylceramide and other glycosphingolipids**

Glycosphingolipids (GSLs) are biosynthetically derived from ceramide backbone linked to an oligosaccharide chain of variable length and complexity. Gangliosides are prominent members of GSLs that are distinguished by the presence of one or more sialic acid residues. GSLs are involved in important physiological processes including differentiation, migration, proliferation and apoptosis (Bektas and Spiegel, 2004; Wedeking and van Echten-Deckert, 2006). Thus, disturbance of GSL metabolism results in various pathological disorders. This is obvious in GSL storage diseases, such as Gaucher and Tay-Sachs disease, in which glucosylceramide and GM2 accumulate, respectively, due to malfunctioning of the proteins responsible for their degradation (Buccoliero and Futerman, 2003).

The simplest GSL, glucosylceramide (GlcCer), in contrast to the apoptotic effect of its biosynthetic precursor ceramide, was reported to have growth stimulatory and anti-apoptotic effects (Datta and Radin, 1988; Marsh *et al.*, 1995; Marchell *et al.*, 1998). Moreover, increased GlcCer synthesis appears to be connected with multidrug resistance (MDR), in which cells lose sensitivity for anti-cancer drugs due to the decreased levels of ceramide (Senchenkov *et al.*, 2001). It is reported that a number of cancer cell lines accumulate this noncytotoxic metabolite (Lavie *et al.*, 1996; Lucci *et al.*, 1998). Therefore, limiting the synthesis of glycolipids could be one approach to dampening drug resistance. Well-known drug resistance modulators such as tamoxifen, verapamil, and cyclosporine A have been shown to exert part of their effect by inhibition of glucosylceramide synthase (Senchenkov *et*

*al.*, 2001; Bleicher and Cabot, 2002). Thus, inhibition of GlcCer synthesis could reduce multidrug resistance and increase ceramide effects.

While GlcCer elicits antiapoptotic role, ganglioside GD3 has been shown to sensitize human hepatoma cells to treatment with ionizing radiation or daunorubicin (Garcia-Ruiz *et al.*, 2000; Paris *et al.*, 2002). Ergo, sialyltransferase II, the enzyme that catalyzes formation of GD3 from GM3 by addition of a sialic acid molecule, might be another good target for anticancer therapy.

### 1.3 Influence of fungal metabolites on sphingolipid metabolism

Since sphingolipids are involved in various cellular functions, each disturbance in sphingolipid homeostasis can lead to serious pathological effects. Thus, strategies which either mimic/antagonize these lipids or modulate their levels could provide novel therapeutic possibilities. Several inhibitors of SL biosynthesis have been described. They have been isolated from natural sources or have been generated by design and chemical synthesis. Most of the synthetic inhibitors are structural analogs of cellular SLs.

Although analogs of natural SLs can possess higher membrane permeability than natural ones (Modica-Napolitano and Aprille, 2001; Senkal *et al.*, 2006), some of them that are synthesized as SL enzyme inhibitors, probably on account of their structural similarity to natural SLs, are also reported to have several physiological functions which may not be related to their enzyme inhibition (Igarashi *et al.*, 1989; Khan *et al.*, 1990; Sweeney *et al.*, 1996). Thus, specific SL enzyme inhibitors are desired.

During the last two decades several compounds have been isolated from natural sources, mostly from fungi, that inhibit the activity of enzymes involved in sphingoid base metabolism. The most representative ones are discussed below.

#### 1.3.1 Inhibitors of serine palmitoyltransferase

The first step of sphingolipid biosynthesis is the condensation of serine and palmitoyl CoA, a reaction catalyzed by serine palmitoyltransferase (SPT) to produce 3-ketodihydrosphingosine. Fungal metabolites that inhibit SPT activity are shown in Figure 1-3-1.

Myriocin (ISP-1), the structure of which resembles that of sphingosine, was initially isolated as an antibiotic and immunosuppressant from a culture broth of *Isaria sinclairi* (Fujita *et al.*, 1994). Myriocin inhibits the activity of SPT, the rate-limiting enzyme in *de novo* biosynthesis of SLs. Thus, ISP-1 inhibits *de novo* formation of all sphingolipids in mammalian cells with  $IC_{50}$  values in the nanomolar range (Miyake *et al.*, 1995). Myriocin is also known to induce apoptosis of cytotoxic T cells (Fujita *et al.*, 1994; Nakamura *et al.*, 1996).

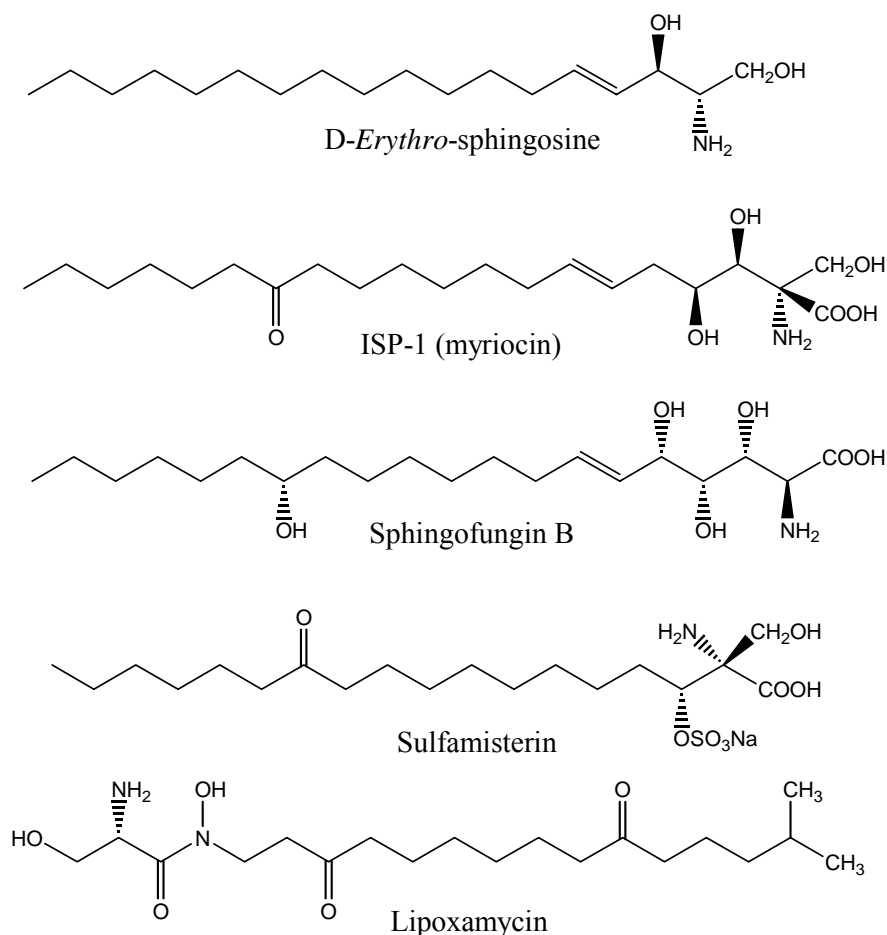


**Figure 1-3-1.** Inhibitors of serine palmitoyltransferase (SPT).

Chemical modification of ISP-1 led to a novel synthetic compound, FTY720 (Figure 1-3-2), which has more potent immunosuppressive activity and less toxicity than ISP-1 (Kiuchi *et al.*, 2000).

Although structurally similar to sphingosine, FTY720, unlike ISP-1, does not inhibit serine palmitoyltransferase. It has been reported that FTY720 is effectively phosphorylated by sphingosine kinase 2 and that FTY720-phosphate (FTY720-P) is a high affinity agonist for sphingosine-1-phosphate (S1P) receptors (Brinkmann and Lynch, 2002; Paugh *et al.*, 2003) which play an important role in inflammatory processes. FTY720 is currently being evaluated by Novartis in Phase III clinical trials for use in transplantation and autoimmune diseases such as multiple sclerosis.

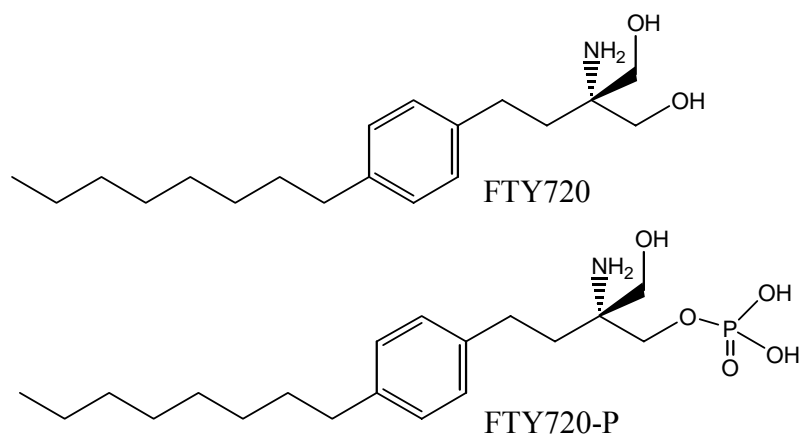


**Figure 1-3-2.** Structures of FTY720 and FTY720-phosphate.

It has been published that only (*S*)-configured enantiomer acts as agonist on S1P receptors (Kiuchi *et al.*, 1998; Albert *et al.*, 2005)

Other sphingosine analogs, the sphingofungins, isolated from two species of thermotolerant fungi, *Aspergillus fumigatus* and *Paecilomyces variotii* (Horn *et al.*, 1992; Zweerink *et al.*, 1992), inhibit activity of mammalian and yeast SPT. Sphingofungin B caused growth inhibition of a Chinese hamster ovary cell line which was due to inhibition of sphingolipid synthesis (Hanada *et al.*, 2000).

Lipoxamycin from *Streptomyces* sp. is an antifungal compound that inhibits SPT from *Saccharomyces cerevisiae* (Mandala *et al.*, 1994).

Viridofungins from *Trichoderma viride* are potent inhibitors of SPT but they also inhibit squalene synthase (Mandala *et al.*, 1997; Onishi *et al.*, 1997), while sulfamisterin, derived from the fungus *Pycnidium* sp., is a specific SPT inhibitor (Yamaji-Hasegawa *et al.*, 2005).

### 1.3.2 Inhibitors of ceramide formation

Fumonisin are a group of mycotoxins initially isolated from corn culture material of *Fusarium moniliforme* (Gelderblom *et al.*, 1998). Later they have been isolated from other *Fusarium* species (i.e. *F. verticillioides* and *F. proliferatum*) and from *Alternaria alternata* (Chen *et al.*, 1992). Until now several fumonisins have been isolated and characterized of which fumonisin B1 is the most toxic. Contamination of food with those toxins causes a neurodegenerative disease of horses called equine leucoencephalomalacia (Marasas *et al.*, 1988) as well as pulmonary edema in pigs (Harrison *et al.*, 1990) and liver and renal damage in numerous animals (Kriek *et al.*, 1981; Voss *et al.*, 1990). Consumption of corn contaminated with *F. moniliforme* has been correlated with human esophageal cancer in areas of southern Africa and China (Yang, 1980). Most or all of the toxicities resulting from





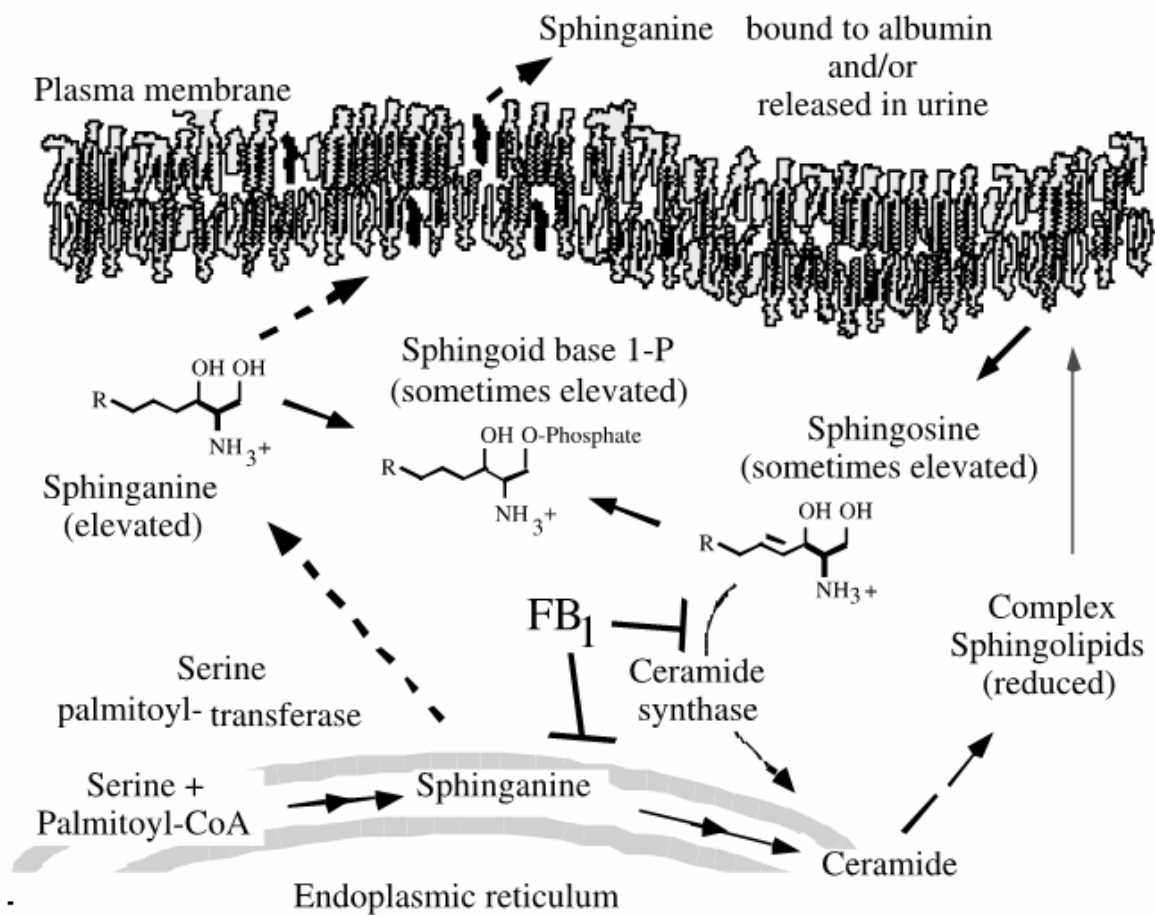


**Figure 1-3-4.** Disruption of SL metabolism by fumonisin B1 (FB1).

Shown are the inhibition of ceramide formation from sphinganine and sphingosine by fumonisin B1, resulting in elevations in these sphingoid bases (and sometimes sphingoid base 1-phosphate) and reduction in complex sphingolipids (Desai *et al.*, 2002).

Alternaria toxin, isolated from *Alternaria alternata* (Shier *et al.*, 1991) (Figure 1-3-5) is a phytotoxin with structural similarity to the sphingolipid backbone. It inhibits SL biosynthesis on the stage of ceramide formation but with less potency than fumonisins (Merrill *et al.*, 1993b).

Australifungin (*Sporomiella australis*) (Figure 1-3-5) is a potent antifungal agent that was reported as an inhibitor of sphinganine *N*-acyltransferase (Mandala *et al.*, 1995).

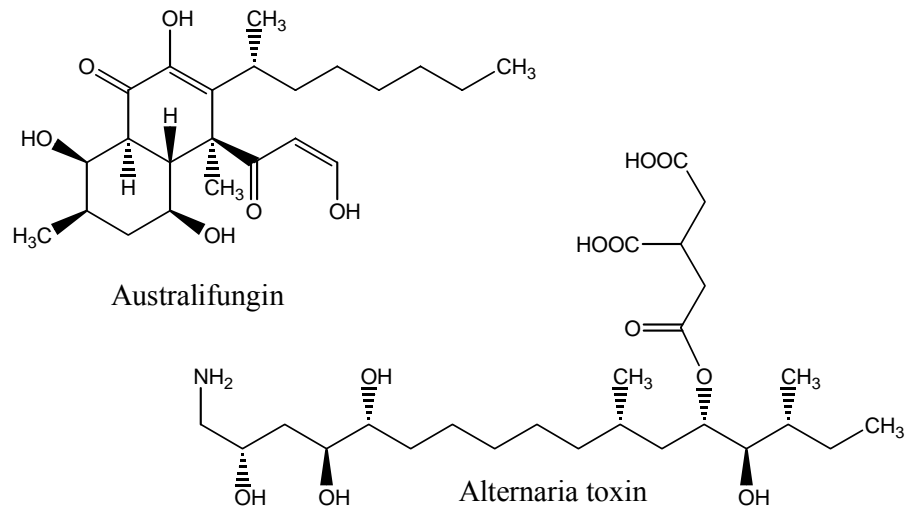


**Figure 1-3-5.** Structures of australifungin and alternaria toxin.

## **2 Scope of the present study**

The main goal of the present study was the isolation of new and preferably biologically active secondary metabolites from marine-derived fungi with an emphasis on such compounds that influence on sphingolipid metabolism.

### **2.1 Biological and chemical screening of fungal extracts**

Selected fungal strains were cultured in small scale and extracted which enabled biological tests and chemical screening. These tests mainly consisted of agar diffusion assays for antibacterial, antifungal and antialgal activity, cytotoxic assays in a panel of 6 cancer cell lines and assays for sphingolipid metabolism alterations. Additional investigations by  $^1\text{H}$  NMR and MS were used for chemical characterization of the fungal extracts. The results obtained with those methods were used for the selection of strains which were subsequently subjected to detailed chemical and biological analyses.

### **2.2 Chemical investigation of selected fungal strains**

In order to isolate pure and biologically active metabolites, selected strains were cultured on a large scale, extracted, and the extracts separated using diverse chromatographic methods, mainly HPLC. The chemical investigations were completed by structure elucidation, using 1D and 2D NMR techniques and by physical characterization of the isolated metabolites.

### **2.3 Biological evaluation of isolated pure compounds**

Pure compounds isolated in this study were tested in the same assays as used for the evaluation of the extracts. Additionally, specific cytotoxicity assays and tests on sphingolipid metabolism were used for the compounds that exhibited potent activity in order to describe their mechanism of action.

### 3 Materials and methods

#### 3.1 Fungal strains

##### 3.1.1 Isolation of the fungal strains

All chemically investigated fungal strains, described in this study, were obtained from fungal culture collection of Professor G. M. König (Institute for Pharmaceutical Biology, University of Bonn), and were isolated by Ekaterina Eguereva or by former Ph. D. students Dr. Ulrich Höller and Dr. Christine Klemke.

##### 3.1.1.1 Isolation from algal material

After sterilization of the algal material with 70 % ethanol, algal samples were rinsed with sterile water and pressed onto agar plates to detect any residual fungal spores on their surface. The water used for media was artificial sea water (ASW) containing the following salts: [(g/L): KBr (0.1), NaCl (23.48), MgCl<sub>2</sub> x H<sub>2</sub>O (10.61), CaCl<sub>2</sub> x 2H<sub>2</sub>O (1.47), KCl (0.66), SrCl<sub>2</sub> x 6H<sub>2</sub>O (0.04), Na<sub>2</sub>SO<sub>4</sub> (3.92), NaHCO<sub>3</sub> (0.19), H<sub>3</sub>BO<sub>3</sub> (0.03)]. Sterilized algae were then cut into pieces and placed on agar plates containing isolation medium: biomalt 20 g/L, 15 g/L agar, 1 L ASW, benzyl penicillin and streptomycin sulphate (250 mg/L). Fungal colonies growing out of the algal tissue were transferred onto medium for sporulation: 15 g/L agar and 20 g/L biomalt extract in artificial sea water (Klemke, PhD Thesis).

##### 3.1.1.2 Isolation from the sponge

Fungal strains were isolated by inoculating small pieces of the inner tissue of the sponge on glucose peptone yeast extract agar at room temperature: Glucose 1 g/L, peptone from Soya 0.5 g/L, yeast extract 0.1 g/L, streptomycin sulfate 250 mg/L, agar 15 g/L, 1 L ASW (Höller *et al.*, 2000). Fungal colonies growing out of the tissue of the sponge were transferred to medium for sporulation (15 g/L agar, 20 g/L biomalt extract, 1 L ASW).

##### 3.1.2 Fungal strains for chemical investigation

All strains, described in this study, were identified by the Centraalbureau voor Schimmelcultures, Utrecht, The Netherlands.

*Aspergillus terreus* was isolated from the alga *Cystoseira* sp. collected around Greece.

*Emericella nidulans* var. *acristata* (Fennell & Raper) Subramanian was isolated from a green alga collected from Sardinia (Italy, Mediterranean Sea).

*Spicellum roseum* (Nicot & Roquebert) was isolated from the sponge *Ectyplasia perox* collected around the Caribbean island of Dominica.

*Arthrinium sacchari* (Speg) M.B. Ellis anamorph of *Apiospora montagnei* Saccardo was isolated from the green alga collected at the Adriatic Coast (Croatia).

*Paecilomyces lilacinus* (Thom) Samson was isolated from unidentified algae sample collected around the Island of Tenerife.

*Fusarium oxysporum* was isolated from the alga *Pelvetia* sp. collected at South Atlantic Coast (France).

*Fusarium dimerum* complex (contains many species) was isolated from the sponge *Callyspongia* sp. collected in Australia.

### **3.1.3 Cultivation of fungal strains**

Fungal strains were cultivated in Fernbach flasks at room temperature for one to three months (specific cultivation conditions see in the “Results” chapter). The solid media used for the cultivation were (a) biomalt agar medium (20 g/L biomalt, 17 g/L agar and ASW), (b) peptone agar medium (20 g/L biomalt, 10 g/L peptone form Soya, 17 g/L agar and ASW), or (c) malt-yeast agar medium (4 g/L yeast extract, 10 g/L malt extract, 4 g/L glucose, 15 g/L agar and ASW, pH 7.3). For the screening examinations fungal strains were cultivated in Petri dishes for one month on three different media: (a) biomalt agar medium, (b) malt-yeast agar medium, or (c) czapek agar medium (35 g/L Czapek solution agar, 15 g/L agar and ASW).

## **3.2 Chromatography**

### **3.2.1 Thin layer chromatography (TLC)**

TLC was carried out using either TLC aluminium sheets silica gel 60 F<sub>254</sub> (Merck) or TLC aluminium sheets RP-18 F<sub>254</sub> (Merck) as stationary phase. Standard chromatograms of fungal extracts and fractions were prepared by applying 20 µL of solution (5 mg/mL) to a TLC plate

and using PE/acetone or MeOH/H<sub>2</sub>O mixtures as mobile phases under saturated conditions. Chromatograms were detected under UV light (254 and 366 nm), and with vanillin-H<sub>2</sub>SO<sub>4</sub> (0.5 g vanillin dissolved in a mixture of 85 ml methanol, 10 mL acetic acid and 5 mL sulphuric acid, TLC plate heated at 110°C after spraying) giving colored spots on a white plate.

### 3.2.2 Vacuum liquid chromatography (VLC)

Sorbents for VLC were silica gel 60 (0.063-0.200 mm, Merck) or Polygoprep 60 C<sub>18</sub> (0.05 mm, Macherey-Nagel). Columns were filled with the appropriate sorbent, compressed under vacuum and soaked with PE or MeOH. Before applying the sample solution, the columns were equilibrated with the first designated eluent.

### 3.2.3 Size exclusion chromatography (SEC)

Sephadex<sup>TM</sup> LH-20 (0.018-0.111 mm, Pharmacia Biotech AB; size exclusion material) was used as column material with MeOH as eluent. Before applying the sample solution, the column was wet packed with MeOH.

### 3.2.4 High performance liquid chromatography (HPLC)

HPLC was performed on either (a) a Merck-Hitachi system equipped with an L-6200A pump, an L-4500A photodiode array detector, a D-6000A interface with D-7000 HSM software and a Rheodyne 7725i injection system or (b) a Waters system, controlled by Waters millennium software, consisting of a 717 plus autosampler, 600 controller pump with in-line degasser and a 996 photodiode array detector. A third system (c) was equipped with a Rheodyne 7725i injection system, a Waters 515 HPLC pump, a Knauer RI detector K-2300 and a Linseis L 250 E recorder. Columns used were:

- A: Knauer Eurospher-100, C-8, 250 x 8 mm, 5 µm
- B: Knauer Si Eurospher-100, 250 x 8 mm, 5 µm
- C: Macherey-Nagel Nucleodur 100-5 C<sub>18</sub>, 250 x 4.6 mm, 5 µm
- D: Phenomenex Synergi Hydro-RP, 250 x 4.6 mm, 4 µm
- E: Phenomenex Synergi Max-RP, 250 x 4.6 mm, 4 µm
- F: Phenomenex Max C<sub>12</sub>, 250 x 4.6 mm, 5µm
- G: Phenomenex Chirex 3126 (D), 4.6 x 5 mm, 5 µm

Typical flow rates were 1.5 or 2.0 mL/min (250 x 8 mm column), or 1.0 mL/min (250 x 4.6 mm column). All solvents, except H<sub>2</sub>O, were distilled prior to use. The eluents were degassed under reduced pressure.

### 3.3 Structure elucidation

Structures were elucidated mainly using one and two dimensional NMR techniques and various MS methods. Furthermore optical rotation and UV parameters as well as IR properties provided additional information. Additionally, calculated NMR data of the assumed structures with ACD software helped to elucidate most structures. Identity of isolated compounds with compounds reported in literature was stated, based on <sup>1</sup>H NMR and <sup>13</sup>C NMR, spectroscopic data, and specific optical rotation. Based on literature searches, using the MarinLit database, Sci Finder-database and Antibase, the structures were designed as known or as new.

#### 3.3.1 NMR spectroscopy

All NMR spectra of extracts and pure compounds were recorded using either a Bruker Avance 300 DPX operating at 300 MHz (<sup>1</sup>H) and 75 MHz (<sup>13</sup>C) or a Bruker Avance 500 DRX spectrometer operating at 500 MHz for <sup>1</sup>H and 125 MHz for <sup>13</sup>C, respectively.

Spectra of pure compounds were processed using Bruker 1D WIN-NMR, 2D WIN-NMR or XWIN-NMR Version 2.6, 3.1 and 3.5 software. Spectra were referenced to residual solvent signals with resonances at  $\delta_{H/C}$  3.35/49.0 for CD<sub>3</sub>OD,  $\delta_{H/C}$  7.26/77.0 for CDCl<sub>3</sub>,  $\delta_{H/C}$  2.04/29.8 for (CD<sub>3</sub>)<sub>2</sub>CO. From DEPT experiments multiplicity for <sup>13</sup>C could be derived: s = C, d = CH, t = CH<sub>2</sub>, q = CH<sub>3</sub>. Structural assignments were based on spectra resulting from one or more of the following NMR experiments: <sup>1</sup>H, <sup>13</sup>C, DEPT135, <sup>1</sup>H-<sup>1</sup>H COSY, <sup>1</sup>H-<sup>13</sup>C direct correlation (HMQC and HSQC), <sup>1</sup>H-<sup>13</sup>C long range correlation (HMBC), <sup>1</sup>H-<sup>1</sup>H NOESY and <sup>1</sup>H selective NOE.

#### 3.3.2 Mass spectrometry

Mass spectral measurements were performed by Ms. C. Sondag (Department of Chemistry, University of Bonn) using a Kratos MS 50 (EI), Kratos Concept 1H (FAB) and a Finnigan MAT 95 (EI, ESI) spectrometer.

HPLC-MS (ESI) measurements were conducted by Dr. A. Krick, Institute for Pharmaceutical Biology, Bonn, Germany employing an Agilent 1100 Series HPLC including DAD (205 nm), with reversed phase C<sub>18</sub> column (Macherey-Nagel Nucleodur 100, 125 x 2 mm, 5  $\mu$ m) and



gradient elution (from MeOH/H<sub>2</sub>O 10/90 to MeOH/H<sub>2</sub>O 100/0 in 20 min, MeOH 100% for 10 min, with added NH<sub>4</sub>Ac, 2 mmol), coupled with an API 2000, Triple Quadrupole, LC/MS/MS, Applied Biosystems/MDS Sciex and ESI source.

### 3.3.3 UV measurements

UV spectra were recorded on a Perkin-Elmer Lambda 40 with UV WinLab Version 2.80.03 software, using 1.0 cm quartz cells. Compounds were measured in methanol. The molar absorption coefficient was determined in accordance with the Lamber-Beer-Law:

$$A = \varepsilon \times c \times b \Leftrightarrow \varepsilon \left[ \frac{L}{\text{mol} \times \text{cm}} \right] = \frac{A}{c \left[ \frac{\text{mol}}{L} \right] \times b [\text{cm}]}$$

A = absorption at peak maximum

c = concentration

b = layer thickness of solution

### 3.3.4 IR spectroscopy

IR spectra were recorded as film, using a Perkin-Elmer FT-IR Spectrum BX spectrometer together with Spectrum v3.01 software.

### 3.3.5 Optical rotation

Optical rotation measurements were conducted on a Jasco model DIP-140 polarimeter (1 dm, 1 cm<sup>3</sup> cell). The samples were dissolved in methanol and measured at  $\lambda=589$  nm corresponding to the sodium D line at room temperature. Specific optical rotation  $[\alpha]_D^T$  was calculated pursuant to:

$$[\alpha]_D^T = \frac{100 \times \alpha}{c \times l}$$

T: temperature [°C]

D: sodium D line at  $\lambda=589$

c: concentration [g/100 mL]

d: cell length [dm]

For each compound at least 10 measurements were accomplished and the average value was calculated and assigned as  $\alpha$ .

### 3.3.6 Molecular modeling

The configurations of spicellamide A and B were revealed by conformation search (Boltzmann jump) using the CVFF1.01 force field refined with 500 iterations of smart minimization as implemented in the Cerius<sup>2</sup> 4.0 (MSI) molecular modeling software package. Calculations were performed using a Silicon Graphics O<sub>2</sub> workstation (Irix 6.5.6).

## 3.4 Amino acids analysis

### 3.4.1 Marfey's method

Depsipeptides (spicellamide A and B, 0.4 mg each) were hydrolyzed with 6 M HCl (0.5 mL) at 110 °C for 16 h. After concentration to dryness, the residues were dissolved in H<sub>2</sub>O (50  $\mu$ L). A 1 % 1-fluoro-2,4-dinitrophenyl-5-L-alaninamide (FDAA) solution in acetone (Marfey's reagent, 100  $\mu$ L) and 1 M NaHCO<sub>3</sub> (20 $\mu$ L) were added. In this manner FDAA reacts with the  $\alpha$ -amino group of L- and D-amino acids yielding diastereomers (Figure 3-1A) which can be separated by HPLC due to large differences in their capacity factors which come from intramolecular H-bonding (Figure 3-1B) (Bhushan and Bruckner, 2004). The mixtures were incubated at 80 °C for 40 min, cooled down to room temperature, neutralized with 2 M HCl (10  $\mu$ L), and evaporated to dryness (Marfey, 1984).

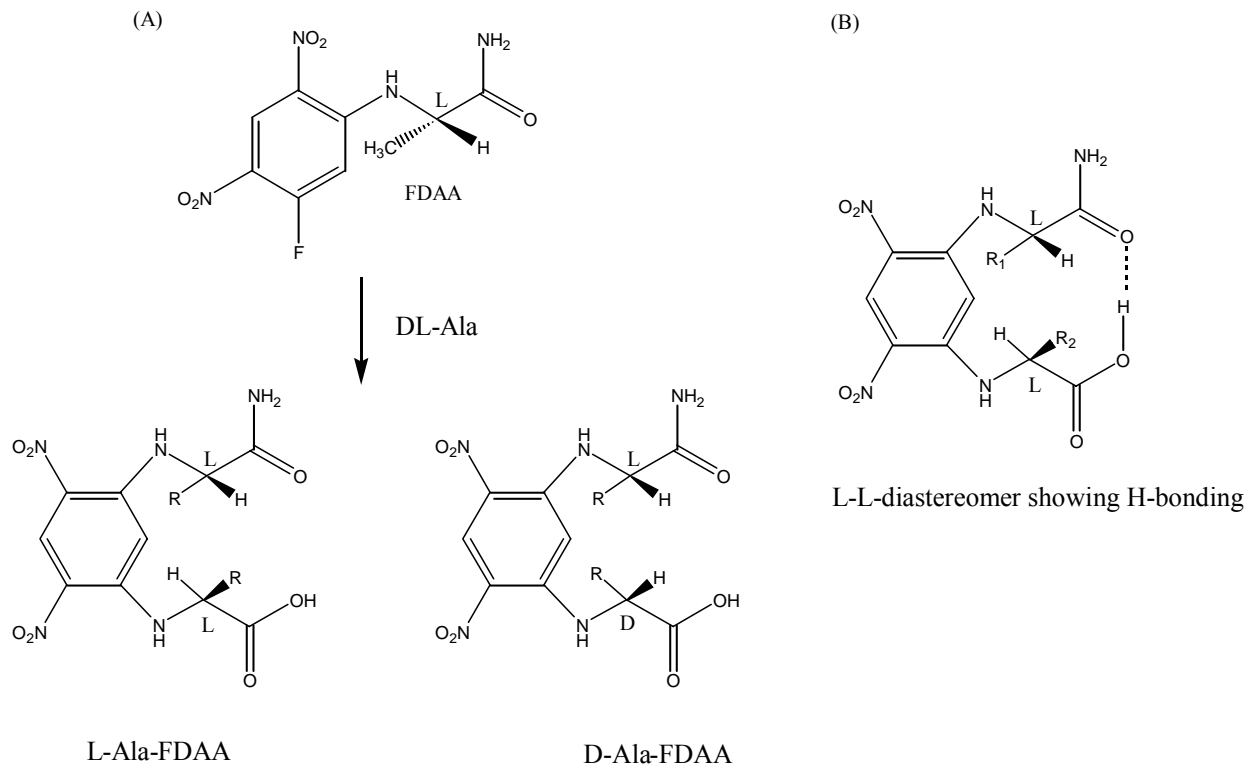


**Figure 3-1.** (A) Formation of L-L and L-D diastereomers. (B) Structure of L-L-diastereomer showing H bonding (Brückner and Keller-Hoehl, 1990).

The residues were resuspended in DMSO (100  $\mu$ L) and subjected to HPLC-MS using a reversed-phase  $C_{18}$  column (Macherey-Nagel Nucleodur 100, 125 x 2 mm, 5  $\mu$ m) and gradient elution (from MeOH/H<sub>2</sub>O 10/90 to MeOH/H<sub>2</sub>O 100/0 in 20 min, MeOH 100% for 10 min, with added NH<sub>4</sub>Ac, 2 mmol). The retention times and molecular weights of the FDAA derivatives of standards were compared with those of hydrolyzed depsipeptide samples.

### **3.5 Cell culture**

#### **3.5.1 Primary cultured neurons**

Cells were prepared from cerebella of six-day-old NMRI (Navy Marine Research Institute) mice, which were bred in the animal house of the University of Bonn (Germany), according to Trenkner and Sidman (Trenkner and Sidman, 1977). The cerebellum was dissected out and immersed in  $\text{Ca}^{2+}/\text{Mg}^{2+}$ -free isotonic solution (CMF) under sterile conditions, washed three times in CMF and incubated in trypsin/DNase for 14 min at room temperature. Trypsin/DNase solution was removed and the cells were washed three times with 10 % heat-inactivated horse serum (30 min at 57 °C) in Dulbecco's modified Eagle's medium (DMEM). The cells were then dissociated by repeated passage through a constricted Pasteur pipette in a DNase solution (10 % horse serum + 0.05 % DNase in DMEM) and collected by centrifugation at room temperature for 7 min at 1000g. The cells were suspended in DMEM containing 10 % heat-inactivated horse serum and plated onto poly-L-lysine-coated 8 cm<sup>2</sup> Petri dishes (6 x 10<sup>6</sup> cells/dish). At 24 h after plating, cytosine arabinose was added to the medium (4 x 10<sup>-5</sup> M) to arrest the division of non-neuronal cells. After 5-6 days in culture, cells were used for metabolic studies. Experiments were performed in minimum essential medium (MEM) containing 0.3 % horse serum and 1 % cytosine arabinoside.

#### **3.5.2 Neuroblastoma B104 cell line**

The rat neuroblastoma B104 cell line (ICLCATL99008) that originates in the central nervous system (Schubert *et al.*, 1974). Neuroblastoma B104 cells were routinely cultured in DMEM, supplemented with 2 mM glutamine, 10 % heat-inactivated fetal calf serum, and antibiotics (penicillin 100 U/l and streptomycin 100 mg/l). For experiments, cells were subcultured in 8 cm<sup>2</sup> Petri dishes. Medium was renewed every 48 h until confluency was reached. Experiments were performed in MEM supplemented with 0.3 % heat-inactivated fetal calf serum.

#### **3.5.3 Sphingolipid labeling in cultured cells**

From the culture dishes medium was removed, and the cells were rinsed two times with MEM supplemented with 0.3 % horse serum and 1 % cytosine arabinoside (cerebellar neurons), or with 0.3 % fetal calf serum (neuroblastoma B104 cells). The cells were then incubated in the same media containing substances, wanted to be tested, diluted in 70 % ethanol, or only 70 % ethanol as control. Incubation temperature was 35.5 °C for primary cultured neurons, and 37

°C for neuroblastoma B104 cells, while the saturation with CO<sub>2</sub> was 5 % for the both cell types. For the sphingolipid analysis, 4 h after the stimulation of the cells, 1 µCi/ml of either [<sup>14</sup>C] serine or [<sup>14</sup>C] galactose were added in the medium.

#### **3.5.4 Cell viability assay**

Cell viability was tested in CellTiter-Blue Cell Viability Assay (Promega) that is based on the conversion of resazurin to the fluorescent product resorufin exclusively by metabolically active (viable) cells. The neuroblastoma B104 cell line or primary cultured neurons were cultured in 8 cm<sup>2</sup> Petri dishes as described above. After 24 h of the incubation with different fungal metabolites, 100 µL of CellTiter-Blue reagent (resazurin) were added to each cell culture dish and incubation continued for 1 h. Then an aliquot of 100 µL from each culture dish was transferred to a 96-well microtiter plate and fluorescence of resorufin was recorded (544<sub>Ex</sub>/590<sub>Em</sub> nm). The values were presented as percentages of control.

#### **3.5.5 Cell harvesting**

After 24 h of the incubation with different fungal metabolites, cells were washed two times with 500 µL of ice-cold phosphate-buffered saline (PBS), harvested with plastic scraper in 1.5 mL PBS, and centrifuged at 4 °C for 10 min at 3000g. Then PBS was removed and the pellets were stored at -20 °C until the further analysis.

#### **3.5.6 Protein determination**

The protein concentration was determined with the Bradford method in a 96-well microtiter plate (Bradford, 1976). The method is based on the binding of Coomassie Blue to protein which causes a shift in the absorption maximum of the dye from 465 to 595 nm. This increase in absorption at 595 nm is monitored. Bovine serum albumin (BSA) was used as a standard for which was calculated a standard curve from the absorptions obtained from 10 standard solutions ranging from 0 to 250 µg/mL. Always, 20 µL of standard or aliquots of protein sample (see Chapter 3.6.1) were added to 200 µL of Bradford reagent (Coomassie-blue R250) diluted 1:5 in Millipore water. The microtiter plate was incubated for 10 min in the absence of light and the absorption measurements and calculations of sample concentrations were carried out photometrically on a Multiskan Ascent readout instrument.

### **3.6 Sphingolipid analysis**

Sphingolipid extraction and analysis by thin layer chromatography (TLC) were done according to van Echten-Deckert (van Echten-Deckert, 2000).

#### **3.6.1 Extraction of lipids**

The cell pellets were suspended in 400  $\mu$ L of water and homogenized by repeated passage through plastic pipette tips. At this step aliquots for other measurements were taken (e.g. protein determination, see Chapter 3.5.6). For the extraction of total lipids, 5.85 mL mixture of chloroform-methanol (2:1, v/v) was added to the homogenized pellets. Extraction was performed for 24 h at 50 °C with continuous stirring. To avoid solvent loss by evaporation during extraction, screw-capped Pyrex tubes with Teflon inlays were used throughout. After extraction, denatured protein particles were removed by passing the samples through cotton wadding introduced into glass Pasteur pipettes, which were used as filtration columns. Prior to application of the lipid extract, the wadding filter was rinsed with 0.5 mL of extraction solvent chloroform-methanol-water (20:10:2, v/v/v). The filtered sample was collected in a new screw-capped Pyrex tube with Teflon inlay placed under the pipette tip. Finally, the wadding filter was rinsed with 2 mL of extraction solvent that was collected in the same tube. The solvent was evaporated under a stream of nitrogen.

#### **3.6.2 Removal of lipid contaminants**

Phospholipids, extracted along with sphingolipids, comigrate with sphingolipid separation by TLC, and therefore they should be removed from lipid extracts. For the removal of phospholipids, extracts were dissolved in 2.5 mL of methanol and sonicated for 5 min in a sonifier (Sonorex RK 100, Bandelin, Berlin, Germany). Then 62.5  $\mu$ L of sodium hydroxide (4 M stock solution in water) was added. After shaking for 2 hours at 37 °C, samples were neutralized by addition of about 10  $\mu$ L of concentrated acetic acid. Finally the solvent was evaporated under a stream of nitrogen.

#### **3.6.3 Removal of salts by reversed-phase chromatography**

Small hydrophilic molecules such as salts, amino acids, sugars, small peptides extracted along with sphingolipids, as well as salts formed by addition of sodium hydroxide, interfere with lipid behavior during separation by TLC. Reversed-phase liquid chromatography (RP-LC) was used to remove polar nonlipid contaminants. The silica gel RP18 (silica gel LiChroprep

RP18, 40-63  $\mu\text{m}$ , Merck) used for RP-LC was suspended in chloroform-methanol (2:1, v/v) and shaken for 30 min. After the gel was settled down supernatant was removed. The gel was resuspended in methanol (1:1, v/v), shaken for 30 min, settled down and the supernatant was removed. This step was repeated 3-4 times with fresh methanol. Finally, the gel suspended in methanol was stored at 4 °C until the use.

For the column preparation, small pieces of silanized glass fiber wadding (Macherey-Nagel) were introduced into glass Pasteur pipettes and 2 mL of the silica gel RP18 suspension was added. The columns were rinsed two times with 1 mL of chloroform-methanol-0.1 M potassium chloride (3:48:47, v/v/v). In the mean time, samples were dissolved in 1 mL of methanol and sonicated for 5 min. Then 1 mL of ammonium acetate (300 mM in H<sub>2</sub>O) was added to each sample, and the samples were applied to the columns. Empty sample tubes were rinsed two times with 0.5 mL of ammonium acetate (200 mM in methanol-water, 1:1, v/v) which was applied to the column. Columns were washed with 6 mL of water to elute all polar contaminants. Then new tubes were placed under each column. Lipids were eluted with 1 mL of methanol and 8 mL of chloroform-methanol (1:1, v/v). Solvent was evaporated under a stream of nitrogen.

#### **3.6.4 Separation of sphingolipids by thin-layer chromatography**

Sphingolipids were separated by thin layer chromatography using glass-backed silica gel 60 precoated TLC plates (Merck). Samples were dissolved in maximum 50 $\mu\text{L}$  of chloroform-methanol-water (20:10:2, v/v/v) and applied as 1 cm bands on the TLC plate using small glass capillaries (length 50 mm, diameter 0.5 mm, Hilgenberg, Malsfeld, Germany). TLC plates were dried overnight in a desiccator under vacuum before development.

The solvents used for the development of chromatograms were freshly mixed and added to the tank at least 90 min prior to initiating chromatography for the formation of the vapor-liquid equilibrium. The solvent system used for the separation of most sphingolipids was the mixture of chloroform-methanol-0.22% aqueous CaCl<sub>2</sub> (60:35:8, v/v/v). For a good resolution of ceramide, the TLC plate was run twice consecutively in chloroform-methanol-acetic acid (190:9:1, v/v/v). Neutral sphingolipids (glucosylceramide, lactosylceramide, sphingomyelin, GM3 and sphingosine) were separated in solvent system of chloroform-methanol-2 M aqueous ammonia (65:25:4, v/v/v).

After running, TLC plates were removed from the tank, and solvents were allowed to evaporate. Sphingolipids were visualized by autoradiography using the bio-imaging analyzer

Fujix Bas1000 software, TINA 2.09 (Raytest, Straubenhardt, Germany) and identified by  $R_f$  values of standards.

### 3.6.5 Lactosylceramide synthase (LacCer) assay

In a total volume of 50  $\mu$ l, the assay mixture contained 100  $\mu$ M GlcCer (Biotrend, Cologne, Germany), 100  $\mu$ g of Triton X-100, 64 mM sodium cacodylate (Sigma-Aldrich, Steinheim, Germany), HCl buffer (pH 7.35), 10 mM  $Mn^{2+}$ , 10 mM  $Mg^{2+}$ , 20 mM CDP-choline (Sigma-Aldrich, Steinheim, Germany), 500  $\mu$ M UDP-galactose (Sigma-Aldrich, Steinheim, Germany) and 500  $\mu$ M UDP- $^{14}C$  galactose (8000 cpm/nmol), and 100  $\mu$ g of cell protein. Incubation was for 30 min at 37 °C. Radioactivity of the reaction product was quantified in a liquid scintillation counter. The radioactive product of the enzyme assay co-migrated with authentic lactosylceramide when applied to TLC (solvent system: chloroform, methanol, 0.22% aqueous  $CaCl_2$  (60:35:8, by volume)). Blanks containing no glycolipid acceptor were run in parallel.

### 3.7 Reverse transcription-polymerase chain reaction (RT-PCR)

Total RNA was isolated from neuroblastoma B104 cells and cerebellar neurons using the RNeasy mini kit and the RNaseFreeDNaseI-set (Qiagen GmbH, Hilden, Germany) following provider's instructions. The principle of the procedure of the kit is the selective binding of RNA to a silica membrane while the rest of the cell components are washed away.

As starting material, cells were disrupted by addition of buffer containing 1 %  $\beta$ -mercaptoethanol (Sigma) and homogenized to reduce viscosity of lysates. Afterwards, 70 % ethanol was added to provide proper binding conditions to the silica-gel membrane of the columns provided by the kit. Finally, RNA was eluted in 60  $\mu$ L of water. The concentration ( $\mu$ g/mL) of isolated RNA was quantified by measuring RNA/protein absorption (260/280 nm) using spectrophotometer (SmartSpec<sup>TM</sup>Plus, Bio-Rad).

To obtain DNA copy (cDNA), approximately 0.4  $\mu$ g of total RNA was reverse-transcribed using SuperScript II First-Strand Synthesis System for RT-PCR with Hexamer Random Primers (Invitrogen, Karlsruhe, Germany) according to manufacturer's instructions. Semiquantitative PCR was performed using the both gene-specific primers pairs (representing intron spanning sequences, respectively) for LacCer synthase: 5'-CCTCCCTCCACATTTCTCC-3' (forward), 5'-ATCTTCCTCTGCCCTACCA-3' (reverse), 23 cycles; and 5'-CATGATCAGGCTGTATACCAATAAA-3' (forward), 5'-



CTTGTATTATTGCCTTCGGGATA-3' (reverse), 25 cycles with similar results; for 18 S rRNA: 5'-AAACGGCTACCACATCCAAG-3' (forward), 5'-CCTCCAATGGATCCTCGTTA-3' (reverse), 7 cycles. All reactions were carried out with taq DNA polymerase (Invitrogen, Karlsruhe, Germany) in a MJ PTC 200 thermal cycler (Biozym, Hess. Oldendorf, Germany). Annealing was at 59 °C and product size was between 100 and 150 base pairs.

In order to observe PCR products they were run on a 1.7 % agarose gel (agarose in Tris-Acetate-EDTA buffer). For analysis, 10 % ethidium bromide was added to the gel to allow visualization under a UV lamp. Samples were applied on the gel with 10 % of loading dye and run with power supply of 120V, 110A for 60 min.

### 3.7.1 RT-PCR protocols

#### RNA isolation

Cells (8 cm<sup>2</sup> Petri dish) were washed two times with 1 mL of sterile 37 °C warm PBS, harvested with plastic scraper in 600 µL of buffer containing 1 % β-mercaptoethanol (Sigma) and homogenized to reduce viscosity of lysates. Isolation of RNA was performed using the RNeasy mini kit and the RNaseFreeDNaseI-set (Qiagen GmbH, Hilden, Germany). The protocol used is summarized as follows:

- Mix 600 µL of lysis buffer with 600 µL 70 % EtOH
- Load 700 µL of the sample into column and centrifuge (20 s, 10000 rpm), discard waste, load rest of the sample and repeat the procedure
- Add 350 µL wash buffer RW1, centrifuge (20 s, 10000 rpm), discard waste
- Mix 10 µL DNase with 70 µL RDD buffer, add on the membrane and leave for 15 min
- Add 350 µL wash buffer RW1, centrifuge (20 s, 10000 rpm), discard waste
- Add 500 µL wash buffer RPE (+ EtOH), centrifuge (20 s, 10000 rpm), discard waste, repeat and centrifuge (2 min, 10000 rpm), discard waste and centrifuge to dry (1 min, max)
- Place column in tube, add 30 µL RNase free water, centrifuge (1 min, 10000 rpm), add another 30 µL RNase free water and repeat the procedure

#### Reverse transcription

<u>PrimerMix</u>	1 x [µL]
Random Hexamers	1
dNTP-Mix	1
H <sub>2</sub> O	3

Add PrimerMix to 5  $\mu$ L RNA.

65 °C 5 min

0 °C 2 min

<u>MasterMix</u>	1 x [ $\mu$ L]
10X RT Buffer	2
MgCl <sub>2</sub>	2
H <sub>2</sub> O	2
DTT	2
RNase Out	1
SS III	1

Add MasterMix to each sample.

25 °C 10 min

50 °C 50 min

85 °C 5 min

0 °C 2 min

Add 1  $\mu$ L RNaseH, spin with the pipette.

37 °C 20 min

### **Polymerase chain reaction**

<u>MasterMix</u>	1 x [ $\mu$ L]
10X Buffer	4
Forward-Primer	2
Reverse-Primer	2
dNTP-Mix	1
H <sub>2</sub> O	28.5
Taq	0.5

Add PrimerMix to 2  $\mu$ L cDNA, spin with the pipette, centrifuge (Short).

Example of PCR program:

Initial denaturation step: 94 °C 2:30 min

Cycle Step 1 – Denaturation: 94 °C 0:30 min

Cycle Step 2 – Annealing 55-60 °C 0:30 min (dependent upon primer used)

Cycle Step 3 – Elongation 68 °C 1:0 min

Repeat cycle steps accordingly between 7 to 35 times.

Final Elongation Step: 68 °C 9:0 min

Cooling: 0 °C 5:0 min

PCR products were either stored at 4 °C or ran on a 1 % agarose gel for analysis.

### **3.8 MRP1- and Pgp-related transport activities**

MRP1- and Pgp-related transport activities were investigated by using the fluorescent probes 5-carboxyfluorescein diacetate (CFDA) and rhodamine-123 (Rh123) in efflux and accumulation assays (Neyfakh, 1988; Laupeze *et al.*, 1999). The neuroblastoma B104 cells and cerebellar neurons were cultivated in 8 cm<sup>2</sup> Petri dishes at 37 °C (neuroblastoma) or 35.5 °C (cerebellar neurons) and 5% CO<sub>2</sub>. At confluence, cells were washed twice with Hank's balanced salt solution (HBSS) (1.3 mM CaCl<sub>2</sub>, 5.4 mM KCl, 0.44 mM KH<sub>2</sub>PO<sub>4</sub>, 0.83 mM MgSO<sub>4</sub>, 137 mM NaCl, 4.2 mM NaHCO<sub>3</sub>, 0.34 mM Na<sub>2</sub>HPO<sub>4</sub> and 25 mM D-glucose, pH 7.2 – 7.6) at 37 °C.

#### **3.8.1 MRP1- and Pgp-mediated accumulation assay**

For MRP1- and Pgp-mediated accumulation assay cells were pre-incubated 1 h at 37 °C with HBSS containing ethanol (2% v/v) or tested compounds (30 μM 8-deoxy-trichothecin, 30 μM trichodermol, 20 μM MK571 and 15 μM cyclosporine A). CFDA (2 μM, MRP1-assay) and Rh-123 (20 μM, Pgp-assay) were then added for an incubation of 2 h at 37 °C. The accumulation of CFDA and Rh-123 was stopped by washing the cells five times with cold PBS and the cells were lysed with 0.1 % Triton X-100 at room temperature. Fluorescence of CFDA and Rh-123 in media and cell lysates was measured using a spectrofluorometer (Labsystems Fluoroskan II, GMI, USA) at a wavelength of 485 nm for excitation and 538 nm for emission.

#### **3.8.2 MRP1- and Pgp-mediated efflux assay**

For MRP1- and Pgp-mediated drug efflux assay cells were loaded with 2 μM CFDA in the presence or absence of the MRP1 inhibitor MK571 (20 μM), or with 20 μM Rh-123 in the presence or absence of the Pgp inhibitor cyclosporine A (15 μM) for 2 h at 37 °C. Cells were then washed five times with HBSS and incubated with HBSS containing 30 μM 8-deoxy-trichothecin, 30 μM trichodermol, 20 μM MK571 (MRP1-assay), 15 μM cyclosporine A

(Pgp-assay) or ethanol (2% v/v) as a control. After incubation for 1 h at 37 °C, cells were washed five times with cold PBS and lysed with 0.1 % Triton X-100 at room temperature. The fluorescent of CFDA and Rh-123 in media and cell lysates was measured as described above.

### 3.9 Biological tests

#### 3.9.1 Agar diffusion assay

Antimicrobial tests of extracts and HPLC fractions were performed by E. Neu following the method described by Schulz *et al.* (Schultz *et al.*, 1995). The bacteria *Bacillus megaterium* de Bary (Gram positive) and *Escherichia coli* (Migula) Castellani & Chambers (gram negative), the fungi *Microbotryum violaceum* (Pers.) Roussel (Ustomycetes), *Eurotium rubrum* (formerly *E. repens*) König, Spieckermann & Bremer (Ascomycetes) (all from DSMZ; Braunschweig, Germany), *Mycotypha microspora* Fenner (Zygomycetes) and the green microalga *Chlorella fusca* Shih Krass (Chlorophyceae) (both kindly provided by B. Schulz, Institute of Microbiology, University of Braunschweig, Germany) were used as test organisms.

Sample solutions contained 1 mg/mL per test sample. 50  $\mu$ L (equivalent to 50  $\mu$ g) of each solution were pipetted onto a sterile antibiotic filter disk (Schleicher & Schuell 2668), which was then placed onto the appropriate agar medium and sprayed with a suspension of the test organism. Growth media, preparation of spraying suspensions, and conditions of incubation were carried out according to Schulz *et al.* (Schultz *et al.*, 1995). For tested samples, a growth inhibition zone  $\geq 3$  mm or a complete inhibition  $\geq 1$  mm, measured from the edge of the filter disk, were regarded as a positive result; growth inhibition: growth of the appropriate test organism was significantly inhibited compared to a negative control; complete inhibition: no growth at all in the appropriate zone. Benzyl penicillin (1 mg/mL MeOH), streptomycin (1 mg/mL MeOH) and miconazole (1 mg/2 mL DCM) were used as positive controls.

#### 3.9.2 Cytotoxicity test against human cancer cell lines

All cytotoxicity data were provided by Dr. G. Kelter and Dr. A. Maier, Oncotest GmbH, Institute for Experimental Oncology, Freiburg, Germany. For screening purpose cytotoxicity of fungal extracts against the following six cell lines were performed according to Roth *et al.* (Roth *et al.*, 1999): GXF 251L (gastric), LXFL 529L (large cell lung carcinoma), MEXF 462NL (melanoma), RXF 486L (renal), UXF 1138L (uterus carcinoma), MAXF 401NL (breast carcinoma). Extracts were tested in concentrations of 10  $\mu$ g/mL.

The cytotoxicity of pure compounds was tested at Oncotest GmbH using 36 human tumor cell lines. The origin of the donor xenografts was described in Fiebig *et al.* (Fiebig *et al.*, 1992):

---

Bladder	BXF 1218L, BXF T24
CNS	CNXF 498NL, CNXF SF268
Colorectal	CXF HCT116, CXF HT29, CXF SW620
Gastric	GXF 251L
Lung	LXF 1121L, LXF 289L, LXF 526L, LXF 529L, LXF 629L, LXF H460
Mammary	MAXF 401NL, MAXF MCF7
Melanoma	MEXF 276L, MEXF 394NL, MEXF 462NL, MEXF 541L, MEXF 520L
Ovary	OVXF 1619L, OCXF 899L, OVXF OVCAR3
Pancreas	PAXF 1657L, PAXF PANC1
Prostate	PRXF 22RV1, PRXF DU145, PRXF LNCAP, PRXF PC3M
Pleuralmesothelioma	PXF 1752L
Renal	RXF 1781L, RXF 393NL, RXF 486L, RXF 944L, RXF UO31
Uterus body	UXF 1138L

Cell death of  $\geq 70\%$  was regarded as active while moderate activity was defined as 50-70 % cell death.

### 3.9.3 Immunostimulating activity

All immunostimulating analyses were performed by Dr. M. Maurer, Oncotest GmbH, Institute for Experimental Oncology, Freiburg, Germany. The immunostimulating effects of selected pure compounds were investigated by analyzing the stimulation of cytokine production by peripheral blood mononuclear cells (PBMCs) from healthy donors as described in Kralj *et al.* (Kralj *et al.*, 2006). The cytokines IL-2, IL-4, IL-6, IL-10, TNF- $\alpha$ , and IFN- $\gamma$  were quantitatively measured with a Coulter Cytomics FC500 cytometer using the cytometric bead array (Morgan *et al.*, 2004). The results were analyzed with the Coulter Cytomics Bead Array Analysis program.

### 3.10 Chemicals and other materials

#### 3.10.1 Apparatus and expendable materials

Agarose gel electrophoresis	ComPhor Midi; Biozym (Oldendorf, Germany)
Analytical balance	Sartorius (Göttingen, Germany)
Autoclave	Labortechnik (Oberschleissheim, Germany)
Balance	Sartorius (Göttingen, Germany)
Bench centrifuge	Centrifuge 5417R; Eppendorf (Hamburg, Germany)
Cell culture flasks	Costar (Cambridge, MA/USA)
Cell scrapers	Costar (Cambridge, MA/USA)
Centrifuge	Megafuge 2.0 R; Heraeus Multifuge 3 S-R; Heraeus (Hanau, Germany)
Centrifuge tubes, 15 mL	Greiner (Nürtingen, Germany)
Centrifuge tubes, 50 mL	Falcon (Heidelberg, Germany)
Plastic tubes, 0.5/1.5/2.0 mL	Eppendorf (Hamburg, Germany)
Fernbach flasks (1800 mL)	Schott Duran (Wertheim, Germany)
Filter paper	Macherey-Nagel (Düren, Germany)
Fluorimeter	Digitalfluorimeter Modell 8-9; Locarte, Dynex Hybaid Labsystems (Frankfurt, Germany)
Gel analyzing system	AlphaDigiDoc; Biozym (Oldendorf, Germany)
Heating-agitator	IKA Werke (Staufen, Germany)
Imager-Plates (Screens)	BAS MS 2040 Imaging Plate, Raytest (Staubenhardt, Germany)
Incubators	Heraeus (Hanau, Germany) Memmert (Schwabach, Germany)
Incubation shaker	Ika-Labortechnik (Staufen, Germany)
Laminar flow	Biohazard; Gelaire (Mailand, Italy)

	Heraeus (Hanau, Germany)
Microtiter plates	Falcon (Heidelberg, Germany)
Parafilm	AAC (Greenwich, USA)
Petri dishes, 8 cm <sup>2</sup>	Falcon (Heidelberg, Germany)
57/143 cm <sup>2</sup>	Greiner (Nürtingen, Germany)
Photometer	Smart Spec 3000; Biorad (Munich, Germany)
pH-Meter	InoLab WTW (Weilheim, Germany)
Pipettes	Eppendorf Research 0.5-10, 2-20, 10-200, 100-1000 (Hamburg, Germany)
Pipette tips	Greiner (Nürtingen, Germany)
Rotational evaporator	Heidolph (Kelheim, Germany)
Röntgen cassette	Chronex; DuPont (de Nemour, France)
Pyrex tubes	VWR (Darmstadt, Germany)
Scintillation counter	Packard Tricarb 1600 TR (Rodgau Jügesheim, Germany)
Scintillation vials	Packard (Frankfurt, Germany)
Shaking water bath	Gesellschaft für Labortechnik (Burgwedel, Germany)
Sonicator	Sonorex RK 100, Bandelin (Berlin, Germany)
Spectrofluorometer	Labsystems Fluoroskan II, GMI (Minnesota, USA)
Thermal cycler	MJ Research PTC-200 (Biozym, Hess. Oldendorf, Germany) SmartSpec <sup>TM</sup> Plus, Bio-Rad (CA/USA)
Ultrasonicator	Sonifer B12 with water cooled cup-horn; Branson Sonic Power Company (Danbury, USA)
Vortex	Bender-Hohlbein (Zürich, Switzerland)
Voltage supply source	Consort; Biometra (Göttingen, Germany) PowerPac 3000; BioRad (Munich, Germany)
Water filtration apparatus	EasypureUV/UF; Barnstedt/Werner



(Leverkusen, Germany)  
MembraPure; Millipore (Schwalbach,  
Germany)

### 3.10.2 Cell culture media

DMEM	PAA Laboratories (Pasching, Austria)
MEM	PAA Laboratories (Pasching, Austria)
HBSS	Sigma-Aldrich (Steinheim, Germany)

### 3.10.3 Chemicals and solvents

All solvents were research grade and supplied by Infracor or BASF. Acetone, CHCl<sub>3</sub>, CH<sub>2</sub>Cl<sub>2</sub>, EtOAc, MeOH and PE were distilled prior to use. Water used was de-ionised using a IBM Wasseraufbereitung VC 30 WE. Water for HPLC was de-ionised using a Millipore (milli-Q<sup>®</sup> academic) system.

Acetic acid	Merck (Darmstadt, Germany)
Acetone-d <sub>6</sub> 99.8%	Deutero GmbH (Kastellaun, Germany)
Acetonitrile	KMF (Lohmar, Germany)
Acetyl chloride	Lancaster (Frankfurt/Main, Germany)
Agar	Fluka (Buchs, Switzerland)
Agarose EEO	AppliChem (Darmstadt, Germany)
D-Alanine 99%	Sigma-Aldrich (Steinheim, Germany)
L-alanine 99%	Sigma-Aldrich (Steinheim, Germany)
N-Methyl-DL-alanine	Sigma-Aldrich (Steinheim, Germany)
N-Methyl-L-alanine	Sigma-Aldrich (Steinheim, Germany)
Ammonium acetate	Merck (Darmstadt, Germany)
Ammonium hydroxide	Merck (Darmstadt, Germany)
Benzyl penicillin	Fluka (Buchs, Switzerland)
Biomalt	Villa Natura (Kirn, Germany)
Bovine serum albumin	Sigma-Aldrich (Steinheim, Germany)
CaCl <sub>2</sub>	Merck (Darmstadt, Germany)
CDP-choline	Sigma-Aldrich (Steinheim, Germany)

---

CFDA	Fluka (Buchs, Switzerland)
Chloroform	Merck (Darmstadt, Germany)
Chloroform-d <sub>1</sub> 99.8%	Deutero GmbH (Kastellaun, Germany)
Coomassie-blue R260	Serva (Heidelberg, Germany)
CuSO <sub>4</sub>	Merck (Darmstadt, Germany)
Cyclosporin A	Fluka (Buchs, Switzerland)
Cytosine arabinose	Sigma-Aldrich (Steinheim, Germany)
Czapek Solution Agar	Becton Dickinson (MD, USA)
Dimethylsulphoxide	AppliChem (Darmstadt, Germany)
DNase	Roche (Mannheim, Germany)
Ethanol	Riedel de Haen (Seelze, Germany)
Ethidium bromide	AppliChem (Darmstadt, Germany)
1-Fluoro-2,4-dinitrophenyl-5-L-alaninamide	Sigma-Aldrich (Steinheim, Germany)
Foetal bovine serum	PAA Laboratories (Pasching, Austria)
Glucose	Merck (Darmstadt, Germany)
Glutamax®	Sigma-Aldrich (Steinheim, Germany)
H <sub>3</sub> BO <sub>3</sub>	Serva (Heidelberg, Germany)
HCl, 37%	Merck (Darmstadt, Germany)
H <sub>2</sub> SO <sub>4</sub>	Merck (Darmstadt, Germany)
D-Hydroxyisocaproic acid	Bachem (Weil am Rhein, Germany)
L-Hydroxyisocaproic acid	Bachem (Weil am Rhein, Germany)
D-Hydroxyisovaleric acid	Fluka (Buchs, Switzerland)
L-Hydroxyisovaleric acid	Fluka (Buchs, Switzerland)
Horse serum	Cytogen (Berlin, Germany)
KBr	Merck (Darmstadt, Germany)
KCl	Merck (Darmstadt, Germany)
KH <sub>2</sub> PO <sub>4</sub>	Merck (Darmstadt, Germany)
Lichenysin A	kindly provided by Dr. Golyshin (Department of Environmental Microbiology, Braunschweig, Germany)
Malt-extract	Roth (Karlsruhe, Germany)
Methanol	Fluka (Buchs, Switzerland)
Methanol-d <sub>4</sub> 99.8 % D	Deutero GmbH (Kastellaun, Germany)
MgCl <sub>2</sub> × 6 H <sub>2</sub> O	Merck (Darmstadt, Germany)

MK571	Alexis biochemicals (Lausen, Switzerland)
MnCl <sub>2</sub> x 4 H <sub>2</sub> O	Merck (Darmstadt, Germany)
NaCl	Merck (Darmstadt, Germany)
NaHCO <sub>3</sub>	Merck (Darmstadt, Germany)
NaOH	Merck (Darmstadt, Germany)
Na <sub>2</sub> SO <sub>4</sub>	Merck(Darmstadt, Germany)
Penicillin/Streptomycin	Biomol GmbH (Hamburg, Germany)
Peptone from Soya	Fluka (Buchs, Switzerland)
N-Methyl-D-phenylalanine	Sigma-Aldrich (Steinheim, Germany)
N-Methyl-L-phenylalanine	Sigma-Aldrich (Steinheim, Germany)
Rhodamine-123	Sigma-Aldrich (Steinheim, Germany)
Sephadex® LH-20	Pharmacia Biotech (Uppsala, Sweden)
Sodium cacodylate	Sigma-Aldrich (Steinheim, Germany)
SrCl <sub>2</sub> × 6 H <sub>2</sub> O	Merck (Darmstadt, Germany)
Streptomycin sulphate	Fluka (Buchs, Switzerland)
Surfactin	kindly provided by Dr. Golyshin (Department of Environmental Microbiology, Braunschweig, Germany)
Taq DNA polymerase	Invitrogen (Karlsruhe, Germany)
Tetrahydrofuran-d <sub>8</sub>	Deutero GmbH (Kastellaun, Germany)
Tris-Acetate-EDTA buffer	AppliChem (Darmstadt, Germany)
Tritone-X 100	Sigma-Aldrich (Steinheim, Germany)
Tween 20	Roth (Karlsruhe, Germany)
UDP-Galactose	Sigma-Aldrich (Steinheim, Germany)
Yeast extract	Roth (Karlsruhe, Germany)
Vanillin	Merck (Darmstadt, Germany)

All other chemicals were supplied by Merck (Darmstadt, Germany), Fluka (Buchs, Switzerland), Roth (Karlsruhe, Germany) and Sigma-Aldrich (Steinheim, Germany).

### 3.10.4 Kits

CellTiter-Blue Cell Viability Assay	Promega (Mannheim, Germany)
-------------------------------------	-----------------------------

RNeasy mini kit	Qiagen GmbH (Hilden, Germany)
RNaseFreeDNaseI-set	Qiagen GmbH (Hilden, Germany)

### 3.10.5 Lipids

Glucosylceramide	Matreya LLC (PA/USA)
Lactosylceramide	Matreya LLC (PA/USA)

### 3.10.6 Primers

All primers were purchased from Invitrogen (Karlsruhe, Germany) and diluted to final concentration of 2.5 nmol.

LacCer synthase	5`-CCTCCCTCCACATTTCTCC-3` (forward)
	5`-ATCTTCCTCTGCCCTACCA-3` (reverse)
18 S rRNA	5`-CATGATCAGGCTGTATACCAATAAAA-3` (forward)
	5`-CTTGTATTATTGCCTTCGGGATA-3` (reverse)
18 S rRNA	5`-AAACGGCTACCACATCCAAG-3` (forward)
	5`-CCTCCAATGGATCCTCGTTA-3` (reverse)

### 3.10.7 Radioactivity

L-[3- <sup>14</sup> C] serine	Amersham Biosciences (Braunschweig, Germany)
D-[U- <sup>14</sup> C] galactose	Amersham Biosciences (Braunschweig, Germany)
UDP-D-[U- <sup>14</sup> C] galactose	Amersham Biosciences (Braunschweig, Germany)
<sup>14</sup> C <sub>8</sub> -Lactosyl-S-Ceramide	synthesized by Dr. G. Schwarzmann
<sup>14</sup> C <sub>8</sub> -Glucosyl-S-Ceramide	synthesized by Dr. G. Schwarzmann
<sup>14</sup> C <sub>8</sub> -GM3	synthesized by Dr. G. Schwarzmann

**3.10.8 Solutions and buffers**

Ca <sup>2+</sup> /Mg <sup>2+</sup> -free isotonic solution (CMF)	Isotonic solution I	50 % (v/v)
	Isotonic solution II	49.5 % (v/v)
	Phenol-red	0.3 % (v/v)
	NaHCO <sub>3</sub>	0.2 % (v/v)
Coomassie-blue R260-stock solution	Coomassie-blue R260	0.05 % (w/v)
	Ethanol	25 %
	85 % Phosphoric acid	50 % (v/v)
Isotonic solution I	Glucose	0.4 % (w/v)
	KCl	0.06 % (w/v)
	NaCl	1.6 % (w/v)
Isotonic solution II	KH <sub>2</sub> PO <sub>4</sub>	0.005%(w/v)
	NaH <sub>2</sub> PO <sub>4</sub>	0.01 % (w/v)
	KCl	3 mM
Phosphate buffered saline (PBS)	KH <sub>2</sub> PO <sub>4</sub>	1.5 mM
	NaCl	140 mM
	Na <sub>2</sub> HPO <sub>4</sub>	16 mM
	H <sub>3</sub> BO <sub>3</sub>	100 mM
Poly-L-lysine-solution, pH 8.4	Poly-L-lysine	1 mg/100 ml

## 4 Results

### 4.1 Screening of fungal extracts for biologically active metabolites

In this study marine-derived fungi were taken as a source of biologically active natural products.

For screening purposes the strains were cultivated on 500 mL of solid media in Petri dishes. Each strain was cultivated on three different media: biomalt agar medium (BMS), malt-yeast agar medium (MYA) and czapek agar medium (CZ). After one month of cultivation, fungal biomass, together with the medium, was homogenized and extracted three times with 100 mL ethyl acetate. Each extract was characterized by  $^1\text{H}$  NMR and LC-MS, and tested in different biological assays.

The major criterion for selection of fungi for further tests and analyses was the significant cytotoxic activity. The selected cytotoxic strains were further screened for their influence on sphingolipid metabolism. On the basis of their biological activity and/or chemical characteristics ( $^1\text{H}$  NMR and MS data), some of the fungal strains were chosen for mass cultivation and detailed chemical and biological examinations.

#### 4.1.1 Screening of fungal extracts for cytotoxic activity

Extracts of 82 fungal strains, cultivated on three different media, were screened for their cytotoxic activity against six human cancer cell lines in a concentration of 10  $\mu\text{g}/\text{mL}$ . The results of the most active extracts are given in Tables 4-1-1. Out of 82 tested strains, 29 strains (35.4 %) exhibited an activity with test/control value smaller than 30 % in at least one cell line. If a strain showed activity in more than one medium, only the extract from the most active medium was counted. Most of the active extracts revealed high activity against uterus and lung carcinoma, while only few showed activity against a gastric cancer cell line. Extract 652 of the fungal strain *Emericella nidulans* (not listed in the tables below) was tested in a panel of 36 cell lines and effected tumor activity in 31 out of 36 cell lines at 5  $\mu\text{g}/\text{mL}$ , which is indicative of possible high antitumor effects.

According to the antitumor activity,  $^1\text{H}$  NMR and LC-MS data, extracts marked in blue in Table 4-1-1 were chosen for further studies.

Tables 4-1-1. In vitro antitumor activity of selected fungal strains.<sup>1</sup>

		concentration: 10 µg/ml																				
		1. run					2. run					both runs										
		cell line: Tumor Typ / Name / FU control										1. + 2. Run										
		mean	s.d.	GXF	LXFL	MAXF	MEXF	RXF	UXF	mean	s.d.	GXF	LXFL	MAXF	MEXF	RXF	UXF	mean	tot.	%		
fungal extract <sup>2</sup>	%	T/C [%]	act.*	251L	529L	401NL	462NL	486L	1138L	%	T/C [%]	act.*	251L	529L	401NL	462NL	486L	1138L	T/C	act.**	act.*	
1	738BMS	100	5	4	5	3	13	8	2	2	100	5	3	5	2	8	8	2	3	5	12	100
2	96BMS	100	9	6	18	5	12	15	3	2	100	9	6	15	5	13	14	4	2	9	12	100
3	74MYA	100	9	7	19	5	13	13	1	3	100	9	6	15	6	15	12	2	3	9	12	100
4	74BMS	100	10	7	17	6	15	17	3	2	100	8	6	16	6	11	11	2	2	9	12	100
5	273MYA	100	10	7	16	7	17	14	2	2	100	9	6	15	8	16	11	2	3	9	12	100
6	96CZ	100	10	7	19	5	17	13	3	2	100	9	6	16	5	15	14	3	3	10	12	100
7	71MYA	100	10	6	16	9	15	15	3	3	100	9	5	16	7	14	12	4	3	10	12	100
8	96MYA	100	10	7	18	6	18	14	3	3	100	10	8	21	5	15	15	3	3	10	12	100
9	620MYA	83	17	11	15	9	19	22	36	2	83	23	28	17	10	16	17	78	2	20	10	83
10	193BMS	100	18	9	24	11	22	19	29	4	67	23	12	28	13	23	32	39	5	21	10	83
11	727BMS	83	22	13	40	11	26	21	28	4	67	21	12	37	12	30	15	28	5	22	9	75
12	74CZ	83	18	10	24	10	33	19	12	8	67	27	18	32	11	38	25	58	11	22	9	75
13	738CZ	67	25	18	43	27	14	13	49	5	83	32	20	37	30	16	18	72	27	29	9	75
14	741BMS	67	32	17	53	23	28	29	50	8	83	27	12	30	24	26	27	45	9	29	9	75
15	18MYA	67	31	28	37	25	22	17	83	4	50	35	30	39	28	20	30	92	3	33	7	58
16	585-2	50	36	20	61	26	21	32	59	15	50	32	15	49	22	18	30	53	23	34	6	50
17	190CZ	50	38	27	25	19	35	50	86	12	50	41	30	28	25	38	38	101	18	40	6	50
18	194MYA	83	18	9	32	13	16	18	20	6	0	49	11	44	44	52	50	69	37	33	5	42
19	16BMS	50	28	24	54	11	58	31	3	9	33	58	33	81	78	90	76	7	65	43	5	42
20	211MYA	33	39	27	37	17	31	56	82	8	33	40	25	37	24	34	56	80	11	40	4	33
21	85MYA	33	46	31	72	14	41	54	86	7	33	48	27	66	27	48	50	88	12	47	4	33
22	211BMS	33	40	15	43	23	48	48	58	17	17	46	18	81	35	48	49	66	16	43	3	25
23	12BMS	17	61	25	77	60	16	52	81	78	33	43	20	67	43	21	52	18	58	52	3	25
24	193MYA	17	43	21	41	33	39	62	69	12	17	45	22	44	34	41	58	78	13	44	2	17
25	741MYA	17	43	19	65	39	50	35	57	13	17	47	21	80	41	53	35	53	16	45	2	17
26	187CZ	17	53	20	53	40	55	62	84	25	17	58	23	61	46	60	70	91	22	56	2	17
27	75BMS	33	51	28	75	83	37	23	70	17	0	77	22	79	116	72	57	82	54	64	2	17
28	54MYA	17	70	34	102	100	46	71	86	14	17	69	30	93	88	56	73	90	16	70	2	17
29	192BMS	17	48	20	42	41	35	53	86	29	0	53	20	59	44	35	61	87	33	50	1	8
30	244BMS	17	49	15	42	44	47	58	73	28	0	55	19	41	68	51	56	85	30	52	1	8
31	187MYA	17	46	19	50	44	32	61	73	19	0	59	19	55	74	37	63	85	39	53	1	8
32	192CZ	17	53	21	50	53	38	58	90	28	0	54	24	51	41	46	52	101	32	54	1	8
33	132BMS	17	53	17	41	63	74	51	65	27	0	59	17	85	57	66	49	62	35	56	1	8
34	193CZ	17	59	23	65	56	37	75	91	28	0	65	21	64	80	47	77	90	35	62	1	8
35	192MYA	0	47	18	44	41	34	50	80	30	0	53	20	57	45	38	51	91	37	50	0	0
36	136BMS	0	74	16	91	52	59	80	89	71	0	79	9	83	62	78	76	87	85	76	0	0
37	187BMS	0	72	10	80	87	63	68	69	64	0	85	2	87	87	87	83	81	83	78	0	0
38	57BMS	0	81	18	86	109	80	84	73	54	0	77	19	67	107	85	69	80	52	79	0	0
39	585-3	0	73	12	81	58	56	76	85	79	0	89	15	88	112	76	71	89	97	81	0	0
40	35BMS	0	81	10	77	98	69	83	80	80	0	84	8	68	90	90	87	85	84	83	0	0

		concentration: 10 µg/ml																			
		1. run					2. run					both runs									
		cell line: Tumor Typ / Name / FU control										1. + 2. Run									
		mean	s.d.	GXF	LXFL	MAXF	MEXF	RXF	UXF	mean	s.d.	GXF	LXFL	MAXF	MEXF	RXF	UXF	mean	tot.	%	
fungal extract <sup>2</sup>	%	T/C [%]	act.*	251L	529L	401NL	462NL	486L	1138L	%	T/C [%]	act.*	251L	529L	401NL	462NL	486L	1138L	T/C	act.**	act.*
1	706MYA	67	34	21	15	39	28	8	50	36	19	20	43	43	10	26	7	58			
2	712CZ	50	31	17	17	62	73	9	67	30	18	20	76	88	10	38	7	58			
3	714MYA	33	49	39	19	57	104	12	50	36	22	26	41	99	24	44	5	42			
4	588MYA	33	47	23	37	45	33	12	33	38	17	40	49	46	17	34	4	33			
5	706CZ	50	41	25	23	34	36	10	17	32	32	41	58	59	24	35	4	33			
6	706SPG	50	26	39	30	63	62	27	0	34	59	35	61	89	37	47	3	25			
7	726BMS	17	83	33	31	51	37	25	17	80	32	32	56	54	30	45	2	17			
8	719CZ	33	32	41	22	60	87	12	0	41	67	30	81	89	35	50	2	17			
9	714BMS	17	39	41	30	73	94	31	17	33	49	29	65	89	34	51	2	17			
10	714CZ	33	67	56	28	99	3	46	0	67	82	38	81	98	72	61	2	17			
11	717CZ	17	49	63	20	80	82	30	0	68	82	43	97	81	42	61	1	8			
12	598BMS	17	71	23	113	93	100	89	0	97	98	104	75	93	99	88	1	8			
13	630MYA	17	121	25	94	101	93	87	0	94	95	103	67	95	96	89	1	8			
14	705CZ	17	104	20	113	94	88	104	0	84	96	118	107	95	95	93	1	8			
15	588BMS	0	81	63	68	81	77	53	0	59	58	67	79	71	59	68	0	0			
16	588CZ	0	75	60	82	89	93	84	0	72	78	78	48	95	69	77	0	0			
17	715CZ	0	69	68	62	99	92	54	0	91	90	90	66	93	86	80	0	0			
18	628CZ	0	98	96	90	88	93	60	0	83	91	95	99	86	50	86	0	0			
19	315/3	0	117	95	68	96	89	73	0	94	93	80	90	79	71	87	0	0			
20	729MYA	0	95	77	93	66	90	102	0	94	93	94	82	72	90	87	0	0			
21	588SPG	0	121	49	122	103	80	81	0	87	86	105	75	77	70	88	0	0			
22	588MB	0	81	85	77	100	92	92	0	77	111	92	99	88	84	90	0	0			
23	723CZ	0	106	88	107	101	92	69	0	103	89	102	33	95	105	91	0	0			
24	716BMS	0	101	37	90	105	106	85	0	87	67	104	115	107	84	91	0	0			
25	711MYA	0	92	85	101	103	88	51	0	96	102	99	110	95	71	91	0	0			
26	710BMS	0	98	103	84	95	94	80	0	97	78	102	100	80	93	92	0	0			
27	712BMS	0	103	91	112	80	83	97	0	89	84	92	84	98	95	92	0	0			
28	707BMS	0	109	94	92	103	97	52	0	96	105	112	113	95	41	92	0	0			
29	722BMS	0	63	48	109	91	101	95	0	102	105	103	91	99	107	93	0	0			
30	729BMS	0	89	87	88	99	111	60	0	87	106	97	104	105	82	93	0	0			
31	711CZ	0	75	103	123	104	79	70	0	103	100	109	66	86	97	93	0	0			
32	711BMS	0	96	81	82	96	93	90	0	103	90	125	88	82	91	93	0	0			
33	719BMS	0	93	95	95	109	87	65	0	102	99	95	87	9							

#### 4.1.2 Antimicrobial and antialgal activities of fungal extracts

Cytotoxic fungal extracts (marked in blue in Tables 4-1-1.) were tested for their antimicrobial and antialgal activities in a concentration of 1 mg/mL. The active extract (Table 4-1-2) originated from the strain *Spicellum roseum* (strain nr. 74) with inhibition zones of 5 and 11 mm against *Eurotium rubrum* and *Mycotypha microspora*, respectively. A strain of *Fusarium oxysporum* (strain nr. 588) exhibited antibacterial and antifungal activities, inhibiting the growth of *Bacillus megaterium* (5 mm) and *Mycotypha microspora* (3 mm). Antifungal activity was exhibited also by the strain *Arthrinium sacchari* (strain nr. 727) which showed a zone of 4 mm growth inhibition of *Mycotypha microspora*. All other strains showed slightly or no antimicrobial activity while algal growth was not inhibited by any of the tested strains.

**Table 4-1-2.** Results of agar diffusion assay of cytotoxic fungal extracts.

Extract <sup>1</sup>	Fungal strain	Inhibition of test organism (mm)					
		<i>Escherichia coli</i>	<i>Bacillus megaterium</i>	<i>Microbotryum violaceum</i>	<i>Eurotium rubrum</i>	<i>Mycotypha microspora</i>	<i>Chlorella fusca</i>
12 BMS	<i>Monochaetia</i> sp.	0	0	0	3	0	0
16 BMS	<i>Stagonospora</i> sp.	0	0	0	0	0	0
18 MYA	<i>Fusarium dimerum</i>	0	0	0	0	0	0
74 BMS	<i>Spicellum roseum</i>	0	0	0	5	11	0
75 BMS	<i>Phoma</i> sp.	0	0	0	0	0	0
85 MYA	<i>Sporothrix</i> sp.	0	0	0	0	0	0
96 BMS	<i>Microsphaeropsis</i> sp.	0	0	0	0	0	0
187 CZ	<i>Monodictys putredinis</i>	0	0	0	0	0	0
190 CZ	<i>Ulocladium</i> sp.	0	0	0	0	0	0
193 BMS	<i>Paecilomyces lilacinus</i>	0	0	0	0	0	0
194 MYA	<i>Alternaria japonica</i>	0	0	0	0	0	0
211 MYA	<i>Paecilomyces</i> sp.	0	0	0	0	0	0
273 MYA	<i>Acremonium</i> sp.	0	0	0	0	0	0
588 MYA	<i>Fusarium oxysporum</i>	0	5	0	0	3	0
598 BMS	<i>Fusarium</i> sp.	0	0	0	0	0	0
620 MYA	<i>Chaetomium</i> sp.	0	0	0	0	0	0
630 MYA	<i>Rhinochladella</i> sp.	0	0	0	0	0	0
652 BMS	<i>Emericella nidulans</i>	0	2	0	0	0	0
705 CZ	GrKo2 EtOH	0	0	0	0	0	0
712 CZ	<i>Microsphaeropsis</i> sp.	0	0	0	0	0	0
714 MYA	<i>Trichoderma harzianum</i>	0	0	0	0	0	0
726 BMS	Cro2 CA EtOH <sub>a</sub>	0	0	0	0	0	0
727 BMS	<i>Arthrinium sacchari</i>	0	0	0	0	4	0
738 BMS	<i>Acremonium sclerotigenum</i>	0	2	0	0	0	0
741 BMS	<i>Phoma macrostoma</i>	0	0	0	0	0	0
A. T.	<i>Aspergillus terreus</i>	0	0	0	0	0	0

<sup>1</sup> This number refers to the fungal collection (Institute for Pharmaceutical Biology, Bonn); BMS, biomalt-agar medium; MYA, malt-yeast medium, CZ, czapek agar medium.

#### 4.1.3 Influence of fungal extracts on sphingolipid metabolism

Of 25 tested cytotoxic fungal extracts, seven altered sphingolipid metabolism. The influence of fungal extracts on sphingolipid metabolism (Figure 4-1-1) of cerebellar neurons and neuroblastoma cells was studied by following the incorporation of L-[3-<sup>14</sup>C] serine into cellular sphingolipids (Figure 4-1-1).



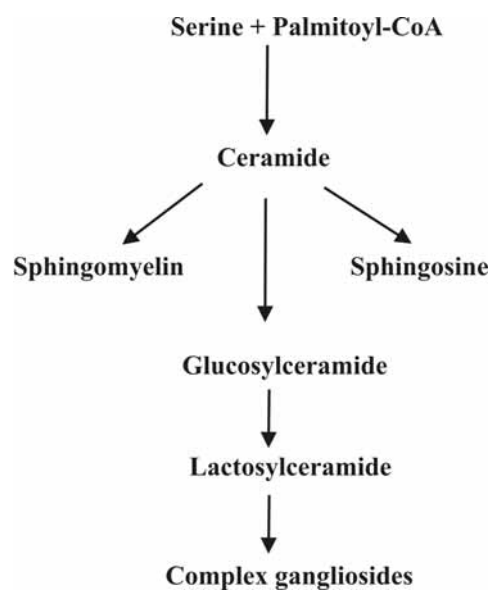


**Figure 4-1-1.** Scheme of sphingolipid pathway.

As shown in Figure 4-1-2, cells incubated with extracts 96, 738, 588 and 74 exhibited an accumulation of glucosylceramide (GlcCer) along with the reduced levels of lactosylceramide (LacCer) and complex gangliosides (A, D), which indicated an inhibitory activity of these extracts on formation of LacCer and gangliosides (Figure 4-1-1). Increased levels of ceramide were noticed in extracts 18, 96 and 738 (B). Fungal extract 193 showed reduced levels of GlcCer, LacCer and complex gangliosides (A), while extract 16 displayed alterations in the levels of LacCer and sphingosine/sphinganine (So/Sa) (C) when compared to control cells.

The activity of fungal extracts on sphingolipid pathway was the main lead for the selection of strains for further investigations. Hence, all strains which showed any modifications in sphingolipids were chosen for detailed examinations. Also, the extracts with no influence on sphingolipids but with prominent cytotoxic activity and/or interesting  $^1\text{H}$  NMR and MS data were selected for a large-scale cultivation and further studies.

Thus, the following strains were investigated in this study:

Extract No. <sup>1</sup>	Isolation No. <sup>2</sup>	Taxonomy of fungal strain
16	193 A 26	<i>Stagonospora</i> sp.
18	193 A 28	<i>Fusarium dimerum</i>
74	193 H 15	<i>Spicellum roseum</i>
96	193 H 48	<i>Microsphaeropsis</i> sp.
193	195 21 W	<i>Paecilomyces lilacinus</i>
588	Fr S1 5N	<i>Fusarium oxysporum</i>
652	Sar 14 15E	<i>Emericella nidulans</i> var. <i>acristata</i>
727	Cro2 CA EtOHb	<i>Arthrinium sacchari</i>
738	Lau 4K CM	<i>Acremonium sclerotigenum</i>
A. T.	GrK4 5N	<i>Aspergillus terreus</i>

<sup>1,2</sup> Numbers refers to the fungal collection (Institute for Pharmaceutical Biology, Bonn).

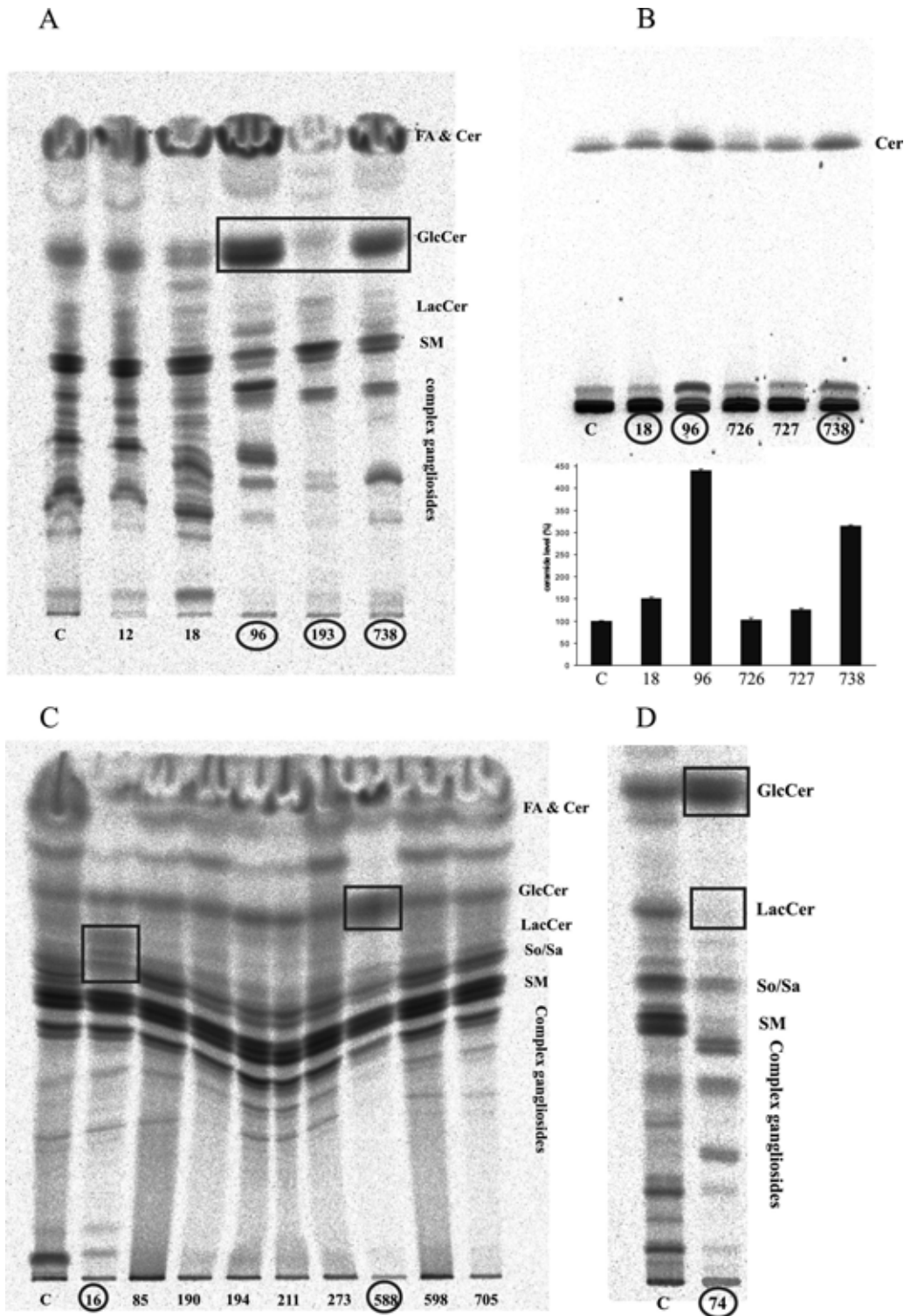


**Figure 4-1-2.** Effects of fungal extracts on SL metabolism.

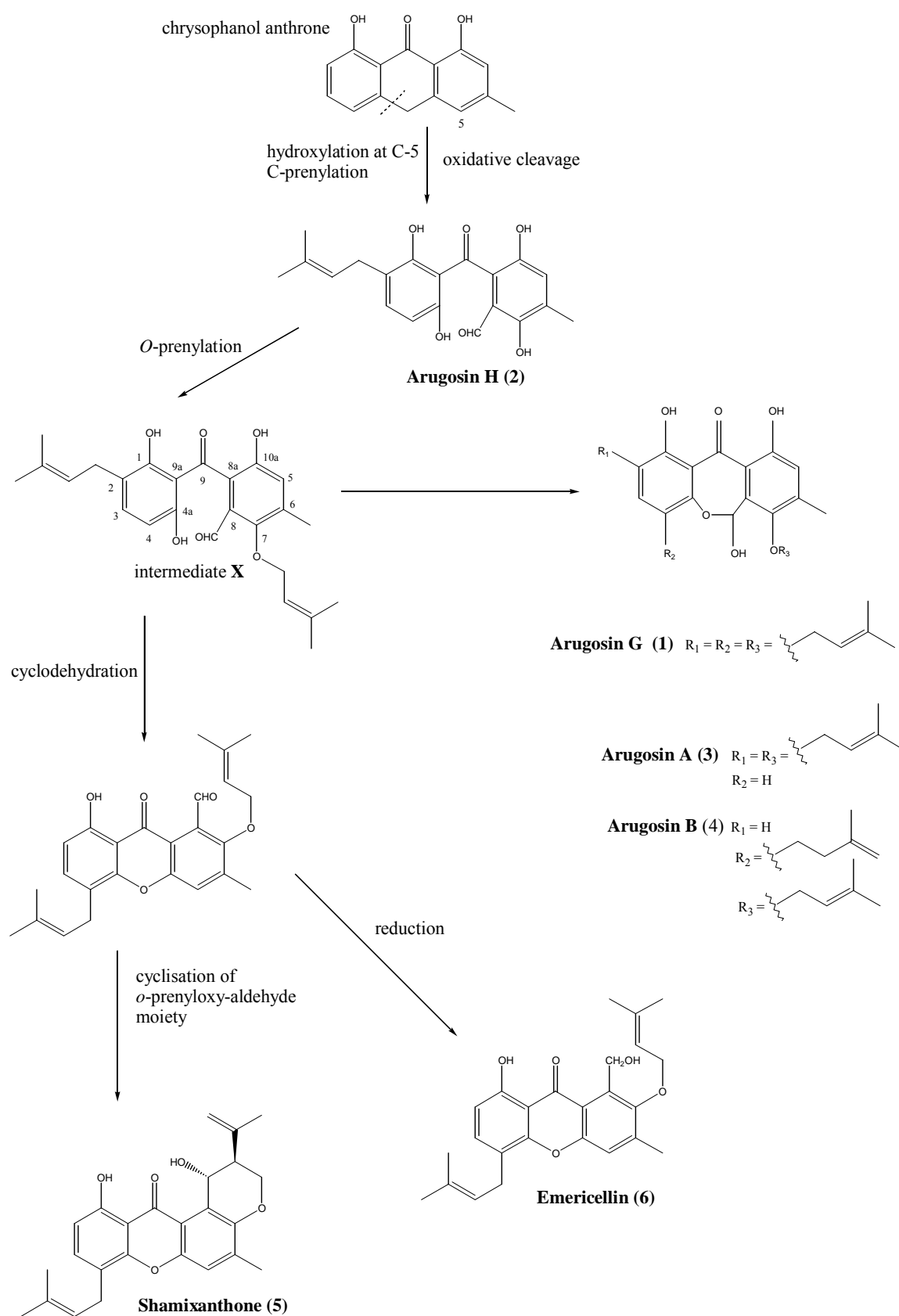
Primary cultured neurons (A, B and D) or neuroblastoma cells (C) were incubated in the absence (C, control) or presence of different fungal extracts (10  $\mu\text{g}/\text{mL}$ ). After 4 h 1  $\mu\text{Ci}$  of [ $^{14}\text{C}$ ]serine was added to the medium. Twenty hours later cells were harvested and lipids were extracted, isolated, separated by TLC, and detected as described in Materials and Methods. TLC plates were developed in  $\text{CHCl}_3$ -MeOH-0.22 % aqueous  $\text{CaCl}_2$  (60:35:8; v/v/v) (plates A, C and D), or in  $\text{CHCl}_3$ -MeOH- $\text{CH}_3\text{COOH}$  (190:9:1; v/v/v) (plate B). FA, fatty acids; Cer, ceramide; GlcCer, glucosylceramide; LacCer, lactosylceramide; So, sphingosine; Sa, Sphinganine; SM, sphingomyelin.

## 4.2 Arugosins G and H: Prenylated polyketides from the marine-derived fungus *Emericella nidulans* var. *acristata* (Strain number 652)

### 4.2.1 Introduction

*Emericella nidulans* var. *acristata* was isolated from a green alga collected around Sardinia in the Mediterranean Sea. HPLC-MS and HPLC-DAD investigations of various extracts identified this fungus as a producer of several polyketide type metabolites. The crude extract also showed cytotoxicity toward six cultured tumour cell lines with a mean IC<sub>70</sub> of 8.30 µg/mL. Two new compounds from the arugosin family, arugosins G (**1**) and H (**2**) were isolated together with the known arugosins A and B (**3** and **4**). Apart from arugosins, which possess a benzophenone skeleton, and the biosynthetically related (Scheme 4-2-1) xanthenes **5**, **6**, **9** and **10**, the indole alkaloid **7**, and the furanone **8** were obtained. A prominent feature of most of these metabolites is their substitution with a prenyl moiety, with the isoprene unit being attached either to a carbon atom of the polyketide nucleus or connected *via* an ether bridge. The fungus *Emericella nidulans* var. *acristata* was cultivated on a solid biomalt medium with added artificial sea salt. Successive fractionation of the EtOAc extract by normal phase vacuum liquid chromatography (VLC), followed by separation over Sephadex, and normal and reversed phase HPLC yielded two new (**1** and **2**), and eight known (**3** - **10**) compounds. Arugosins A and B (**3** and **4**) were isolated as a mixture, as in all previous investigations (Ballantine *et al.*, 1970; Kawahara *et al.*, 1988). The structural elucidation of compounds **1** and **2** is based on NMR and MS data and on comparison of data with those of the known compounds **3** and **4**.

**Scheme 4-2-1.** Proposed biosynthetic relationship of *Emericella nidulans* var. *acristata* secondary metabolites.



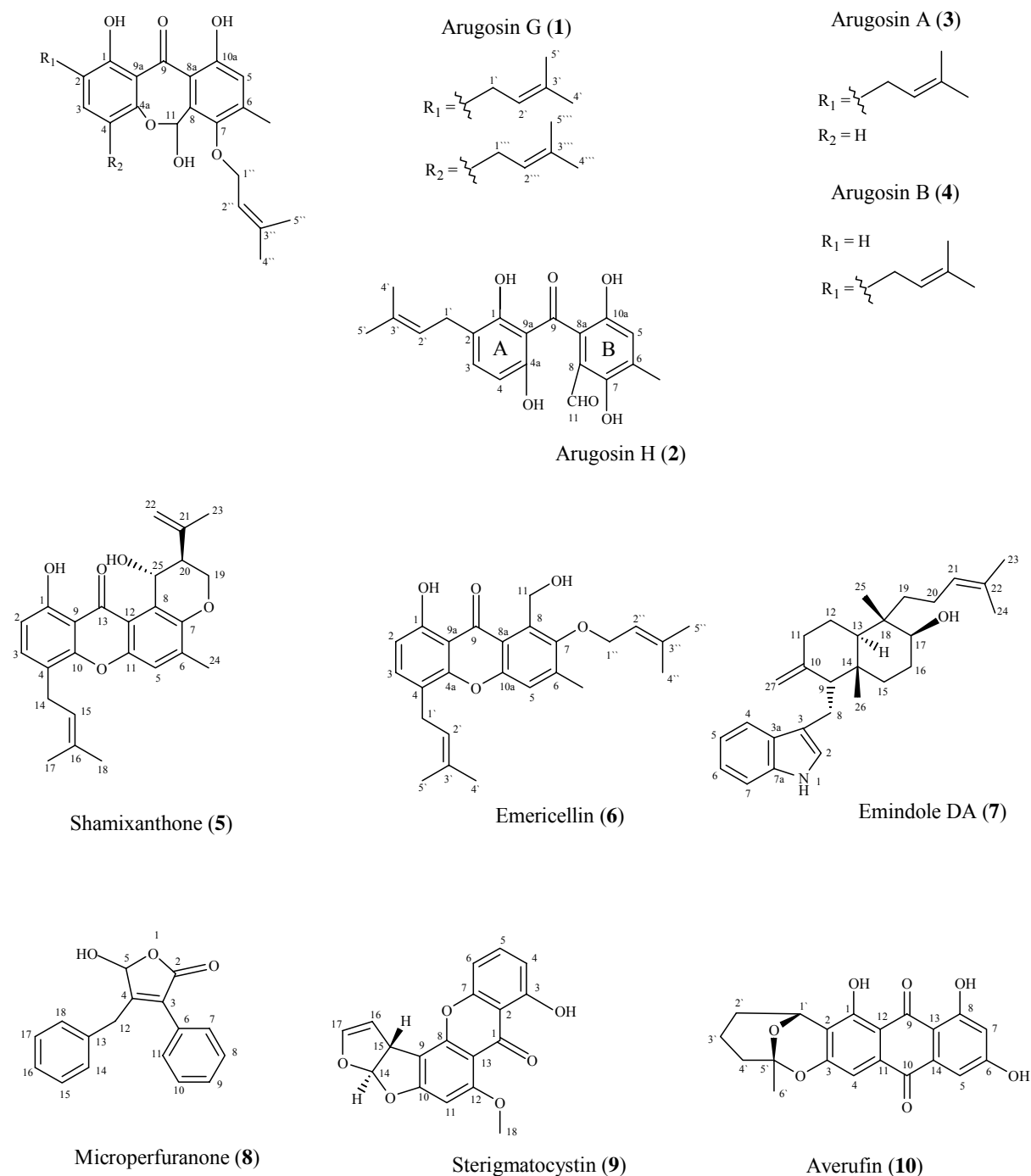
#### 4.2.2 Cultivation, extraction and isolation

The fungus (*Emericella nidulans* var. *acristata*, strain number 620, Sar 14 15E) was cultivated at room temperature for one month in 32 x 8 L Fernbach flasks. The solid biomalt medium contained 20 g/L of Biomalt, 17 g/L agar and artificial seawater. The fungal biomass, including the medium, was homogenized using an Ultra-Turrax and the mixture was extracted with EtOAc (3 x 8 L). After evaporation of the organic phase 47 g of dark purple oil was obtained. The extract was fractionated by VLC (Si gel 60, 0.063-0.200 mm) with a CH<sub>2</sub>Cl<sub>2</sub> - EtOAc - MeOH gradient, to yield 11 fractions. Of these, fractions 2 - 6, on the basis of TLC results, were combined and separated on a Sephadex LH-20 column, with MeOH as eluent to give 5 fractions (1-5). Sephadex fraction 2 was further separated on a normal phase HPLC column (Knauer Si Eurospher-100, 250 x 8 mm, 5 μm), eluting with petroleum ether/acetone 9:1 and yielded 10 fractions (S1-S10). Of these, fractions S3 was identified as a mixture of compounds **3** and **4**, whereas fraction S7 contained compound **7**, fraction S10 compound **2**, and fraction S10 compound **10**. Fraction S1 was separated into compounds **5** and **6** with hexane/EtOAc 20:1 using normal phase HPLC (Knauer Si Eurospher-100, 250 x 8 mm, 5 μm). Fraction S2 was eluted on reversed phase HPLC (Phenomenex Max C<sub>12</sub>, 250 x 4.6 mm, 5 μm) with MeOH/H<sub>2</sub>O 9:1 and yielded compound **1**. Sephadex Fraction 5 gave compound **8** after fractionation on reversed phase (Knauer, Eurospher-100, C-8, 250 x 8 mm, 5 μm) HPLC with MeOH/H<sub>2</sub>O 8:2. Sephadex fraction 3 was further fractionated using reversed phase HPLC (Knauer C<sub>8</sub> Eurospher-100, 250 x 8 mm, 5 μm) with gradient elution from MeOH/H<sub>2</sub>O 7:3 to MeOH in 90 min, 1.5 mL/min, to afford compound **9**.

#### 4.2.3 Results and discussion

The molecular formula of compound **1** was established by high-resolution mass measurement (HREIMS) as C<sub>30</sub>H<sub>36</sub>O<sub>6</sub> implying 13 degrees of unsaturation. The <sup>13</sup>C NMR spectrum showed 30 signals for 7 x CH<sub>3</sub>, 3 x CH<sub>2</sub>, 6 x CH and 14 x C. These data also revealed the presence of 10 double bonds (1 x CO, 9 x C=C) (Table 4-2-1). Thus, compound **1** was tricyclic. Considering the molecular formula and the IR data ( $\nu_{\max}$  3438 cm<sup>-1</sup>), it was obvious that three protons had to be present as hydroxyl groups. UV maxima at 305 and 366 nm pointed towards an extended aromatic moiety. This was supported by two singlet resonances in the <sup>1</sup>H NMR spectrum at  $\delta$ 7.26 and  $\delta$ 6.89 for two aromatic protons. A <sup>1</sup>H NMR resonance at  $\delta$ 7.03 could be attributed to H-11, which is attached to a doubly oxygenated carbon resonating at 92.2

ppm, as evident from the  $^{13}\text{C}$  NMR and HSQC spectrum. These structural features suggested compound **1** to be an arugosin derivative, i.e. closely related to arugosin A (**3**) and B (**4**).



The major difference between the NMR data for **3** and **4**, and **1** was the presence of signals for nine additional protons ( $\delta_{\text{H}}$  1.70, 3.29, 5.30; H-1'''' to H-5''') and five further carbons ( $\delta_{\text{C}}$  17.8, 25.8, 28.4, 123.4, 132.5; C-1'''' to C-5''') (Table 4-2-2) in the case of **1**.

**Table 4-2-1.** 1D and 2D NMR spectral data for compound **1**

Atom Number	<sup>13</sup> C <sup>a,b</sup> ( $\delta$ in ppm)	<sup>1</sup> H <sup>a,b</sup> ( $\delta$ ppm, mult., <i>J</i> in Hz)	Članak I. OSY <sup>a,b</sup>	Članak II. MBC <sup>a,c</sup>	F
1	160.5 (C)				
2	122.9 (C)				
3	138.8 (CH)	7.26 (s)	1 <sup>'d</sup> , 1 <sup>''''d</sup>	1, 4a, 9a <sup>d</sup> , 1', 1 <sup>''''</sup>	
4	122.9 (C)				
4a	150.0 (C)				
5	120.9 (CH)	6.89 (s)	6-Me	7, 8 <sup>d</sup> , 8a, 9 <sup>d</sup> , 10a	
6	141.8 (C)				
6-Me	16.9 (CH <sub>3</sub> )	2.35 (s)		5, 6, 7, 8 <sup>d</sup>	
7	146.3 (C)				
8	133.2 (C)				
8a	119.6 (C)				
9	199.4 (C)				
9a	114.9 (C)				
10a	157.6 (C)				
11	92.2 (CH)	7.03 (s)		7, 8a, 10a <sup>d</sup>	
1'	29.4 (CH <sub>2</sub> )	3.24 (brd, 7.32)	2', 3,	1, 3, 2', 3'	
2'	123.8 (CH)	5.23 (t, 7.32)	1'	1'	
3'	132.8 (C)				
4'	25.8 (CH <sub>3</sub> )	1.67 (s)		2', 3', 5'	
5'	17.8 (CH <sub>3</sub> )	1.70 (brs)		2', 3', 4'	
1''	72.2 (CH <sub>2</sub> )	4.42 (d, 7.32)	2''	2'', 3'', 7	
2''	120.8 (CH)	5.59 (t, 7.32)	1''	1''	
3''	138.9 (C)				
4''	25.8 (CH <sub>3</sub> )	1.78 (s)		2'', 3'', 5''	
5''	18.0 (CH <sub>3</sub> )	1.69 (s)		2'', 3'', 4''	
1 <sup>''''</sup>	28.4 (CH <sub>2</sub> )	3.29 (d, 7.32)	2 <sup>''''</sup> , 3	3, 4a <sup>d</sup> , 2 <sup>''''</sup> , 3 <sup>''''</sup>	
2 <sup>''''</sup>	123.4 (CH)	5.30 (t, 7.32)	1 <sup>''''</sup>	1 <sup>''''</sup>	
3 <sup>''''</sup>	132.5 (C)				
4 <sup>''''</sup>	25.8 (CH <sub>3</sub> )	1.70 (brs)		2 <sup>''''</sup> , 3 <sup>''''</sup> , 5 <sup>''''</sup>	
5 <sup>''''</sup>	17.8 (CH <sub>3</sub> )	1.70 (brs)		2 <sup>''''</sup> , 3 <sup>''''</sup> , 4 <sup>''''</sup>	
1-OH		13.21 (s)	3 <sup>d</sup>	1, 2, 3 <sup>d</sup> , 9 <sup>d</sup> , 9a	
10a-OH		10.59 (s)		5, 6 <sup>d</sup> , 8a, 10a	
11-OH		6.73 (brs)		8 <sup>d</sup>	

<sup>a</sup>Acetone-d<sub>6</sub>, 300/75.5 MHz. <sup>b</sup>Assignments are based on extensive 1D and 2D NMR measurements (HMBC, HSQC, COSY). <sup>c</sup>Numbers refer to carbon resonances. <sup>d</sup>Weak signal.

The  $^1\text{H}$ - $^1\text{H}$  COSY correlation (Table 4-2-1) between  $\text{H}_2\text{-2}''''$  and  $\text{H}_2\text{-1}''''$ , and  $^1\text{H}$ - $^{13}\text{C}$  HMBC correlations between  $\text{H}_2\text{-1}''''$  and  $\text{C-2}''''$  and  $\text{C-3}''''$ , and between both  $\text{H}_3\text{-4}''''$  and  $\text{H}_3\text{-5}''''$  and  $\text{C-2}''''$  and  $\text{C-3}''''$ , suggested compound **1** to contain a third 3-methylbut-2-enyl group, which was corroborated by the mass difference between **1** and **3** or **4**. The position of this additional group in compound **1** was deduced from HMBC correlations between  $\text{H}_2\text{-1}''''$  and both  $\text{C-4a}$  and  $\text{C-3}$ . Thus, it was evident that the 3-methylbut-2-enyl group replaced the aromatic proton  $\text{H-4}$  of compound **3** (Table 4-2-2), a deduction supported by  $^1\text{H}$  NMR data, which showed the absence of the signal at  $\delta_{\text{H}}$  6.44 ( $\text{H-4}$  in **3**) (Kawahara *et al.*, 1988). All other spin systems deduced from the  $^1\text{H}$ - $^1\text{H}$  COSY and HMBC correlations were consistent with the proposed structure for **1** (Figure 4-2-1). Thus, the new compound **1** is the 4-(3-methylbut-2-enyl) derivative of **3**. Due to the similarity between compounds **1** and **3** or **4**, we propose the name arugosin G.

As already stated by Gloer *et al.* for arugosin F (Hein *et al.*, 1998), arugosin G also has a small negative optical rotation. Due to the small amount of compound isolated, we did not determine whether the hemiacetal function of arugosin G gives rise to an enantiomeric mixture. The stereochemistry of arugosins A-F has not been reported.

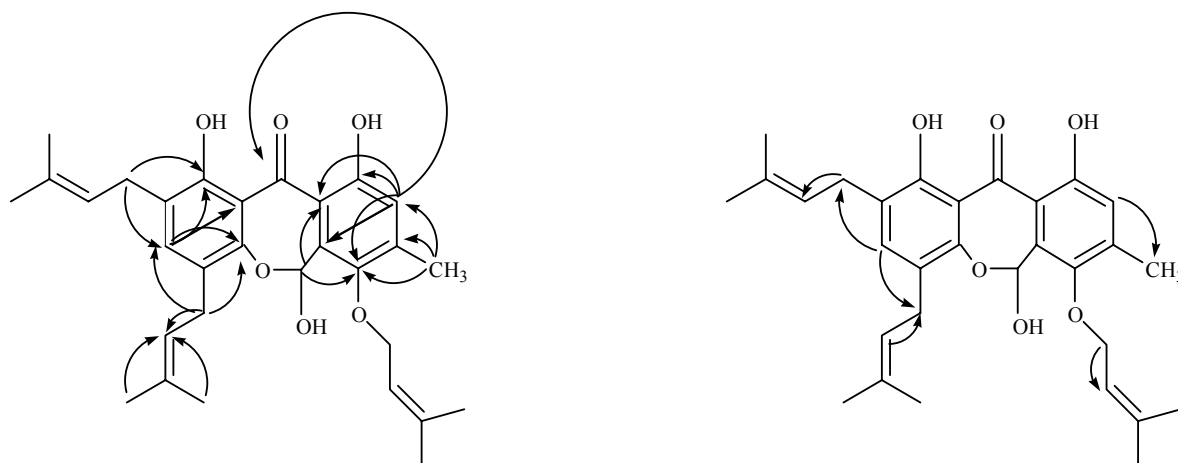


**Figure 4-2-1.** Significant HMBC (left, from H to C) and  $^1\text{H}$ - $^1\text{H}$  COSY (right) correlations for arugosin G (**1**).



**Table 4-2-2.**  $^1\text{H}$  and  $^{13}\text{C}$  NMR spectral data for compounds **3** and **4**

Atom Number	$^{13}\text{C}^{\text{a,b}}$ ( $\delta$ in ppm)		$^1\text{H}^{\text{a,b}}$ ( $\delta$ ppm, mult., $J$ in Hz)	
	(3)	(4)	(3)	(4)
1	163.2 (C)	162.2 (C)		
2	122.7 (C)	120.3 (CH)		6.57 (d, 6.22)
3		138.0 (CH)	7.32 (d, 6.22) 6.22)	7.05 (d, 6.22)
4	119.6 (CH)	119.8 (C)	6.43 (d, 6.22)	
4a	153.3 (C)	152.0 (C)		
5		120.7 (CH)		6.93-6.89 (brs)
6		141.9 (C)		
6-Me		17.0 (CH <sub>3</sub> )		2.34 (s)
7		146.4 (C)		
8		133.1 (C)		
8a	115.2 (C)	114.6 (C)		
9		199.3 (C)		
9a	111.6 (C)	111.4 (C)		
10a	157.6 (C)	157.5 (C)		
11	92.3 (CH)	92.0 (CH)		6.93-6.89 (brs)
1'	28.3 (CH <sub>2</sub> )	27.8 (CH <sub>2</sub> )		3.27 (brd, 7.32)
2'	123.8 (CH)	123.5 (CH)		5.31 (t, 7.32)
3'		133.0 (C)		
4'		25.9 (CH <sub>3</sub> )		1.70-1.66 (brs)
5'		18.0 (CH <sub>3</sub> )		1.70-1.66 (brs)
1''	72.2 (CH <sub>2</sub> )	72.1 (CH <sub>2</sub> )		4.40 (t, 7.32)
2''		120.9 (CH)		5.56 (t, 7.32)
3''	139.1 (C)	138.5 (C)		
4''		25.9 (CH <sub>3</sub> )		1.70-1.66 (brs)
5''		18.0 (CH <sub>3</sub> )		1.70-1.66 (brs)
OH			13.37 (s) (s)	12.77
OH			10.60 (s) (s)	10.55

<sup>a</sup>Acetone- $d_6$ , 300/75.5 MHz. <sup>b</sup>Assignments are based on extensive 1D and 2D NMR measurements (HMBC, HSQC, COSY).

The molecular formula of compound **2** was found to be  $\text{C}_{20}\text{H}_{20}\text{O}_6$  as deduced from HREIMS and NMR data, implying 11 degrees of unsaturation. The  $^{13}\text{C}$  NMR spectrum showed 20 carbon signals attributable to 3 x CH<sub>3</sub>, 1 x CH<sub>2</sub>, 5 x CH and 11 x C (Table 4-2-3). Considering

the molecular formula and according to the IR data ( $\nu_{\max}$  3237  $\text{cm}^{-1}$ ), it was evident that the four remaining protons had to be part of hydroxyl groups. The  $^1\text{H}$  and  $^{13}\text{C}$  NMR chemical shifts and HSQC spectra, suggested the presence of one carbonyl ( $\delta_{\text{C}}$  200.4) and one aldehyde ( $\delta_{\text{C}}$  196.2,  $\delta_{\text{H}}$  9.86) group, a deduction supported by IR absorptions at  $\nu_{\max}$  1698 and 1615  $\text{cm}^{-1}$ , and seven C=C double bonds. These data, together with the number of unsaturations, required two rings within the molecule, both of which were aromatic.

**Table 4-2-3.** 1D and 2D NMR spectral data for compound **2**

Atom Number	$^{13}\text{C}^{\text{a,b}}$ ( $\delta$ in ppm)	$^1\text{H}^{\text{a,b}}$ ( $\delta$ ppm, mult., $J$ in Hz)	Članak III. OSY $^{\text{a,b}}$	Članak IV. MBC $^{\text{a,c}}$
1	162.0 (C)			
2	121.0 (C)			
3	138.4 (CH)	7.19 (d, 8.20)	1 $^{\text{d}}$ , 4	1, 1 $^{\text{d}}$ , 4a,
4	106.8 (CH)	6.29 (d, 8.20)		2, 4a $^{\text{d}}$ , 9 $^{\text{d}}$ , 9a
4a	159.4 (C)			
5	127.5 (CH)	7.04 (s)	6-Me	7, 8a, 9 $^{\text{d}}$ , 10a $^{\text{d}}$
6	128.6 (C)			
6-Me	15.3 (CH <sub>3</sub> )	2.07 (s)		5, 7, 8
7	154.5 (C)			
8	117.6 (C)			
8a	131.7 (C)			
9	200.4 (C)			
9a	113.0 (C)			
10a	146.0 (C)			
11	196.2 (CH)	9.86 (s)		
1 $^{\text{d}}$	27.8 (CH <sub>2</sub> )	3.24 (d, 7.32)	4 $^{\text{d}}$ , 5 $^{\text{d}}$	1, 2, 3, 2 $^{\text{d}}$ , 3 $^{\text{d}}$ , 4 $^{\text{d}}$ , 5 $^{\text{d}}$
2 $^{\text{d}}$	123.1 (CH)	5.29 (t, 7.32)	1 $^{\text{d}}$ , 4 $^{\text{d}}$ , 5 $^{\text{d}}$	1 $^{\text{d}}$ , 4 $^{\text{d}}$ , 5 $^{\text{d}}$
3 $^{\text{d}}$	132.8 (C)			
4 $^{\text{d}}$	25.9 (CH <sub>3</sub> )	1.69 (s)		3 $^{\text{d}}$ , 5 $^{\text{d}}$
5 $^{\text{d}}$	17.8 (CH <sub>3</sub> )	1.69 (s)		3 $^{\text{d}}$ , 4 $^{\text{d}}$
OH		12.84 (s)		
OH		11.30 (s)		

<sup>a</sup>Acetone- $d_6$ , 300/75.5 MHz. <sup>b</sup>Assignments are based on extensive 1D and 2D NMR measurements (HMBC, HSQC, COSY). <sup>c</sup>Numbers refer to carbon resonances. <sup>d</sup>Weak signal.

The  $^1\text{H}$  NMR data showed three aromatic protons, two of them (H-3 and H-4) with an ortho coupling, and the third one (H-5) as a singlet. The  $^1\text{H}$  NMR spectrum also contained a

resonance for an aryl methyl group ( $\delta$  2.07, H<sub>3</sub>-6-Me), and two hydrogen-bonded phenolic OH groups ( $\delta$  12.84 and 11.30). The location of the carbonyl group (C-9), as a link between two aromatic rings at the position C-8a and C-9a, was supported by weak HMBC correlations from both H-4 and H-5 to C-9. The <sup>1</sup>H NMR signals observed at  $\delta$  1.69 (CH<sub>3</sub>-4' and CH<sub>3</sub>-5'),  $\delta$  3.24 (CH<sub>2</sub>-1') and  $\delta$  5.29 (CH-2') were assigned to a 3-methylbut-2-enyl group, according to the <sup>1</sup>H-<sup>1</sup>H COSY correlations between H<sub>2</sub>-1' and H-2', and HMBC correlations between all H<sub>2</sub>-1', H<sub>3</sub>-4' and H<sub>3</sub>-5', to C-3'. The position of the 3-methylbut-2-enyl group was proven to be at C-2 by correlations in the <sup>1</sup>H-<sup>1</sup>H COSY spectrum between H-3 and H<sub>2</sub>-1', and in the HMBC spectrum between H<sub>2</sub>-1' and C-1, C-2 and C-3. Carbon C-4a had to be hydroxylated due to its resonance in the <sup>13</sup>C NMR spectrum ( $\delta$  159.4). An ortho coupling between H-3 and H-4, and HMBC correlations between H-4 and C-2, C-4a (weak), C-9 (weak) and C-9a and between H-3 and C-4a and C-1 confirmed the substitution pattern of the aromatic ring A.

The remaining two hydroxyls, the aldehyde, and the methyl group resided at the aromatic ring B. Correlations from the <sup>1</sup>H-<sup>1</sup>H COSY between H-5 and H<sub>3</sub>-6Me and HMBC correlations from H<sub>3</sub>-6Me to C-5 and C-7, and from H-5 to C-7, C-8a, C-9 (weak), and C-10a (weak) indicated the position of the methyl group at C-6 and the positions of the carbons C-5 and C-7 in the aromatic ring B. Hydroxylation of C-7 was suggested by its <sup>13</sup>C NMR chemical shift at  $\delta_c$  154.5. Although, the position of the aldehyde group showed no coupling with any of the neighboring carbons, its position was assigned to C-8 on the basis of C-8 being the only remaining nonprotonated carbon. These results are consistent with a bicyclic arugosin structure with the middle ring open. This deduction is supported by biosynthetic considerations (Scheme 4-2-1) (Holker *et al.*, 1974; Chexal *et al.*, 1975). For compound **2** the name arugosin H is proposed.

The structures of arugosin A and B (**3** and **4**) (Ballantine *et al.*, 1973), shamixanthone (**5**) (Holker *et al.*, 1974; Chexal *et al.*, 1975), emericellin (**6**) (Kawahara *et al.*, 1988), emindole DA (**7**) (Nozawa *et al.*, 1987), microperfuraneone (**8**) (Fujimoto *et al.*, 1998), sterigmatocystin (**9**) (Pachler *et al.*, 1976; Cox *et al.*, 1977), and averufin (**10**) (Gorst-Allman *et al.*, 1977) were identified by comparing their spectroscopic data and optical rotations with published values.

Fungi of the genus *Emericella* (anamorph: *Aspergillus*) produce a great diversity of secondary metabolites (Hensens *et al.*, 1991; Itabashi *et al.*, 1992; Itabashi *et al.*, 1996; Fujimoto *et al.*, 2000). Among them is a family of compounds called arugosins which are of interest with regard to the biosynthesis of several structural types of fungal polyketides, e.g. anthrones,

anthraquinones, benzophenones, xanthenes (Chexal *et al.*, 1974; Holker *et al.*, 1974; Chexal *et al.*, 1975). Arugosin A and B, two substituted dibenz[*b,e*]oxepins, are the major metabolites of *Aspergillus rugulosus* (Ballantine *et al.*, 1970), *A. varicolor* (Chexal *et al.*, 1975), and *A. silvaticus* (Kawahara *et al.*, 1988). Arugosin C (Ballantine *et al.*, 1973), D (Chexal *et al.*, 1975), and E (Kawahara *et al.*, 1988) also occur in *Aspergillus* spp., whereas arugosin F was found in *Ascodesmis sphaerospora* (Hein *et al.*, 1998). Biosynthetic studies (Chexal *et al.*, 1974; Holker *et al.*, 1974; Chexal *et al.*, 1975) suggested that the bi- and tricyclic arugosins and compounds from xanthone family are biogenetically related. Arugosin H (**2**) may be derived from chrysophanol anthrone which undergoes oxidative cleavage to form the aldehyde function, followed by C-prenylation and hydroxylation (see Scheme 4-2-1). The aldehyde function can be converted to a hemiacetal function as seen in the further prenylated and tricyclic arugosins G, A, and B (**1**, **3** and **4**). Alternatively, cyclodehydration of the benzophenone intermediate yields shamixanthone (**5**) and emericellin (**6**).

On the other hand, a member of indole diterpenes, emindole DA (**7**) is formed by epoxidation of a common intermediate, 3-geranylgeranylindole and subsequent cyclization (Fueki *et al.*, 2004), while sterigmatocystin (**9**) and averufin (**10**) as precursors of aflatoxins, toxic and carcinogenic fungal metabolites, are biosynthesized from norsolorinic acid which undergoes 12 to 17 enzymatic reactions (Yabe and Nakajima, 2004) to form **9** and **10**. Thus, the isolation of compounds **1** – **10** testifies, once more, about a diversity of natural products and a complexity of metabolic pathways in one strain.

Compounds **1** – **10** were tested in antibacterial, antifungal and antialgal assays (Schultz *et al.*, 1995) at the 50 µg/disk level. Compound **2** showed inhibition zones against *Mycotypha microspora* (3 mm) and *Chlorella fusca* (2 mm); compounds **3** and **4** (as a mixture) were active against *Bacillus megaterium* (4 mm), while compound **9** and **10** inhibited *M. microspora* (11 mm and 3.5 mm, respectively) and *C. fusca* (5 mm and 3 mm, respectively).

The effects of the crude extract as well as the pure compounds **1** – **8** on tumor growth *in vitro* were investigated in a survival and proliferation assay in a panel of 36 human tumor cell lines representing 11 different tumor types. Anti-tumor activity was defined as test/control value smaller than 50% compared to the untreated control cells. The crude extract effected anti-tumor activity in all 36 cell lines (100%) at 50 µg/mL, in 31 out of the 36 cell lines (86%) at 5 µg/mL, and in 2/36 (6%) cell lines at 0.5 µg/mL. This is indicative for a selective and concentration-dependent antitumor activity of this extract and one or more of its ingredients.

Among the pure compounds, compound **7** gave the highest activity score, exhibiting a mean  $IC_{50}$  value of 5.5  $\mu\text{g/mL}$ . At a concentration of 10  $\mu\text{g/mL}$  33 out of 36 cell lines (92%) were inhibited. As expected, the reference compound adriamycin tested in parallel in the same assays was more potent ( $IC_{50}$  0.016  $\mu\text{g/mL}$ ). Compounds **3** and **4** were active in 7 out of the 36 cell lines (19%) at the highest concentration of 10  $\mu\text{g/mL}$ . The other five compounds showed either only marginal or no anti-tumour activity *in vitro*.

Compounds **9** (sterigmatocystin) and **10** (averufin) are known from the literature (Wang and Groopman, 1999; Bungler *et al.*, 2004) to be potent cytotoxic agents and were thus not evaluated in the current study.

The immunostimulating effects of compounds **1** - **8** were investigated by analysing the stimulation of cytokine production by PBMCs from two healthy donors. All compounds were tested at concentrations of 0.1 and 1  $\mu\text{g/mL}$ . These concentrations were not cytotoxic in the monolayer cytotoxicity and proliferation assay. LPS at 1  $\mu\text{g/mL}$ , PMA at 10  $\text{ng/mL}$ , and ionomycin at 1  $\mu\text{g/mL}$  were used as positive controls. Twenty-four hours after exposure of PBMCs to the test compounds, PBMC supernatants were quantitatively tested for IL-2, IL-4, IL-6, IL-10, TNF- $\alpha$  and IFN- $\gamma$  by flow cytometry with the Cytometric Bead Array (CBA) (Morgan *et al.*, 2004). None of the compounds induced the production of any of the cytokines. Negative PI-staining of PBMCs after removal of the supernatant confirmed that the failure of the test compounds to induce cytokine production by PBMCs was not due to cytotoxicity.

Arugosin G (**1**) was isolated as bright yellow solid (2.8 mg). UV (MeOH)  $\lambda_{\text{max}}$  ( $\log \epsilon$ ) 226 nm (sh) (4.20), 271 nm (3.84), 305 nm (3.82), 366 nm (3.75); IR (ATR)  $\nu_{\text{max}}$  3438, 2920, 1608, 1477, 1422, 1344, 1213, 1115, 1071, 998;  $^1\text{H}$  and  $^{13}\text{C}$  NMR spectral data (see Table 4-2-1); HREIMS  $m/z$  492.2517 (calcd for  $\text{C}_{30}\text{H}_{36}\text{O}_6$  492.2512);  $[\alpha]_{\text{D}}^{24}$  -1.1° ( $c$  0.29, MeOH).

Arugosin H (**2**) was isolated as bright orange solid (10.8 mg). UV (MeOH)  $\lambda_{\text{max}}$  ( $\log \epsilon$ ) 225 nm (4.50), 274 nm (4.33), 291nm (sh) (4.21), 382 nm (3.93); IR (ATR)  $\nu_{\text{max}}$  3237, 2921, 1698, 1615, 1417, 1353, 1222, 1111, 1047, 982, 899, 816  $\text{cm}^{-1}$ ;  $^1\text{H}$  and  $^{13}\text{C}$  NMR spectral data (see Table 4-2-3); HREIMS  $m/z$  356.1266 (calcd for  $\text{C}_{20}\text{H}_{20}\text{O}_6$  356.1260).

Arugosin A and B (**3**, **4**) were isolated as a viscous, yellow oil (80.3 mg).  $^1\text{H}$  and  $^{13}\text{C}$  NMR spectral data (see Table 4-2-2).

Shamixanthone (**5**) was isolated as yellow needles (4.0 mg).  $^1\text{H}$  NMR (300 MHz,  $\text{CDCl}_3$ );  $\delta$  12.60 (1H, s, 1-OH), 7.44 (1H, d,  $J = 8.42$ , H-3), 7.30 (1H, s, H-5), 6.74 (1H, d,  $J = 8.42$ , H-2), 5.41 (1H, s, H-25), 5.31 (1H, t,  $J = 7.32$ , H-15), 4.80 (1H, s, H-22a), 4.59 (1H, s, H-22b), 4.45-4.32 (2H, m, H<sub>2</sub>-19), 3.50 (2H, d,  $J = 7.32$ , H<sub>2</sub>-14), 2.74 (1H, s, H-20), 2.36 (3H, s, H<sub>3</sub>-24), 1.85 (3H, s, H<sub>3</sub>-23), 1.80 (3H, s, H<sub>3</sub>-17), 1.75 (3H, s, H<sub>3</sub>-18);  $^{13}\text{C}$  NMR (75.5 MHz,  $\text{CDCl}_3$ )  $\delta$  184.5 (s, C-13), 159.7 (s, C-1), 152.8 (s, C-10), 152.2 (s, C-11), 149.4 (s, C-7), 142.6 (s, C-21), 138.3 (s, C-6), 136.5 (d, C-3), 133.3 (s, C-16), 121.7 (d, C-15), 121.0 (s, C-8), 119.3 (d, C-5), 118.9 (s, C-4), 116.9 (s, C-12), 112.3 (t, C-22), 109.7 (d, C-2), 109.2 (s, C-9), 64.6 (t, C-19), 63.2 (d, C-25), 45.0 (d, C-20), 27.5 (t, C-14), 25.8 (q, C-18), 22.6 (q, C-23), 17.9 (q, C-17), 17.4 (q, C-24);  $\text{C}_{25}\text{H}_{26}\text{O}_5$  (406.18);  $[\alpha]_D^{24} +10.0^\circ$  ( $c$  0.51,  $\text{CHCl}_3$ ), (lit. (Chexal *et al.*, 1974);  $[\alpha]_D^{24} +11.9^\circ$  ( $c$  1.92,  $\text{CHCl}_3$ ); (Bringmann *et al.*, 2003);  $[\alpha]_D^{24} +25.2^\circ$  ( $c$  0.33,  $\text{CHCl}_3$ )).

Emericellin (**6**) was isolated as yellow oil (5.1 mg).  $^1\text{H}$  NMR (300 MHz,  $\text{CDCl}_3$ );  $\delta$  12.51 (1H, s, 1-OH), 7.42 (1H, d,  $J = 8.05$ , H-3), 7.30 (1H, s, H-5), 6.70 (1H, d,  $J = 8.05$ , H-2), 5.60 (1H, t,  $J = 6.95$ , H-2''), 5.28 (1H, t,  $J = 6.95$ , H-2'), 5.06 (2H, s, H<sub>2</sub>-11), 4.43 (2H, d,  $J = 6.95$ , H<sub>2</sub>-1''), 3.47 (2H, d,  $J = 6.95$ , H<sub>2</sub>-1'), 2.45 (3H, s, H<sub>3</sub>-6Me), 1.80 (3H, s, H<sub>3</sub>-5''), 1.78 (3H, s, H<sub>3</sub>-5'), 1.74 (3H, s, H<sub>3</sub>-4''), 1.71 (3H, s, H<sub>3</sub>-4');  $^{13}\text{C}$  NMR (75.5 MHz,  $\text{CDCl}_3$ )  $\delta$  184.6 (s, C-9), 159.9 (s, C-1), 154.0 (s, C-10a), 152.8 (s, C-4a), 152.6 (s, C-7), 142.6 (s, C-6), 139.1 (s, C-3''), 136.9 (d, C-3), 134.2 (s, C-8), 133.3 (s, C-3'), 121.6 (d, C-2''), 119.6 (d, C-2'), 119.4 (d, C-5), 119.0 (s, C-8a), 118.9 (s, C-4), 117.9 (s, C-9a), 110.0 (d, C-2), 72.2 (t, C-1''), 57.1 (t, C-11), 27.4 (t, C-1'), 25.9 (q, C-5''), 25.8 (q, C-5'), 18.1 (q, C-4''), 17.9 (q, C-4'), 17.7 (q, C-6Me);  $\text{C}_{25}\text{H}_{28}\text{O}_5$  (408.19).

Emindole DA (**7**) was isolated as bright yellow solid (8.5 mg).  $^1\text{H}$  NMR (300 MHz,  $(\text{CD}_3)_2\text{CO}$ );  $\delta$  7.52 (1H, d,  $J = 7.68$ , H-5), 7.31 (1H, d,  $J = 7.68$ , H-7), 7.06-7.02 (1H, m, H-2), 6.98 (1H, d,  $J = 1.10$ , H-6), 6.96 (1H, d,  $J = 1.10$ , H-4), 5.15 (1H, t,  $J = 6.95$ , H-21), 4.43 (1H, s, H-27a), 4.09 (1H, s, H-27b), 3.63-3.58 (1H, brs, H-17), 3.15 (1H, dd,  $J = 4.03, 14.64$ , H-8a), 2.77 (1H, dd,  $J = 10.25, 14.64$ , H-8b), 2.38 (1H, dt,  $J = 5.12, 13.54, 27.08$ , H-11a), 2.16-2.06 (3H, m, H-11b, H<sub>2</sub>-20), 2.08 (1H, s, H-9), 1.86-1.80 (1H, m, H-13), 1.75-1.70 (2H, m, H<sub>2</sub>-16), 1.67 (3H, s, H<sub>3</sub>-24), 1.64 (3H, s, H<sub>3</sub>-23), 1.41 (2H, m, H<sub>2</sub>-12), 1.31-1.27 (2H, m, H<sub>2</sub>-19), 1.26-1.23 (2H, m, H<sub>2</sub>-15), 0.99 (3H, s, H<sub>3</sub>-26), 0.81 (3H, s, H<sub>3</sub>-25);  $^{13}\text{C}$  NMR (75.5 MHz,  $(\text{CD}_3)_2\text{CO}$ )  $\delta$  149.6 (s, C-10), 137.6 (s, C-7a), 131.0 (s, C-22), 128.6 (s, C-3a), 126.3 (d, C-21), 123.5 (d, C-6), 121.6 (d, C-2), 119.3 (d, C-5), 119.0 (d, C-4), 115.3 (s, C-3), 112.0 (d, C-

7), 110.0 (t, C-27), 73.4 (d, C-17), 59.7 (d, C-9), 41.8 (s, C-18), 39.5 (d, C-13), 38.6 (s, C-14), 38.1 (t, C-19), 35.3 (t, C-15), 31.5 (t, C-11), 28.6 (t, C-16), 25.9 (q, C-24), 24.1 (t, C-8), 23.8 (t, C-12), 23.7 (q, C-26), 22.5 (t, C-20), 17.8 (q, C-23, C-25);  $C_{28}H_{39}NO$  (405.30);  $[\alpha]_D^{24} -23.4^\circ$  ( $c$  0.86, MeOH), (lit. (Nozawa *et al.*, 1988);  $[\alpha]_D^{24} -30.7^\circ$  ( $c$  2.32, MeOH)).

Microperfuranone (**8**) was isolated as colorless solid (1.5 mg).  $^1H$  NMR (300 MHz,  $(CD_3)_2CO$ );  $\delta$  7.53 (2H, d,  $J = 6.95$ , H-8, H-10), 7.46 (2H, d,  $J = 6.95$ , H-7, H-11), 7.44-7.41 (1H, m, H-9), 7.33-7.24 (5H, m, H-14, H-15, H-16, H-17, H-18), 5.96 (1H, s, H-5), 3.98 (2H, dd,  $J = 14.27$ , 71.35, H<sub>2</sub>-12);  $^{13}C$  NMR (75.5 MHz,  $(CD_3)_2CO$ )  $\delta$  170.8 (s, C-2), 159.6 (s, C-4), 137.5 (s, C-13), 130.8 (s, C-6), 130.2 (s, C-3), 129.9 (s, C-8, C-10), 129.7 (s, C-15, C-17), 129.6 (s, C-9, C-14, C-18), 129.3 (s, C-7, C-11), 127.7 (s, C-16), 97.5 (d, C-5), 32.9 (t, C-12);  $C_{17}H_{14}O_3$  (266.09);  $[\alpha]_D^{24} -4.4^\circ$  ( $c$  0.27, MeOH), (lit. (Fujimoto *et al.*, 1998);  $[\alpha]_D^{24} -6.8^\circ$  ( $c$  0.60, MeOH)).

Sterigmatocystin (**9**) was isolated as white crystals (4.0 mg).  $^1H$  NMR (300 MHz,  $(CD_3)_2CO$ );  $\delta$  13.41 (1H, s, 3-OH), 7.60 (1H, t,  $J = 8.42$ , H-5), 6.96 (1H, s, H-4), 6.93 (1H, s, H-14), 6.72-6.69 (1H, m, H-6), 6.65-6.63 (1H, m, H-17), 6.61 (1H, s, H-11), 5.54 (1H, q,  $J = 2.56$ , 5.12, 8.42, H-16), 4.93-4.89 (1H, m, H-15), 3.96 (3H, s, H<sub>3</sub>-18);  $^{13}C$  NMR (75.5 MHz,  $(CD_3)_2CO$ )  $\delta$  181.7 (s, C-1), 165.7 (s, C-10), 164.4 (s, C-12), 163.2 (s, C-7), 156.0 (s, C-3), 154.9 (s, C-8), 146.2 (d, C-17), 136.7 (d, C-5), 114.5 (d, C-14), 111.6 (d, C-6), 109.6 (s, C-2), 107.7 (s, C-9), 106.9 (d, C-4), 106.4 (s, C-13), 103.4 (d, C-16), 91.5 (d, C-11), 57.0 (q, C-18), 48.7 (d, C-15);  $C_{18}H_{12}O_6$  (324.06);  $[\alpha]_D^{24} -106.2^\circ$  ( $c$  0.25,  $CHCl_3$ ).

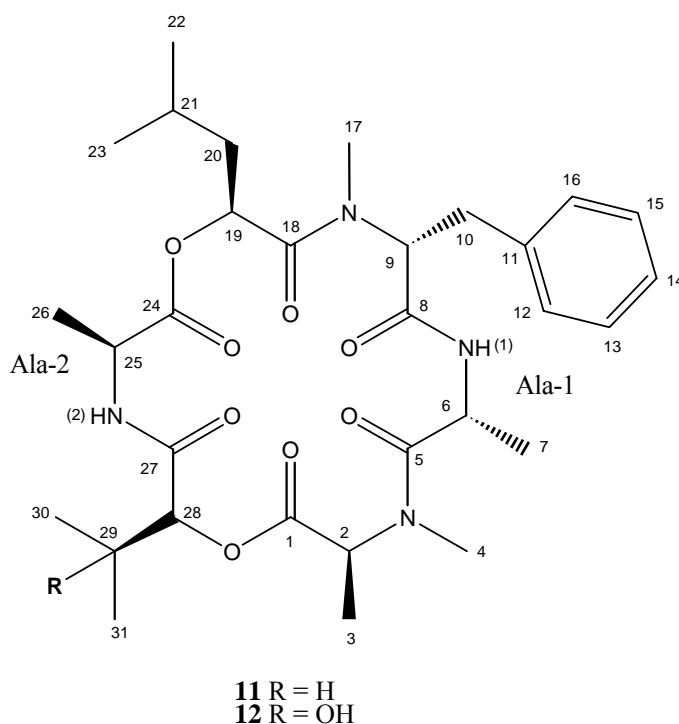
Averufin (**10**) was isolated as orange solid (11.5 mg).  $^1H$  NMR (300 MHz, THF);  $\delta$  7.31 (1H, d,  $J = 2.20$ , H-7), 7.27 (1H, s, H-4), 6.68 (1H, d,  $J = 2.20$ , H-5), 5.43-5.41 (1H, brs, H-1'), 2.18-2.13 (2H, m, H-2'a, H-4'a), 2.00-1.92 (2H, m, H-2'a, H-4'a), 1.73-1.67 (2H, m, H<sub>2</sub>-3'), 1.65 (3H, s, H<sub>3</sub>-6');  $^{13}C$  NMR (75.5 MHz, THF)  $\delta$  192.0 (s, C-9), 182.9 (s, C-10), 167.9 (s, C-6), 167.5 (s, C-8), 162.7 (s, C-3), 161.2 (s, C-1), 137.6 (s, C-14), 135.9 (s, C-11), 118.3 (s, C-2), 111.2 (s, C-12), 111.0 (s, C-13), 110.9 (d, C-7), 110.1 (d, C-5), 109.8 (d, C-4), 103.3 (s, C-5'), 68.6 (d, C-1'), 37.8 (t, C-4'), 29.4 (t, C-2'), 29.2 (q, C-6'), 17.5 (t, C-3');  $C_{20}H_{16}O_7$  (368.09);  $[\alpha]_D^{24} -26.6^\circ$  ( $c$  1.0,  $CHCl_3$ ).

### 4.3 Two New Depsipeptides from the Marine Fungus *Spicellum roseum* (Strain number 74)

#### 4.3.1 Introduction

Cyclic peptides and depsipeptides are of special interest due to their potent biological activities. Cyclodepsipeptides like beauvericin and enniatins are secondary metabolites from different species of *Fusarium* with cytotoxic (Calo *et al.*, 2004), antibiotic (Dobler *et al.*, 1969) and insecticidal effects (Gupta *et al.*, 1991). Moreover, beauvericin was reported to be an inhibitor of acyl-CoA: cholesterol acyltransferase (Tomoda *et al.*, 1992).

In our continuing research on novel bioactive fungal metabolites, we have examined a fungal strain whose extract inhibited the growth of *Eurotium rubrum* and *Mycotypha microspora* in agar diffusion assays, and showed the alternations in sphingolipid metabolism (Chapter 4.6). The bioassay-guided isolation revealed the presence of two known compounds belonging to the trichothecenes, i.e. trichodermol and 8-deoxy-trichothecin (Chapter 4.6) which were responsible for the activity. Further investigations of the crude extract gave two new depsipeptides (**11** and **12**) containing 2-hydroxyisovaleric acid and N-methylphenylalanine. The later two units are also present in beauvericin (Dobler *et al.*, 1969). The structure elucidation and absolute configuration of the beauvericin analogs **11** and **12** are based on NMR and MS data, chiral HPLC and computer modeling.





### 4.3.2 Cultivation, extraction and isolation

The fungal strain (*Spicellum roseum*, strain number 74, 193 H 15) was cultivated at room temperature for one month in 4 L (16 Fernbach flasks) in solid peptone biomalt medium containing 20 g/L of Biomalt, 10 g/L of peptone from Soya, 17 g/L of agar and artificial seawater. The fungal biomass, including the medium, was homogenized using an Ultra-Turrax and the mixture was extracted with EtOAc (4 x 4 L). After evaporation of the organic phase 1.8 g of dark brown oil was obtained. The extract was fractionated by VLC (Si gel 60, 0.063-0.200 mm) with a petroleum ether – EtOAc – MeOH gradient, to yield 8 fractions. Fraction 5 contained depsipeptides and was subjected to HPLC using a reversed-phase column (Phenomenex Synergi Hydro-RP, 250 x 4.60 mm, 4 µm) with MeOH/H<sub>2</sub>O gradient as eluant at a flow rate of 1 mL/min to obtain compounds **11** and **12**.

### 4.3.3 Absolute configuration of spicellamide A (**11**) and spicellamide B (**12**)

Spicellamide A (**11**, 0.4 mg) and spicellamide B (**12**, 0.4 mg) were hydrolyzed with 6 M HCl (0.5 mL) at 110 °C for 16 h. After concentration to dryness, the residues were dissolved in H<sub>2</sub>O (50 µL). A 1 % 1-fluoro-2,4-dinitrophenyl-5-L-alaninamide solution in acetone (Marfey's reagent, 100 µL) and 1 M NaHCO<sub>3</sub> (20µL) were added. The mixtures were incubated at 80 °C for 40 min, cooled down to room temperature, neutralized with 2 M HCl (10 µL), and evaporated to dryness. The residues were resuspended in DMSO (100 µL) and subjected to HPLC-MS using a reversed-phase C<sub>18</sub> column (Macherey-Nagel Nucleodur 100, 125 x 2 mm, 5 µm) and gradient elution (from MeOH/H<sub>2</sub>O 10/90 to MeOH/H<sub>2</sub>O 100/0 in 20 min, MeOH 100% for 10 min, with added NH<sub>4</sub>Ac, 2 mmol). The retention times of the FDAA derivatives of standards were at 8.77 min (L-Ala), 11.47 min (D-Ala), 9.73 min (*N*-Me-L-Ala), 10.84 min (*N*-Me-D-Ala), 13.17 min (*N*-Me-L-Phe) and 13.74 min (*N*-Me-D-Phe). Thus, the presence of *N*-Me-D-Phe, *N*-Me-L-Ala and both D- and L-Ala was determined for both spicellamide A and spicellamide B.

The configuration of hydroxycarboxyl acids was determined by chiral HPLC. Portions of hydrolysate were evaporated to dryness and resuspended in solution which was used as mobile phase (100 µL). Chiral HPLC analyses were carried out using a Phenomenex Chirex 3126 (D), 4.6 x 50 mm column; detection at 254 nm, with 2 mM CuSO<sub>4</sub> in MeCN/H<sub>2</sub>O (15:85) as eluant at a flow rate of 1 mL/min. The retention times of authentic standards were at 8.05 min (L-2-hydroxyisovaleric acid), 11.57 min (D-2-hydroxyisovaleric acid), 24.05 min (L-2-hydroxyisocaproic acid), 27.12 min (D-2-hydroxyisocaproic acid). These analyses revealed that the hydrolysate of **11** consisted of L-2-hydroxyisovaleric and L-2-

hydroxyisocaproic acid moieties. For hydrolysate of **12** the configuration of 2-hydroxyisocaproic acid was determined as L-form.

#### 4.3.4 Results and discussion

The molecular formula of compound **11** was determined by HREIMS and  $^{13}\text{C}$  NMR as  $\text{C}_{31}\text{H}_{46}\text{N}_4\text{O}_8$  implying 11 elements of unsaturation. The  $^1\text{H}$  and  $^{13}\text{C}$  NMR spectral data (Table 4-3-1) revealed six carbonyl carbon signals at  $\delta_{\text{C}}$  173.2, 172.9, 172.3, 170.5, 168.9, and 168.7 and six  $\alpha$ -proton signals at  $\delta_{\text{H}}$  5.62, 5.15, 5.09, 4.87, 4.79, and 3.99 suggesting compound **11** to a peptide-like metabolite composed of six subunits. The  $^1\text{H}$  NMR spectrum showed two signals ( $\delta_{\text{H}}$  6.98 and 7.92) characteristic for amide protons and two signals ( $\delta_{\text{H}}$  3.28 and 2.99) characteristic for N-methyl protons. The chemical shifts of C-19 ( $\delta_{\text{C}}$  71.2) and C-28 ( $\delta_{\text{C}}$  78.1) clearly demonstrated that these carbons are oxygenated, proposing that two of the six carbonyl groups belonged to hydroxycarboxylic acids. Thus, compound **11** was a hexadepsipeptide consisting of four amino acid and two hydroxycarboxylic acid residues. Absorption bands at  $1638\text{ cm}^{-1}$  (amide carbonyls) and  $1742\text{ cm}^{-1}$  (ester carbonyls) in the IR spectrum supported this deduction. Analyses of  $^1\text{H}$ - $^1\text{H}$  COSY and HMBC spectroscopic data disclosed the structures of hydroxycarboxylic and amino acid residues (Table 4-3-1). The presence of an aromatic moiety was clearly visible from  $^1\text{H}$  and  $^{13}\text{C}$  NMR spectra.  $^1\text{H}$ - $^1\text{H}$  COSY correlations between all five aromatic methine groups (CH-12 to CH-16) and H<sub>2</sub>-10, and  $^1\text{H}$ - $^{13}\text{C}$  HMBC couplings between  $\alpha$ -CH-9 and H<sub>2</sub>-10, assigned the aromatic ring to a phenylalanine residue. HMBC correlations from amide methyl protons ( $\delta_{\text{H}}$  2.99) to  $\alpha$ -CH-9 indicated the *N*-phenylalanine residue to be *N*-methylated. Furthermore, three spin systems typical for alanine moieties were found, i.e.  $^1\text{H}$ - $^1\text{H}$  COSY correlations between H-2 and H<sub>3</sub>-3, between H-6 and H<sub>3</sub>-7, and between H-25 and H<sub>3</sub>-26. As deduced from the  $^1\text{H}$ - $^{13}\text{C}$  HMBC correlations between  $\alpha$ -CH-2 and CH<sub>3</sub>-4 ( $\delta_{\text{H}}$  3.28), one of the alanine moieties had a methylated amino group. The other two  $\alpha$ -protons,  $\alpha$ -CH-6 and  $\alpha$ -CH-25, showed couplings to their adjacent amide NH protons, NH (1) ( $\delta_{\text{H}}$  6.98) and NH (2) ( $\delta_{\text{H}}$  7.92), respectively.  $^1\text{H}$ - $^1\text{H}$  couplings between  $\alpha$ -CH-19 and H<sub>2</sub>-20 and between H<sub>2</sub>-20 and H-21, H<sub>3</sub>-22 and H<sub>3</sub>-23 revealed a 2-hydroxyisocaproic acid partial structure. Finally, the last residue of the hexadepsipeptide **11** was evident from  $^1\text{H}$ - $^1\text{H}$  COSY correlations between  $\alpha$ -CH-28 and H-29 and between H-29 and CH<sub>3</sub>-30 and CH<sub>3</sub>-31, and identified as a 2-hydroxyisovaleric acid residue. Determination of the sequence and connection of the six residues (two alanine, *N*-methylalanine, *N*-methylphenylalanine, 2-hydroxyisocaproic acid and 2-hydroxyisovaleric acid moieties) was accomplished from HMBC and NOESY correlations.

**Table 4-3-1.** 1D and 2D NMR spectral data for compound **1** ( $\delta$  in ppm;  $J$  in Hz)

Carbon	$\delta_C^{a,c}$	$\delta_H^{a,c}$	COSY <sup>b,c</sup>	HMBC <sup>b,d</sup>	NOESY <sup>b,c</sup>
1	168.9				
2	61.1	3.99 (q; 6.59)	3	1, 3, 4, 5	3, 4
3	13.9	1.53 (d; 6.59)	2	1, 2	NH2 <sup>w</sup> , 2, 4 <sup>w</sup>
4	37.3	3.28 (s)		2, 5	2, 3 <sup>w</sup> , 6, 7
5	172.3				
6	46.9	4.79 (quint; 6.95)	NH1, 7	5, 7, 8	NH1, 4, 7
7	18.2	1.32 (d; 6.95)	6	5, 6	NH1, 6, 17 <sup>w</sup>
8	168.7				
9	57.5	5.62 (dd; 5.12, 11.71)	10	8, 10, 17, 18	NH1, 10
		3.32 (dd; 5.12, 15.0)	9	8, 9, 11-16, 17	12-16, 9
10	33.6	2.93 (dd; 11.71, 15.0)			
11	138.9				
12	129.7	7.23 (m)	10, 13-16	10	10, 17, 20 <sup>w</sup> , 22 <sup>w</sup> , 23 <sup>w</sup>
13	129.0	7.26 (m)	10, 12, 14-16	10	10, 17, 20 <sup>w</sup> , 22 <sup>w</sup> , 23 <sup>w</sup>
14	127.1	7.19 (m)	10, 12, 13, 15, 16	10	10, 17
15	129.0	7.26 (m)	10, 12-14, 16	10	10, 17, 20 <sup>w</sup> , 22 <sup>w</sup> , 23 <sup>w</sup>
16	129.7	7.23 (m)	10, 12-15	10	10, 17, 20 <sup>w</sup> , 22 <sup>w</sup> , 23 <sup>w</sup>
17	29.5	2.99 (s)		9, 18	NH1, 7 <sup>w</sup> , 12-16, 19, 20 <sup>w</sup> , 22 <sup>w</sup> , 23 <sup>w</sup>
18	173.2				
19	71.2	5.15 (q; 5.49)	20	18, 20, 21	17, 20, 21, 22, 23
20	39.9	1.47 (m); 1.13 (m)	19, 21, 22, 23	19, 21, 22, 23	19, 22, 23
21	24.6	1.17. (m)	20		19
22	22.8	0.78 (d; 6.22)	20	23	17 <sup>w</sup> , 19, 20, 26 <sup>w</sup>
23	23.2	0.75 (d; 6.22)	20	22	17 <sup>w</sup> , 19, 20, 26 <sup>w</sup>
24	172.9				
25	47.5	4.87 (dq; 8.78, 7.32)	NH2, 26	24, 26, 27	NH2, 26
26	19.7	1.42 (d; 7.32)	25	24, 25	NH2, 22-23 <sup>w</sup> , 25, 30-31 <sup>w</sup>
27	170.5				
28	78.1	5.09 (d; 2.56)	29	1, 27, 29, 30, 31	NH2, 29, 30, 31
29	29.2	2.50 (hept d; 7.32, 2.56)	28, 30, 31	30, 31	28, 30, 31
30	19.3	0.92 (d; 7.32)	29	28, 31	26 <sup>w</sup> , 28, 29
31	16.2	0.84 (d; 7.32)	29	28, 30	NH2 <sup>w</sup> , 26 <sup>w</sup> , 28, 29
NH (1)		6.98 (d; 6.95)	6		6, 7, 9, 17
NH (2)		7.92 (d; 8.78)	25		3 <sup>w</sup> , 25, 26, 28, 31 <sup>w</sup>

<sup>a</sup> Acetone-d<sub>6</sub>, 300 MHz. <sup>b</sup> Acetone-d<sub>6</sub>, 500 MHz. <sup>c</sup> Assignments are based on extensive 1D and 2D NMR measurements (HMBC, HSQC, COSY, NOESY). <sup>d</sup> Numbers refer to carbon resonances. <sup>w</sup> Weak signal.

The position of the *N*-methylphenylalanine residue was established by  $^1\text{H}$ - $^{13}\text{C}$  HMBC correlations between  $\alpha$ -H-9 and both C-8 and C-18 and between H<sub>3</sub>-17 and C-18. The  $\alpha$ -proton H-6 showed  $^1\text{H}$ - $^{13}\text{C}$  long range coupling with carbonyl carbon C-8 which connected *N*-methylphenylalanine with one of the alanine residues (Ala-1). These data together with heteronuclear long range couplings of  $\alpha$ -H-6, H<sub>3</sub>-7,  $\alpha$ -H-2 and H<sub>3</sub>-4 with carbonyl carbon C-5 disclosed the location of this alanine residue between *N*-methylphenylalanine and *N*-methylalanine. *N*-methylalanine was further linked to the 2-hydroxyisovaleric acid residue as deduced from HMBC correlations between  $\alpha$ -H-2 and C-1, between H<sub>3</sub>-3 and C-1, and between  $\alpha$ -H-28 and C-1. The carbonyl carbon C-27 showed long range correlations with both  $\alpha$ -H-28 and  $\alpha$ -H-25 which connected the second alanine moiety (Ala-2) to the 2-hydroxyisovaleric acid residue. The  $\alpha$ -proton of the 2-hydroxyisocaproic acid residue H-19 did not show clear HMBC correlations with carbonyl groups but NOESY data suggested that  $\alpha$ -H-19 was bound to C-18. Thus, NOESY correlations were detected between  $\alpha$ -H-19 and CH<sub>3</sub>-17, and between CH<sub>3</sub>-26 and both CH<sub>3</sub>-22 (weak) and CH<sub>3</sub>-23 (weak). This allowed to position the 2-hydroxyisocaproic acid moiety, the last moiety of compound **11**, between *N*-methylphenylalanine and an alanine residue (Ala-2).

To establish the absolute configuration of the four amino acids, compound **11** was hydrolyzed, derivatized with Marfey's reagent and analyzed by HPLC-MS. Comparison of retention times and mass spectral data of hydrolysed products of **11** with those of standards, allowed to deduce the configuration of the amino acids as *N*-Me-D-Phe, *N*-Me-L-Ala, L-Ala and D-Ala. The configuration of the hydroxycarboxylic acids was determined by chiral HPLC analysis of the acid hydrolysate, and determined as L for both, 2-hydroxyisocaproic and 2-hydroxyisovaleric acid.

At this point of the structure elucidation the position of D- and L-alanine had to be solved. Molecular modeling calculations were used to address this problem. Minimum energy conformations of the two possible isomers of **11** (6*S*, 25*R* and 6*R*, 25*S*) were calculated (Figure 4-3-1) and analyzed with regard to the NOESY correlations observed. The most conspicuous difference between the two models was the spatial orientation of proton H-6 and the amide methyl protons (H<sub>3</sub>-4). H-6 and CH<sub>3</sub>-4 showed NOESY correlations, which seemed only possible in the 6*R*, 25*S* isomer. In the model with 6*S*, 25*R* configuration H-6 is positioned below and H<sub>3</sub>-4 above the plane of the depsipeptide ring with a distance of approx. 4.0 Å to each other, while in the model with 6*R*, 25*S* configuration they are on the same side of the plane with a distance of approx. 2.2 Å. Thus, the 6*R*, 25*S* configuration is suggested for compound **11**, for which we propose the trivial name spicellamide A.

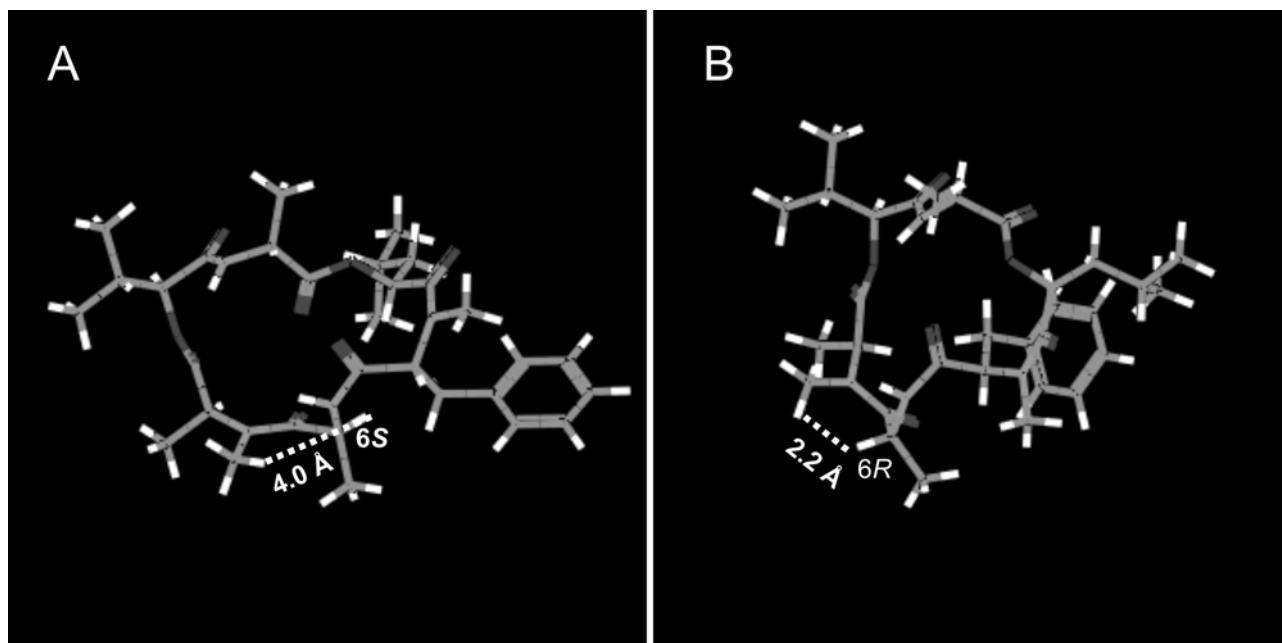


**Figure 4-3-1.** Minimum energy conformation of the 6*S*, 25*R* isomer (A) and 6*R*, 25*S* isomer (B) of **1**.

HREIMS and NMR data of compound **12** imparted a molecular formula of  $C_{31}H_{46}N_4O_9$ . The  $^1H$  and  $^{13}C$  NMR spectral data indicated high structural similarity between compounds **12** and **11**. The only difference was evident from  $^1H$  and  $^{13}C$  NMR chemical shifts of the 2-hydroxyisovaleric acid residue (Table 4-3-2). Hydroxylation of C-29 in **12** was suggested due to its  $^{13}C$  NMR chemical shift at  $\delta_C$  72.2 and due to the missing signal for proton H-29 in the  $^1H$  NMR spectrum of **12**. Thus, 2-hydroxyisovaleric acid was replaced with 2,3-dihydroxyisovaleric acid moiety in compound **2**. All other COSY, HMBC and NOESY correlations were the same as for compound **11**.

The absolute configuration of spicellamide B was also determined by Marfey's method. The HPLC-MS analysis gave the same configurations for the amino acid residues as deduced for **11** (*N*-Me-D-Phe, *N*-Me-L-Ala, L-Ala and D-Ala). Analysis by chiral HPLC revealed the configuration of the 2-hydroxyisocaproic acid residue as L, whereas 2,3-dihydroxyisovaleric acid, however could not be detected after acid hydrolysis due to its instability under acidic conditions. Literature reports proposed that during acidic hydrolysis 2,3-dihydroxy acids dehydrate and decarboxylate (Luesch *et al.*, 2000). Therefore, the configuration of 2,3-dihydroxyisovaleric acid in **12** could not be determined. However, due to the high structural homology of depsipeptides **11** and **12** and the close to identical spectroscopic data we suggested the same configuration for both compounds. For compound **12** the trivial name spicellamide B is proposed.

**Table 4-3-2.** 1D and 2D NMR spectral data for compound **2** ( $\delta$  in ppm;  $J$  in Hz)

Carbon	$\delta_C^{a,c}$	$\delta_H^{a,c}$	COSY <sup>b,c</sup>	HMBC <sup>b,d</sup>	NOESY <sup>b,c</sup>
1	170.1				
2	60.9	4.04 (q; 6.71)	3	1, 3, 4, 5	3, 4
3	13.7	1.53 (d; 6.71)	2	1, 2	2
4	37.3	3.29 (s)		2, 5	2, 6, 7 <sup>w</sup>
5	172.4				
6	46.8	4.81 (quint; 6.71)	7	5, 7, 8	4, 7, 9 <sup>w</sup>
7	18.2	1.32 (d; 6.71)	6	5, 6	6, 17 <sup>w</sup>
8	168.6				
9	57.5	5.62 (dd; 5.19, 11.60)	10	8, 10, 17, 18	10, 12, 13, 15-17
		3.34 (dd; 5.19, 14.95)	9, 12-16	8, 9, 11-16	9, 12, 13, 15, 16
10	33.6	2.93 (dd; 11.60, 14.95)			
11	138.9				
12	129.7	7.23 (m)	10, 13-16	10, 11	9, 10, 17, 19, 21-23 <sup>w</sup>
13	129.0	7.25 (m)	10, 12, 14-16	10, 11	9, 10, 17, 19, 21-23 <sup>w</sup>
14	127.1	7.18 (m)	10, 12, 13, 15, 16	10, 11	21-23 <sup>w</sup>
15	129.0	7.25 (m)	10, 12-14, 16	10, 11	9, 10, 17, 19, 21-23 <sup>w</sup>
16	129.7	7.23 (m)	10, 12-15	10, 11	9, 10, 17, 19, 21-23 <sup>w</sup>
17	29.5	3.0 (s)		9, 18	7 <sup>w</sup> , 9, 12-16, 19, 22 <sup>w</sup> , 23 <sup>w</sup>
18	172.9				
19	71.4	5.18 (dd; 5.49, 8.54,)	20, 21	18, 20, 21	17, 21-23, 26 <sup>w</sup>
20	39.8	1.48 (m)	19, 21	21, 22, 23	
		1.18 (m)			
21	24.5	1.16 (m)	19, 20, 22, 23	22, 23	12-16 <sup>w</sup> , 19, 22, 23
22	22.8	0.75 (d; 6.41)	21		12-16 <sup>w</sup> , 19, 21
23	23.2	0.79 (d; 6.41)	21		12-16 <sup>w</sup> , 19, 21
24	172.9				
25	47.6	4.89 (dq; 8.59, 7.32)	26	24, 26, 27	26
26	19.5	1.45 (d; 7.32)	25	24, 25	19 <sup>w</sup> , 22 <sup>w</sup> , 23 <sup>w</sup> , 25, 30 <sup>w</sup>
27	170.5				
28	77.3	5.04 (s)	30, 31	1, 27, 29, 30, 31	30, 31
29	72.2				
30	25.0	1.21 (s)	28	28, 29	26 <sup>w</sup> , 28
31	26.9	1.11 (s)	28	28, 29	28
NH (1)		6.98 (d; 6.71)			
NH (2)		8.23 (d; 8.59)			

<sup>a</sup> Acetone-d<sub>6</sub>, 300 MHz. <sup>b</sup> Acetone-d<sub>6</sub>, 500 MHz. <sup>c</sup> Assignments are based on extensive 1D and 2D NMR measurements (HMBC, HSQC, COSY, NOESY). <sup>d</sup> Numbers refer to carbon resonances. <sup>w</sup> Weak signal.

Cytotoxicity of both compounds was tested in neuroblastoma cells. Compound **12** exhibited an IC<sub>50</sub> value of 6.2 µg/mL while compound **11** was less cytotoxic with an IC<sub>50</sub> value of 30 µg/mL. In agar diffusion assay both depsipeptides were inactive up to a concentration of 50 µg/plate.

Spicellamide A (**11**): colorless solid (1.5 mg);  $[\alpha]_D^{24} - 59.5^\circ$  (*c* 0.12 MeOH); UV(MeOH)  $\lambda$  250-300 nm (br);  $\lambda_{\max}$  (log  $\epsilon$ ) 203 (4.64), 205 (4.62), 208 (4.60), 227 sh (4.45) nm; IR (ATR)  $\gamma_{\max}$  3364, 2925, 2457, 2361, 1742, 1638, 1454, 1236 cm<sup>-1</sup>; <sup>1</sup>H and <sup>13</sup>C NMR spectral data (see Table 4-3-1); HREIMS *m/z* 602.3312 (calcd for C<sub>31</sub>H<sub>46</sub>N<sub>4</sub>O<sub>8</sub> 602.3316).

Spicellamide B (**12**): colorless solid (1.0 mg);  $[\alpha]_D^{24} - 19.04^\circ$  (*c* 0.11 MeOH); UV(MeOH)  $\lambda_{\max}$  (log  $\epsilon$ ) 203 (4.26), 205 (4.15), 208 (4.04); IR (ATR)  $\gamma_{\max}$  3323, 2926, 2359, 1745, 1638, 1456, 1417, 1230 cm<sup>-1</sup>; <sup>1</sup>H and <sup>13</sup>C NMR spectral data (see Table 4-3-2); HREIMS *m/z* 618.3256 (calcd for C<sub>31</sub>H<sub>46</sub>N<sub>4</sub>O<sub>9</sub> 618.3265).

## 4.4 Lipopeptides from the strain *Fusarium dimerum* complex (Strain number 18)

### 4.4.1 Introduction

Microorganisms are well known producers of biosurfactants that attracted researchers attention in the last 20 years (Cameotra and Makkar, 2004; Singh and Cameotra, 2004). Surfactants are amphiphilic compounds which can reduce surface and interfacial tensions. Due to these properties they increase the solubility, mobility, bioavailability of hydrophobic or insoluble organic compounds. Biosurfactants play an important role in motility of microorganisms and take part in cellular signalling and differentiation as well as in biofilm formation (antibiotic resistance by bacteria) (Van Hamme *et al.*, 2006). Literature distinguishes high- and low-molecular mass surfactants (Rosenberg and Ron, 1999). The high-molecular mass surfactants are proteins, lipopolysaccharides and lipoproteins, while the low-molecular mass surfactants are glycolipids and lipopeptides. The most active and the most investigated cyclic lipopeptide is surfactin. Natural surfactin, produced by bacterial strain *Bacillus subtilis* (Arima *et al.*, 1968), includes a mixture of lipopeptides which differ in chain length of hydroxyl fatty acid residue and in amino acid substitutions of the peptide ring (Figure 4-4-1) (Kowall *et al.*, 1998). A similar surface-active compound, described as lichenysin A, was isolated from *Bacillus licheniformis* by Yakimov *et al.* (Yakimov *et al.*, 1995).

Fungal strain number 18 was identified as *Fusarium dimerum* complex that contains many *Fusarium* species (Centraalbureau voor Schimmelcultures, Utrecht, The Netherlands). *Fusarium* is a large genus of filamentous fungi distributed in soil and in association with plants and marine organisms. Some species produce mycotoxins that can contaminate food and affect human and animal health (Gelderblom *et al.*, 1998; Creppy, 2002). The *Fusarium* extract inhibited the growth of 6 cancer cell lines at the concentration of 30 µg/mL and exhibited an IC<sub>50</sub> value of 9.4 µg/mL. Mass spectra of the crude extract showed series of ions at  $m/z$  [M]<sup>+</sup> 951 to 1008, evidencing the presence of a peptide mixture.

### 4.4.2 Cultivation, extraction and isolation

The fungal strain (*Fusarium dimerum* complex, strain number 18, 193A 28) was cultivated on a solid biomalt medium containing antibiotics (benzyl penicillin and streptomycin sulphate, 250 mg / L). After the colonies were grown, the strain was transferred to a solid malt-yeast agar medium and cultivated in a big scale (10 L) for two months at room temperature. The fungal biomass and the media were homogenized using an Ultra-Turrax and the mixture was



extracted with EtOAc (4 x 8 L). After filtration, the filtrate was dried under reduced pressure to yield 2.5 g of orange extract. The fractionation of the extract by VLC (Si gel 60, 0.063-0.200 mm) with a petroleum ether - DCM - EtOAc - MeOH gradient yielded 11 fractions. In the cytotoxic assay fraction 8 was the most active with an IC<sub>50</sub> value of 8.5 µg/mL. Thus, it was further fractionated by reversed-phase VLC (Polygoprep 60 C<sub>18</sub>, 0.05 mm) with a MeOH - H<sub>2</sub>O gradient into 8 fractions. Of these, the last VLC fraction (eluted only with MeOH) was elucidated as a mixture of lipopeptides (**13**, 400 mg) which could not be further separated.

#### 4.4.3 Results and discussion

The <sup>1</sup>H NMR spectrum of fraction **13** displayed proton signals characteristic for α- and β-protons of a peptide structure, in the regions from 4.0 to 5.3 ppm and from 2.3 to 3.5 ppm, respectively. Also, the <sup>13</sup>C NMR spectrum showed carbonyl carbon signals between 168 and 177 ppm and α-carbon signals between 50 and 63 ppm. The DEPT spectrum revealed signals in the region from 24 to 31 ppm typically for alkyl groups. Taken together, <sup>1</sup>H and <sup>13</sup>C NMR data implied fraction **13** to be a mixture of chemically similar lipopeptides. Literature and data base search indicated similarities to biosurfactants, lichenysins and surfactins, isolated from different species of *Bacillus* (Bonmatin *et al.*, 1995; Yakimov *et al.*, 1995; Kowall *et al.*, 1998).

Surfactin, lichenysin A, B, C are mixtures of cyclic lipopeptides built from variants of a heptapeptide and β-hydroxy fatty acids with different chain lengths. The peptide moiety of surfactin contains two acidic residues (aspartate and glutamate) and five (four leucine and one valine) hydrophobic residues (Bonmatin *et al.*, 1995), whereas in lichenysin A either aspartate or glutamate are present in their amide form (Yakimov *et al.*, 1995) (Figure 4-4-1).

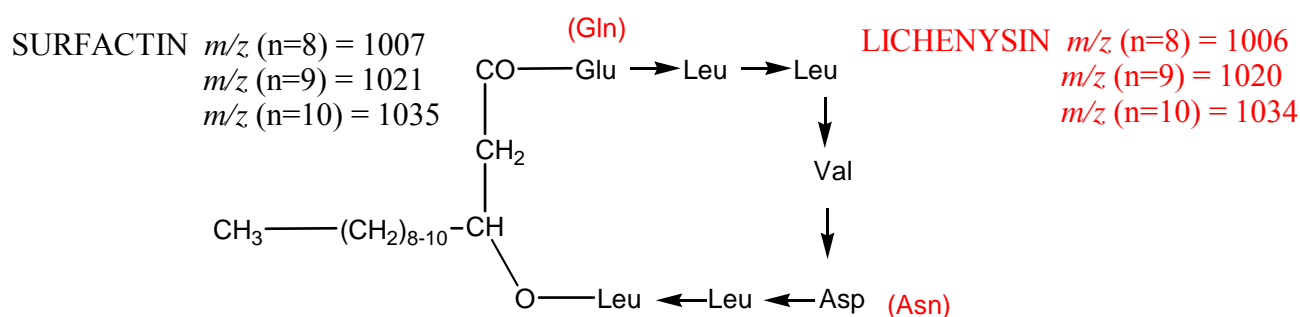


**Figure 4-4-1.** Structures of surfactin and lichenysin

The molecular weights of surfactin and lichenysin of different chain length are calculated considering suggested amino acid residues by Yakimov *et al.*, 1995. In the case when leucine is replaced with valine there is a difference of 14 Da.

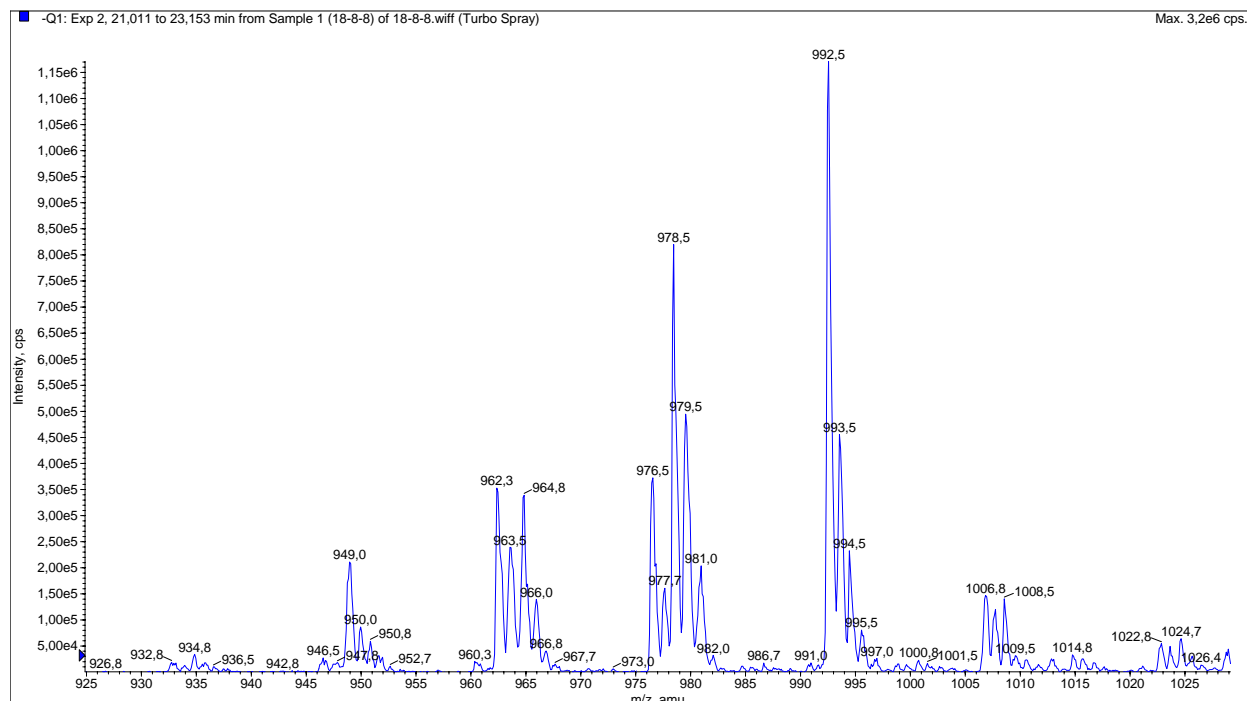
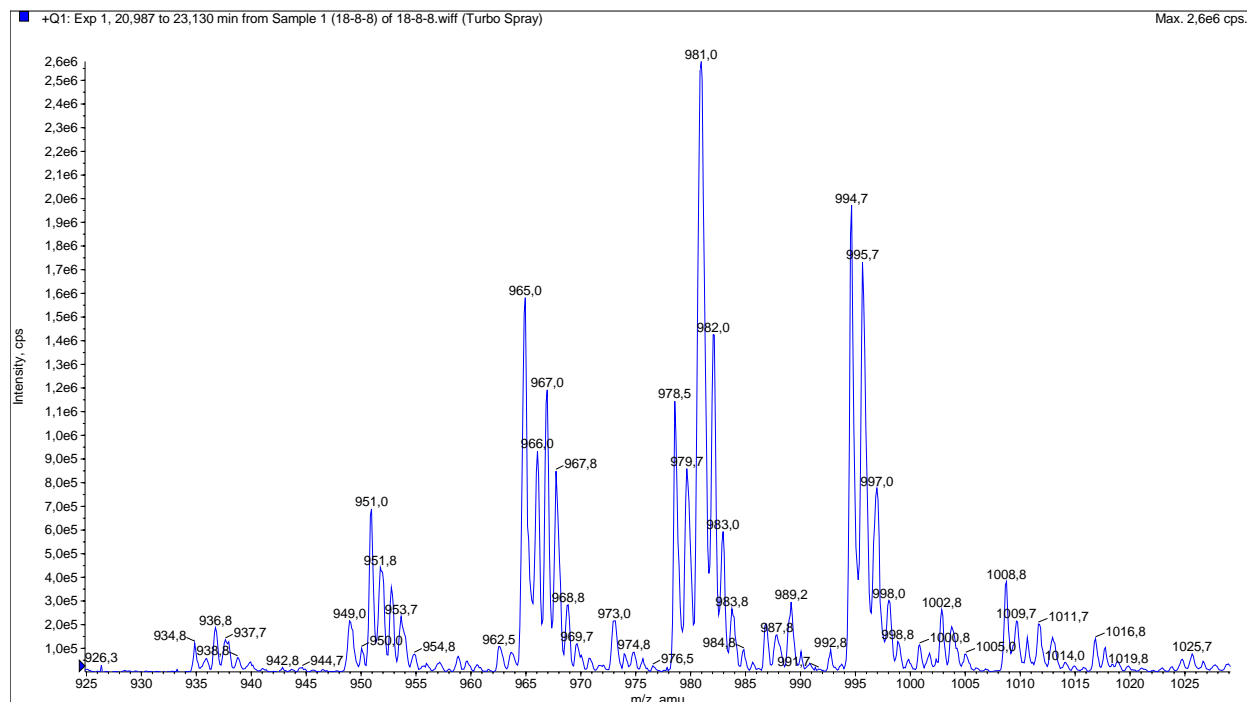
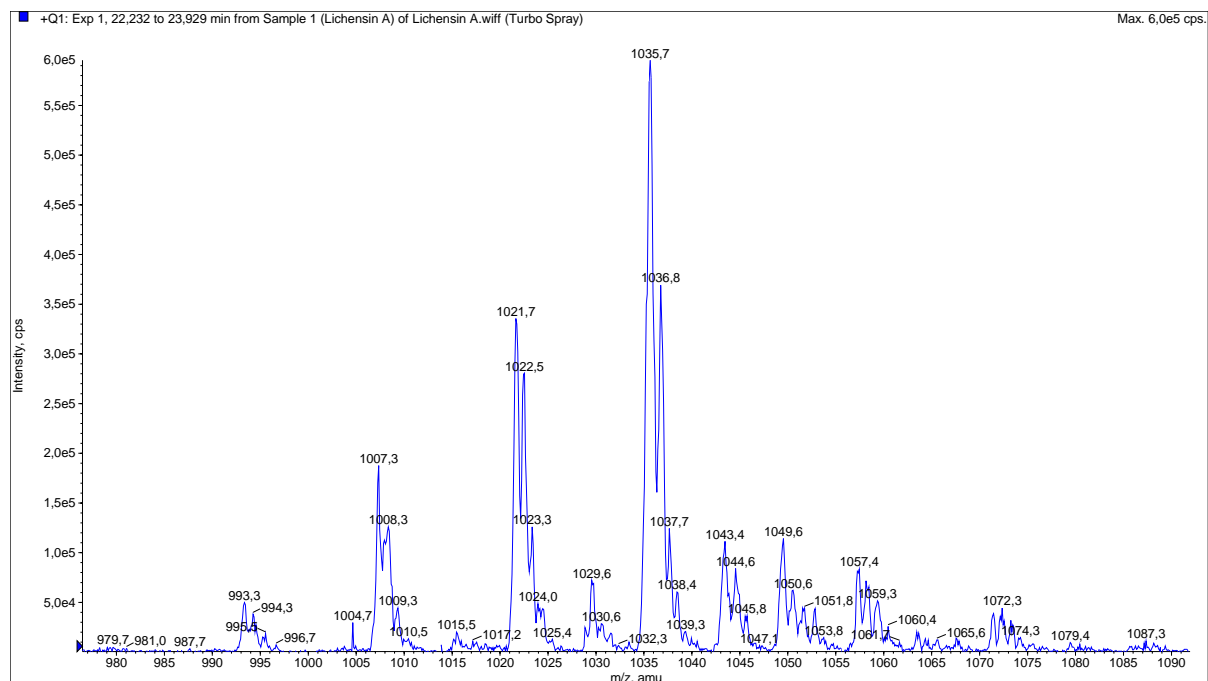


Figure 4-4-2. EIMS spectra of mixture 13.

A



B

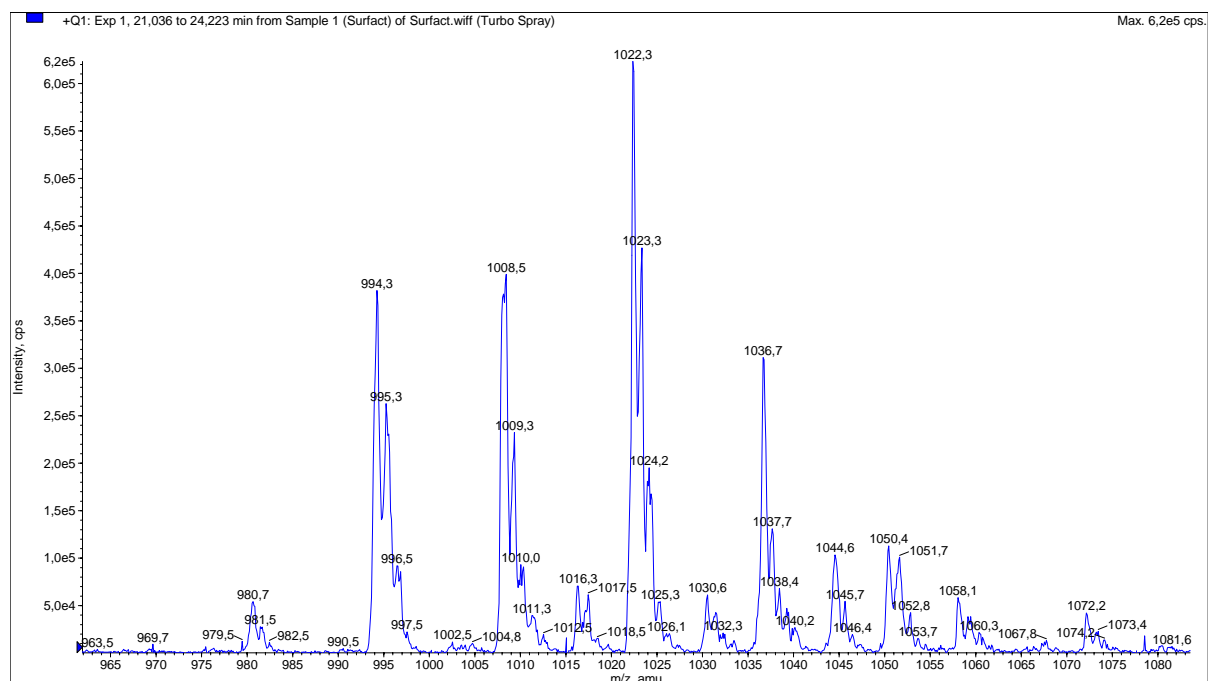


Figure 4-4-3. EIMS spectra of lichensin A (A) and surfactin (B) in positive mode.

The comparison of EIMS spectra of fraction **13** (Figure 4-4-2) to the spectra of both surfactin and lichenysin A (Figure 4-4-3) pointed to the resemblance of fraction **13** to both of them. As seen from mass spectra (Figure 4-4-3), lichenysin A consists of structural analogs that have even-numbered molecular weights ranging from 992 to 1034, while surfactin has odd-numbered molecular weights in the range from 979 to 1035. The difference of 1 Da in molecular weight is due to the presence of the amide form of either glutamic or aspartic acid in lichenysin A. The EIMS analysis of fraction **13** revealed series of ions at  $m/z$  951 to 1008 in the positive-ion mode and at  $m/z$  949 to 1006 in the negative-ion mode, implying a mixture of even- (950, 964, 978) and odd-numbered (979, 993, 1007) molecular weights. Mass shifts of 14 Da between structural analogs come from variations of fatty acid chain, or from replacement of leucine or isoleucine by valine (Horowitz and Griffin, 1991; Peypoux *et al.*, 1991). Literature describes surfactins and lichenysins as mixtures of lipopeptides which alter in lengths of fatty acid chain from C<sub>8</sub> to C<sub>15</sub> and in number of leucine and valine residues, e.g. in molecular weights from 979 to 1035 for surfactin and from 978 to 1034 for lichenysin A (Yakimov *et al.*, 1995; Kowall *et al.*, 1998). Analysis of mass spectra imparted fraction **13** (Figure 4-4-2) as a mixture of lichenysin and surfactin analogs. To confirm the exact structures of lipopeptide analogs further structural elucidation should be performed.

In antimicrobial tests fraction **13** exhibited an antibacterial activity inhibiting growth of *Bacillus megaterium* (2 mm) and *Microbotryum violaceum* (5 mm) at a concentration of 1 µg/µL. The antibacterial activity of surfactins and lichenysins was described previously (Yakimov *et al.*, 1995). *In vitro* antitumor assay revealed an IC<sub>50</sub> value of 7.7 µg/mL (see Appendix).

Since the isolation of surfactins and lichenysins has been reported only from bacteria, mostly from different species of *Bacillus* (Bonmatin *et al.*, 1995; Yakimov *et al.*, 1995; Kowall *et al.*, 1998), *Fusarium dimerum* was cultivated on media supplemented with antibiotics. Although classical microscopic studies did not reveal the presence of bacteria, it is possible that bacteria exist as endosymbionts in the fungus. Thus, further studies are necessary to shed light on the genuine producer organism of the lipopeptides.

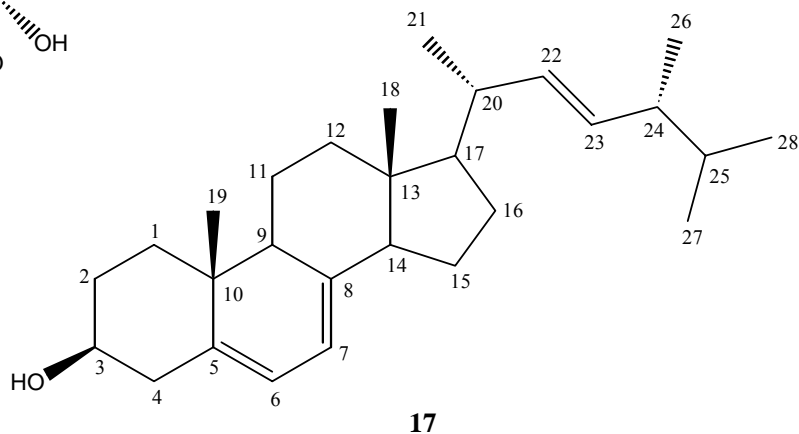
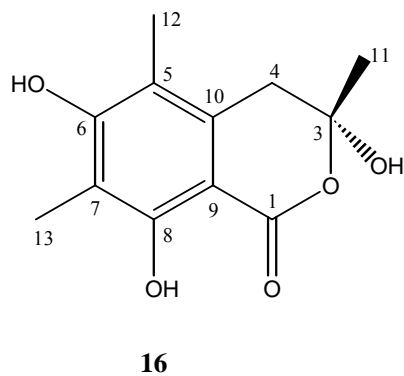
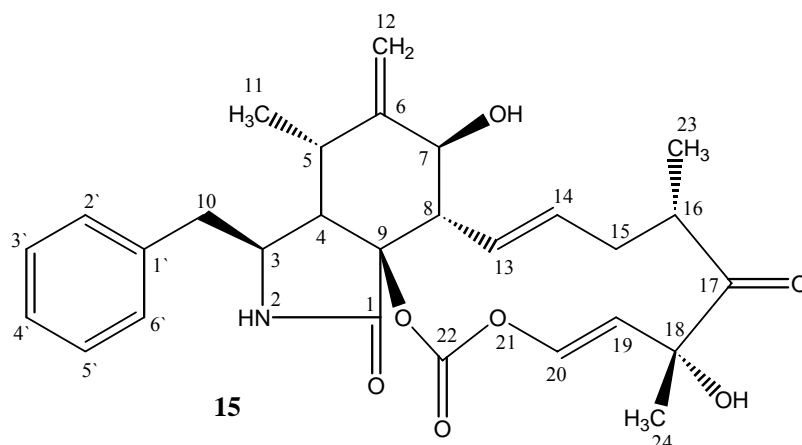
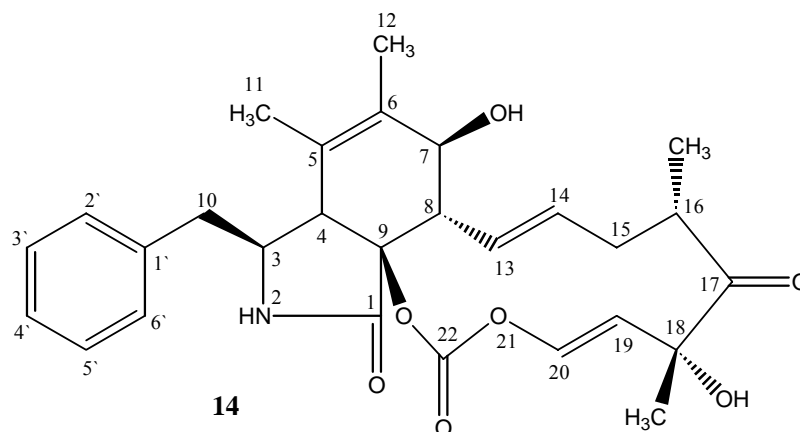
## 4.5 Secondary metabolites from selected marine fungi

### 4.5.1 *Arthrinium sacchari*

In the preliminary screening for antitumor activity in a 6 cell line panel, the extract of the fungus *Arthrinium sacchari* showed antitumor activity in 2 out of 6 cell lines (33%) and in 5 out of 6 cell lines (83%) at a concentrations of 3  $\mu\text{g/mL}$  and 30  $\mu\text{g/mL}$ , respectively. In agar diffusion assay the crude extract displayed inhibition zone against *Mycotypha microspora* of 4 cm at 250  $\mu\text{g/disc}$ . The biological activity in the mentioned assays and  $^1\text{H}$  NMR data addressed the fungus for detailed investigations.

The fungal strain (*Arthrinium sacchari*, strain number 727, Cro2 CA EtOHb) was cultivated at room temperature for one and a half month in Fernbach flasks. The solid biomalt medium (11 L) contained 20 g/L of Biomalt, 17 g/L agar and artificial seawater. Mycelia and medium were homogenized using an Ultra-Turrax®, and the mixture was extracted with EtOAc (3 x 8 L). After the evaporation of the organic phase, 4.6 g of dark red oil was obtained. The extract was applied on VLC (Si gel 60, 0.063-0.200 mm), with a  $\text{CH}_2\text{Cl}_2$ /acetone/MeOH gradient, to bring 11 fractions. In cytotoxic assay VLC fraction 3 revealed the highest activity with a mean  $\text{IC}_{50}$  value of 3.3  $\mu\text{g/mL}$  while all other fractions did not show desirable activity in concentration less than 30  $\mu\text{g/mL}$ . VLC fraction 3 was fractionated by another VLC (Si gel 60, 0.063-0.200 mm), with a  $\text{CH}_2\text{Cl}_2$ /EtOAc/MeOH gradient, into 10 further fractions. The cytotoxic activity was indicated to subfraction 3.5 (a mean  $\text{IC}_{50}$  value of 0.17  $\mu\text{g/mL}$ ) which was separated on reversed-phase HPLC (Macherey-Nagel Nucleodur 100-5  $\text{C}_{18}$ , 250 x 4.6 mm, 5  $\mu\text{m}$ ) with MeOH/ $\text{H}_2\text{O}$  (6:4; flow 0.8 mL/min) and yielded compounds **14** and **15**. Subfraction 3.2 was eluted with petroleum ether/acetone (8:2; flow 1.5 mL/min) on normal-phase HPLC column (Knauer Eurospher-100, C-8, 250 x 8 mm, 5  $\mu\text{m}$ ) and gave compounds **16** and **17**.

Structure elucidation of compounds **14-17** was accomplished with 1D and 2D NMR data, mass spectrometry and data base search. The structure of compounds **14** and **15** was assigned to group of cytochalasins, structure of **16** to coumarins and of **17** to sterols.



Cytochalasin K (**14**) and its  $\Delta^{6,12}$  isomer (**15**) are formally isolated from *Aspergillus clavatus* by Steyn and van Heerden (Steyn and van Heerden, 1982). In antitumor activity assay compounds **14** and **15** displayed a mean IC<sub>50</sub> value of 1.59  $\mu\text{g/mL}$  and 0.014  $\mu\text{g/mL}$ , respectively. At a concentration of 1  $\mu\text{g/mL}$  compound **15** showed higher activity inhibiting growth of 30 cell lines out of 36 (83 %), and at a concentration of 10  $\mu\text{g/mL}$  growth of 34 out

of 36 cell lines (94 %), while compound **14** inhibited 6 % (2/36) cell lines at 1  $\mu\text{g/mL}$  and 23/36 cell lines (64 %) at 10  $\mu\text{g/mL}$  (see Appendix).

Sclerotinin B (**16**) was first isolated by Sassa *et al.* (Sassa *et al.*, 1968) as plant growth promoting metabolite. In an antitumor assay compound **16** did not affect the growth of any cell type.

Ergosterol (**17**) is a common lipid produced by most of the fungi (Shirane *et al.*, 1996). Ergosterol showed a mean  $\text{IC}_{50}$  value of 4.67  $\mu\text{g/mL}$  inhibiting growth of 27 out of 36 cell lines (75 %) at a concentration of 10  $\mu\text{g/mL}$  without selectivity on a specific tumor type.

None of the compounds showed any activity in the agar diffusion assay.

Cytochalasin K (**14**) was isolated as white crystals (14.6 mg).  $^1\text{H}$  NMR (300 MHz,  $\text{CDCl}_3$ );  $\delta$  7.31 (2H, d,  $J = 6.95$ , H-3', H-5'), 7.28 (1H, s, H-4'), 7.15 (2H, d,  $J = 6.95$ , H-2', H-6'), 6.64 (1H, d,  $J = 11.34$ , H-20), 6.23-6.15 (1H, m, H-13), 5.65 (1H, d,  $J = 11.34$ , H-19), 5.43-5.33 (1H, m, H-14), 3.93-3.89 (2H, m, H-4, H-7), 3.52-3.48 (1H, m, H-3), 2.98-2.90 (1H, m, H-16), 2.84-2.66 (4H, m, H-8, H<sub>2</sub>-10, H-15a), 2.17 (1H, s, H-15b), 1.67 (3H, s, H<sub>3</sub>-11), 1.50 (3H, s, H<sub>3</sub>-18Me), 1.48 (3H, s, H<sub>3</sub>-12), 1.17 (3H, d,  $J = 6.59$ , H<sub>3</sub>-16Me);  $^{13}\text{C}$  NMR (75.5 MHz,  $\text{CDCl}_3$ )  $\delta$  211.5 (s, C-17), 170.2 (s, C-1), 149.0 (s, C-22), 142.4 (d, C-20), 136.6 (s, C-1'), 133.6 (d, C-14), 131.7 (s, C-5), 129.3 (d, C-2', C-6', C-13), 128.9 (d, C-3', C-5'), 127.1 (d, C-4'), 125.2 (s, C-6), 120.4 (d, C-19), 86.3 (s, C-9), 77.2 (s, C-18), 70.0 (d, C-7), 59.1 (d, C-3), 49.9 (d, C-8), 48.2 (d, C-4), 44.0 (t, C-10), 40.9 (d, C-16), 39.0 (t, C-15), 24.6 (q, C-18Me), 20.2 (q, C-16Me), 17.6 (q, C-12), 14.0 (q, C-11);  $\text{C}_{28}\text{H}_{33}\text{NO}_7$  (495.23);  $[\alpha]_D^{24} +23.8^\circ$  (c 0.45, MeOH).

$\Delta^{6,12}$  isomer of Cytochalasin K (**15**) was isolated as white crystals (9.7 mg).  $^1\text{H}$  NMR (300 MHz,  $\text{CDCl}_3$ );  $\delta$  7.32-7.29 (3H, brs, H-3', H-4', H-5'), 7.15-7.12 (2H, brs, H-2', H-6'), 6.54 (1H, d,  $J = 11.34$ , H-20), 5.77-5.68 (1H, m, H-13), 5.62 (1H, d,  $J = 11.34$ , H-19), 5.37 (1H, s, H-12a), 5.33-5.29 (1H, brs, H-14), 5.16 (1H, s, H-12b), 3.81 (1H, brs, H-7), 3.33 (2H, brs, H-3, H-5), 3.04-2.86 (4H, brs, H-4, H-8, H-10a, H-16), 2.73-2.58 (2H, brs, H-10b, H-15a), 2.17 (1H, s, H-15b), 1.50 (3H, s, H<sub>3</sub>-24), 1.16 (3H, s, H<sub>3</sub>-23), 1.11 (3H, s, H<sub>3</sub>-11);  $^{13}\text{C}$  NMR (75.5 MHz,  $\text{CDCl}_3$ )  $\delta$  211.8 (s, C-17), 169.2 (s, C-1), 152.7 (s, C-22), 149.5 (s, C-6), 142.2 (d, C-20), 136.6 (s, C-1'), 133.8 (d, C-14), 129.3 (d, C-2', C-6'), 128.9 (d, C-3', C-5'), 128.2 (d, C-

13), 127.2 (d, C-4'), 120.2 (d, C-19), 114.5 (t, C-12), 86.2 (s, C-9), 76.8 (s, C-18), 69.3 (d, C-7), 53.6 (d, C-3), 48.7 (d, C-8), 47.9 (d, C-4), 44.4 (t, C-10), 40.8 (d, C-16), 38.7 (t, C-15), 32.0 (d, C-5), 24.2 (q, C-24), 20.2 (q, C-23), 14.6 (q, C-11); C<sub>28</sub>H<sub>33</sub>NO<sub>7</sub> (495.23);  $[\alpha]_D^{24} +8.3^\circ$  (*c* 0.66, MeOH).

Sclerotinin B (**16**) was isolated as a pale brown solid (3.1 mg). <sup>1</sup>H NMR (300 MHz, (CD<sub>3</sub>)<sub>2</sub>CO); δ 3.85 (2H, s, H<sub>2</sub>-4), 2.57 (3H, s, H<sub>3</sub>-11), 2.14 (3H, s, H<sub>3</sub>-12), 2.13 (3H, s, H<sub>3</sub>-13); <sup>13</sup>C NMR (75.5 MHz, (CD<sub>3</sub>)<sub>2</sub>CO) δ 172.2 (s, C-1), 158.2 (s, C-6), 158.0 (s, C-8), 132.4 (s, C-10), 120.0 (s, C-7), 118.1 (s, C-5), 110.8 (s, C-3, C-9), 37.3 (t, C-4), 32.1 (q, C-11), 12.1 (q, C-12), 8.8 (q, C-13); C<sub>12</sub>H<sub>14</sub>O<sub>5</sub> (238.08);  $[\alpha]_D^{24} -15.1^\circ$  (*c* 0.28, MeOH).

Ergosterol (**17**) was isolated as amorphous white powder (2.8 mg). <sup>1</sup>H NMR (300 MHz, (CD<sub>3</sub>)<sub>2</sub>CO); δ 5.52 (1H, dd, *J* = 2.20, 5.85, H-6), 5.38-5.34 (1H, m, H-7), 5.26-5.22 (2H, m, H-22, H-23), 3.55-3.43 (1H, m, H-3), 2.39 (1H, d, *J* = 14.27, H-4a), 2.23 (1H, d, *J* = 14.27, H-4b), 2.09 (1H, s, H-20), 1.98-1.83 (5H, m, H<sub>2</sub>-2, H-9, H-16a, H-17), 1.81-1.75 (2H, m, H-1, H-24), 1.71-1.62 (3H, m, H<sub>2</sub>-11, H-15a), 1.50-1.45 (1H, m, H-25), 1.43-1.34 (2H, m, H-14, H-16b), 1.33-1.29 (1H, m, H-15b), 1.28 (2H, s, H<sub>2</sub>-12), 1.05 (3H, d, *J* = 6.59, H<sub>3</sub>-21), 0.93 (3H, s, H<sub>3</sub>-19), 0.91 (3H, s, H<sub>3</sub>-28), 0.85 (3H, d, *J* = 5.12, H<sub>3</sub>-27), 0.82 (3H, d, *J* = 5.12, H<sub>3</sub>-26), 0.66 (3H, s, H<sub>3</sub>-18); <sup>13</sup>C NMR (75.5 MHz, (CD<sub>3</sub>)<sub>2</sub>CO) δ 141.6 (s, C-5), 141.3 (s, C-8), 136.6 (d, C-23), 132.7 (d, C-22), 119.9 (d, C-6), 117.4 (d, C-7), 70.2 (d, C-3), 56.5 (d, C-14), 55.2 (d, C-17), 47.1 (d, C-9), 43.7 (d, C-24), 53.5 (s, C-13), 41.8 (t, C-4), 41.3 (d, C-20), 39.9 (t, C-12), 39.2 (t, C-1), 37.8 (s, C-10), 33.8 (d, C-25), 32.8 (t, C-2), 29.0 (t, C-16), 23.7 (t, C-15), 21.7 (t, C-11), 21.5 (q, C-21), 20.3 (q, C-27), 19.9 (q, C-26), 18.1 (q, C-28), 16.6 (q, C-19), 12.3 (q, C-18); C<sub>28</sub>H<sub>44</sub>O (396.34);  $[\alpha]_D^{24} -51.0^\circ$  (*c* 0.19, MeOH).

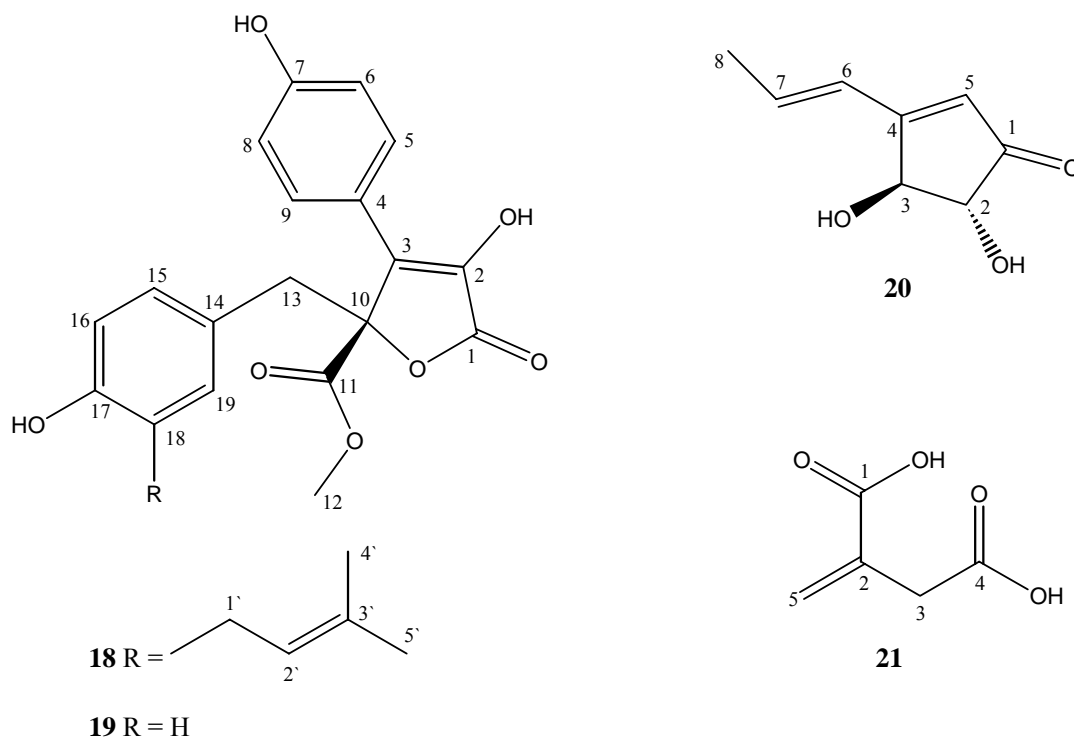
#### 4.5.2 *Aspergillus terreus*

*Aspergillus* species are highly aerobic and are found in almost all oxygen-rich environments. Some of the metabolites produced by *Aspergillus terreus*, like lovastatin – inhibitor of cholesterol synthesis, are of great clinical importance (Manzoni *et al.*, 1998). On the basis of the interesting <sup>1</sup>H NMR spectrum of the crude extract, the strain was chosen for further analysis.

Mycelia and 4L of solid biomalt medium were diluted with water (100 mL/L) and homogenized using an Ultra-Turrax® T25 at 5000 rpm for 2 minutes. The resulting mixture was exhaustively extracted with EtOAc (3 x 4 L), filtrated and evaporated under reduced



pressure to yield 2.0 g of dark red extract. The EtOAc extract was fractionated by VLC (Si gel 60, 0.063-0.200 mm), normal-phase silica (gradient dichloromethan – EtOAc - methanol) to give 16 fractions. According to  $^1\text{H}$  NMR spectral data fractions 4, 5 and 7 were further fractionated on normal-phase HPLC column (Knauer Si Eurospher-100, 250 x 8 mm, 5 $\mu\text{m}$ ) using different mixtures of petroleum ether and acetone. VLC fraction 4 was separated into compounds **18** (butyrolactone I) and **19** (butyrolactone II) with petroleum ether/acetone (7:3; flow 2.0 mL/min). VLC fraction 7 yielded terrein (**20**) with petroleum ether/acetone (1:1; flow 2.0 mL/min). And finally, elution of VLC fraction 5 with petroleum ether/acetone (7:3; flow 2.0 mL/min) afforded itaconic acid (**21**).



All compounds were previously isolated also from *Aspergillus terreus*. Butyrolactone I (**18**) and II (**19**) are first time described in 1983 (Nitta *et al.*, 1983), terrein (**20**) and itaconic acid (**21**) in 1935 (Raistrick and Smith, 1935).

In a cytotoxic assay and agar diffusion tests none of the compounds show significant activity (see Appendix).

Butyrolactone I (**18**) was isolated as red solid (73.2 mg).  $^1\text{H}$  NMR (300 MHz,  $(\text{CD}_3)_2\text{CO}$ );  $\delta$  9.06 (1H, s, 2-OH), 8.88 (1H, s, 7-OH), 8.08 (1H, s, 17-OH), 7.64 (2H, d,  $J = 8.78$ , H-5, H-9),

6.97 (2H, d,  $J = 8.78$ , H-6, H-8), 6.56 (2H, brs, H-16, H-19), 6.49 (1H, s, H-15), 5.07 (1H, t,  $J = 6.95$ , H-2'), 3.72 (3H, s, H<sub>3</sub>-12), 3.45 (2H, s, H<sub>2</sub>-13), 3.10 (2H, d,  $J = 6.95$ , H<sub>2</sub>-1'), 1.61 (3H, s, H<sub>3</sub>-4'), 1.54 (3H, s, H<sub>3</sub>-4'); <sup>13</sup>C NMR (75.5 MHz, (CD<sub>3</sub>)<sub>2</sub>CO)  $\delta$  170.9 (s, C-11), 168.6 (s, C-1), 158.8 (s, C-7), 154.7 (s, C-17), 139.0 (s, C-3), 132.4 (s, C-3'), 132.3 (d, C-15), 130.1 (d, C-5, C-9), 129.5 (d, C-19), 128.1 (s, C-2), 127.9 (s, C-14), 124.9 (s, C-18), 123.3 (d, C-2'), 122.8 (s, C-4), 116.6 (d, C-6, C-8), 115.0 (d, C-16), 85.9 (s, C-10), 53.7 (q, C-12), 39.2 (t, C-13), 28.5 (t, C-1'), 25.9 (q, C-4'), 17.7 (q, C-5'); C<sub>24</sub>H<sub>24</sub>O<sub>7</sub> (424.15);  $[\alpha]_D^{24} +55.4^\circ$  ( $c$  1.0, EtOH), (lit. (Nitta *et al.*, 1983);  $[\alpha]_D^{24} +86.0^\circ$  ( $c$  0.5, EtOH)).

Butyrolactone II (**19**) was isolated as dark orange solid (37.8 mg). <sup>1</sup>H NMR (300 MHz, (CD<sub>3</sub>)<sub>2</sub>CO);  $\delta$  7.69 (2H, d,  $J = 8.78$ , H-5, H-9), 7.01 (2H, d,  $J = 8.78$ , H-6, H-8), 6.72 (2H, d,  $J = 8.78$ , H-15, H-19), 6.62 (2H, d,  $J = 8.78$ , H-16, H-18), 3.83 (3H, s, H<sub>3</sub>-12), 3.53 (2H, s, H<sub>2</sub>-13); <sup>13</sup>C NMR (75.5 MHz, (CD<sub>3</sub>)<sub>2</sub>CO)  $\delta$  170.8 (s, C-11), 168.6 (s, C-1), 158.9 (s, C-7), 157.3 (s, C-17), 139.0 (s, C-3), 132.2 (d, C-15, C-19), 130.0 (d, C-5, C-9), 128.2 (s, C-2), 124.8 (s, C-14), 122.7 (s, C-4), 116.6 (d, C-6, C-8), 115.4 (d, C-16, C-18), 85.9 (s, C-10), 53.7 (q, C-12), 39.1 (t, C-13); C<sub>19</sub>H<sub>16</sub>O<sub>7</sub> (356.09);  $[\alpha]_D^{24} +42.5^\circ$  ( $c$  1.4, EtOH), (lit. (Nitta *et al.*, 1983);  $[\alpha]_D^{24} +85.0^\circ$  ( $c$  1.0, EtOH)).

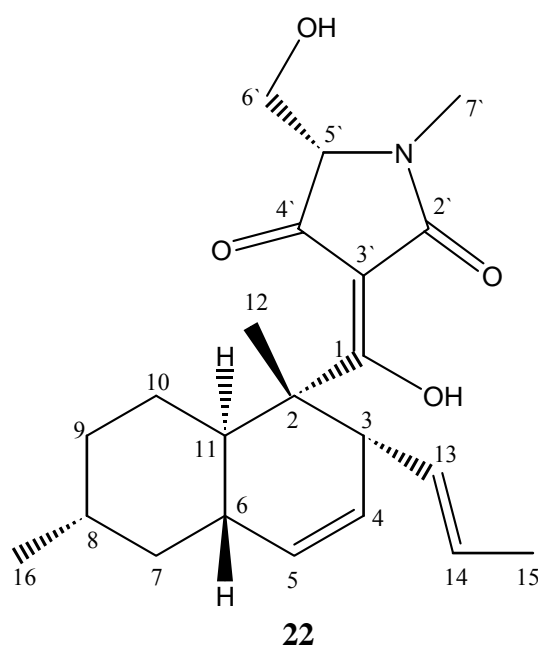
Terrein, 5,6-dihydroxy-4-(1-propenyl)cyclopent-4-en-7-one (**20**) was isolated as white crystals (140.7 mg). <sup>1</sup>H NMR (300 MHz, (CD<sub>3</sub>)<sub>2</sub>CO);  $\delta$  6.87-6.75 (1H, m, H-7), 6.42 (1H, d,  $J = 15.73$ , H-6), 5.95 (1H, s, H-5), 4.72 (1H, s, H-2), 4.07 (1H, d,  $J = 2.20$ , H-3), 1.89 (3H, dd,  $J = 1.46, 6.95$ , H<sub>3</sub>-8); <sup>13</sup>C NMR (75.5 MHz, (CD<sub>3</sub>)<sub>2</sub>CO)  $\delta$  203.6 (s, C-1), 169.1 (s, C-4), 140.1 (d, C-7), 126.3 (d, C-6), 125.7 (s, C-5), 82.2 (d, C-2), 77.8 (d, C-3), 19.3 (q, C-8); C<sub>8</sub>H<sub>10</sub>O<sub>3</sub>; (154.06);  $[\alpha]_D^{24} +168.0^\circ$  ( $c$  1.2, H<sub>2</sub>O), (lit. (Grove, 1954);  $[\alpha]_D^{24} +192.0^\circ$  ( $c$  0.2, H<sub>2</sub>O)).

Itaconic acid (**21**) was isolated as white crystals (132.6 mg). <sup>1</sup>H NMR (300 MHz, (CD<sub>3</sub>)<sub>2</sub>CO);  $\delta$  6.26 (1H, d,  $J = 1.10$ , H-5a), 5.80 (1H, d,  $J = 1.10$ , H-5b), 3.34 (2H, d,  $J = 1.10$ , H<sub>2</sub>-3); <sup>13</sup>C NMR (75.5 MHz, (CD<sub>3</sub>)<sub>2</sub>CO)  $\delta$  172.2 (s, C-1), 167.8 (s, C-4), 135.8 (s, C-2), 128.4 (t, C-5), 37.6 (t, C-3); C<sub>5</sub>H<sub>6</sub>O<sub>4</sub> (130.03).

#### 4.5.3 *Fusarium oxysporum*

The extract of the fungus *Fusarium oxysporum* exhibited an IC<sub>50</sub> value of 6.5  $\mu$ g/mL in *in vitro* antitumor assay inhibiting growth of 5 out of 6 cell lines in a concentration of 30  $\mu$ g/mL. Moreover, the screening tests in sphingolipid metabolism assay revealed an accumulation of

glucosylceramide (Figure 4-1-2). Therefore, the strain *Fusarium oxysporum* (strain number 588, Fr S1 5N) was selected for mass-cultivation (10 L (40 Fernbach flasks) of solid malt-yeast agar medium, room temperature for 3 months). The fungal biomass, including the medium, was homogenized using an Ultra-Turrax and the mixture was extracted with EtOAc (4 x 8 L). After evaporation of the organic phase 1.5 g of brown oil was obtained. The extract was fractionated by VLC (Si gel 60, 0.063-0.200 mm) with a petroleum ether - EtOAc - MeOH gradient, to yield 8 fractions. Fractions 3 and 4 were combined together according to  $^1\text{H}$  NMR and LC/MS data, and the cytotoxic assay in which they exhibited an  $\text{IC}_{50}$  value of 2.4  $\mu\text{g/mL}$  in a 6 cell line panel. In addition, both fractions induced an accumulation of glucosylceramide along with reduction of downstream glycosphingolipids. Thus, they were further fractionated by reversed-phase VLC (Polygoprep 60  $\text{C}_{18}$ , 0.05 mm) with a MeOH -  $\text{H}_2\text{O}$  gradient to give 5 fractions. Of these, fraction 2 was eluted with MeOH/ $\text{H}_2\text{O}$  (9:1) on reversed-phase HPLC (Macherey-Nagel Nucleodur 100-5  $\text{C}_{18}$ , 250 x 4.6 mm, 5  $\mu\text{m}$ , flow 2.5 mL) to yield compound **22**.



Structure elucidation of compound **22** was achieved with  $^1\text{H}$  and  $^{13}\text{C}$  NMR spectra, mass spectrometry and literature search. Equisetin was isolated previously by Phillips *et al.* (Phillips *et al.*, 1989) from *Fusarium equiseti*. In agar diffusion assay equisetin exhibited an antibacterial and antifungal activity inhibiting growth of *Bacillus megaterium* (11 mm), *Microbotryum violaceum* (5 mm), *Eurotium rubrum* (4 mm) and *Mycotypha microspora* (5

mm). Compound **22** also exhibited an IC<sub>50</sub> value of 4.8 µg/mL in *in vitro* antitumor activity assay.

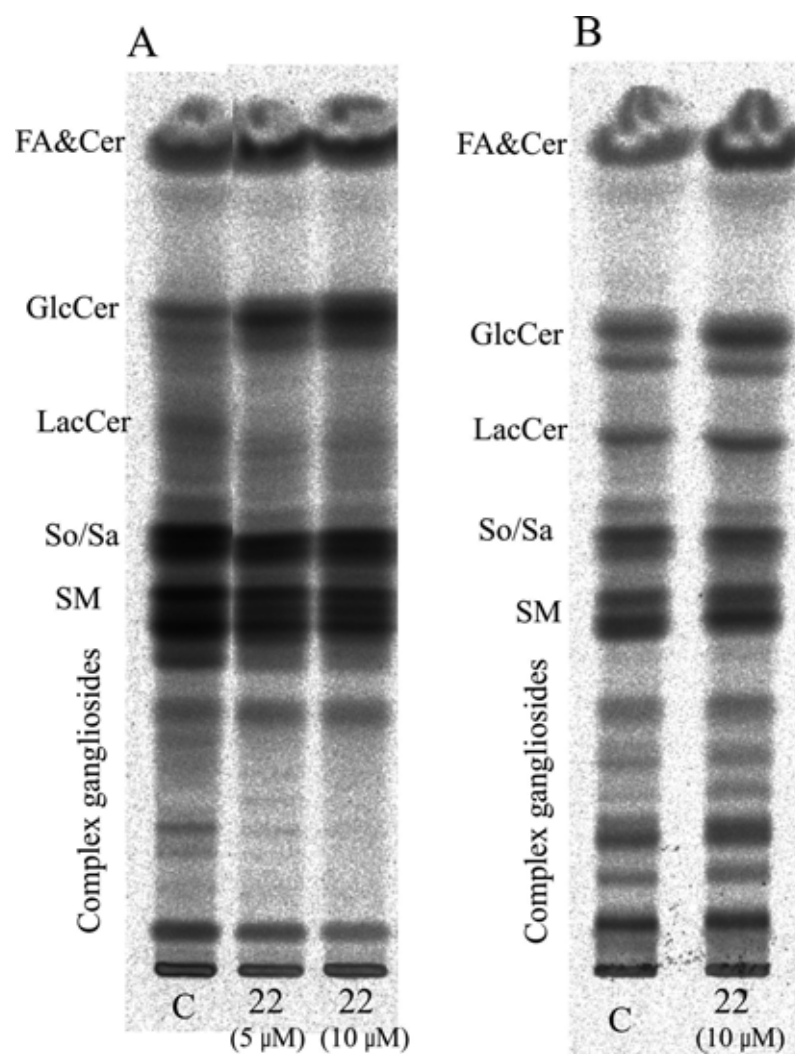


**Figure 4-5-1.** Effect of equisetin (**22**) on glycosphingolipid metabolism of neuroblastoma cells (A) and primary cultured neurons (B).

Cells were incubated in the absence (C, control) or presence of indicated concentrations of equisetin. After 4 h 1 µCi of [<sup>14</sup>C]serine was added to the medium. Twenty hours later cells were harvested and lipids were extracted, isolated, separated by TLC, and detected as described in Materials and Methods. TLC plates were developed in chloroform-methanol-0.22 % aqueous CaCl<sub>2</sub> (60:35:8; v/v/v). FA, fatty acids; Cer, ceramide; GlcCer, glucosylceramide; LacCer, lactosylceramide; So, sphingosine; Sa, sphinganine; SM, sphingomyelin; \*, unidentified bands.

The influence of equisetin on sphingolipid metabolism was studied by following the incorporation of L-[3-<sup>14</sup>C] serine into cellular sphingolipids of cerebellar neurons and neuroblastoma B104 cells. Incubation of neuroblastoma cells with 5 µM and 10 µM of equisetin revealed a 3fold increased content of GlcCer along with the reduced levels of

LacCer and complex gangliosides (Figure 4-5-1A), whereas in primary cultured neurons levels of glycosphingolipids in cell treated with compound **22** (10  $\mu$ M) were comparable with the control cells (Figure 4-5-1B). However, further experiments in neuroblastoma cells showed that the potency of equisetin to alter glycosphingolipid metabolism is dependent on cell confluence and the passage number of cell line. Thus, the experiments could not give reliable results and, for that reason, no further investigations were conducted.

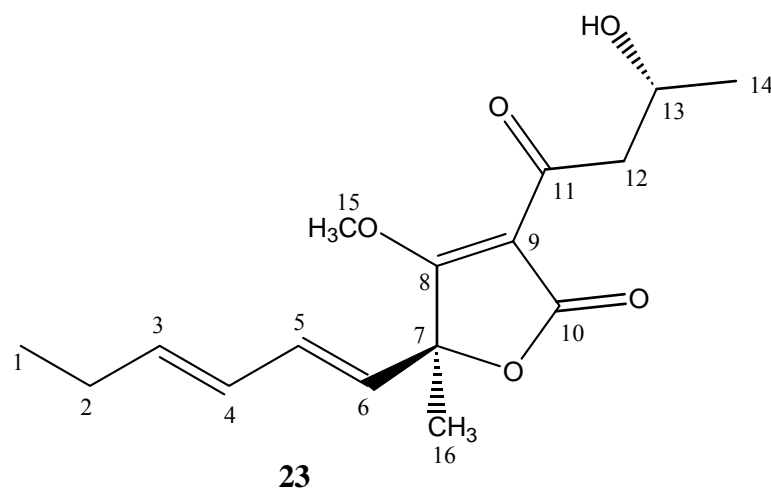
Equisetin (**22**) was isolated as colourless oil (65 mg).  $^1\text{H}$  NMR (300 MHz,  $(\text{CD}_3)_2\text{CO}$ );  $\delta$  5.40-5.39 (2H, brs, H-4, H-5), 5.23-5.21 (2H, brs, H-13, H-14), 4.00 (2H, dd,  $J = 3.50, 12.00$ , H<sub>2</sub>-6'), 3.70 (1H, t,  $J = 3.50, 7.00$ , H-5'), 3.37 (1H, s, H-3), 3.06 (3H, s, H<sub>3</sub>-7'), 2.08 (1H, s, H-10a), 1.85-1.79 (6H, m, H-6, H<sub>2</sub>-7, H<sub>2</sub>-9, H-11), 1.52 (1H, s, H-8), 1.56 (3H, d,  $J = 6.50$ , H<sub>3</sub>-15), 1.46 (3H, s, H<sub>3</sub>-12), 1.09 (1H, s, H-10b), 0.94 (3H, d,  $J = 6.50$ , H<sub>3</sub>-16);  $^{13}\text{C}$  NMR (75.5 MHz,  $(\text{CD}_3)_2\text{CO}$ )  $\delta$  197.1 (s, C-4'), 191.0 (s, C-1), 177.8 (s, C-2), 132.0 (d, C-5), 130.6 (d, C-13), 127.4 (d, C-4), 127.3 (d, C-14), 101.6 (s, C-3'), 68.8 (d, C-5'), 60.0 (t, C-6'), 45.7 (s, C-2), 49.0 (d, C-3), 43.0 (t, C-7), 39.4 (d, C-11), 39.2 (d, C-6), 36.4 (t, C-9), 34.1 (d, C-8), 28.7 (t, C-10), 27.5 (q, C-7'), 22.8 (q, C-16), 17.7 (q, C-15), 15.2 (q, C-12);  $\text{C}_{22}\text{H}_{31}\text{NO}_4$  (373.23);  $[\alpha]_{\text{D}}^{24} -99^\circ$  (c 1.13  $\text{CHCl}_3$ ).

#### 4.5.4 *Paecilomyces lilacinus*

The extract of the fungus *Paecilomyces lilacinus* inhibited growth of 2 out of 6 cancer cell lines at the concentration of 3  $\mu\text{g}/\text{mL}$  exhibiting an  $\text{IC}_{50}$  value of 0.09  $\mu\text{g}/\text{mL}$ . Also, preliminary tests on sphingolipid metabolism showed reduced levels of ceramide and glycosphingolipids (Figure 4-1-2) which addressed the fungus for detailed studies.

The fungus (*Paecilomyces lilacinus*, strain number 193, 195 21 W) was cultivated at room temperature for one month in 4 L of solid biomalt agar medium containing 20 g/L Biomalt, 17 g/L agar and artificial sea water. Mycelia and medium were homogenized using an Ultra-Turrax and the resulting mixture was exhaustively extracted with EtOAc and filtrated. The filtrate was evaporated under reduced pressure to yield 0.8 g of dark brown gum. The extract was fractionated by VLC (Si gel 60, 0.063-0.200 mm), with a hexane - petroleum ether – EtOAc – MeOH gradient, to yield 10 fractions. Unfortunately, none of the fractions and the extract by its self showed any alterations in sphingolipid metabolism. Thus, a bioassay-guided isolation was done according to the cytotoxic activity. Fractions 7 and 8 showed an  $\text{IC}_{50}$  value of 0.01  $\mu\text{g}/\text{mL}$  and of 0.9  $\mu\text{g}/\text{mL}$ , respectively, in a 6 cell line panel cytotoxic assay. Both fractions displayed similar  $^1\text{H}$  NMR and LC/MS spectra and, thus, were combined to be

fractionated by reversed-phase VLC (Polygoprep 60 C<sub>18</sub>, 0.05 mm) with a MeOH – H<sub>2</sub>O gradient to give 5 fractions. Of these, fraction 3 was purified on reversed-phase (Phenomenex Synergi Hydro-RP, 250 x 4.60 mm, 4 μm, flow 1.0 mL/min) HPLC with MeOH - H<sub>2</sub>O gradient into compound **23**.



Gregatin D was first isolated in 1975 by Kobayashi and Ui (Kobayashi and Ui, 1975) as phytotoxic substance. In our antitumor assay in a panel of 36 human tumor cell lines gregatin D displayed an IC<sub>50</sub> value of 9.4 μg/mL inhibiting growth of 3 out of 36 cell lines in a concentration of 30 μg/mL.

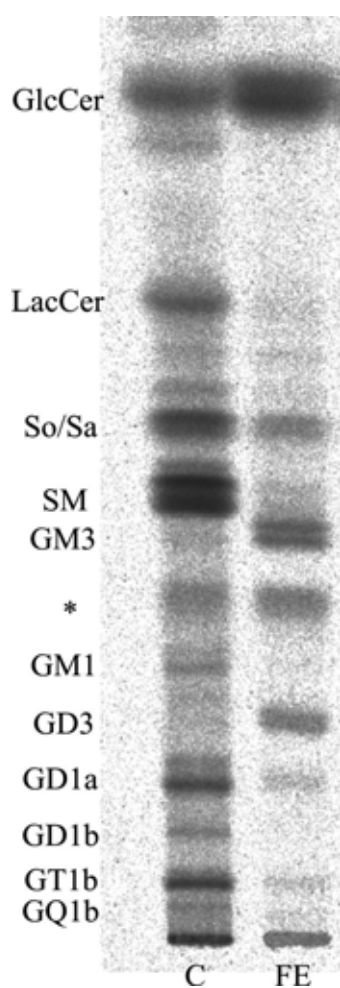
Compound **23** and the extract from mass cultivation did not show any effect on sphingolipid metabolism.

Gregatin D (**23**) was isolated as orange oil (14.8 mg). <sup>1</sup>H NMR (300 MHz, MeOD); δ 6.45-6.35 (1H, m, H-5), 6.03 (1H, t, *J* = 14.64, H-4), 5.90-5.82 (1H, m, H-3), 5.58 (1H, d, *J* = 14.64, H-6), 4.29 (1H, brs, H-13), 3.95-3.83 (5H, m, H<sub>2</sub>-12, H<sub>3</sub>-15), 2.14 (2H, t, *J* = 7.32, H<sub>2</sub>-2), 1.52 (3H, s, H<sub>3</sub>-16), 1.29 (3H, d, *J* = 5.85, H<sub>3</sub>-14), 1.04 (3H, t, *J* = 7.32, H<sub>3</sub>-1); <sup>13</sup>C NMR (75.5 MHz, MeOD) δ 206.4 (s, C-10), 197.5 (s, C-11), 170.0 (s, C-8), 140.3 (d, C-3), 133.4 (d, C-5), 129.2 (d, C-4), 126.7 (d, C-6), 112.4 (s, C-9), 92.1 (s, C-7), 66.9 (d, C-13), 56.7 (q, C-15), 49.5 (t, C-12), 26.7 (t, C-2), 24.0 (q, C-14), 22.7 (q, C-16), 13.8 (q, C-1); C<sub>16</sub>H<sub>22</sub>O<sub>5</sub> (294.15); [α]<sub>D</sub><sup>24</sup> + 102° (*c* 0.99 CHCl<sub>3</sub>), (lit. (Kobayashi and Ui, 1975); [α]<sub>D</sub><sup>24</sup> + 152.0° (*c* 0.93 CHCl<sub>3</sub>)).

## 4.6 Influence of fungal metabolites from the strain *Spicellum roseum* on sphingolipid metabolism

### 4.6.1 Alterations of glycosphingolipid profile by the extract of *Spicellum roseum*

Preliminary screening studies for the influence of fungal extracts on sphingolipid metabolism imparted the extract of fungal strain *Spicellum roseum* as a producer of metabolites with potential impact on SLs.



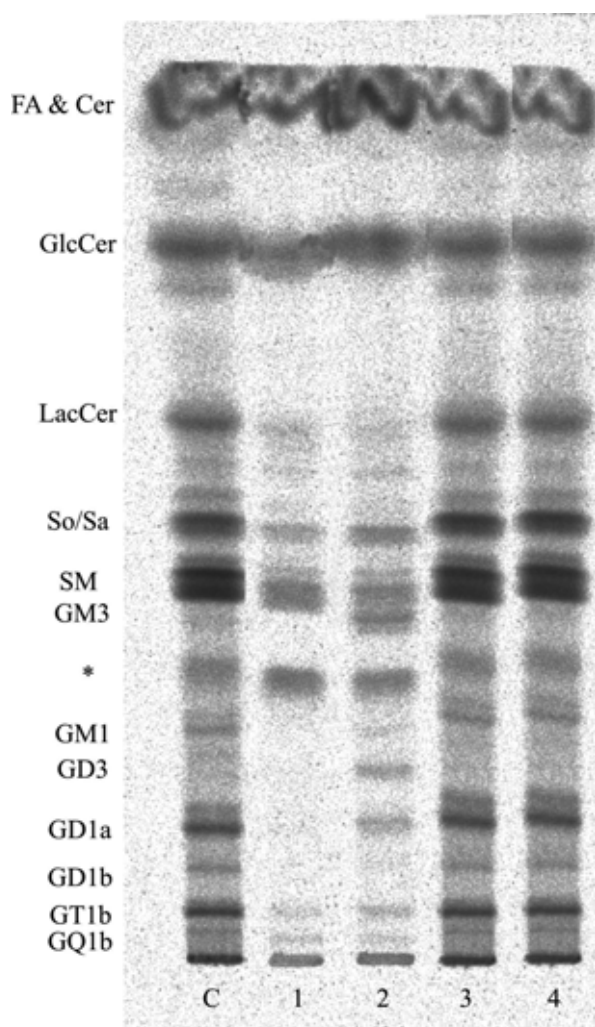
The effect of the fungal extract (FE) on *de novo* sphingolipid biosynthesis of cerebellar neurons was studied by following the incorporation of L-[3-<sup>14</sup>C] serine into cellular sphingolipids. Cells incubated with 10 µg/mL of FE exhibited an accumulation of GlcCer, GM3 and GD3 while the formation of LacCer and more complex gangliosides was reduced (Figure 4-6-1). These observations were similar to the effects of fungal metabolite brefeldin A (BFA), previously published by van Echten *et al.* (van Echten *et al.*, 1990b), with the exception concerning LacCer formation. In contrast to BFA that was shown to induce accumulation of newly formed LacCer (van Echten *et al.*, 1990b), the fungal extract clearly reduced its formation. Therefore, the extract of fungal strain *Spicellum roseum* was subjected to further investigation.

**Figure 4-6-1.** Influence of the fungal extract of strain *Spicellum roseum* on [<sup>14</sup>C] serine incorporation into sphingolipids of primary cultured neurons.

Cells were incubated in the absence (C, control) or presence of fungal extract (FE, 10 µg/mL). After 4 h 1 µCi of [<sup>14</sup>C]serine was added to the medium. Twenty hours later cells were harvested and lipids were extracted, isolated, separated by TLC, and detected as described in Materials and Methods. TLC plates were developed in chloroform-methanol-0.22 % aqueous CaCl<sub>2</sub> (60:35:8; v/v/v). The terminology of gangliosides (GQ1b, GT1b, GD1b, GD1a, GD3, GM1 and GM3) is according to Svenerholm (Svenerholm, 1963). GlcCer, glucosylceramide; LacCer, lactosylceramide; So, sphingosine; Sa, sphinganine; SM, sphingomyelin; \*, unidentified bands.

#### 4.6.2 Cultivation, extraction and bioassay-guided isolation

The fungal strain *Spicellum roseum* (strain number 74; 193 H 15) was isolated from the sponge *Ectyplasia perox* as previously described (Höller *et al.*, 2000). The strain was cultivated on a solid biomalt medium (10 L) for two months. The fungal biomass, together with media, was homogenized using an Ultra-Turrax® and extracted with EtOAc (3x8L). After the evaporation of the organic phase 4.0 g of dark brown extract was obtained. The extract was fractionated by VLC with a petroleum ether-acetone-methanol gradient into four fractions.



Primary cultured neurons were incubated with different VLC fractions and their influence on *de novo* SL synthesis was followed by incorporation of L-[3-<sup>14</sup>C] serine into cellular sphingolipids. Figure 4-6-2 clearly shows that cells treated with fractions 1 and 2 exhibited alterations of glycosphingolipids while cells treated with fractions 3 and 4 showed no difference in expression of SLs when compared to control cells. As seen on Figure 4-6-2, both fractions (1 and 2) increased the levels of GlcCer and reduced the levels of LacCer. Additionally, fraction 1 reduced the expression of all gangliosides which was less in the case for fraction 2. Therefore, VLC fractions 1 and 2 were addressed for further investigation and isolation of the compounds responsible for exhibited activity.

**Figure 4-6-2.** Influence of VLC fractions of the extract from *Spicellum roseum* on sphingolipid metabolism of primary cultured neurons.

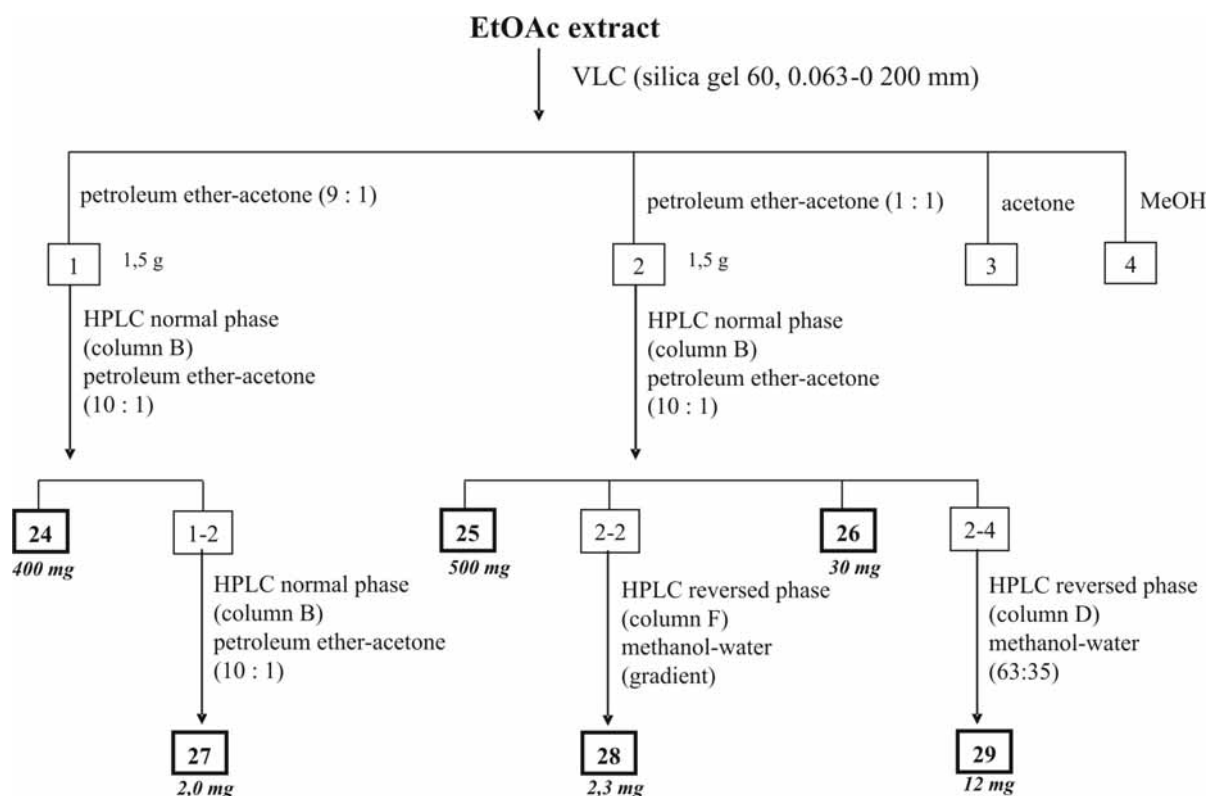
Cells were incubated in the absence (C, control) or presence of VLC fractions (1, 2, 3, 4; 10 µg/mL). After 4 h 1 µCi of [<sup>14</sup>C]serine was added to the medium. Twenty hours later cells were harvested and lipids were extracted, isolated, separated by TLC, and detected as described in Materials and Methods. TLC plates were developed in chloroform-methanol-0.22 % aqueous CaCl<sub>2</sub> (60:35:8; v/v/v). The terminology of gangliosides (GQ1b, GT1b, GD1b, GD1a, GD3, GM1 and GM3) is according to Svennerholm (Svennerholm, 1963). FA, fatty acids; Cer,



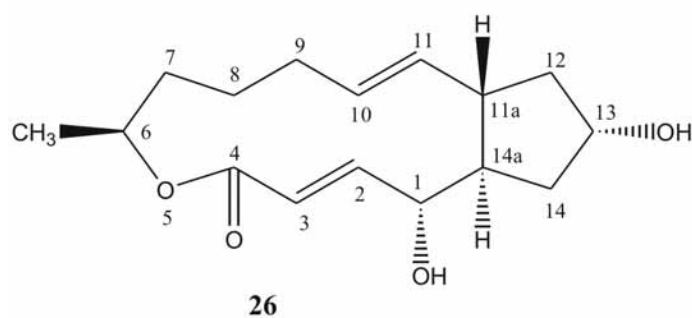
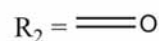
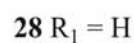
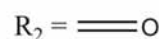
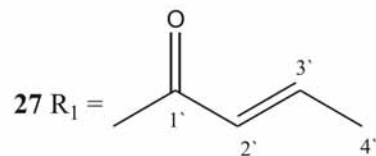
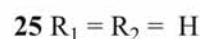
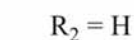
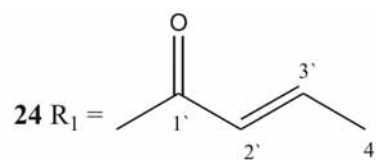
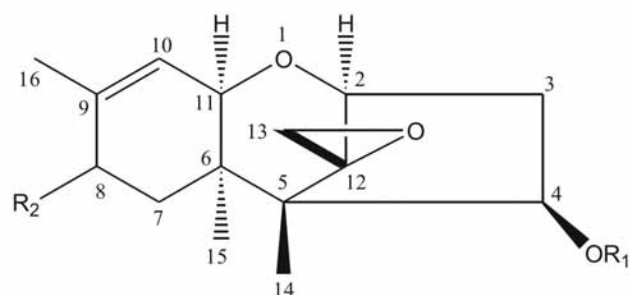
ceramide; SM, sphingomyelin; So, sphingosine; Sa, sphinganine; GlcCer, glucosylceramide; LacCer, lactosylceramide; \*, unidentified bands.

The fractionation of VLC fractions and the isolation of the compounds **24** – **29** are shown in Scheme 4-6-1.

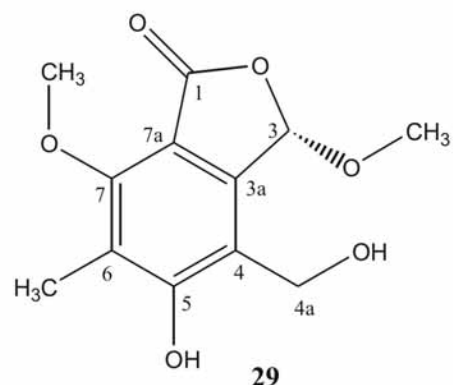
**Scheme 4-6-1.** Extract fractionation and the isolation of compounds **24-29**.



Structure elucidation of compounds **24-29** was accomplished with 1D and 2D NMR data, mass spectrometry and data base search. Compounds **24**, **25**, **27** and **28** are sesquiterpenoid metabolites that belong to the family of trichothecenes. Trichothecenes have various effects on eukaryotic cells. Their biological activity will be discussed later (Chapter 4.6.4). Isolation, chemical characteristics and biosynthetic studies of trichothecenes are well described in literature – compounds **25**, **27**, **28** (Hanson *et al.*, 1974), compound **24** (Plattner *et al.*, 1988; Tanaka *et al.*, 2001). The  $^1\text{H}$  and  $^{13}\text{C}$  NMR data of brefeldin A (**26**) were similar with those published by Glaser *et al.* (Glaser *et al.*, 2000). Compound **29** was described previously (Achenbach *et al.*, 1985).



26



29

8-deoxy-trichothecin (**24**) was isolated as colorless oil (400 mg).  $^1\text{H}$  NMR (300 MHz,  $(\text{CD}_3)_2\text{CO}$ );  $\delta$  6.45-6.34 (1H, m, H-3'), 5.77 (1H, dd,  $J = 1.83, 11.34$ , H-2'), 5.63 (1H, dd,  $J = 3.66, 7.68$ , H-4), 5.33 (1H, d,  $J = 5.12$ , H-10), 3.66-3.62 (2H, m, H-2, H-11), 3.00 (1H, d,  $J = 4.39$ , H-13a), 2.80 (1H, d,  $J = 4.39$ , H-13b), 2.48 (1H, dd,  $J = 8.05, 15.32$ , H-3a), 2.11 (3H, dd,  $J = 1.83, 6.95$ , H<sub>3</sub>-4'), 1.96-1.85 (4H, m, H-3b, H-7a, H<sub>2</sub>-8), 1.66 (3H, s, H<sub>3</sub>-16), 1.45-1.41 (1H, m, H-7b), 0.93 (3H, s, H<sub>3</sub>-15), 0.67 (3H, s, H<sub>3</sub>-14);  $^{13}\text{C}$  NMR (75.5 MHz,  $(\text{CD}_3)_2\text{CO}$ )  $\delta$  166.5 (s, C-1'), 145.9 (d, C-3'), 139.3 (s, C-9), 121.4 (d, C-2'), 120.4 (d, C-10), 79.6 (d, C-2), 75.3 (d, C-4), 71.1 (d, C-11), 66.0 (s, C-12), 49.8 (s, C-5), 47.8 (t, C-13), 41.1 (s, C-6), 37.3 (t, C-3), 28.6 (t, C-8), 25.1 (t, C-7), 23.3 (q, C-16), 16.2 (q, C-15), 15.5 (q, C-4'), 6.2 (q, C-14);  $\text{C}_{19}\text{H}_{26}\text{O}_4$  (318.18);  $[\alpha]_{\text{D}}^{24} -5.5^\circ$  ( $c$  1.0, MeOH).

Trichodermol (**25**) was isolated as white crystals (500 mg).  $^1\text{H}$  NMR (300 MHz,  $(\text{CD}_3)_2\text{CO}$ );  $\delta$  5.29 (1H, d,  $J = 5.49$ , H-10), 4.38 (1H, dd,  $J = 3.29, 7.32$ , H-4), 3.55 (1H, d,  $J = 5.12$ , H-2), 3.49 (1H, d,  $J = 5.49$ , H-11), 2.91 (1H, d,  $J = 4.76$ , H-13a), 2.70 (1H, d,  $J = 4.76$ , H-13b),

2.39 (1H, dd,  $J = 7.32, 15.37$ , H-3a), 1.93-1.90 (3H, m, H-7a, H<sub>2</sub>-8), 1.77-1.75 (1H, m, H-3b), 1.63 (3H, s, H<sub>3</sub>-16), 1.42-1.39 (1H, m, H-7b), 0.81 (3H, s, H<sub>3</sub>-15), 0.73 (3H, s, H<sub>3</sub>-14); <sup>13</sup>C NMR (75.5 MHz, (CD<sub>3</sub>)<sub>2</sub>CO)  $\delta$  139.0 (s, C-9), 120.7 (d, C-10), 79.7 (d, C-11), 73.4 (d, C-4), 70.9 (d, C-2), 66.1 (s, C-12), 49.5 (s, C-5), 47.1 (t, C-13), 40.7 (s, C-6), 40.2 (t, C-3), 28.6 (t, C-8), 25.1 (t, C-7), 23.2 (q, C-16), 16.0 (q, C-15), 6.4 (q, C-14); C<sub>15</sub>H<sub>22</sub>O<sub>3</sub> (250.16);  $[\alpha]^{24}_{\text{D}} - 26.6^{\circ}$  ( $c$  1.0, CHCl<sub>3</sub>), (lit. (Krohn *et al.*, 2003);  $[\alpha]^{24}_{\text{D}} - 30.0^{\circ}$  ( $c$  0.1, CHCl<sub>3</sub>)).

Brefeldin A (**26**) was isolated as white crystals (30 mg). <sup>1</sup>H NMR (300 MHz, MeOD);  $\delta$  7.50 (1H, dd,  $J = 3.29, 15.37$ , H-2), 5.89 (1H, d,  $J = 1.83$ , H-3), 5.84-5.75 (1H, m, H-10), 5.32 (1H, dd,  $J = 8.78, 14.27$ , H-11), 4.87-4.79 (1H, m, H-6), 4.26 (1H, t,  $J = 5.12$ , H-13), 4.08 (1H, d,  $J = 1.83$ , H-1), 2.49-2.38 (1H, m, H-11a), 2.21-2.12 (1H, m, H-12a), 2.06-2.01 (2H, m, H-9a, H-14x), 1.94-1.79 (5H, m, H-7a, H-8a, H-9b, H-14y, H-14a), 1.67-1.58 (1H, m, H-7b), 1.53-1.44 (1H, m, H-12b), 1.28 (3H, d,  $J = 6.22$ , H<sub>3</sub>-15), 0.99-0.88 (1H, m, H-8); <sup>13</sup>C NMR (75.5 MHz, MeOD)  $\delta$  168.3 (s, C-4), 155.1 (d, C-2), 138.1 (d, C-11), 131.4 (d, C-10), 117.8 (d, C-3), 76.6 (d, C-1), 73.2 (d, C-6), 73.0 (d, C-13), 53.2 (d, C-14a), 45.5 (d, C-11), 44.1 (t, C-12), 41.8 (t, C-14), 35.0 (t, C-7), 33.0 (t, C-9), 28.0 (t, C-8), 21.1 (q, C-15); C<sub>16</sub>H<sub>24</sub>O<sub>4</sub> (280.17);  $[\alpha]^{24}_{\text{D}} + 89.7^{\circ}$  ( $c$  1.6, MeOH), (lit. (Härrilä *et al.*, 1963);  $[\alpha]^{24}_{\text{D}} + 96.0^{\circ}$  (MeOH)).

Trichothecin (**27**) was isolated as amorphous white solid (2.0 mg). <sup>1</sup>H NMR (500 MHz, CDCl<sub>3</sub>);  $\delta$  6.49 (1H, d,  $J = 4.76$ , H-10), 6.44-6.32 (1H, m, H-3'), 5.83 (1H, d,  $J = 11.71$ , H-2'), 5.58 (1H, q,  $J = 2.93, 6.95$ , H-4), 3.96-3.93 (2H, m, H-2, H-11), 3.14 (1H, d,  $J = 3.66$ , H-13a), 2.91-2.85 (2H, m, H-7a, H-13b), 2.63 (1H, dd,  $J = 8.05, 16.10$ , H-3a), 2.30 (1H, d,  $J = 14.64$ , H-7b), 2.15 (3H, d,  $J = 6.59$ , H<sub>3</sub>-4'), 1.92-1.89 (1H, m, H-3b), 1.83 (3H, s, H<sub>3</sub>-15), 1.07 (3H, s, H<sub>3</sub>-16), 0.72 (3H, s, H<sub>3</sub>-14); <sup>13</sup>C NMR (125 MHz, CDCl<sub>3</sub>)  $\delta$  198.7 (s, C-8), 166.2 (s, C-1'), 146.2 (d, C-3'), 138.2 (s, C-9), 137.1 (d, C-10), 120.3 (d, C-2'), 79.6 (d, C-2), 73.3 (d, C-4), 70.1 (d, C-11), 65.5 (s, C-12), 47.5 (s, C-5), 47.5 (t, C-13), 43.7 (s, C-6), 42.1 (t, C-7), 37.0 (t, C-3), 18.5 (q, C-16), 15.5 (q, C-4'), 15.4 (q, C-15), 5.7 (q, C-14); C<sub>19</sub>H<sub>24</sub>O<sub>5</sub> (332.16);  $[\alpha]^{24}_{\text{D}} + 22.0^{\circ}$  ( $c$  0.1, CH<sub>2</sub>Cl<sub>2</sub>), (lit. (Loukaci *et al.*, 2000);  $[\alpha]^{24}_{\text{D}} + 29.3^{\circ}$  ( $c$  1.59, CH<sub>2</sub>Cl<sub>2</sub>)).

Trichothecolone (**28**) was isolated as amorphous white solid (2.3 mg). <sup>1</sup>H NMR (500 MHz, (CD<sub>3</sub>)<sub>2</sub>CO);  $\delta$  6.47 (1H, dd,  $J = 1.46, 5.85$ , H-10), 4.42 (1H, dd,  $J = 3.29, 7.32$ , H-4), 3.94 (1H, d,  $J = 5.85$ , H-11), 3.72 (1H, d,  $J = 5.12$ , H-2), 2.98 (1H, d,  $J = 4.03$ , H-13a), 2.86-2.81 (2H, m, H-7a, H-13b), 2.52 (1H, dd,  $J = 7.32, 15.37$ , H-3a), 2.17 (1H, dd,  $J = 1.46, 15.37$ , H-7b), 1.93-1.85 (1H, m, H-3b), 1.71 (3H, s, H<sub>3</sub>-16), 0.92 (3H, s, H<sub>3</sub>-15), 0.75 (3H, s, H<sub>3</sub>-14);

$^{13}\text{C}$  NMR (125 MHz,  $(\text{CD}_3)_2\text{CO}$ )  $\delta$  199.1 (s, C-8), 138.7 (d, C-10), 137.6 (s, C-9), 80.4 (d, C-11), 72.6 (d, C-4), 70.5 (d, C-2), 66.1 (s, C-12), 49.7 (s, C-5), 46.8 (t, C-13), 44.0 (s, C-6), 42.8 (t, C-7), 40.2 (t, C-3), 18.4 (q, C-15), 15.3 (q, C-16), 6.1 (q, C-14);  $\text{C}_{15}\text{H}_{20}\text{O}_4$  (264.14);  $[\alpha]_{\text{D}}^{24} +25.0^\circ$  (*c* 0.2,  $\text{CHCl}_3$ ), (lit. (Loukaci *et al.*, 2000);  $[\alpha]_{\text{D}}^{24} +22.5^\circ$  (*c* 1,  $\text{CHCl}_3$ )).

3-*O*-Alkylcyclopolacid (**29**) was isolated as pale yellow solid (12.0 mg).  $^1\text{H}$  NMR (300 MHz, MeOD);  $\delta$  6.73 (1H, s, H-3), 4.0 (8H, d,  $J = 2.56$ ,  $\text{H}_3\text{-1}'$ ,  $\text{H}_3\text{-2}'$ ,  $\text{H}_2\text{-4a}$ ), 2.26 (3H, s,  $\text{H}_3\text{-6Me}$ );  $^{13}\text{C}$  NMR (75.5 MHz, MeOD)  $\delta$  169.3 (s, C-1), 166.5 (s, C-7), 159.2 (s, C-5), 149.2 (s, C-3a), 115.4 (s, C-6), 108.0 (s, C-4), 107.6 (s, C-7a), 97.0 (d, C-3), 65.3 (t, C-4a), 56.9 (q, C-1'), 56.4 (q, C-2'), 10.3 (q, C-6Me);  $\text{C}_{12}\text{H}_{14}\text{O}_6$  (254.08);  $[\alpha]_{\text{D}}^{24} -0.4^\circ$  (*c* 0.9, MeOH).

### 4.6.3 Brefeldin A – uncoupling of ganglioside biosynthesis

Primary cultured neurons were incubated with isolated pure compounds **24-29** and their interference with glycosphingolipid (GSL) metabolism was studied using [ $^{14}\text{C}$ ] galactose as the radioactively labeled precursor.

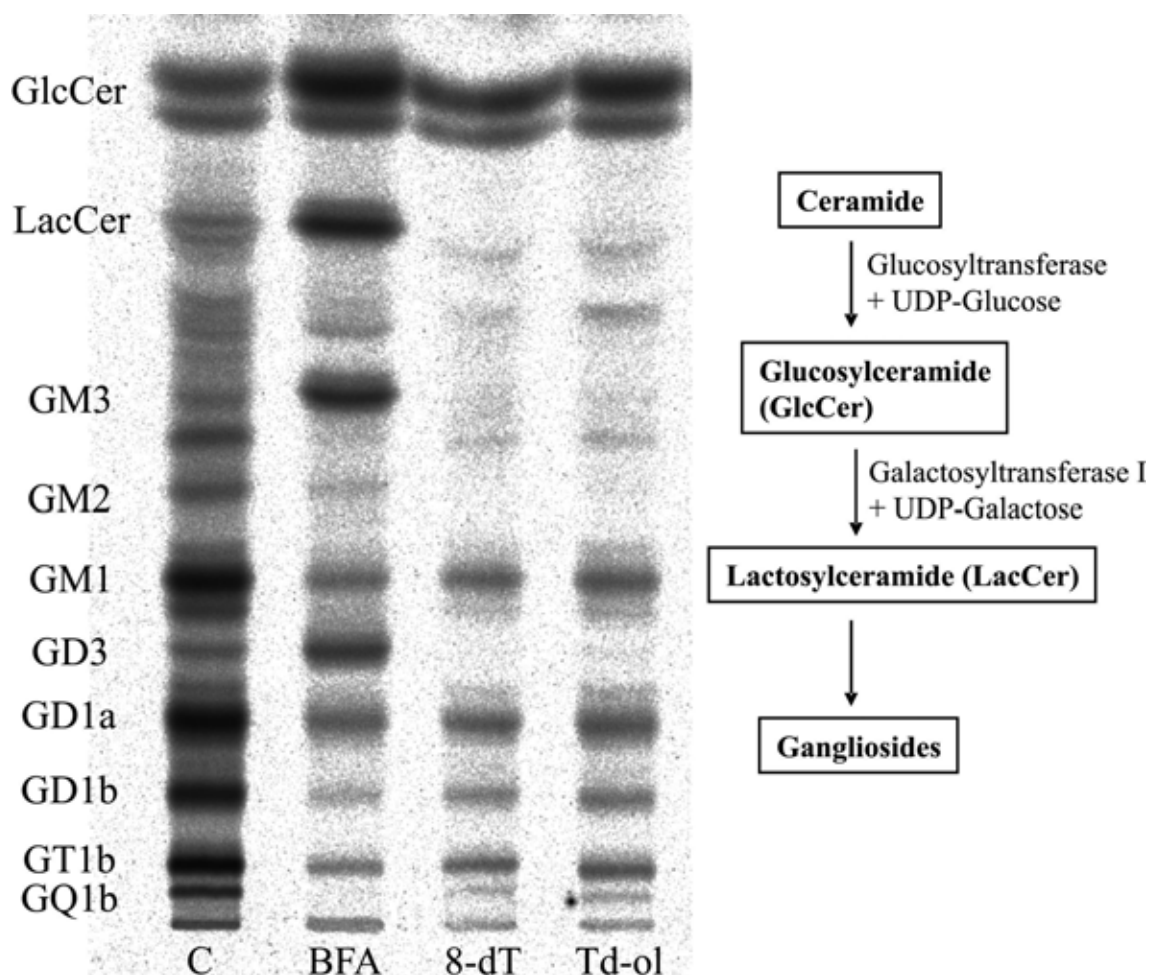


**Figure 4-6-3.** Effect of brefeldin A and of two tricothecenes isolated from *Spicellum roseum* crude extract on the incorporation of [ $^{14}\text{C}$ ] galactose into glycosphingolipids of primary cultured cerebellar neurons.

Cells were incubated in the absence (C, control) or presence of brefeldin A (BFA, 20  $\mu\text{M}$ ), 8-deoxy-trichotheclin (8-dT, 30  $\mu\text{M}$ ) or trichodermol (Td-ol, 30  $\mu\text{M}$ ). After 4 h 1 $\mu\text{Ci}$  of [ $^{14}\text{C}$ ]galactose was added into the medium. Twenty hours later cells were harvested and lipids were extracted, isolated, separated by TLC, and visualized as described in *Materials and Methods*. TLC plates were developed in chloroform-methanol-0.22 % aqueous  $\text{CaCl}_2$  (60:35:8; v/v/v). The terminology of gangliosides (GQ1b, GT1b, GD1b, GD1a, GD3, GM1, GM2 and GM3) is according to Svenerholm (Svenerholm, 1963). GlcCer, glucosylceramide; LacCer, lactosylceramide.

Brefeldin A (BFA, **26**) induced the accumulation of labeled GlcCer, LacCer, GM3 and GD3 (Figure 4-6-3) confirming previously published data (van Echten *et al.*, 1990b; Sadeghlar *et*

*al.*, 2000). Brefeldin A (26), a macrocyclic lactone, is a fungal metabolite originally isolated from *Penicillium brefeldianum* (Härri *et al.*, 1963). It has been reported that BFA blocks protein transport from the endoplasmatic reticulum (ER) to Golgi. This causes a redistribution of the proximal Golgi into the ER and a block of transport from these compartments to the distal Golgi (Donaldson and Klausner, 1994). Since GlcCer, LacCer, GM3 and GD3 are synthesized in the proximal Golgi (Figure 4-6-4), BFA uncouples ganglioside biosynthesis beyond GM3 and GD3 and, in that way, causes the accumulation of GlcCer, LacCer, GM3 and GD3 in cells (van Echten *et al.*, 1990b; Sadeghlar *et al.*, 2000).

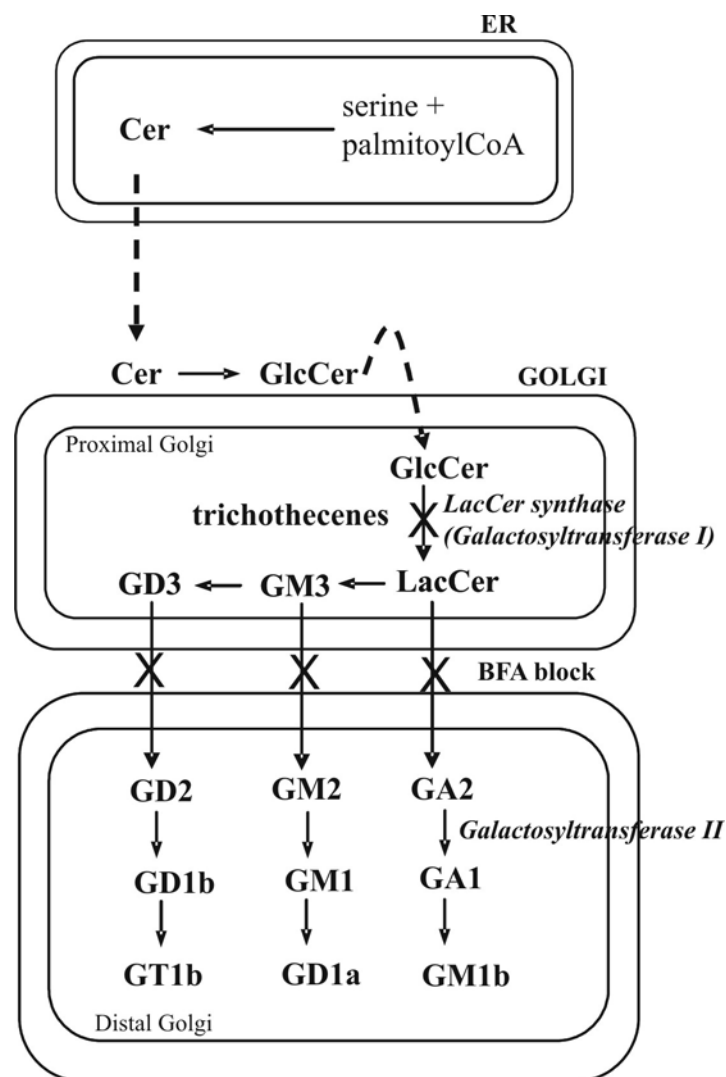


**Figure 4-6-4.** Scheme of glycosphingolipid biosynthesis.

Modified from Giraud and Maccioni (Giraud and Maccioni, 2003). ER, endoplasmatic reticulum; Cer, ceramide; GlcCer, glucosylceramide; LacCer, lactosylceramide; BFA, brefeldin A. The terminology of gangliosides (GM3, GD3, GD2, GM2, GA2, GD1b, GM1, GA1, GT1b, GD1a, GM1b) is according to Svenerholm (Svenerholm, 1963).

#### 4.6.4 Effect of trichothecene derivatives on glycosphingolipid metabolism

As shown in Figure 4-6-3, cells treated with trichothecene derivatives, 8-deoxy trichothecin (8-dT, **24**) or trichodermol (Td-ol, **25**), exhibited accumulation of GlcCer whereas the formation of LacCer and of all other GSLs located distal of LacCer was markedly impeded. The bands representing more complex gangliosides, which are metabolically derived from GM3 and GD3, can be explained by the glycosylation of the respective endogenous precursors to act as acceptors for the added [ $^{14}\text{C}$ ] galactose (van Echten *et al.*, 1990a). These findings led to the assumption that the two trichothecenes interfere with LacCer formation in neurons (see also Figure 4-6-4).

The other two isolated compounds from the trichothecene family, trichothecin (**27**) and trichothecolone (**28**), showed the same effect as compounds **24** (8-dT) and **25** (Td-ol) (data not shown). Therefore, all further experiments were performed only with compounds **24** and **25**, and the obtained results were taken as equivalence for compounds **27** and **28**.

Compound **29** did not show any modification on sphingolipid pathway.

The influence of 8-deoxy-trichothecin (8-dT, **24**) and trichodermol (Td-ol, **25**) on sphingolipid biosynthesis was studied in primary cultured cerebellar neurons and neuroblastoma cells by following the incorporation of L-[3- $^{14}\text{C}$ ] serine into cellular sphingolipids. In cells incubated for 24 hours with 8-dT (30  $\mu\text{M}$ ) and Td-ol (30  $\mu\text{M}$ ) a 3fold increased content of *de novo* formed GlcCer was detected along with a 5fold reduced amount of LacCer as well as of all downstream gangliosides, when compared with control cells (Figure 4-6-5). These results indicate that 8-dT as well as Td-ol blocked the formation of LacCer thereby causing the accumulation of GlcCer. As shown in Figure 4-6-5, formation of sphingomyelin and of long chain sphingoid bases was not affected. Note that in the presence of the applied trichothecene concentration for 24 hours cell viability always amounted about 70 % of untreated controls.

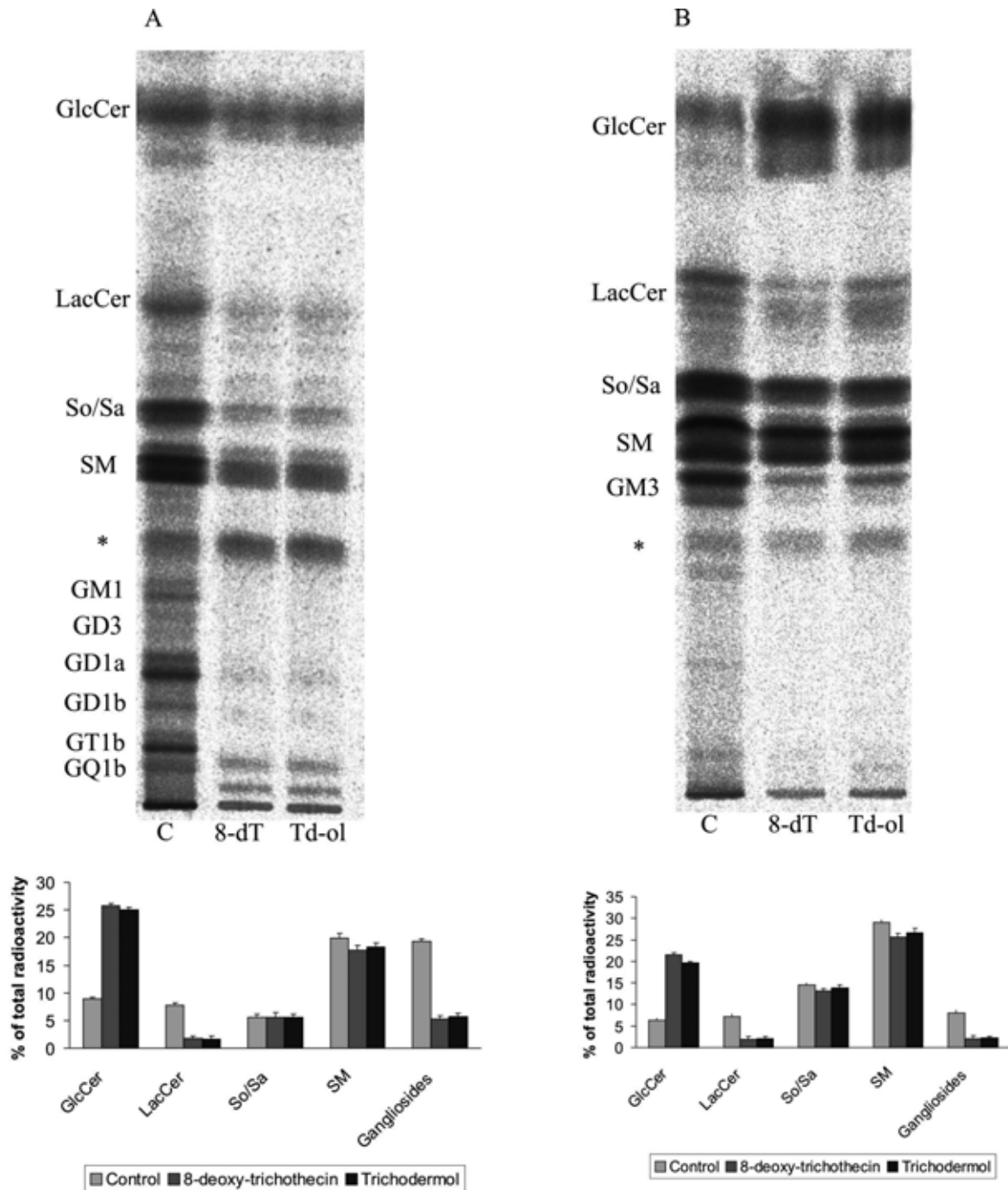


**Figure 4-6-5.** Effect of 8-deoxy-trichothechin and trichodermol on [ $^{14}\text{C}$ ] serine incorporation into sphingolipids of primary cultured cerebellar neurons (A) and neuroblastoma B104 cells (B).

Cells were incubated in the absence (C, control) or presence of 30  $\mu\text{M}$  8-deoxy-trichothechin (8-dT) or trichodermol (Td-ol), as indicated. After 4 h 1  $\mu\text{Ci}$  of [ $^{14}\text{C}$ ]serine was added to the medium. Twenty hours later cells were harvested and lipids were extracted, isolated, separated by TLC, visualized by autoradiography and quantitatively evaluated as described under Materials and Methods. TLC plates were developed in chloroform-methanol-0.22 % aqueous  $\text{CaCl}_2$  (60:35:8; v/v/v). In the two histograms the amount of radioactivity determined in the respective lipid fraction is expressed relative to total lipid associated radioactivity. Data are from one representative out of three independent experiments that gave similar results. Note that the content of de novo



formed sphingomyelin (SM) and also of free long chain bases (So/Sa) is not affected by tricothecenes in both cell types. The terminology of gangliosides (GQ1b, GT1b, GD1b, GD1a, GD3, GM1 and GM3) is according to Svennerholm (Svennerholm, 1963). GlcCer, glucosylceramide; LacCer, lactosylceramide; Sa, sphinganine; SM, sphingomyelin; So, sphingosine; \*, unidentified bands.

#### 4.6.4.1 Influence of tricothecenes on lactosylceramide synthase in neural cells

Reduction of lactosylceramide biosynthesis by tricothecenes could be due either to an inhibitory effect of these compounds on the enzyme responsible for LacCer formation by catalyzing the addition of galactose to GlcCer or to an interference of tricothecenes with the translocation of GlcCer from the cytosolic face where it is formed to the luminal face of the Golgi membrane where it is used for LacCer formation.

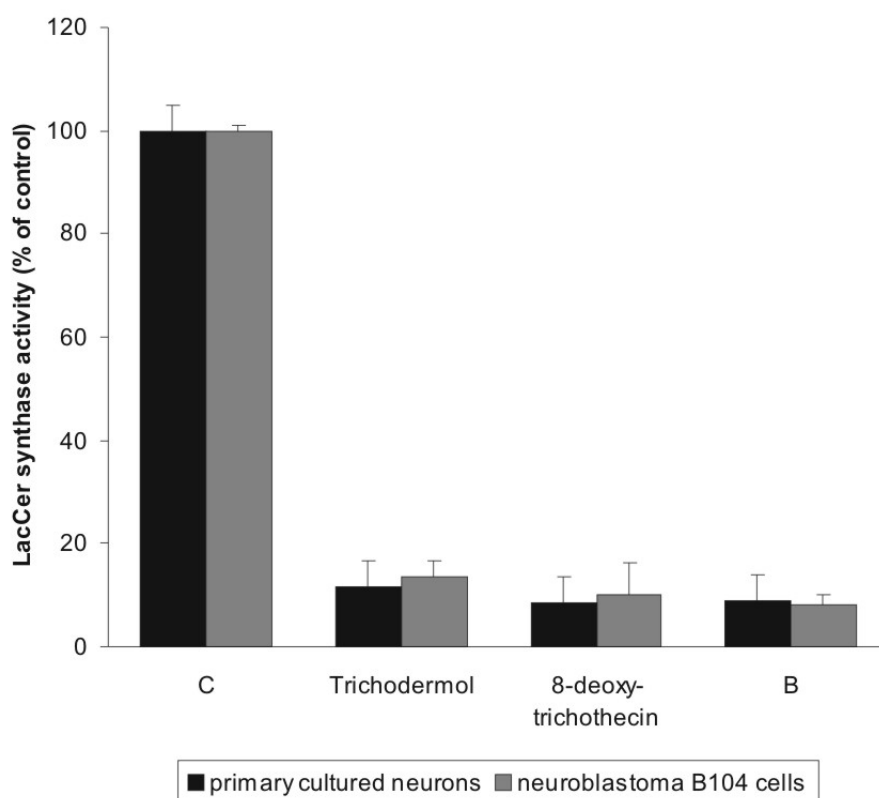


**Figure 4-6-6.** Effect of 8-deoxy-tricothecin and trichodermol on LacCer synthase of neural cells.

Cells were cultivated in the presence of 30  $\mu$ M of 8-deoxy-tricothecin (8-dT) or trichodermol (Td-ol), respectively. After 24 h cells were harvested and LacCer synthase activity was assessed in cell homogenate as described in Materials and Methods. Blanks (B) with boiled cell homogenate were run in parallel.

To examine both possibilities, we first analyzed whether tricothecenes act as inhibitors of LacCer synthase (galactosyltransferase I). Cells were preincubated prior to determination of

LacCer synthase activity for 24 h with 30  $\mu\text{M}$  of trichothecene derivatives. The results shown in Figure 4-6-6 reveal a decrease of LacCer synthase activity by about 90% in both cell types treated with trichodermol or 8-deoxy-trichothecin, when compared to control cells. This effect was concentration dependent (Figure 4-6-7) with half maximal inhibition at 0.5  $\mu\text{M}$  for 8-deoxy-trichothecin and 1  $\mu\text{M}$  for trichodermol. These findings demonstrate that 8-dT (**24**) and Td-ol (**25**) reduce catalytic activity of LacCer synthase in cultured cells.

However, *in vitro* the same concentrations of trichothecenes directly added to the assay mixture, exhibited no effect on LacCer synthase activity (data not shown). These observations indicate that cell integrity plays a crucial role for the effect of both, trichodermol and 8-deoxy-trichothecin on LacCer synthase activity.

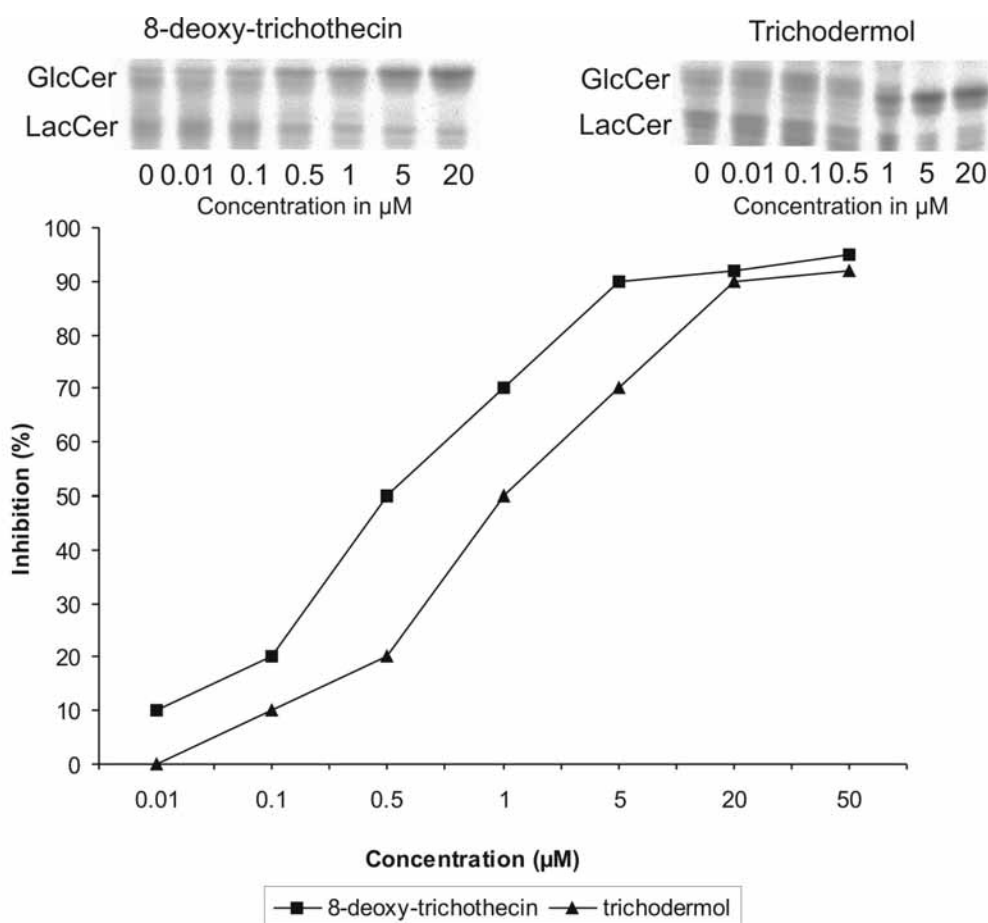


**Figure 4-6-7.** Concentration dependence of the effect of 8-deoxy-trichothecin and of trichodermol on the incorporation of [ $^{14}\text{C}$ ] serine into sphingolipids of neuroblastoma B104 cells.

Cells were incubated with the indicated concentrations of 8-deoxy-trichothecin (8-dT) and of trichodermol (Td-ol). After 4 h 1  $\mu\text{Ci}$  of [ $^{14}\text{C}$ ] serine was added into the cultured medium. After 20 h cells were harvested and lipids were extracted, isolated, separated by TLC, and detected as described under Materials and Methods. TLC

plates were developed in chloroform-methanol-0.22 % aqueous  $\text{CaCl}_2$  (60:35:8; v/v/v). The results are presented as percentages of control and are means from three independent experiments.

We then analyzed whether the compounds affect transcription of LacCer synthase. As illustrated in Figure 4-6-8A in neuroblastoma cells treated with 8-deoxy-trichothecin and trichodermol, respectively, transcription of LacCer synthase mRNA was markedly decreased amounting only about 20% of untreated controls. By contrast, in primary cultured neurons (Figure 4-6-8B) the level of mRNA was the same in control cells and in cells treated with trichothecenes. Collectively, these findings show that the trichothecene derivatives, 8-dT (**24**) and Td-ol (**25**), isolated from *Spicellum roseum* decrease LacCer synthase activity in both cell types, albeit by different mechanisms: in neuroblastoma cells they interfere with enzyme transcription, while in cerebellar neurons they act on a post-transcriptional level.

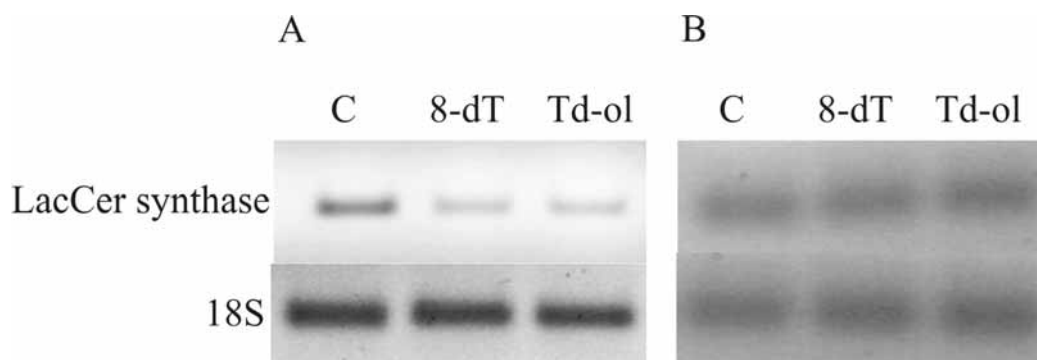


**Figure 4-6-8.** Effect of 8-deoxy-trichothecin and of trichodermol on mRNA levels of LacCer synthase in neuroblastoma B104 cells (A) and in primary cultured neurons (B).

Cells were incubated for 24 h in the absence (control) or presence of 8-deoxy-trichothecin (Td-ol, 30  $\mu\text{M}$ ) or of trichodermol (8-dT, 30  $\mu\text{M}$ ). Levels of LacCer synthase mRNA were determined by RT-PCR as described in Materials and Methods. Shown is one representative of three different experiments, each performed with double determinations.

#### 4.6.4.2 Influence of trichothecenes on galactosyltransferase II

Galactosyltransferase II catalyses the transfer of galactose from UDP-galactose to gangliosides GA2, GM2 and GD2 generating the formation of GA1, GM1 and GD1b, respectively (Figure 4-6-4). Galactosyltransferase I (LacCer synthase), whose activity was inhibited by trichothecenes (Chapter 4.6.4.1), shows 96 % identity with galactosyltransferase II in terms of amino acid sequence (Nomura *et al.*, 1998).

To test if compounds **24** and **25** also inhibit galactosyltransferase II, neuroblastoma cells were treated with 8-dT (**24**, 30  $\mu\text{M}$ ) and Td-ol (**25**, 30  $\mu\text{M}$ ) and labelled either with [ $^{14}\text{C}_8$ ]

lactosylceramide or [ $^{14}\text{C}_8$ ] GM3. As shown in Figure 4-6-9, both compounds had no influence on a-series gangliosides formation (GM1 and GD1a). However, levels of b-series gangliosides (GD1b, GT1b, GQ1b) in cells treated with trichothecene derivatives were visibly reduced. These observations suggest that trichothecenes have an additional effect on GSL expression which includes reduced formation of acidic gangliosides.

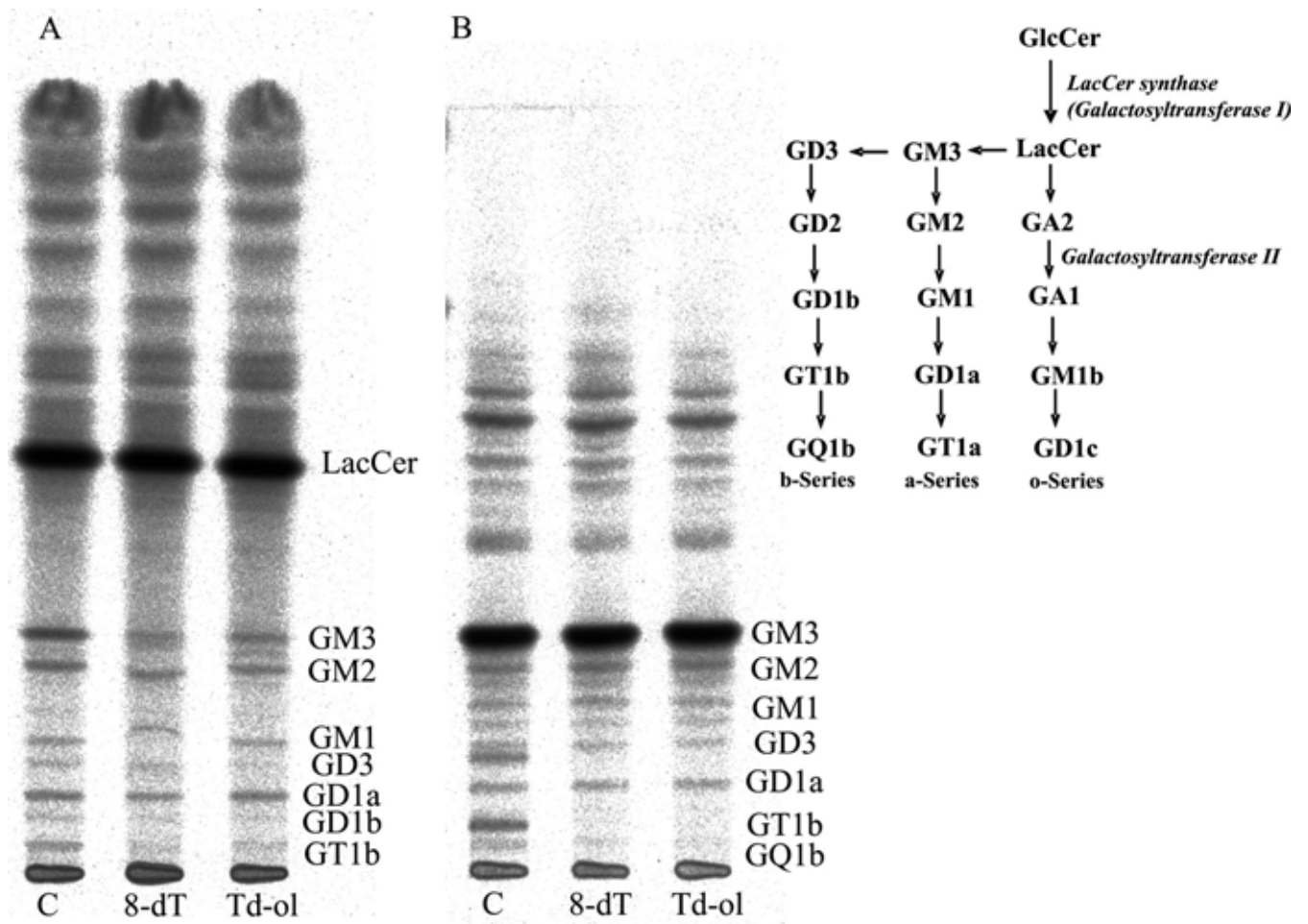


**Figure 4-6-9.** Effect of 8-deoxy-trichothecin (8-dT) and trichodermol (Td-ol) on [ $^{14}\text{C}_8$ ] LacCer (A) and [ $^{14}\text{C}_8$ ] GM3 (B) incorporation into glycosphingolipids of neuroblastoma B104 cells.

Cells were incubated in the absence (C, control) or presence of 30  $\mu\text{M}$  8-deoxy-trichothecin (8-dT) or trichodermol (Td-ol), as indicated. After 4 h 1  $\mu\text{Ci}$  of [ $^{14}\text{C}_8$ ]LacCer or [ $^{14}\text{C}_8$ ]GM3 were added to the medium. Twenty hours later cells were harvested and lipids were extracted, isolated, separated by TLC, visualized by autoradiography and quantitatively evaluated as described under Materials and Methods. TLC plates were developed in chloroform-methanol-0.22 % aqueous  $\text{CaCl}_2$  (60:35:8; v/v/v). Data are from one representative out of three independent experiments that gave similar results. The terminology of gangliosides (GQ1b, GT1b, GD1b, GD1a, GD3, GM1, GM2 and GM3) is according to Svennerholm (Svennerholm, 1963). LacCer, lactosylceramide.

#### 4.6.4.3 Influence of trichothecenes on the translocation of glucosylceramide

Next, we examined whether trichothecenes also affect GlcCer translocation from the cytosolic side, where it is formed to the luminal side where it is galactosylated to yield LacCer (Figure 4-6-4).

First, we analyzed the activity of Pgp (also known as ABCB1) and MRP1 (also known as ABCC1), two potential translocators of GlcCer, towards known fluorescent substrates. In both cell types, the ability of cyclosporin A (CsA) (10 $\mu$ M), an inhibitor of Pgp activity as well as of MK571 (20 $\mu$ M), an inhibitor of MRP1 activity was tested using rhodamine-123 (R-123) and/or 5-carboxyfluorescein diacetate (CFDA) as fluorescent substrates for Pgp and MRP1, respectively. In both cell types CsA showed no effect on efflux of R-123 indicating that Pgp was not active towards this substrate in neural cells. On the other hand MK571 caused significant accumulation of CFDA (Figure 4-6-10) in neuroblastoma cells but not in cerebellar neurons, pointing to an activity of MRP1 towards the used substrate only in neuroblastoma cells.

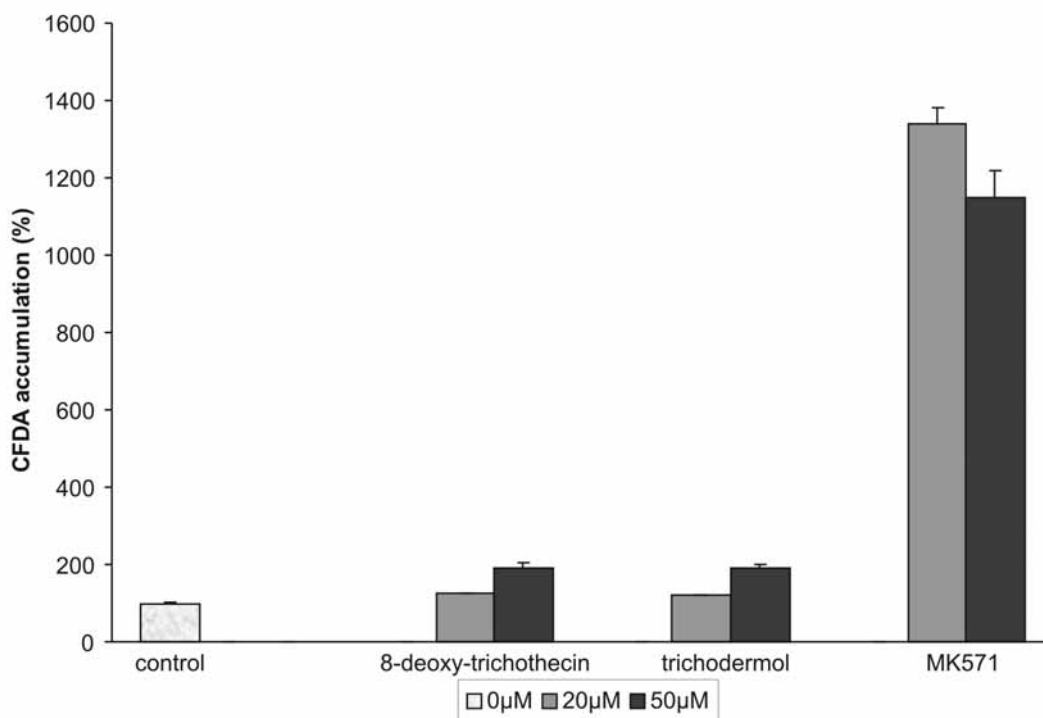


**Figure 4-6-10.** Effect of 8-deoxy-trichothecin (8-dT) and of trichodermol (Td-ol) on MRP1 transport activity in neuroblastoma B104.

Transport activity was assessed over 2 h by CFDA accumulation assay as described in Materials and Methods. MK571 was used as a positive control. Results are given relative to untreated controls and represent means from three independent experiments.

Since MRP1 was only demonstrated to function as a translocator for short chain lipid analogs across cellular membranes (Raggers *et al.*, 1999) we tested whether MRP1 also acts as a flippase for endogenous long-chain glucosylceramide across the Golgi membrane. Therefore, neuroblastoma B104 cells were incubated with different concentrations of MK571 and the incorporation of L-[3-<sup>14</sup>C] serine into cellular GSLs was followed. As illustrated in Figure 4-6-11, levels of labeled GlcCer in MK571 treated cells were 3-4fold higher than in control cells. However, the amounts of labeled LacCer and other GSLs were comparable with those of control cells (not shown), indicating that additional mechanisms exist that obviously allow translocation of sufficient amounts of GlcCer for *de novo* GSL biosynthesis. In primary cultured neurons, however, no changes either in GlcCer or in downstream GSL biosynthetic labelling were observed in the presence of MK571. These observations suggested MRP1 to function as a GlcCer translocase across Golgi membranes at most in neuroblastoma B104 cells.

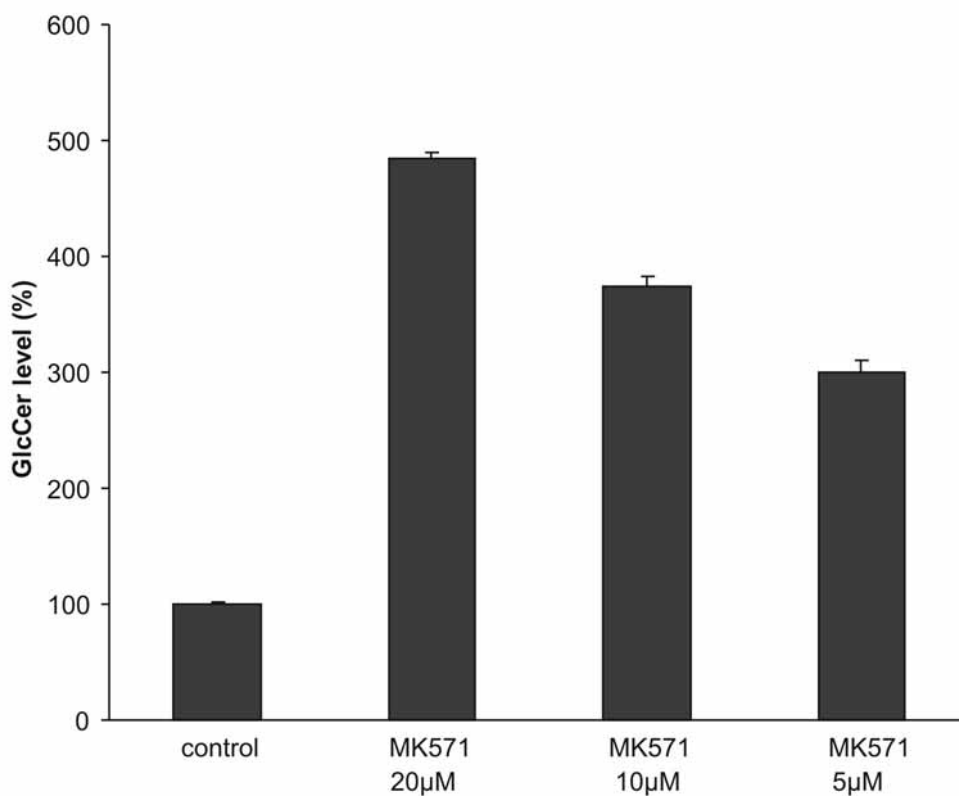


**Figure 4-6-11.** Effect of MK571 on [<sup>14</sup>C] serine incorporation into sphingolipids of neuroblastoma B104 cells.

Cells were incubated in the absence (C, control) or presence of the indicated concentrations of MK571. After 4 h 1µCi of [<sup>14</sup>C]serine was added to the medium. Twenty hours later cells were harvested and lipids were extracted, isolated, separated by TLC, and detected as described under Materials and Methods. TLC plates were developed in chloroform-methanol-0.22 % aqueous CaCl<sub>2</sub> (60:35:8; v/v/v). GlcCer bands were scraped and their

radioactivity was quantified in a liquid scintillation counter. The results are presented as percentages of control and are means from three independent experiments.

We therefore tested the effect of 8-dT and Td-ol on CFDA accumulation in neuroblastoma cells. As shown in Figure 4-6-10, neither 8-dT (**24**) nor Td-ol (**25**) altered CFDA accumulation. It thus appears that 8-deoxy-trichothecin and trichodermol do not affect the function of ABC transporters.

#### **4.6.4.4 Influence of trichothecenes on ceramide level in neural cells**

Trichothecenes are well known apoptotic compounds (Yang *et al.*, 2000; Pestka and Smolinski, 2005). Ceramide, a biosynthetic precursor and also a catabolic product of GlcCer, has been shown to be involved in many forms of apoptosis (Pettus *et al.*, 2002; Gulbins, 2003). Therefore, we investigated the influence of compounds **24** and **25** on the formation of ceramide.

The incorporation of L-[3-<sup>14</sup>C] serine into ceramide was studied in primary cultured neurons and neuroblastoma cells after incubation of the cells with compounds **24** (8-dT, 30  $\mu$ M) or **25** (Td-ol, 30  $\mu$ M) for 24 h. In neuroblastoma cells trichothecenes significantly elevated level of ceramide (3-4fold), while in cerebellar neurons there was no difference between trichothecene-treated and control cells (Figure 4-6-12).

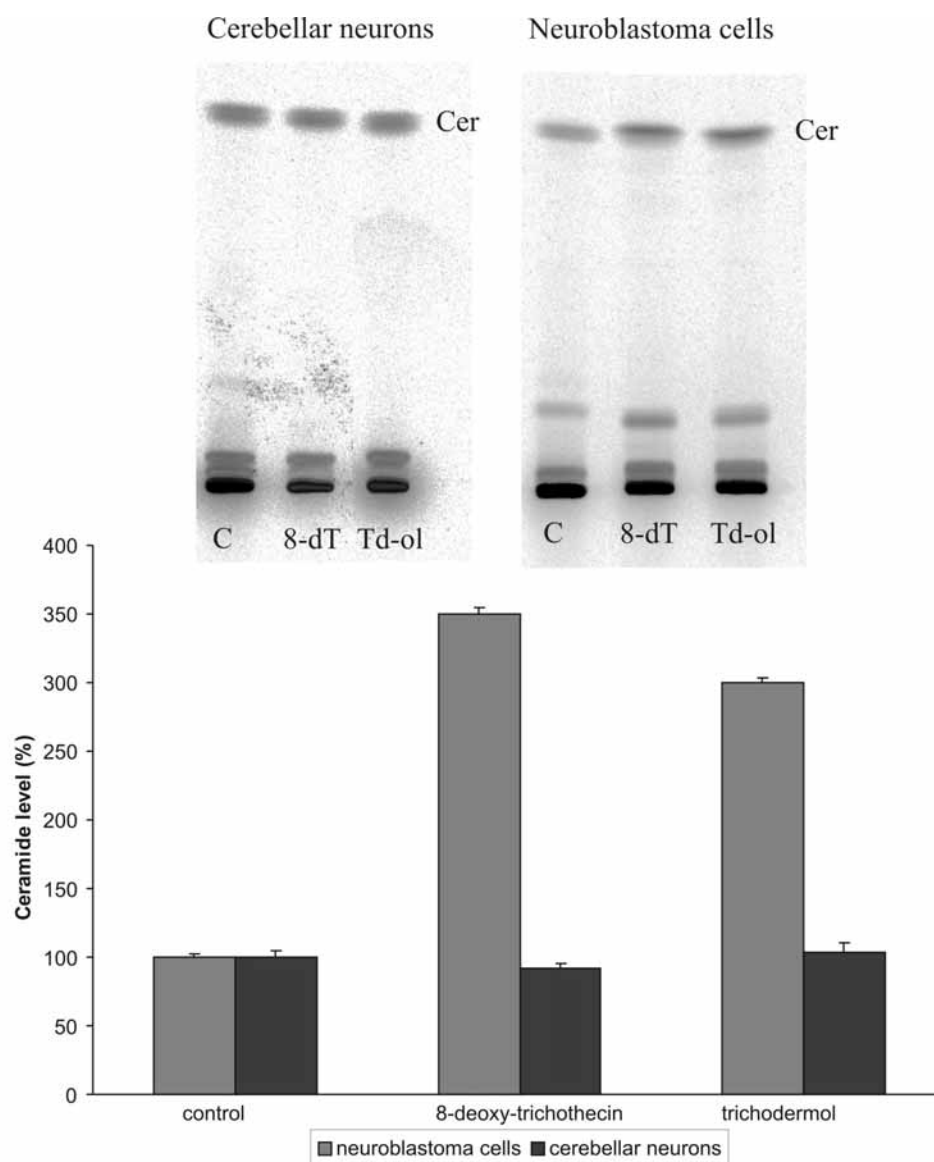


**Figure 4-6-12.** Effect of 8-deoxy-trichothecin (8-dT, **24**) and of trichodermol (Td-ol, **25**) on ceramide level in neuroblastoma cells and primary cultured neurons.

Cells were incubated in the absence (C, control) or presence of 8-dT (30  $\mu$ M) or Td-ol (30  $\mu$ M). After 4 h 1  $\mu$ Ci of [ $^{14}$ C]serine was added to the medium. Twenty hours later cells were harvested and lipids were extracted, isolated, separated by TLC, and detected as described under Materials and Methods. TLC plates were developed in chloroform-methanol-acetic acid (190:9:1; v/v/v). Ceramide bands were scraped and their radioactivity was quantified in a liquid scintillation counter. The results are presented as percentages of control and are means from three independent experiments.

These findings demonstrate, once more, that trichothecenes exhibit different mechanism of action in cerebellar neurons and neuroblastoma cells.



## 5 Discussion

The focus of this study was the investigation of marine-derived fungi aiming to find natural products with potent biological activity and/or novel chemical structures. Fungi are an extremely valuable source of novel natural products with a wide array of biological activities (König and Wright, 1996; Blunt *et al.*, 2005). Several fungal metabolites, e.g. fumagillin, illudin S (McMorris, 1999; Butler, 2005; Furness *et al.*, 2005; Senzer *et al.*, 2005), are undergoing clinical trials as antitumour compounds and inspired the current study. Also, fungal metabolites are reported to interfere with sphingolipids (SLs), compounds of eukaryotic cells that are connected with different signaling pathways including regulation of cell growth and death (Merrill *et al.*, 1993a; Mandala *et al.*, 1994). The isolated fungal metabolites and their biological activity are discussed below according to the results presented in the previous chapter.

### 5.1 Selection of fungal strains

Search for new anticancer drugs is today of utmost importance for therapy. Natural products are an important source of anticancer drugs (Simmons *et al.*, 2005; Altmann and Gertsch, 2007). Therefore, fungal strains from the culture collection of the Institute for Pharmaceutical Biology (Bonn) were screened in a panel of six human tumor cell lines in cooperation with Oncotest GmbH, Institute for Experimental Oncology (Freiburg). The results of the present study are based on cytotoxic screening of around 80 fungal strains. Due to the significant advances in cancer biology much of the research is focused on cancer-specific mechanisms and molecular targets (McLaughlin *et al.*, 2003). Sphingolipids, mediators of apoptosis and cell growth, were recognized in the last 20 years as molecules with an important role in cancer pathogenesis and treatment (Ogretmen and Hannun, 2004; Radin, 2004; Modrak *et al.*, 2006). Hence, the extracts of fungal strains with cytotoxic activity were screened for their interference with sphingolipid metabolism. In preliminary screening studies out of 25 cytotoxic extracts seven showed alterations in expression of sphingolipids (Figure 4-1-2, Chapter 4-1-2) and were, thus, chosen for mass cultivation. Though, extracts of the strains *Emericella nidulans*, *Arthrimum sacchari* and *Aspergillus terreus* did not interfere with sphingolipids, they were selected for further studies due to interesting NMR (low field  $^1\text{H}$  NMR resonances) and MS data ( $m/z$  900-1100).

After large scale cultivation and extraction some of the fungal strains revealed a different profile of biological activity as compared with that of the screening extracts. Extracts of the strains *Microsphaeropsis* sp. and *Acremonium sclerotigenum* (strain number 96 and 738, respectively) lost their cytotoxic effects together with the effect on SLs. The activity on SL metabolism was lost in extracts from the strains of *Fusarium dimerum* and *Paecilomyces lilacinus*.

The loss of biological activity is one of the problems encountered when screening for biological compounds in microorganisms. It may be explained by physiological changes of fungal strains which loose, due to many passages, the ability to produce their active metabolites.

## 5.2 Isolated natural products

A major problem within natural product isolation is rediscovery of already known compounds. A careful selection of organisms based on taxonomy may not help, especially when dealing with fungi. Certain fungal secondary metabolites are often found in more than one species and some are typical for several genera. Also, the output of LC-MS spectra of extracts or VLC fractions is usually a list of possible candidates, and it is hard to determine whether the peaks belong to known compounds or not, especially when molecular weights are smaller than 500 Da. Thus, the selection of strains in the current project was based on biological activity of extracts and VLC fractions.

It has to be stated, however, that most of the isolated compounds responsible for the bioactivity of the extracts were known.

The cytotoxic effect of the *Emericella nidulans* extract resulted from the toxicity of sterigmatocystin (**9**) and averufin (**10**), biosynthetic precursors of aflatoxins (Yabe and Nakajima, 2004). Aflatoxins are metabolites of different species of *Aspergillus* that induce DNA damage and immune suppression, and are associated with toxicity and carcinogenicity in animals and humans (Bennett and Klich, 2003; Preston and Williams, 2005).

Bioassay-guided isolation of cytotoxic compounds from an *Arthrinium sacchari* extract revealed the presence of cytochalasins (**14**, **15**), a group of toxic metabolites known from different genera of fungi (Liu, 2005) which show a wide range of biological activities. Many cytochalasins bind to actin filaments and block polymerization and elongation of actin which leads to the inhibition of cell division and apoptotic responses (Cooper, 1987; Rubtsova *et al.*,

1998). They have also been reported to inhibit HIV-1 protease (Lingham *et al.*, 1992) and to have antibiotic and antitumor activities (Carter, 1967; Mookerjee *et al.*, 1981).

Trichothecenes (**24**, **25**, **27** and **28**) were identified as the major compounds in a strain of *Spicellum roseum*. They are well described in the literature as cytotoxic compounds that bind to eukaryotic ribosomes and inhibit translation (Pestka and Smolinski, 2005).

The bioassay-guided isolation is not always a suitable approach in the isolation of new natural products. Mostly, the activity of extracts or VLC fractions comes from the presence of known compounds. The reason for that is probably due to the general validity of the assays used. Preliminary antitumor assays consider only the percentage of dead cells and, by that, are not suitable for detailed analysis and selection.

New fungal metabolites (**1**, **2**, **11**, **12**) elucidated in this study were isolated in small amounts (1.5 – 3.0 mg) and usually had no significant biological activity. These, compounds present as “traces” are biosynthetic products of specific metabolic pathways of a certain fungus. Compounds **1** and **2** belong to a family of arugosins which are of interest with regard to the biosynthesis of several structural types of fungal polyketides, e.g. anthrones, anthraquinones, benzophenones and xanthenes (Chexal *et al.*, 1974; Holker *et al.*, 1974; Chexal *et al.*, 1975). Compounds **11** and **12** are cyclodepsipeptides, analogs of beauvericin and enniatins which were reported to have cytotoxic and antibiotic activity (Dobler *et al.*, 1969; Calo *et al.*, 2004). Thus, they clearly demonstrate the chemical diversity of fungal-derived natural products.

### 5.3 Interference of fungal metabolites with sphingolipid metabolism

In the current study the influence of cytotoxic fungal extracts on sphingolipid metabolic pathway has been investigated. Sphingolipid metabolism bears potential valuable targets for cancer therapy since sphingolipids are involved in important cellular functions (Fox *et al.*, 2006; Ogretmen, 2006). Isolation of sphingolipids, their purification and separation in individual species is well described by van Echten-Deckert (van Echten-Deckert, 2000). Thin layer chromatography has proven to be a valuable method for metabolic studies of lipids. In this study the influence of fungal metabolites on SL biosynthesis was examined in primary cultured neurons and neuroblastoma cells by following the incorporation of L-[3-<sup>14</sup>C] serine into cellular sphingolipids. For examination of specific glycosphingolipids other labeled precursors were also used. Neurons are enriched in complex gangliosides which enables their detection (van Echten-Deckert and Herget, 2006), whereas neuroblastoma cell line originates

in central nervous system (Schubert *et al.*, 1974). Interference of fungal toxins trichothecenes with sphingolipids is discussed below.

### 5.3.1 Trichothecenes – alterations of glycosphingolipid profiles

In a screening approach we investigated the effect of more than 20 different crude extracts from fungal species of the genera *Fusarium*, *Acremonium*, *Trichoderma*, *Microsphaeropsis*, *Chaetomium* and *Arthrinium* on sphingolipid metabolism in neural cells. Most interesting was a crude extract of the fungal strain *Spicellum roseum*. When added to the culture medium it displayed a similar effect with that previously described in the presence of brefeldin A (BFA) in primary cultured neurons (van Echten *et al.*, 1990b; Sadeghlar *et al.*, 2000) except that no accumulation but rather a strongly reduced formation of *de novo* biosynthesized LacCer was observed. Further fractionation of the crude extract indeed revealed BFA as one of the components produced by *Spicellum roseum*. The effect of BFA known to induce an accumulation of newly formed GlcCer, LacCer, GM3 and GD3 along with a reduction of the formation of complex gangliosides and also of sphingomyelin due to the redistribution of the proximal Golgi into the endoplasmatic reticulum was obviously accompanied by an additional effect regarding LacCer formation. Indeed two additional compounds were identified which belong to the trichothecene family.

Trichodermol (Td-ol, **25**) was described as an isolate from different fungal species (Grove, 1988; Krohn *et al.*, 2003), while its isocrotonyl ester 8-deoxy-trichothecin (8-dT, **24**) was identified so far only in *Spicellum roseum* (Plattner *et al.*, 1988; Tanaka *et al.*, 2001). The trichothecenes are a group of about 180 diverse sesquiterpenoid metabolites produced by various fungal species of the genera *Fusarium*, *Trichothecium*, *Cephalosporum* and *Stachybotrys* (Grove, 1988; Grove, 2000). Consumption of food contaminated with these mycotoxins causes severe pathological effects in animals and humans (Lautraite *et al.*, 1997; Li *et al.*, 1999; Pestka and Smolinski, 2005). Trichothecenes are cytotoxic compounds that have multiple inhibitory effects on eukaryotic cells (summarized in review (Rocha *et al.*, 2005)) like inhibition of protein, DNA and RNA synthesis (Ji *et al.*, 1994). At the molecular level, trichothecenes inhibit the peptidyltransferase reaction by binding to the 60S ribosomal subunit, suggesting that one of the cytotoxic mechanisms is translational inhibition (Ueno, 1984). Later, it was shown that trichothecenes activate mitogen-activated protein kinases (MAPKs) which induce the production of proinflammatory cytokines, implying the immune system as the most important target of trichothecenes (Shifrin and Anderson, 1999; Zhou *et al.*, 2003; Pestka *et al.*, 2004). Despite a vast number of studies on various effects of this

mycotoxin family, results described in this study are the first report on an interference of tricothecenes with GSL metabolism.

The analysis of the effects of tricothecenes on sphingolipid metabolism showed that both compounds blocked de novo formation of LacCer (lactosylceramide) and of its downstream derivatives (Figure 4-6-4, Chapter 4-6), leading simultaneously to an accumulation of GlcCer in neural cells. A similar uncoupling of GSL biosynthesis at the level of LacCer synthase was described in embryonic chicken neurons incubated with epoxy-glucosylceramide, a synthetic analog of GlcCer (Zacharias *et al.*, 1994). Like shown for this truncated GlcCer-analog, cell integrity was also required for the inhibitory action of tricothecenes in the two neural cell types investigated in the present study. Thus, a reduction of LacCer synthase activity was observed only after pretreatment of neural cells with tricothecenes but not when directly added to the enzyme assay *in vitro*. This of course raised the question whether not the enzyme itself but a flippase responsible for the translocation of the substrate from the cytosolic face, where it is formed, to the luminal face, where it is galactosylated, might be the *in vivo* target of tricothecenes action. In neuroblastoma B104 cells we could clearly show that this was not the case. However, in these cells both tricothecenes clearly decreased transcription of LacCer synthase, which explains the importance of cell integrity for the inhibitory effect in this cell type. On the other hand in primary cultured cerebellar neurons we could detect neither a protein responsible for GlcCer translocation nor an effect of tricothecenes on transcription of LacCer synthase. Obviously in terminally differentiated post-mitotic neurons different metabolic requirements imply different regulatory mechanisms when compared with undifferentiated rapidly dividing neuroblastoma cells. Terminally differentiated neurons exhibit a characteristic ganglioside composition, which is known to change upon cell transformation (van Echten-Deckert and Herget, 2006) (see also Figure 4-6-5, Chapter 4-6). Although the exact function of certain complex ganglioside species is not known yet, the development of mouse models deficient in gangliosides clearly document the essential function of these complex membrane components for brain development and function (Proia, 2004; Yamashita *et al.*, 2005).

It is thus not surprising that in rapidly dividing neuroblastoma cells tricothecenes act on the transcriptional level whereas in terminally differentiated post-mitotic neurons a fine tuning on post-transcriptional and/or post-translational level appears to be decisive for the activity of LacCer synthase, which yields the common precursor for all cellular complex GSLs. Note that LacCer synthase has been purified and cloned from rat brain about one decade ago

(Nomura *et al.*, 1998). Different mechanisms of action in different cell types are also demonstrated in ceramide level of trichothecene treated cells. Both trichothecene derivatives increased cellular level of ceramide in neuroblastoma cells but not in cerebellar neurons. Yet, these effects require detailed investigations in future studies.

Collectively these data document a new effect of two trichothecene derivatives in neural cells. Trichodermol (**25**) and 8-deoxy-trichothecin (**24**) considerably interfere with the activity of LacCer synthase albeit by different cell type specific mechanisms. As a consequence GSL biosynthesis is uncoupled at the level of LacCer accompanied by the accumulation of GlcCer.

As already mentioned, one of the most important effects of trichothecenes is the modulation of the immune system by inducement of the production of proinflammatory cytokines and chemokines (Pestka *et al.*, 2004). It is known that sphingolipids can act as regulators and mediators of inflammatory responses (El Alwani *et al.*, 2006). Memon *et al.* (Memon *et al.*, 2001) reported that inflammation caused by bacterial endotoxin lipopolysaccharide increased ceramide and glucosylceramide content in Syrian hamsters. These results suggest a possible role of GlcCer in inflammation and, by that, a possible relation between the inflammatory effects of trichothecenes on one side and trichothecene-induced GlcCer accumulation on the other side.

Moreover, it was demonstrated (Yang *et al.*, 2000; Zhou *et al.*, 2005) that trichothecenes, although strong apoptotic compounds, initiate competing apoptotic and survival pathways. Since GlcCer was reported to have growth stimulatory and anti-apoptotic effects (Datta and Radin, 1988; Marsh *et al.*, 1995; Marchell *et al.*, 1998), in contrast to its metabolic precursor ceramide, there is a possibility that GlcCer accumulation induced by trichothecenes to act as a link between trichothecenes and survival pathways.

However, further studies will clarify the fate and physiological consequence of accumulated GlcCer in trichothecene-treated cells and also the correlation of known effects of trichothecenes with those presented here.

#### **5.4 General discussion**

As already discussed above, a general bioassay-guided isolation (cytotoxicity and antimicrobial assays) is not always a favorable for the isolation of new compounds with potent biological activity. However, when a specific cellular function is recognized as a target

for potential therapeutics and used for screening, there are more chances for the isolation of compounds that serve as tools for biological research and/or are leads for clinical medicines.

Various sphingolipid metabolites appear to modulate various cellular events including proliferation, differentiation, and apoptosis. These sphingolipid-regulated processes are crucial in cancer development and progression, and influence the efficacy of anti-cancer therapeutics. In addition, defects of enzymes catalyzing SL degradation are responsible for various genetic, so called sphingolipid storage diseases.

Till today, only few compounds of natural origin and several synthetic compounds are known to interfere with sphingolipid metabolism. Considering plenty of cellular functions regulated by SLs and their importance, sphingolipid metabolism represents a wealthy source for pharmacological targets.

## 6 Summary

Development of new drugs, especially in the area of oncological and infectious diseases, represents today one of the most important research fields. An analysis of the number of chemotherapeutic agents and their sources shows that over 60 % of approved drugs are derived from natural compounds. The marine environment is a tremendous source of natural products. Moreover, many of the new compounds isolated from marine micro- and macroorganisms showed prominent biological effects, mostly antibiotic and cytotoxic activities. Drug development is now turning toward potentially more selective ways (e.g. inducement of certain signaling molecules) in disease treatments, especially when concerning cancer. Sphingolipids (SLs) are ubiquitous constituents of eukaryotic cellular membranes that are involved in cell growth, proliferation, differentiation and apoptosis. These sphingolipid-regulated processes are crucial in cancer development and progression, and influence efficacy of anti-cancer therapeutics. Pharmacological or molecular manipulations of any of the enzymes involved in SL metabolism have been proposed as new strategies in the treatment of cancer or diseases caused by disrupted sphingolipid balance. The toxic effects of some fungal metabolites were related to their ability to interfere with SL metabolism. The aim of this study was the investigation of secondary metabolites produced by marine-derived fungi with cytotoxic properties and the isolation of new compounds with potent biological activity, preferably with the potential to influence sphingolipid metabolism.

Extracts of seven fungal strains, including five algal-derived and two sponge-derived strains, were chemically investigated. This investigation resulted in the isolation and structure elucidation of 29 pure compounds. Four compounds, arugosin G and H, spicellamide A and B, proved to be new. Arugosins G and H, together with arugosins A and B, were isolated from algicolous fungus *Emericella nidulans* var. *acristata*. They are benzophenone derivatives, biosynthetically related to xanthenes, which showed moderate antitumor activity toward individual tumor cell lines. Cyclohexadepsipeptides spicellamide A and B, isolated from sponge-derived fungus *Spicellum roseum*, exhibited an IC<sub>50</sub> value of 30 µg mL<sup>-1</sup> and 6.2 µg mL<sup>-1</sup>, respectively, in neuroblastoma cells.

Bioassay-guided isolation of cytotoxic compounds revealed the presence of cytochalasins from an *Arthrinium sacchari* extract, of aflatoxins from an *Emericella nidulans* var. *acristata* extract and of trichothecenes from a *Spicellum roseum* extract.



Trichothecenes are cytotoxic compounds that have several inhibitory effects on eukaryotic cells. Tests on sphingolipid metabolism exhibited alterations in the expression of glycosphingolipids by two compounds from trichothecene family, 8-deoxy-trichothecin and trichodermol. In cerebellar neurons and neuroblastoma cells both compounds inhibit lactosylceramide synthase activity and induce an accumulation of glucosylceramide (Figure 6-1). These data describe a new effect of trichothecenes. However, further studies have to clarify the fate and physiological consequence of accumulated glucosylceramide and also its correlations with known effects of trichothecenes.

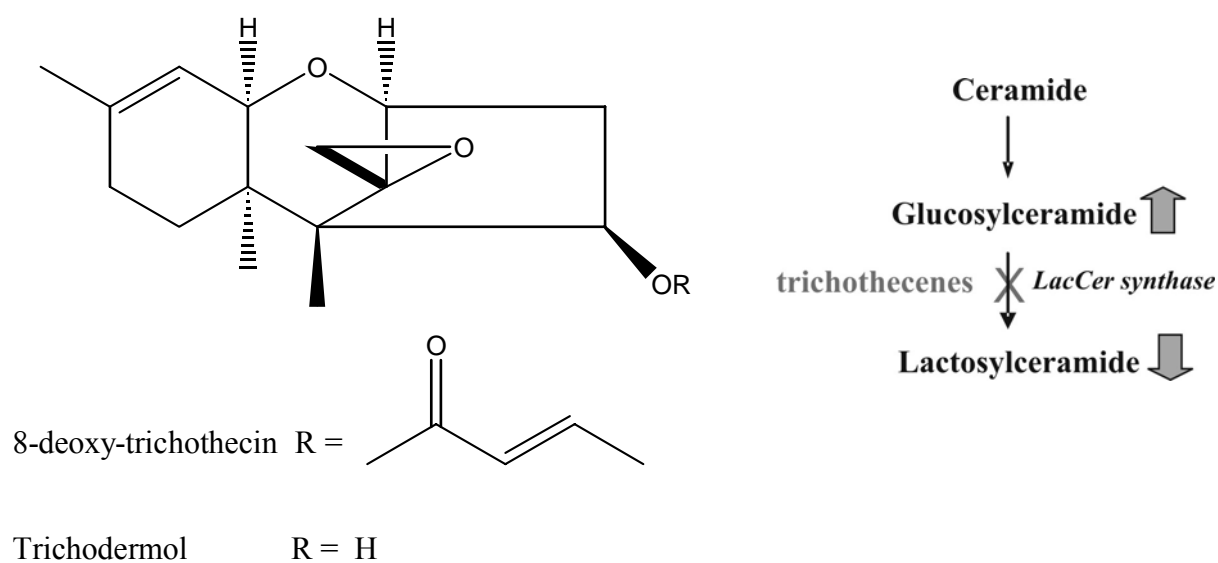


**Figure 6-1.** Structures of trichothecene derivatives and their interference with sphingolipids.

Trichothecenes inhibit the activity of lactosylceramide (LacCer) synthase which leads to the accumulation of glucosylceramide level and reduction of lactosylceramide level in the cells.

Fungal metabolites are recognized as a valuable source of new and biologically active metabolites. Since sphingolipid metabolites modulate various cellular events, they are a wealthy source of pharmacological targets. Results obtained in this study demonstrate that targeting specific cellular pathways, e. g. sphingolipid metabolism, in a combination with additional biological assays, e. g. cytotoxic tests, represents good strategy in detection of new chemical structures and/or compounds with desirable biological effects.

## 7 References

Achenbach H, Muehlenfeld A, Brillinger GU **1985**. Metabolites from microorganisms. XXX. Phthalides and chromanols from *Aspergillus duricaulis*. *Liebigs Ann Chem* 8, 1596-1628.

Adachi-Yamada T, Gotoh T, Sugimura I, Tateno M, Nishida Y, Onuki T, Date H **1999**. De novo synthesis of sphingolipids is required for cell survival by down-regulating c-Jun N-terminal kinase in *Drosophila* imaginal discs. *Mol Cell Biol* 19, 7276-7286.

Albert R, Hinterding K, Brinkmann V, Guerini D, Muller-Hartwig C, Knecht H, Simeon C, Streiff M, Wagner T, Welzenbach K, Zecri F, Zollinger M, Cooke N, Francotte E **2005**. Novel immunomodulator FTY720 is phosphorylated in rats and humans to form a single stereoisomer. Identification, chemical proof, and biological characterization of the biologically active species and its enantiomer. *J Med Chem* 48, 5373-5377.

Altmann KH, Gertsch J **2007**. Anticancer drugs from nature--natural products as a unique source of new microtubule-stabilizing agents. *Nat Prod Rep* 24, 327-357.

Arima K, Kakinuma A, Tamura G **1968**. Surfactin, a crystalline peptidelipid surfactant produced by *Bacillus subtilis*: isolation, characterization and its inhibition of fibrin clot formation. *Biochem Biophys Res Commun* 31, 488-494.

Bajjalieh SM, Martin TF, Floor E **1989**. Synaptic vesicle ceramide kinase. A calcium-stimulated lipid kinase that co-purifies with brain synaptic vesicles. *J Biol Chem* 264, 14354-14360.

Ballantine JA, Ferrito V, Hassall CH, Jenkins ML **1973**. The biosynthesis of phenols. XXIV. Arugosin C, a metabolite of a mutant strain of *Aspergillus rugulosus*. *J Chem Soc [Perkin 1]* 17, 1825-1830.

Ballantine JA, Francis DJ, Hassall CH, Wright JL **1970**. The biosynthesis of phenols. XXI. The molecular structure of arugosin, a metabolite of a wild-type strain of *Aspergillus rugulosus*. *J Chem Soc [Perkin 1]* 9, 1175-1182.

Barenholz Y **2004**. Sphingomyelin and cholesterol: from membrane biophysics and rafts to potential medical applications. *Subcell Biochem* 37, 167-215.

Bektas M, Spiegel S **2004**. Glycosphingolipids and cell death. *Glycoconj J* 20, 39-47.

Belofsky GN, Jensen PR, Renner MK, Fenical W **1998**. New cytotoxic sesquiterpenoid nitrobenzoyl esters from a marine isolate of the fungus *Aspergillus versicolor*. *Tetrahedron* 54, 1715-1724.

Bennett JW, Klich M **2003**. Mycotoxins. *Clin Microbiol Rev* 16, 497-516.

Bhadury P, Mohammad BT, Wright PC **2006**. The current status of natural products from marine fungi and their potential as anti-infective agents. *J Ind Microbiol Biotechnol* 33, 325-337.

Bhushan R, Bruckner H **2004**. Marfey's reagent for chiral amino acid analysis: a review. *Amino Acids* 27, 231-247.

Bleicher RJ, Cabot MC **2002**. Glucosylceramide synthase and apoptosis. *Biochim Biophys Acta* 1585, 172-178.

Blunt JW, Copp BR, Munro MH, Northcote PT, Prinsep MR **2005**. Marine natural products. *Nat Prod Rep* 22, 15-61.

- Bonmatin J-M, Labbe H, Grangemard I, Peypoux F, Maget-Dana R, Ptak M, Michel G **1995**. Production, isolation and characterization of [Leu4]- and [Ile4]surfactins from *Bacillus subtilis*. *Lett Pept Sci* 2, 41-47.
- Bose R, Verheij M, Haimovitz-Friedman A, Scotto K, Fuks Z, Kolesnick R **1995**. Ceramide synthase mediates daunorubicin-induced apoptosis: an alternative mechanism for generating death signals. *Cell* 82, 405-414.
- Bradford MM **1976**. A rapid and sensitive method for the quantitation of microgram quantities of protein utilizing the principle of protein-dye binding. *Anal Biochem* 72, 248-254.
- Bringmann G, Lang G, Steffens S, Gunther E, Schaumann K **2003**. Evariquinone, isoemicellin, and stromemycin from a sponge derived strain of the fungus *Emericella varicolor*. *Phytochemistry* 63, 437-443.
- Brinkmann V, Lynch KR **2002**. FTY720: targeting G-protein-coupled receptors for sphingosine 1-phosphate in transplantation and autoimmunity. *Curr Opin Immunol* 14, 569-575.
- Brückner H, Keller-Hoehl C **1990**. HPLC separation of DL-amino acids derivatized with N<sup>2</sup>-(5-fluoro-2,4-dinitrophenyl)-L amino acids amides. *Chromatographia* 30, 621-629.
- Buccoliero R, Futerman AH **2003**. The roles of ceramide and complex sphingolipids in neuronal cell function. *Pharmacol Res* 47, 409-419.
- Bugni TS, Ireland CM **2004**. Marine-derived fungi: a chemically and biologically diverse group of microorganisms. *Nat Prod Rep* 21, 143-163.
- Bunger J, Westphal G, Monnich A, Hinnendahl B, Hallier E, Muller M **2004**. Cytotoxicity of occupationally and environmentally relevant mycotoxins. *Toxicology* 202, 199-211.
- Butler MS **2005**. Natural products to drugs: natural product derived compounds in clinical trials. *Nat Prod Rep* 22, 162-195.
- Cabot MC, Giuliano AE, Volner A, Han TY **1996**. Tamoxifen retards glycosphingolipid metabolism in human cancer cells. *FEBS Lett* 394, 129-131.
- Calo L, Fornelli F, Ramires R, Nenna S, Tursi A, Caiaffa MF, Macchia L **2004**. Cytotoxic effects of the mycotoxin beauvericin to human cell lines of myeloid origin. *Pharmacol Res* 49, 73-77.
- Cameotra SS, Makkar RS **2004**. Recent applications of biosurfactants as biological and immunological molecules. *Curr Opin Microbiol* 7, 262-266.
- Carter SB **1967**. Effects of cytochalasins on mammalian cells. *Nature* 213, 261-264.
- Charles AG, Han TY, Liu YY, Hansen N, Giuliano AE, Cabot MC **2001**. Taxol-induced ceramide generation and apoptosis in human breast cancer cells. *Cancer Chemother Pharmacol* 47, 444-450.
- Chen J, Mirocha CJ, Xie W, Hogge L, Olson D **1992**. Production of the Mycotoxin Fumonisin B(1) by *Alternaria alternata* f. sp. *lycopersici*. *Appl Environ Microbiol* 58, 3928-3931.
- Chexal KK, Fouweather C, Holker JSE, Simpson TJ, Young K **1974**. The biosynthesis of fungal metabolites. Part III. Structure of shamixanthone and tajixanthone, metabolites of *Aspergillus varicolor*. *J Chem Soc [Perkin 1]*, 1584-1593.

- Chexal KK, Holker JS, Simpson TJ **1975**. The biosynthesis of fungal metabolites. Part VI. Structures and biosynthesis of some minor metabolites from variant strains of *Aspergillus varicolor*. *J Chem Soc [Perkin 1]*, 549-554.
- Ciacci-Zanella JR, Merrill AH, Jr., Wang E, Jones C **1998**. Characterization of cell-cycle arrest by fumonisin B1 in CV-1 cells. *Food Chem Toxicol* 36, 791-804.
- Cooper JA **1987**. Effects of cytochalasin and phalloidin on actin. *J Cell Biol* 105, 1473-1478.
- Coste H, Martel MB, Got R **1986**. Topology of glucosylceramide synthesis in Golgi membranes from porcine submaxillary glands. *Biochim Biophys Acta* 858, 6-12.
- Cox RH, Churchill F, Cole RJ, Dormer JW **1977**. Carbon-13 nuclear magnetic resonance studies of the structure and biosynthesis of versiconal acetate. *J Am Chem Soc* 99, 3159-3161.
- Creppy EE **2002**. Update of survey, regulation and toxic effects of mycotoxins in Europe. *Toxicol Lett* 127, 19-28.
- Cuvillier O **2002**. Sphingosine in apoptosis signaling. *Biochim Biophys Acta* 1585, 153-162.
- Cuvillier O, Pirianov G, Kleuser B, Vanek PG, Coso OA, Gutkind S, Spiegel S **1996**. Suppression of ceramide-mediated programmed cell death by sphingosine-1-phosphate. *Nature* 381, 800-803.
- da Rocha AB, Lopes RM, Schwartzmann G **2001**. Natural products in anticancer therapy. *Curr Opin Pharmacol* 1, 364-369.
- Datta SC, Radin NS **1988**. Stimulation of liver growth and DNA synthesis by glucosylceramide. *Lipids* 23, 508-510.
- De Rosa MF, Sillence D, Ackerley C, Lingwood C **2004**. Role of multiple drug resistance protein 1 in neutral but not acidic glycosphingolipid biosynthesis. *J Biol Chem* 279, 7867-7876.
- Desai K, Sullards MC, Allegood J, Wang E, Schmelz EM, Hartl M, Humpf HU, Liotta DC, Peng Q, Merrill AH, Jr. **2002**. Fumonisin and fumonisin analogs as inhibitors of ceramide synthase and inducers of apoptosis. *Biochim Biophys Acta* 1585, 188-192.
- Dickson RC **1998**. Sphingolipid functions in *Saccharomyces cerevisiae*: comparison to mammals. *Annu Rev Biochem* 67, 27-48.
- Dobler M, Dunitz JD, Krajewski J **1969**. Structure of the K<sup>+</sup> complex with enniatin B, a macrocyclic antibiotic with K<sup>+</sup> transport properties. *J Mol Biol* 42, 603-606.
- Donaldson JG, Klausner RD **1994**. ARF: a key regulatory switch in membrane traffic and organelle structure. *Curr Opin Cell Biol* 6, 527-532.
- Donia M, Hamann MT **2003**. Marine natural products and their potential applications as anti-infective agents. *Lancet Infect Dis* 3, 338-348.
- Duan RD **2005**. Anticancer compounds and sphingolipid metabolism in the colon. *In Vivo* 19, 293-300.
- El Alwani M, Wu BX, Obeid LM, Hannun YA **2006**. Bioactive sphingolipids in the modulation of the inflammatory response. *Pharmacol Ther* 112, 171-183.

- Fairchild CR, Johnston KJ, Peterson RW, Cornell LA, Bifario M, Raventos-Suarez C, *al. e* **1998**. Halimide, a novel cytotoxic marine natural product, destabilizes microtubules and demonstrates *in vivo* antitumor activity. *Proc Am Ass Cancer Res* 39, 165.
- Fiebig HH, Berger DP, Dengler WA, Wallbrecher E, Winterhalter BR **1992**. Combined *in vitro/in vivo* test procedure with human tumor xenografts. Basel, Karger. 321-351.
- Fleming A **1929**. On the bacterial action of cultures of a penicillium, with special reference to their use in the isolation of *B. influenzae*. *Br J Exp Pathol* 10, 226-236.
- Fox TE, Finnegan CM, Blumenthal R, Kester M **2006**. The clinical potential of sphingolipid-based therapeutics. *Cell Mol Life Sci* 63, 1017-1023.
- Fueki S, Tokiwano T, Toshima H, Oikawa H **2004**. Biosynthesis of indole diterpenes, emindole, and paxilline: involvement of a common intermediate. *Org Lett* 6, 2697-2700.
- Fujimoto H, Nakamura E, Okuyama E, Ishibashi M **2000**. Immunomodulatory constituents from an ascomycete, *Emericella aurantio-brunnea*. *Chem Pharm Bull (Tokyo)* 48, 1436-1441.
- Fujimoto H, Satoh Y, Yamaguchi K, Yamazaki M **1998**. Monoamine oxidase inhibitory constituents from *Anixalla micropertusa*. *Chem Pharm Bull (Tokyo)* 46, 1506-1510.
- Fujita T, Inoue K, Yamamoto S, Ikumoto T, Sasaki S, Toyama R, Chiba K, Hoshino Y, Okumoto T **1994**. Fungal metabolites. Part 11. A potent immunosuppressive activity found in *Isaria sinclairii* metabolite. *J Antibiot (Tokyo)* 47, 208-215.
- Furness MS, Robinson TP, Ehlers T, Hubbard RBt, Arbiser JL, Goldsmith DJ, Bowen JP **2005**. Antiangiogenic agents: studies on fumagillin and curcumin analogs. *Curr Pharm Des* 11, 357-373.
- Futerman AH, Pagano RE **1991**. Determination of the intracellular sites and topology of glucosylceramide synthesis in rat liver. *Biochem J* 280 ( Pt 2), 295-302.
- Futerman AH, van Meer G **2004**. The cell biology of lysosomal storage disorders. *Nat Rev Mol Cell Biol* 5, 554-565.
- Garcia-Ruiz C, Colell A, Paris R, Fernandez-Checa JC **2000**. Direct interaction of GD3 ganglioside with mitochondria generates reactive oxygen species followed by mitochondrial permeability transition, cytochrome c release, and caspase activation. *Faseb J* 14, 847-858.
- Gelderblom WCA, Jaskiewicz K, Marasas WFO, Thiel PG, Horak RM, Vleggaar R, Kriek NPJ **1998**. Fumonisin - novel mycotoxins with cancer promoting activity produced by *Fusarium moniliforme*. *Appl Environ Microbiol* 54, 1806-1811.
- Giraud CG, Maccioni HJ **2003**. Ganglioside glycosyltransferases organize in distinct multienzyme complexes in CHO-K1 cells. *J Biol Chem* 278, 40262-40271.
- Glaser R, Shiftan D, Froimowitz M **2000**. NMR structure determination of brefeldin-A, a 13-membered ring fungal metabolite. *Magn Reson Chem* 38, 274-280.
- Goni FM, Alonso A **2002**. Sphingomyelinases: enzymology and membrane activity. *FEBS Lett* 531, 38-46.
- Gorst-Allman CP, Pachler KGR, Steyn PS, Wessels PL **1977**. Carbon-13 nuclear magnetic resonance assignments of some fungal C<sub>20</sub> anthraquinones; their biosynthesis in relation to that of aflatoxin B<sub>1</sub>. *J Chem Soc [Perkin 1]*, 2181-2188.

- Griffith EC, Su Z, Niwayama S, Ramsay CA, Chang YH, Liu JO **1998**. Molecular recognition of angiogenesis inhibitors fumagillin and ovalicin by methionine aminopeptidase 2. *Proc Natl Acad Sci U S A* 95, 15183-15188.
- Grove JF **1954**. The structure of terrein. *J Chem Soc*, 4693-4694.
- Grove JF **1988**. Non-macrocyclic trichothecenes. *Nat Prod Rep* 5, 187-209.
- Grove JF **2000**. Non-macrocyclic trichothecenes. Part 2. *Prog Chem Org Nat Prod* 69, 1-70.
- Gulbins E **2003**. Regulation of death receptor signaling and apoptosis by ceramide. *Pharmacol Res* 47, 393-399.
- Gupta S, Krasnoff SB, Underwood NL, Renwick JA, Roberts DW **1991**. Isolation of beauvericin as an insect toxin from *Fusarium semitectum* and *Fusarium moniliforme* var. *subglutinans*. *Mycopathologia* 115, 185-189.
- Han CK, Ahn SK, Choi NS, Hong RK, Moon SK, Chun HS, Lee SJ, Kim JW, Hong CI, Kim D, Yoon JH, No KT **2000**. Design and synthesis of highly potent fumagillin analogues from homology modeling for a human MetAP-2. *Bioorg Med Chem Lett* 10, 39-43.
- Hanada K **2005**. Sphingolipids in infectious diseases. *Jpn J Infect Dis* 58, 131-148.
- Hanada K, Nishijima M, Fujita T, Kobayashi S **2000**. Specificity of inhibitors of serine palmitoyltransferase (SPT), a key enzyme in sphingolipid biosynthesis, in intact cells. A novel evaluation system using an SPT-defective mammalian cell mutant. *Biochem Pharmacol* 59, 1211-1216.
- Hanada K, Nishijima M, Kiso M, Hasegawa A, Fujita S, Ogawa T, Akamatsu Y **1992**. Sphingolipids are essential for the growth of Chinese hamster ovary cells. Restoration of the growth of a mutant defective in sphingoid base biosynthesis by exogenous sphingolipids. *J Biol Chem* 267, 23527-23533.
- Hannun YA **1994**. The sphingomyelin cycle and the second messenger function of ceramide. *J Biol Chem* 269, 3125-3128.
- Hannun YA, Luberto C, Argraves KM **2001**. Enzymes of sphingolipid metabolism: from modular to integrative signaling. *Biochemistry* 40, 4893-4903.
- Hannun YA, Obeid LM **2002**. The Ceramide-centric universe of lipid-mediated cell regulation: stress encounters of the lipid kind. *J Biol Chem* 277, 25847-25850.
- Hanson JR, Marten T, Siverns M **1974**. Studies in terpenoid biosynthesis. Part XII. Carbon-13 nuclear magnetic resonance spectra of the trichothecenes and the biosynthesis of trichothecolone from [<sup>13</sup>C]mevalonic acid. *J Chem Soc [Perkin 1]*, 1033-1036.
- Härrä E, Loeffler W, Sigg HP, Stähelin H, Tamm C **1963**. Über die Isolierung neuer Stoffwechselprodukte aus *Penicillium brefeldianum* DODGE. *Helv Chim Acta* 138-139, 1235-1243.
- Harrison LR, Colvin BM, Greene JT, Newman LE, Cole JR, Jr. **1990**. Pulmonary edema and hydrothorax in swine produced by fumonisin B1, a toxic metabolite of *Fusarium moniliforme*. *J Vet Diagn Invest* 2, 217-221.
- Hassler DF, Bell RM **1993**. Ceramidases: enzymology and metabolic roles. *Adv Lipid Res* 26, 49-57.
- Hein SM, Gloer JB, Koster B, Malloch D **1998**. Arugosin F: a new antifungal metabolite from the coprophilous fungus *Ascodesmis sphaerospora*. *J Nat Prod* 61, 1566-1567.

- Hensens OD, Zink D, Williamson JM, Lotti VJ, Chang RSL, Goetz MA **1991**. Variocolin, a sesterterpenoid of novel skeleton from *Aspergillus varicolor* MF138. *J Org Chem* 56, 3399-3403.
- Holker JSE, Lapper RD, Simpson TJ **1974**. The biosynthesis of fungal metabolites. Part IV. Tajixanthone:  $^{13}\text{C}$  nuclear magnetic resonance spectrum and feedings with  $[1-^{13}\text{C}]$ - and  $[2-^{13}\text{C}]$ -acetate. *J Chem Soc [Perkin 1]*, 2135-2140.
- Höller U, Wright AD, Matthee GF, König GM, Draeger S, Aust HJ, Schulz B **2000**. Fungi from marine sponges: diversity, biological activity and secondary metabolites. *Mycol Res* 11, 1354-1365.
- Horn WS, Smith JL, Bills GF, Raghoobar SL, Helms GL, Kurtz MB, Marrinan JA, Frommer BR, Thornton RA, Mandala SM **1992**. Sphingofungins E and F: novel serinepalmitoyl transferase inhibitors from *Paecilomyces variotii*. *J Antibiot (Tokyo)* 45, 1692-1696.
- Horowitz S, Griffin WM **1991**. Structural analysis of *Bacillus licheniformis* 86 surfactant. *J Ind Microbiol* 7, 45-52.
- Igarashi Y, Hakomori S, Toyokuni T, Dean B, Fujita S, Sugimoto M, Ogawa T, el-Ghendy K, Racker E **1989**. Effect of chemically well-defined sphingosine and its N-methyl derivatives on protein kinase C and src kinase activities. *Biochemistry* 28, 6796-6800.
- Ikeda M, Kihara A, Igarashi Y **2004**. Sphingosine-1-phosphate lyase SPL is an endoplasmic reticulum-resident, integral membrane protein with the pyridoxal 5'-phosphate binding domain exposed to the cytosol. *Biochem Biophys Res Commun* 325, 338-343.
- Ingber D, Fujita T, Kishimoto S, Sudo K, Kanamaru T, Brem H, Folkman J **1990**. Synthetic analogues of fumagillin that inhibit angiogenesis and suppress tumour growth. *Nature* 348, 555-557.
- Itabashi T, Nozawa K, Miyaji M, Udagawa S, Nakajima S, Kawai K **1992**. Falconensis A, B, C and D, new compounds related to azaphilone, from *Emericella falconensis* 40, 3142-3144.
- Itabashi T, Ogasawara N, Nozawa K, Kawai K **1996**. Isolation and structures of new azaphilone derivatives, falconensis E-G, from *Emericella falconensis* and absolute configurations of falconensis A-G. *Chem Pharm Bull* 44, 2213-2217.
- Iwamoto C, Minoura K, Oka T, Ohta T, Hagishita S, Numata A **1999**. Absolute stereostructures of novel cytotoxic metabolites, penostatins A-E, from a *Penicillium* species separated from an *Enteromorpha* alga. *Tetrahedron* 55, 14353-14368.
- Iwamoto C, Yamada T, Ito T, Minoura K, Numata A **2001**. Cytotoxic cytochalasans from a *Penicillium* species separated from a marine alga. *Tetrahedron* 57, 2997-3004.
- Jaffrezou JP, Levade T, Bettaieb A, Andrieu N, Bezombes C, Maestre N, Vermeersch S, Rouse A, Laurent G **1996**. Daunorubicin-induced apoptosis: triggering of ceramide generation through sphingomyelin hydrolysis. *Embo J* 15, 2417-2424.
- Jensen PR, Fenical W **2000**. Drugs from the Sea. *Basel, Karger (ed. Fusetani, N.)*, 6-29.
- Ji X, Ke Y, Ning T, Liang Y, Wang D, Shi G **1994**. Effects of sterigmatocystin and T-2 toxin on the induction of unscheduled DNA synthesis in primary cultures of human gastric epithelial cells. *Nat Toxins* 2, 115-119.
- Kanoh K, Kohno S, Asari T, Harada T, Katada J **1997**. (-)-Phenylahistin: a new mammalian cell cycle inhibitor produced by *Aspergillus ustus*. *Bioorg Med Chem Lett* 7, 2847-2852.

- Kanoh K, Kohno S, Katada J, Hayashi Y, Muramatsu M, Uno I **1999a**. Antitumor activity of phenylahistin in vitro and in vivo. *Biosci Biotechnol Biochem* 63, 1130-1133.
- Kanoh K, Kohno S, Katada J, Takahashi J, Uno I **1999b**. (-)-Phenylahistin arrests cells in mitosis by inhibiting tubulin polymerization. *J Antibiot (Tokyo)* 52, 134-141.
- Kawahara N, Nozawa K, Nakajima S, Kawai K **1988**. Studies on fungal products. Part 15. Isolation and structure determination of arugosin E from *Aspergillus silvaticus* and cycloisomerellin from *Emericella striata*. *J Chem Soc [Perkin 1]*, 907-911.
- Khan WA, Dobrowsky R, el Touny S, Hannun YA **1990**. Protein kinase C and platelet inhibition by D-erythro-sphingosine: comparison with N,N-dimethylsphingosine and commercial preparation. *Biochem Biophys Res Commun* 172, 683-691.
- Killough JH, Magill GB, Smith RC **1952**. The treatment of amebiasis with fumagillin. *Science* 115, 71-72.
- Kim S, LaMontagne K, Sabio M, Sharma S, Versace RW, Yusuff N, Phillips PE **2004**. Depletion of methionine aminopeptidase 2 does not alter cell response to fumagillin or bengamides. *Cancer Res* 64, 2984-2987.
- Kim YM, An JJ, Jin YJ, Rhee Y, Cha BS, Lee HC, Lim SK **2007**. Assessment of the anti-obesity effects of the TNP-470 analog, CKD-732. *J Mol Endocrinol* 38, 455-465.
- Kiuchi M, Adachi K, Kohara T, Minoguchi M, Hanano T, Aoki Y, Mishina T, Arita M, Nakao N, Ohtsuki M, Hoshino Y, Teshima K, Chiba K, Sasaki S, Fujita T **2000**. Synthesis and immunosuppressive activity of 2-substituted 2-aminopropane-1,3-diols and 2-aminoethanols. *J Med Chem* 43, 2946-2961.
- Kiuchi M, Adachi K, Kohara T, Teshima K, Masubuchi Y, Mishina T, Fujita T **1998**. Synthesis and biological evaluation of 2,2-disubstituted 2-aminoethanols: analogues of FTY720. *Bioorg Med Chem Lett* 8, 101-106.
- Klemke C **PhD Thesis**. Isolation, cultivation and biological screening of marine endophytic fungi and structure elucidation of new fungal secondary metabolites. 2004 University of Bonn, Germany.
- Kobayashi K, Meguro S, Yoshimoto T, Namikoshi M **2003**. Absolute structure, biosynthesis, and anti-microtubule activity of phomopsidin, isolated from a marine-derived fungus *Phomopsis* sp. *Tetrahedron* 59, 455-459.
- Kobayashi K, Ui T **1975**. Isolation of phytotoxic substances produced by *Cephalosporium gregatum* Allington and Chamberlain. *Tetrahedron Lett* 47, 4119-4122.
- Kok JW, Sietsma H **2004**. Sphingolipid metabolism enzymes as targets for anticancer therapy. *Curr Drug Targets* 5, 375-382.
- Kolter T, Sandhoff K **2006**. Sphingolipid metabolism diseases. *Biochim Biophys Acta* 1758, 2057-2079.
- König GM, Kehraus S, Seibert SF, Abdel-Lateff A, Muller D **2006**. Natural products from marine organisms and their associated microbes. *Chembiochem* 7, 229-238.
- König GM, Wright AD **1996**. Marine natural products research: current directions and future potential. *Planta Med* 62, 193-211.



- Kowall M, Vater J, Kluge B, Stein T, Franke P, Ziessow D **1998**. Separation and Characterization of Surfactin Isoforms Produced by *Bacillus subtilis* OKB 105. *J Colloid Interface Sci* 204, 1-8.
- Kralj A, Kehraus S, Krick A, Eguereva E, Kelter G, Maurer M, Wortmann A, Fiebig HH, König GM **2006**. Arugosins G and H: prenylated polyketides from the marine-derived fungus *Emericellanidulans* var. *acristata*. *J Nat Prod* 69, 995-1000.
- Kriek NP, Kellerman TS, Marasas WF **1981**. A comparative study of the toxicity of *Fusarium verticillioides* (= *F. moniliforme*) to horses, primates, pigs, sheep and rats. *Onderstepoort J Vet Res* 48, 129-131.
- Krohn K, Steingrover K, Aust HJ, Draeger S, Schulz B **2003**. Biologically active metabolites from fungi, 17. 8- $\alpha$ -acetoxyverrol, a new member of the trichothecene sesquiterpenes. *Nat Prod Res* 17, 67-70.
- Kruger EA, Figg WD **2000**. TNP-470: an angiogenesis inhibitor in clinical development for cancer. *Expert Opin Investig Drugs* 9, 1383-1396.
- Lannert H, Gorgas K, Meissner I, Wieland FT, Jeckel D **1998**. Functional organization of the Golgi apparatus in glycosphingolipid biosynthesis. Lactosylceramide and subsequent glycosphingolipids are formed in the lumen of the late Golgi. *J Biol Chem* 273, 2939-2946.
- Laupeze B, Amiot L, Courtois A, Vernhet L, Drenou B, Fauchet R, Fardel O **1999**. Use of the anionic dye carboxy-2',7'-dichlorofluorescein for sensitive flow cytometric detection of multidrug resistance-associated protein activity. *Int J Oncol* 15, 571-576.
- Lautraite S, Parent-Massin D, Rio B, Hoellinger H **1997**. In vitro toxicity induced by deoxynivalenol (DON) on human and rat granulomonocytic progenitors. *Cell Biol Toxicol* 13, 175-183.
- Lavie Y, Cao H, Bursten SL, Giuliano AE, Cabot MC **1996**. Accumulation of glucosylceramides in multidrug-resistant cancer cells. *J Biol Chem* 271, 19530-19536.
- Lee HS, Choi WK, Son HJ, Lee SS, Kim JK, Ahn SK, Hong CI, Min HK, Kim M, Myung SW **2004**. Absorption, distribution, metabolism, and excretion of CKD-732, a novel antiangiogenic fumagillin derivative, in rats, mice, and dogs. *Arch Pharm Res* 27, 265-272.
- Lee HW, Cho CS, Kang SK, Yoo YS, Shin JS, Ahn SK **2007**. Design, synthesis, and antiangiogenic effects of a series of potent novel fumagillin analogues. *Chem Pharm Bull (Tokyo)* 55, 1024-1029.
- Li FQ, Luo XY, Yoshizawa T **1999**. Mycotoxins (trichothecenes, zearalenone and fumonisins) in cereals associated with human red-mold intoxications stored since 1989 and 1991 in China. *Nat Toxins* 7, 93-97.
- Lingham RB, Hsu A, Silverman KC, Bills GF, Dombrowski A, Goldman ME, Darke PL, Huang L, Koch G, Ondeyka JG, et al. **1992**. L-696,474, a novel cytochalasin as an inhibitor of HIV-1 protease. III. Biological activity. *J Antibiot (Tokyo)* 45, 686-691.
- Liu JK **2005**. N-containing compounds of macromycetes. *Chem Rev* 105, 2723-2744.
- Liu S, Widom J, Kemp CW, Crews CM, Clardy J **1998**. Structure of human methionine aminopeptidase-2 complexed with fumagillin. *Science* 282, 1324-1327.
- Loukaci A, Kayser O, Bindseil K, Siems K, Frevert J, Abreu PM **2000**. New trichothecenes isolated from *Holarrhena floribunda*. *J Nat Prod* 63, 52-56.
- Lucci A, Cho WI, Han TY, Giuliano AE, Morton DL, Cabot MC **1998**. Glucosylceramide: a marker for multiple-drug resistant cancers. *Anticancer Res* 18, 475-480.

- Lucci A, Han TY, Liu YY, Giuliano AE, Cabot MC **1999**. Modification of ceramide metabolism increases cancer cell sensitivity to cytotoxics. *Int J Oncol* 15, 541-546.
- Lucero HA, Robbins PW **2004**. Lipid rafts-protein association and the regulation of protein activity. *Arch Biochem Biophys* 426, 208-224.
- Luesch H, Yoshida WY, Moore RE, Paul VJ, Mooberry SL **2000**. Isolation, structure determination, and biological activity of Lyngbyabellin A from the marine cyanobacterium *lyngbya majuscula*. *J Nat Prod* 63, 611-615.
- Malisan F, Testi R **2002**. GD3 ganglioside and apoptosis. *Biochim Biophys Acta* 1585, 179-187.
- Mandala SM, Frommer BR, Thornton RA, Kurtz MB, Young NM, Cabello MA, Genilloud O, Liesch JM, Smith JL, Horn WS **1994**. Inhibition of serine palmitoyl-transferase activity by lipoxamycin. *J Antibiot (Tokyo)* 47, 376-379.
- Mandala SM, Thornton RA, Frommer BR, Curotto JE, Rozdilsky W, Kurtz MB, Giacobbe RA, Bills GF, Cabello MA, Martin I, et al. **1995**. The discovery of australifungin, a novel inhibitor of sphinganine N-acyltransferase from *Sporormiella australis*. Producing organism, fermentation, isolation, and biological activity. *J Antibiot (Tokyo)* 48, 349-356.
- Mandala SM, Thornton RA, Frommer BR, Dreikorn S, Kurtz MB **1997**. Viridifungins, novel inhibitors of sphingolipid synthesis. *J Antibiot (Tokyo)* 50, 339-343.
- Mandon EC, Ehse I, Rother J, van Echten G, Sandhoff K **1992**. Subcellular localization and membrane topology of serine palmitoyltransferase, 3-dehydrosphinganine reductase, and sphinganine N-acyltransferase in mouse liver. *J Biol Chem* 267, 11144-11148.
- Manzoni M, Rollini M, Bergomi S, Cavazzoni V **1998**. Production and purification of statins from *Aspergillus terreus* strains. *Biotechnol Techn* 12, 529-532.
- Marasas WF, Kellerman TS, Gelderblom WC, Coetzer JA, Thiel PG, van der Lugt JJ **1988**. Leukoencephalomalacia in a horse induced by fumonisin B1 isolated from *Fusarium moniliforme*. *Onderstepoort J Vet Res* 55, 197-203.
- Marchell NL, Uchida Y, Brown BE, Elias PM, Holleran WM **1998**. Glucosylceramides stimulate mitogenesis in aged murine epidermis. *J Invest Dermatol* 110, 383-387.
- Marfey P **1984**. Determination of D-amino acids. II. Use of a bifunctional reagent, 1,5-difluoro-2,4-dinitrobenzene. *Carlsberg Res Commun* 49, 591-596.
- Marsh NL, Elias PM, Holleran WM **1995**. Enhancement of epidermal glucosylceramide content stimulates mitogenesis in murine epidermis. *J Clin Invest* 95, 2903-2909.
- Marui S, Itoh F, Kozai Y, Sudo K, Kishimoto S **1992**. Chemical modification of fumagillin. I. 6-O-acyl, 6-O-sulfonyl, 6-O-alkyl, and 6-O-(N-substituted-carbamoyl)fumagillols. *Chem Pharm Bull (Tokyo)* 40, 96-101.
- Maruta H, He H, Tikoo A, Nur-e-Kamal M **1999**. Cytoskeletal tumor suppressors that block oncogenic RAS signaling. *Ann N Y Acad Sci* 886, 48-57.
- McCloskey DE, Kaufmann SH, Prestigiacomo LJ, Davidson NE **1996**. Paclitaxel induces programmed cell death in MDA-MB-468 human breast cancer cells. *Clin Cancer Res* 2, 847-854.
- McLaughlin F, Finn P, La Thangue NB **2003**. The cell cycle, chromatin and cancer: mechanism-based therapeutics come of age. *Drug Discov Today* 8, 793-802.

- McMorris TC **1999**. Discovery and development of sesquiterpenoid derived hydroxymethylacylfulvene: a new anticancer drug. *Bioorg Med Chem* 7, 881-886.
- Memon RA, Holleran WM, Uchida Y, Moser AH, Grunfeld C, Feingold KR **2001**. Regulation of sphingolipid and glycosphingolipid metabolism in extrahepatic tissues by endotoxin. *J Lipid Res* 42, 452-459.
- Merrill AH, Jr., Sullards MC, Wang E, Voss KA, Riley RT **2001**. Sphingolipid metabolism: roles in signal transduction and disruption by fumonisins. *Environ Health Perspect* 109 Suppl 2, 283-289.
- Merrill AH, Jr., van Echten G, Wang E, Sandhoff K **1993a**. Fumonisin B1 inhibits sphingosine (sphinganine) N-acyltransferase and de novo sphingolipid biosynthesis in cultured neurons in situ. *J Biol Chem* 268, 27299-27306.
- Merrill AH, Jr., Wang E, Gilchrist DG, Riley RT **1993b**. Fumonisin and other inhibitors of de novo sphingolipid biosynthesis. *Adv Lipid Res* 26, 215-234.
- Michel C, van Echten-Deckert G, Rother J, Sandhoff K, Wang E, Merrill AH, Jr. **1997**. Characterization of ceramide synthesis. A dihydroceramide desaturase introduces the 4,5-trans-double bond of sphingosine at the level of dihydroceramide. *J Biol Chem* 272, 22432-22437.
- Miyake Y, Kozutsumi Y, Nakamura S, Fujita T, Kawasaki T **1995**. Serine palmitoyltransferase is the primary target of a sphingosine-like immunosuppressant, ISP-1/myriocin. *Biochem Biophys Res Commun* 211, 396-403.
- Modica-Napolitano JS, Aprille JR **2001**. Delocalized lipophilic cations selectively target the mitochondria of carcinoma cells. *Adv Drug Deliv Rev* 49, 63-70.
- Modrak DE, Gold DV, Goldenberg DM **2006**. Sphingolipid targets in cancer therapy. *Mol Cancer Ther* 5, 200-208.
- Mookerjee BK, Cuppoletti J, Rampal AL, Jung CY **1981**. The effects of cytochalasins on lymphocytes. Identification of distinct cytochalasin-binding sites in relation to mitogenic response and hexose transport. *J Biol Chem* 256, 1290-1300.
- Morgan E, Varro R, Sepulveda H, Ember JA, Apgar J, Wilson J, Lowe L, Chen R, Shivraj L, Agadir A, Campos R, Ernst D, Gaur A **2004**. Cytometric bead array: a multiplexed assay platform with applications in various areas of biology. *Clin Immunol* 110, 252-266.
- Nakamura S, Kozutsumi Y, Sun Y, Miyake Y, Fujita T, Kawasaki T **1996**. Dual roles of sphingolipids in signaling of the escape from and onset of apoptosis in a mouse cytotoxic T-cell line, CTLL-2. *J Biol Chem* 271, 1255-1257.
- Neyfakh AA **1988**. Use of fluorescent dyes as molecular probes for the study of multidrug resistance. *Exp Cell Res* 174, 168-176.
- Nitta K, Fujita N, Yoshimura T, Arai K, Yamamoto Y **1983**. Metabolic products of *Aspergillus terreus*. IX. Biosynthesis of butyrolactone derivatives isolated from strains IFO 8835 and 4100. *Chem Pharm Bull* 31, 1528-1533.
- Nomura T, Takizawa M, Aoki J, Arai H, Inoue K, Wakisaka E, Yoshizuka N, Imokawa G, Dohmae N, Takio K, Hattori M, Matsuo N **1998**. Purification, cDNA cloning, and expression of UDP-Gal: glucosylceramide beta-1,4-galactosyltransferase from rat brain. *J Biol Chem* 273, 13570-13577.

- Nozawa K, Nakajima S, Kawai K **1988**. Studies on fungal products. Part 17. Isolation and structures of novel indoloditerpenes, emindoles DA and DB, from *Emericella desertorum*: X-ray molecular structure of emindole DA acetate. *J Chem Soc [Perkin 1]*, 1689-1694.
- Nozawa K, Udagawa S, Nakajima S, Kawai K **1987**. Structures of two stereoisomers of a new type of indoloditerpene related to the tremorgenic mycotoxin paxilline, from *Emericella desertorum* and *Emericella striata*. *J Chem Soc Chem Commun*, 1157-1159.
- Numata A, Amagata T, Minoura K, Ito T **1997**. Gymnastatins, novel cytotoxic metabolites produced by a fungal strain from a sponge. *Tetrah Lett* 38, 5675-5678.
- Ogretmen B **2006**. Sphingolipids in cancer: regulation of pathogenesis and therapy. *FEBS Lett* 580, 5467-5476.
- Ogretmen B, Hannun YA **2004**. Biologically active sphingolipids in cancer pathogenesis and treatment. *Nat Rev Cancer* 4, 604-616.
- Onishi JC, Milligan JA, Basilio A, Bergstrom J, Curotto J, Huang L, Meinz M, Nallin-Omstead M, Pelaez F, Rew D, Salvatore M, Thompson J, Vicente F, Kurtz MB **1997**. Antimicrobial activity of viridiodifungins. *J Antibiot (Tokyo)* 50, 334-338.
- Pachler KG, Steyn PS, Vlegaar R, Wessels PL **1976**. Carbon-13 nuclear magnetic resonance assignments and biosynthesis of aflatoxin B1 and sterigmatocystin. *J Chem Soc [Perkin 1]*, 1182-1189.
- Paris R, Morales A, Coll O, Sanchez-Reyes A, Garcia-Ruiz C, Fernandez-Checa JC **2002**. Ganglioside GD3 sensitizes human hepatoma cells to cancer therapy. *J Biol Chem* 277, 49870-49876.
- Paugh SW, Payne SG, Barbour SE, Milstien S, Spiegel S **2003**. The immunosuppressant FTY720 is phosphorylated by sphingosine kinase type 2. *FEBS Lett* 554, 189-193.
- Pestka JJ, Smolinski AT **2005**. Deoxynivalenol: toxicology and potential effects on humans. *J Toxicol Environ Health B Crit Rev* 8, 39-69.
- Pestka JJ, Zhou HR, Moon Y, Chung YJ **2004**. Cellular and molecular mechanisms for immune modulation by deoxynivalenol and other trichothecenes: unraveling a paradox. *Toxicol Lett* 153, 61-73.
- Pettit GR, Numata A, Iwamoto C, Morito H, Yamada T, Goswami A, Clewlow PJ, Cragg GM, Schmidt JM **2002**. Antineoplastic agents. 489. Isolation and structures of meliastatins 1-5 and related euphane triterpenes from the tree *Melia dubia*. *J Nat Prod* 65, 1886-1891.
- Pettus BJ, Chalfant CE, Hannun YA **2002**. Ceramide in apoptosis: an overview and current perspectives. *Biochim Biophys Acta* 1585, 114-125.
- Peypoux F, Bonmatin JM, Labbe H, Das BC, Ptak M, Michel G **1991**. Isolation and characterization of a new variant of surfactin, the [Val7]surfactin. *Eur J Biochem* 202, 101-106.
- Phillips NJ, Goodwin JT, Fraiman A, Cole RJ, Lynn DG **1989**. Characterization of the *Fusarium* toxin equisetin: The use of phenylboronates in structure assignment. *J Am Chem Soc* 111, 8223-8231.
- Plattner RD, Al-Hetti MB, Weisleder D, Sinclair JB **1988**. A new trichothecene from *Trichothecium roseum*. *J Chem Res (M)*, 2461-2473.
- Preston RJ, Williams GM **2005**. DNA-reactive carcinogens: mode of action and human cancer hazard. *Crit Rev Toxicol* 35, 673-683.

- Proia RL **2003**. Glycosphingolipid functions: insights from engineered mouse models. *Philos Trans R Soc Lond B Biol Sci* 358, 879-883.
- Proia RL **2004**. Gangliosides help stabilize the brain. *Nat. Genet.* 36, 1147-1148.
- Radin NS **2004**. Sphingolipids as coenzymes in anion transfer and tumor death. *Bioorg Med Chem* 12, 6029-6037.
- Raggers RJ, van Helvoort A, Evers R, van Meer G **1999**. The human multidrug resistance protein MRP1 translocates sphingolipid analogs across the plasma membrane. *J Cell Sci* 112 ( Pt 3), 415-422.
- Raistrick H, Smith G **1935**. Studies in the biochemistry of micro-organisms: The metabolic products of *Aspergillus terreus* Thom. A new mould metabolic product-terrein. *Biochem J* 29, 606-611.
- Ramstedt B, Slotte JP **2002**. Membrane properties of sphingomyelins. *FEBS Lett* 531, 33-37.
- Renner MK, Jensen PR, Fenical W **1998**. Neomangicols: Structures and Absolute Stereochemistries of Unprecedented Halogenated Sesterterpenes from a Marine Fungus of the Genus *Fusarium*. *J Org Chem* 63, 8346-8354.
- Reynolds CP, Maurer BJ, Kolesnick RN **2004**. Ceramide synthesis and metabolism as a target for cancer therapy. *Cancer Lett* 206, 169-180.
- Riley RT, Enongene E, Voss KA, Norred WP, Meredith FI, Sharma RP, Spitsbergen J, Williams DE, Carlson DB, Merrill AH, Jr. **2001**. Sphingolipid perturbations as mechanisms for fumonisin carcinogenesis. *Environ Health Perspect* 109 Suppl 2, 301-308.
- Rocha O, Ansari K, Doohan FM **2005**. Effects of trichothecene mycotoxins on eukaryotic cells: a review. *Food Addit Contam* 22, 369-378.
- Rosenberg E, Ron EZ **1999**. High- and low-molecular-mass microbial surfactants. *Appl Microbiol Biotechnol* 52, 154-162.
- Roth T, Burger AM, Debgler WA, Willmann H, Fiebig HH **1999**. Human tumor cell lines demonstrating the characteristics of patient tumors as useful models for anticancer drug screening. 145-156.
- Rother J, van Echten G, Schwarzmann G, Sandhoff K **1992**. Biosynthesis of sphingolipids: dihydroceramide and not sphinganine is desaturated by cultured cells. *Biochem Biophys Res Commun* 189, 14-20.
- Rubtsova SN, Kondratov RV, Kopnin PB, Chumakov PM, Kopnin BP, Vasiliev JM **1998**. Disruption of actin microfilaments by cytochalasin D leads to activation of p53. *FEBS Lett* 430, 353-357.
- Sadeghlar F, Sandhoff K, van Echten-Deckert G **2000**. Cell type specific localization of sphingomyelin biosynthesis. *FEBS Lett* 478, 9-12.
- Sassa T, Aoki H, Munakata K **1968**. Plant growth metabolites of *Sclerotinia sclerotiorum*. (II) The synthesis of sclerotinin B. *Tetrahedron Lett* 54, 5703-5705.
- Schmelz EM, Dombrink-Kurtzman MA, Roberts PC, Kozutsumi Y, Kawasaki T, Merrill AH, Jr. **1998**. Induction of apoptosis by fumonisin B1 in HT29 cells is mediated by the accumulation of endogenous free sphingoid bases. *Toxicol Appl Pharmacol* 148, 252-260.
- Schubert D, Heinemann S, Carlisle W, Tarikas H, Kimes B, Patrick J, Steinbach JH, Culp W, Brandt BL **1974**. Clonal cell lines from the rat central nervous system. *Nature* 249, 224-227.

- Schultz B, Sucker J, Aust HJ, Krohn K, Ludewig K, Jones PG, Döring D **1995**. Biologically active secondary metabolites of endophytic *Pezizula* species. *Mycol Res* 99, 1007-1015.
- Senchenkov A, Litvak DA, Cabot MC **2001**. Targeting ceramide metabolism--a strategy for overcoming drug resistance. *J Natl Cancer Inst* 93, 347-357.
- Senkal CE, Ponnusamy S, Rossi MJ, Sundararaj K, Szulc Z, Bielawski J, Bielawska A, Meyer M, Cobanoglu B, Koybasi S, Sinha D, Day TA, Obeid LM, Hannun YA, Ogretmen B **2006**. Potent antitumor activity of a novel cationic pyridinium-ceramide alone or in combination with gemcitabine against human head and neck squamous cell carcinomas in vitro and in vivo. *J Pharmacol Exp Ther* 317, 1188-1199.
- Senzer N, Arsenau J, Richards D, Berman B, MacDonald JR, Smith S **2005**. Irofulven demonstrates clinical activity against metastatic hormone-refractory prostate cancer in a phase 2 single-agent trial. *Am J Clin Oncol* 28, 36-42.
- Shier WT, Abbas HK, Mirocha CJ **1991**. Toxicity of the mycotoxins fumonisins B1 and B2 and *Alternaria alternata* f. sp. *lycopersici* toxin (AAL) in cultured mammalian cells. *Mycopathologia* 116, 97-104.
- Shifrin VI, Anderson P **1999**. Trichothecene mycotoxins trigger a ribotoxic stress response that activates c-Jun N-terminal kinase and p38 mitogen-activated protein kinase and induces apoptosis. *J Biol Chem* 274, 13985-13992.
- Shirane N, Takenaka H, Ueda K, Hashimoto Y, Katoh K, Ishii H **1996**. Sterol analysis of DMI-resistant and -sensitive strains of *Venturia inaequalis*. *Phytochemistry* 41, 1301-1308.
- Simmons TL, Andrianasolo E, McPhail K, Flatt P, Gerwick WH **2005**. Marine natural products as anticancer drugs. *Mol Cancer Ther* 4, 333-342.
- Singh P, Cameotra SS **2004**. Potential applications of microbial surfactants in biomedical sciences. *Trends Biotechnol* 22, 142-146.
- Smith ER, Merrill AH, Jr. **1995**. Differential roles of de novo sphingolipid biosynthesis and turnover in the "burst" of free sphingosine and sphinganine, and their 1-phosphates and N-acyl-derivatives, that occurs upon changing the medium of cells in culture. *J Biol Chem* 270, 18749-18758.
- Soriano JM, Gonzalez L, Catala AI **2005**. Mechanism of action of sphingolipids and their metabolites in the toxicity of fumonisin B1. *Prog Lipid Res* 44, 345-356.
- Spear MA **2007**. Vascular disrupting agent NPI-2358 in phase I study. *American association for cancer research. Annual meeting 2007* Nereus Pharmaceuticals, San Diego, California, Abstract 3987.
- Spiegel S, Milstien S **2003**. Sphingosine-1-phosphate: an enigmatic signalling lipid. *Nat Rev Mol Cell Biol* 4, 397-407.
- Steyn PS, van Heerden FR **1982**. Cytochalasins E and K, toxic metabolites from *Aspergillus clavatus*. *J Chem Soc [Perkin 1]*, 541-544.
- Svennerholm L **1963**. Chromatographic Separation of Human Brain Gangliosides. *J Neurochem* 10, 613-623.
- Sweeney EA, Sakakura C, Shirahama T, Masamune A, Ohta H, Hakomori S, Igarashi Y **1996**. Sphingosine and its methylated derivative N,N-dimethylsphingosine (DMS) induce apoptosis in a variety of human cancer cell lines. *Int J Cancer* 66, 358-366.

- Takahashi C, Numata A, Matsumura E, Minoura K, Eto H, Shingu T, Ito T, Hasegawa T **1994**. Leptosins I and J, cytotoxic substances produced by a *Leptosphaeria* sp. Physico-chemical properties and structures. *J Antibiot (Tokyo)* 47, 1242-1249.
- Takahashi C, Takai Y, Kimura Y, Numata A, Shigematsu N, Tanaka H **1995**. Cytotoxic metabolites from a fungal adherent of a marine alga. *Phytochemistry* 38, 155-158.
- Tanaka H, Plattner RD, Yamagishi R, Minamisawa M, Manabe M, Kawasugi S, Gareis M, Okada G **2001**. 8-deoxy-trichothecin production by *Spicellum roseum* isolated from a cultivated mushroom in Japan. *Mycotoxins* 51, 71-77.
- Thudichum JLW **1884**. Treatise on the chemical constitution of the brain. *London, Bailliere, Tindall and Cox*.
- Tomoda H, Huang XH, Cao J, Nishida H, Nagao R, Okuda S, Tanaka H, Omura S, Arai H, Inoue K **1992**. Inhibition of acyl-CoA: cholesterol acyltransferase activity by cyclodepsipeptide antibiotics. *J Antibiot (Tokyo)* 45, 1626-1632.
- Trenkner E, Sidman RL **1977**. Histogenesis of mouse cerebellum in microwell cultures. Cell reaggregation and migration, fiber and synapse formation. *J Cell Biol* 75, 915-940.
- Ueno Y **1984**. Toxicological features of T-2 toxin and related trichothecenes. *Fundam Appl Toxicol* 4, S124-132.
- van Echten-Deckert G **2000**. Sphingolipid extraction and analysis by thin-layer chromatography. *Methods Enzymol* 312, 64-79.
- van Echten-Deckert G, Herget T **2006**. Sphingolipid metabolism in neural cells. *Biochim Biophys Acta* 1758, 1978-1994.
- van Echten G, Birk R, Brenner-Weiss G, Schmidt RR, Sandhoff K **1990a**. Modulation of sphingolipid biosynthesis in primary cultured neurons by long chain bases. *J Biol Chem* 265, 9333-9339.
- van Echten G, Iber H, Stotz H, Takatsuki A, Sandhoff K **1990b**. Uncoupling of ganglioside biosynthesis by Brefeldin A. *Eur J Cell Biol* 51, 135-139.
- van Echten G, Sandhoff K **1989**. Modulation of ganglioside biosynthesis in primary cultured neurons. *J Neurochem* 52, 207-214.
- van Echten G, Sandhoff K **1993**. Ganglioside metabolism. Enzymology, Topology, and regulation. *J Biol Chem* 268, 5341-5344.
- Van Hamme JD, Singh A, Ward OP **2006**. Physiological aspects. Part 1 in a series of papers devoted to surfactants in microbiology and biotechnology. *Biotechnol Adv* 24, 604-620.
- Van Veldhoven PP **2000**. Sphingosine-1-phosphate lyase. *Methods Enzymol* 311, 244-254.
- Varoglu M, Crews P **2000**. Biosynthetically diverse compounds from a saltwater culture of sponge-derived *Aspergillus niger*. *J Nat Prod* 63, 41-43.
- Voss KA, Plattner RD, Bacon CW, Norred WP **1990**. Comparative studies of hepatotoxicity and fumonisin B1 and B2 content of water and chloroform/methanol extracts of *Fusarium moniliforme* strain MRC 826 culture material. *Mycopathologia* 112, 81-92.
- Wang JS, Groopman JD **1999**. DNA damage by mycotoxins. *Mutat Res* 424, 167-181.

- Watterson KR, Ratz PH, Spiegel S **2005**. The role of sphingosine-1-phosphate in smooth muscle contraction. *Cell Signal* 17, 289-298.
- Wedeking A, van Echten-Deckert G **2006**. Sphingolipid metabolism and function in nerve tissue. Kerala, India, Research Signpost.
- Yabe K, Nakajima H **2004**. Enzyme reactions and genes in aflatoxin biosynthesis. *Appl Microbiol Biotechnol* 64, 745-755.
- Yakimov MM, Timmis KN, Wray V, Fredrickson HL **1995**. Characterization of a new lipopeptide surfactant produced by thermotolerant and halotolerant subsurface *Bacillus licheniformis* BAS50. *Appl Environ Microbiol* 61, 1706-1713.
- Yamaji-Hasegawa A, Takahashi A, Tetsuka Y, Senoh Y, Kobayashi T **2005**. Fungal metabolite sulfamisterin suppresses sphingolipid synthesis through inhibition of serine palmitoyltransferase. *Biochemistry* 44, 268-277.
- Yamashita T, Wu YP, Sandhoff R, Werth N, Mizukami H, Ellis JM, Dupree JL, Geyer R, Sandhoff K, Proia RL **2005**. Interruption of ganglioside synthesis produces central nervous system degeneration and altered axon-glia interactions. *Proc Natl Acad Sci U S A* 102, 2725-2730.
- Yang CS **1980**. Research on esophageal cancer in China: a review. *Cancer Res* 40, 2633-2644.
- Yang GH, Jarvis BB, Chung YJ, Pestka JJ **2000**. Apoptosis induction by the satratoxins and other trichothecene mycotoxins: relationship to ERK, p38 MAPK, and SAPK/JNK activation. *Toxicol Appl Pharmacol* 164, 149-160.
- Zacharias C, van Echten-Deckert G, Plewe M, Schmidt RR, Sandhoff K **1994**. A truncated epoxy-glucosylceramide uncouples glycosphingolipid biosynthesis by decreasing lactosylceramide synthase activity. *J Biol Chem* 269, 13313-13317.
- Zhang J, Alter N, Reed JC, Borner C, Obeid LM, Hannun YA **1996**. Bcl-2 interrupts the ceramide-mediated pathway of cell death. *Proc Natl Acad Sci U S A* 93, 5325-5328.
- Zhang Y, Dickman MB, Jones C **1999**. The mycotoxin fumonisin B1 transcriptionally activates the p21 promoter through a cis-acting element containing two Sp1 binding sites. *J Biol Chem* 274, 12367-12371.
- Zhou HR, Islam Z, Pestka JJ **2003**. Rapid, sequential activation of mitogen-activated protein kinases and transcription factors precedes proinflammatory cytokine mRNA expression in spleens of mice exposed to the trichothecene vomitoxin. *Toxicol Sci* 72, 130-142.
- Zhou HR, Islam Z, Pestka JJ **2005**. Induction of competing apoptotic and survival signaling pathways in the macrophage by the ribotoxic trichothecene deoxynivalenol. *Toxicol Sci* 87, 113-122.
- Zweerink MM, Edison AM, Wells GB, Pinto W, Lester RL **1992**. Characterization of a novel, potent, and specific inhibitor of serine palmitoyltransferase. *J Biol Chem* 267, 25032-25038.



---

## 8 Appendix

Assays were performed as described in the Materials and Methods chapter.

	page
<b>8.1 Results of the cytotoxicity assay</b>	
8.1.1 Cytotoxicity of extracts and VLC fractions	131
8.1.2 Cytotoxicity of isolated compounds	137

## 8.1 Cytotoxicity of extracts and VLC fractions

Fungal strain	code		IC50	IC70	active/total* at				Tumor selectivity		
	König	Oncotest	[µg/ml]	[µg/ml]	3 µg/ml		30 µg/ml		sel. <sup>1)/</sup> total	% select.	rating <sup>2)</sup>
	018MYA-8	MNEB127F	8,511	14,717	0/6	0%	6/6	100%	0/6	0%	-
<b><i>Fusarium</i></b>	018MYA	MNEB119F	9,404	15,817	0/6	0%	6/6	100%	0/6	0%	-
<b><i>dimerum</i></b>	018MYA-9	MNEB128F	9,778	16,050	0/6	0%	6/6	100%	0/6	0%	-
<b>(18 MYA)</b>	018MYA-1	MNEB120F	10,141	16,915	0/6	0%	6/6	100%	0/6	0%	-
	018MYA-7	MNEB126F	10,127	17,626	0/6	0%	6/6	100%	0/6	0%	-
	018MYA-5	MNEB124F	14,091	22,433	0/6	0%	5/6	83%	0/6	0%	-
	018MYA-6	MNEB125F	21,048	29,064	0/6	0%	3/6	50%	0/6	0%	-
	018MYA-4	MNEB123F	21,751	39,031	0/6	0%	2/6	33%	0/6	0%	-
	018MYA-11	MNEB130F	27,744	44,033	0/6	0%	0/6	0%	0/6	0%	-
	018MYA-10	MNEB129F	28,892	59,052	0/6	0%	0/6	0%	0/6	0%	-
	018MYA-2	MNEB121F	>30	>30	0/6	0%	0/6	0%	0/6	0%	-
	018MYA-3	MNEB122F	<30	>30	0/6	0%	0/6	0%	0/6	0%	-
<b><i>Arthrinium</i></b>	727/3	MNEB003	3,302	5,753	3/6	50%	6/6	100%			
<b><i>sacchari</i></b>	727 BMS	MNEB012	4,751	10,288	2/6	33%	5/6	83%			
<b>(727 BMS)</b>	727/4	MNEB004	23,213	>30	0/6	0%	2/6	33%			
	727/1	MNEB001	>30	>30	0/6	0%	0/6	0%			
	727/10	MNEB010	>30	>30	0/6	0%	0/6	0%			
	727/2	MNEB002	28,243	>30	0/6	0%	0/6	0%			

Fungal strain	code		IC50	IC70	active/total* at				Tumor selectivity		
	König	Oncotest	[µg/ml]	[µg/ml]	3 µg/ml		30 µg/ml		sel. <sup>1)</sup> / total	% select.	rating <sup>2)</sup>
	727/5	MNEB005	>30	>30	0/6	0%	0/6	0%			
	727/6	MNEB006	>30	>30	0/6	0%	0/6	0%			
	727/7	MNEB007	>30	>30	0/6	0%	0/6	0%			
	727/8	MNEB008	>30	>30	0/6	0%	0/6	0%			
	727/9	MNEB009	>30	>30	0/6	0%	0/6	0%			
	727-11	MNEB011	>30	>30	0/6	0%	0/6	0%			
subfractionation	727/3-5	MNEB053F	0,172	2,435	3/6	50%	5/6	83%			
of fraction 3	727/3-6	MNEB054F	0,507	1,776	3/6	50%	4/6	66%			
	727/3-4	MNEB052F	0,883	8,607	3/6	50%	3/6	50%			
	727/3-7	MNEB055F	5,353	13,094	1/6	17%	5/6	83%			
	727/3-1	MNEB049F	>30	>30	0/6	0%	0/6	0%			
	727/3-2	MNEB050F	>30	>30	0/6	0%	0/6	0%			
	727/3-3	MNEB051F	>30	>30	0/6	0%	0/6	0%			
	727/3-8	MNEB056F	>30	>30	0/6	0%	0/6	0%			
	727/3-9	MNEB057F	>30	>30	0/6	0%	0/6	0%			
	727/3-10	MNEB058F	>30	>30	0/6	0%	0/6	0%			

Fungal strain	code		IC50	IC70	active/total* at				Tumor selectivity		
	König	Oncotest	[µg/ml]	[µg/ml]	3 µg/ml		30 µg/ml		sel. <sup>1)</sup> / total	% select.	rating <sup>2)</sup>
<i>Fusarium</i>	588MYA	MNEB177F	6,459	15,082	0/6	0%	5/6	83%	1/6	17%	++
<i>oxysporum</i>	588-4	MNEB181F	2,385	5,123	2/6	33%	6/6	100%	0/6	0%	-
<b>(588 MYA)</b>	588-3	MNEB180F	2,351	5,526	2/6	33%	6/6	100%	0/6	0%	-
	588-5	MNEB182F	9,391	17,784	0/6	0%	6/6	100%	0/6	0%	-
	588-7	MNEB184F	11,648	22,016	0/6	0%	4/6	67%	0/6	0%	-
	588-6	MNEB183F	14,142	25,915	0/6	0%	5/6	83%	0/6	0%	-
	588-8	MNEB185F	17,807	30,691	0/6	0%	3/6	50%	0/6	0%	-
	588-1	MNEB178F	>30	>30	0/6	0%	0/6	0%	0/6	0%	-
	588-2	MNEB179F	70,558	>30	0/6	0%	0/6	0%	0/6	0%	-
<i>Paecilomyces</i>	193BMS-8	MNEB104F	0,012	2,589	2/6	33%	3/6	50%	2/6	33%	++
<i>lilacinus</i>	193BMS-10	MNEB106F	0,038	4,060	2/6	33%	2/6	33%	2/6	33%	++
<b>(193 BMS)</b>	193BMS-7	MNEB103F	0,928	4,716	1/6	17%	4/6	67%	2/6	33%	++
	193BMS	MNEB096F	0,091	5,448	2/6	33%	5/6	83%	2/6	33%	++
	193BMS-9	MNEB105F	0,275	3,873	1/6	17%	3/6	50%	1/6	17%	+
	193BMS-4	MNEB100F	1,611	4,372	3/6	50%	6/6	100%	0/6	0%	-
	193BMS-5	MNEB101F	1,659	5,075	1/6	17%	6/6	100%	0/6	0%	-
	193BMS-6	MNEB102F	21,830	>30	0/6	0%	0/6	0%	0/6	0%	-
	193BMS-3	MNEB099F	>30	>30	0/6	0%	0/6	0%	0/6	0%	-

Fungal strain	code		IC50	IC70	active/total* at				Tumor selectivity		
	König	Oncotest	[µg/ml]	[µg/ml]	3 µg/ml		30 µg/ml		sel. <sup>1)</sup> / total	% select.	rating <sup>2)</sup>
	193BMS-1	MNEB097F	>30	>30	0/6	0%	0/6	0%	0/6	0%	-
	193BMS-2	MNEB098F	>30	>30	0/6	0%	0/6	0%	0/6	0%	-
<b><i>Acremonium</i></b>	738BMS-6	MNEB090F	0,331	0,698	6/6	100%	6/6	100%	1/6	17%	+
<b><i>sclerotigenum</i></b>	738BMS-5	MNEB089F	5,311	9,960	1/6	17%	6/6	100%	1/6	17%	+
<b>(738 BMS)</b>	738BMS-7	MNEB091F	0,692	1,340	6/6	100%	6/6	100%	0/6	0%	-
	738BMS-8	MNEB092F	14,036	22,158	0/6	0%	5/6	83%	0/6	0%	-
	738BMS	MNEB084F	13,065	22,917	0/6	0%	4/6	67%	0/6	0%	-
	738CZ	MNEB083F	20,399	31,010	0/6	0%	2/6	33%	0/6	0%	-
	738BMS-4	MNEB088F	37,434	90,759	0/6	0%	0/6	0%	0/6	0%	-
	738BMS-9	MNEB093F	28,035	>30	0/6	0%	0/6	0%	0/6	0%	-
	738BMS-11	MNEB095F	42,753	>30	0/6	0%	0/6	0%	0/6	0%	-
	738BMS-10	MNEB094F	>30	>30	0/6	0%	0/6	0%	0/6	0%	-
	738BMS-3	MNEB087F	>30	>30	0/6	0%	0/6	0%	0/6	0%	-
	738BMS-2	MNEB086F	>30	>30	0/6	0%	0/6	0%	0/6	0%	-
	738BMS-1	MNEB085F	>30	>30	0/6	0%	0/6	0%	0/6	0%	-

Fungal strain	code		IC50	IC70	active/total* at				Tumor selectivity		
	König	Oncotest	[µg/ml]	[µg/ml]	3 µg/ml		30 µg/ml		sel. <sup>1)</sup> / total	% select.	rating <sup>2)</sup>
<i>Microsphaeropsis</i>	96BMS-6	MNEB112F	25,110	29,250	0/6	0%	1/6	17%	0/6	0%	-
<i>sp.</i>	96BMS-5	MNEB111F	>30	29,584	0/6	0%	1/6	17%	0/6	0%	-
<b>(96 BMS)</b>	96BMS-7	MNEB113F	>30	>30	0/6	0%	0/6	0%	0/6	0%	-
	96BMS-4A	MNEB110F	>30	>30	0/6	0%	0/6	0%	0/6	0%	-
	96BMS	MNEB107F	>30	>30	0/6	0%	0/6	0%	0/6	0%	-
	96BMS-3	MNEB108F	>30	>30	0/6	0%	0/6	0%	0/6	0%	-
	96BMS-4	MNEB109F	>30	>30	0/6	0%	0/6	0%	0/6	0%	-
	96BMS-8	MNEB1114F	>30	>30	0/6	0%	0/6	0%	0/6	0%	-
	96BMS-9	MNEB115F	>30	>30	0/6	0%	0/6	0%	0/6	0%	-
	96BMS-10	MNEB116F	>30	>30	0/6	0%	0/6	0%	0/6	0%	-
	96BMS-11	MNEB117F	>30	>30	0/6	0%	0/6	0%	0/6	0%	-
	96BMS-12	MNEB118F	>30	>30	0/6	0%	0/6	0%	0/6	0%	-

Fungal strain	code		IC50 [µg/ml]	IC70 [µg/ml]	active/total* at				Tumor selectivity		
	König	Oncotest			3 µg/ml		30 µg/ml		sel. <sup>1)</sup> / total	% select.	rating <sup>2)</sup>
<i>Stagonospora</i>	16-6	MNEB173F	3,666	6,813	2/6	33%	6/6	100%	2/6	33%	+++
<i>sp.</i>	16-5	MNEB172F	0,700	1,259	6/6	100%	6/6	100%	1/6	17%	++
<b>(16 BMS)</b>	16-8	MNEB175F	7,903	12,231	0/6	0%	4/6	67%	1/6	17%	++
	16-4	MNEB171F	7,409	12,773	1/6	17%	6/6	100%	1/6	17%	++
	16BMS	MNEB167F	1,304	2,851	3/6	50%	6/6	100%	0/6	0%	-
	16-2	MNEB169F	6,781	15,416	0/6	0%	5/6	83%	0/6	0%	-
	16-7	MNEB174F	11,233	18,796	0/6	0%	6/6	100%	0/6	0%	-
	16-3	MNEB170F	10,050	19,312	0/6	0%	6/6	100%	0/6	0%	-
	16-1	MNEB168F	25,703	38,005	0/6	0%	0/6	0%	0/6	0%	-
	16-9	MNEB176F	27,783	38,442	0/6	0%	0/6	0%	0/6	0%	-

Samples were dissolved in methanol and tested in concentrations of 10 µg/mL against six tumor cell lines. Details are given in 3.9.2 chapter. Each test series was run in duplicate.

<sup>1)</sup> individual IC70 < 1/3 mean IC70; for example if mean IC70 = 2.1 µM the threshold for above average sensitivity was IC70 < 0.7 µM

<sup>2)</sup> – (% selective = < 4 %); + (4 % > = 10 %); ++ (10 % > % selective >= 20 %); +++ (% selective > 20 %)

## 8.2 Cytotoxicity of isolated compounds

compound	Identification		Potency		active/total at				Tumor selectivity		
	Oncotest	König	mean IC50 [µg/ml]	mean IC70 [µg/ml]	1 µg/ml		10 µg/ml		select. <sup>1)/</sup> total	% select.	rating <sup>2)</sup>
1	MNSB009	EM 7.2.4	>10	>10					0/36	0%	-
2	MNSB012	EM 7.10	>10	>10					0/36	0%	-
3 and 4	MNSB010	EM 7.3	9,5	>10					0/36	0%	-
5	MNSB006	EM 6.0.8	>10	>10					0/36	0%	-
6	MNSB007	EM 6.0.9	>10	>10					0/36	0%	-
7	MNSB011	EM 7.7	5,5	9,8					0/36	0%	-
8	MNSB008	EM 6.6.2	>10	>10					0/36	0%	-
10	MNSB013	EM 13	0,51	1,6					4/37	11%	++
13	MNSB049	018-8-8	7,706	13,621	1/36	3%	36/36	100%	1/36	3%	-
14	MNSB035	727-V3-5-4	1,59	5,24	2/36	6%	23/36	64%	4/36	11%	++
15	MNSB034	727-V3-5-3	0,014	0,094	30/36	83%	34/36	94%	10/36	28%	+++
16	MNSB033	727-V3-2-11	>10	>10	0/36	0%	0/36	0%	0/36	0%	-
17	MNSB032	727-V3-2-2-3	4,67	8,14	0/36	0%	27/36	75%	0/36	0%	-
18	MNSB041	A. T. 3.4	>10	>10	0/36	0%	0/36	0%	0/36	0%	-
19	MNSB042	A. T. 4.7	>10	>10	0/36	0%	0/36	0%	0/36	0%	-
20	MNSB044	A. T. 7.3	3,473	6,671	0/36	0%	35/36	97%	0/36	0%	-



compound	Identification		Potency		active/total at				Tumor selectivity		
	Oncotest	König	mean IC50 [µg/ml]	mean IC70 [µg/ml]	1 µg/ml		10 µg/ml		select. <sup>1)/total</sup>	% select.	rating <sup>2)</sup>
21	MNSB043	A. T. 5.2	>10	>10	0/36	0%	0/36	0%	0/36	0%	-
22	MNSB045	588-3.4-2.4	4,768	8,754	0/36	0%	25/36	69%	0/36	0%	-
23	MNSB046	193-7.8-3.4	9,403	9,965	0/36	0%	3/36	8%	0/36	0%	-
24	MNSB016	74-v1-5	0,07	0,15					2/36	6%	+
25	MNSB017	74-v2-2	0,17	0,42					2/36	6%	+
26	MNSB031	74-v2-8-4	0,005	0,014	34/36	94%	35/36	97%	8/36	22%	+++
29	MNSB030	74-v2-9-1	>10	>10	0/36	0%	0/36	0%	0/36	0%	-

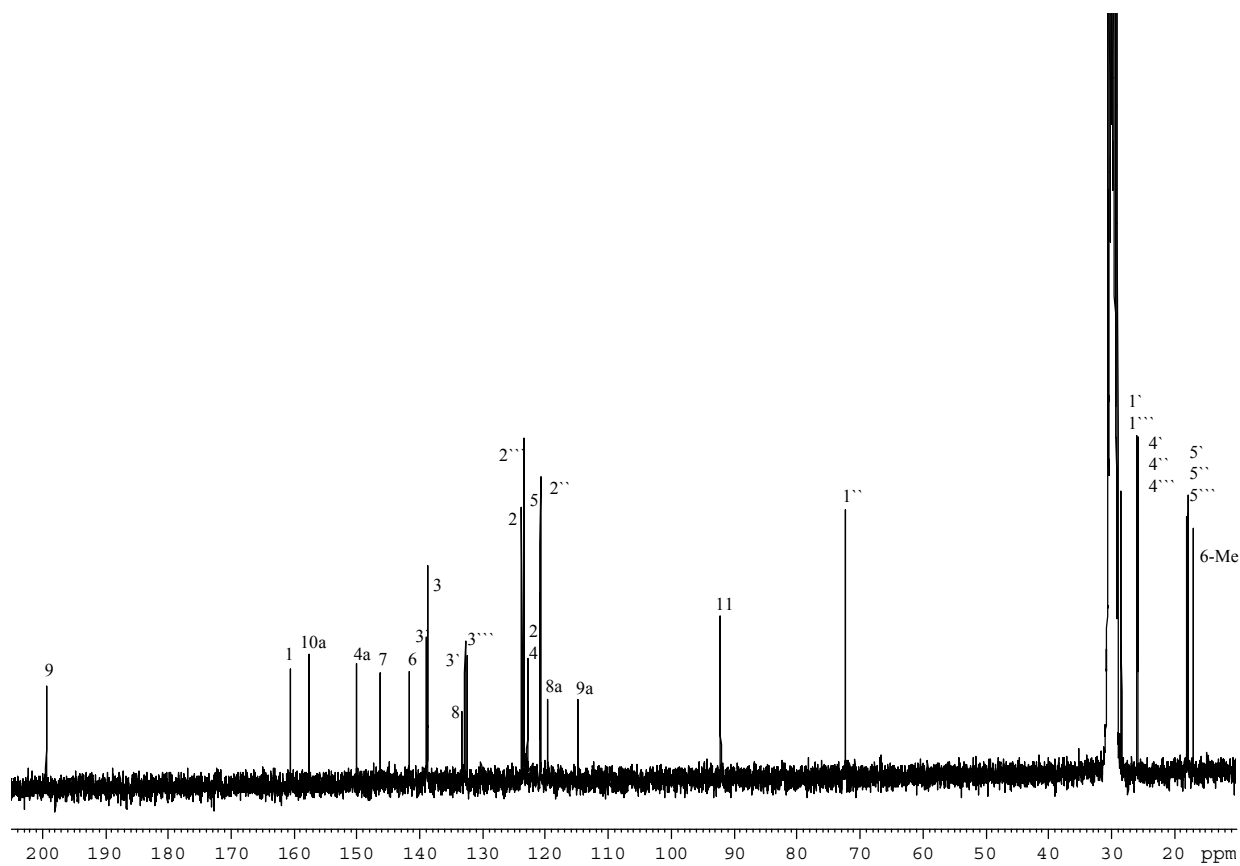
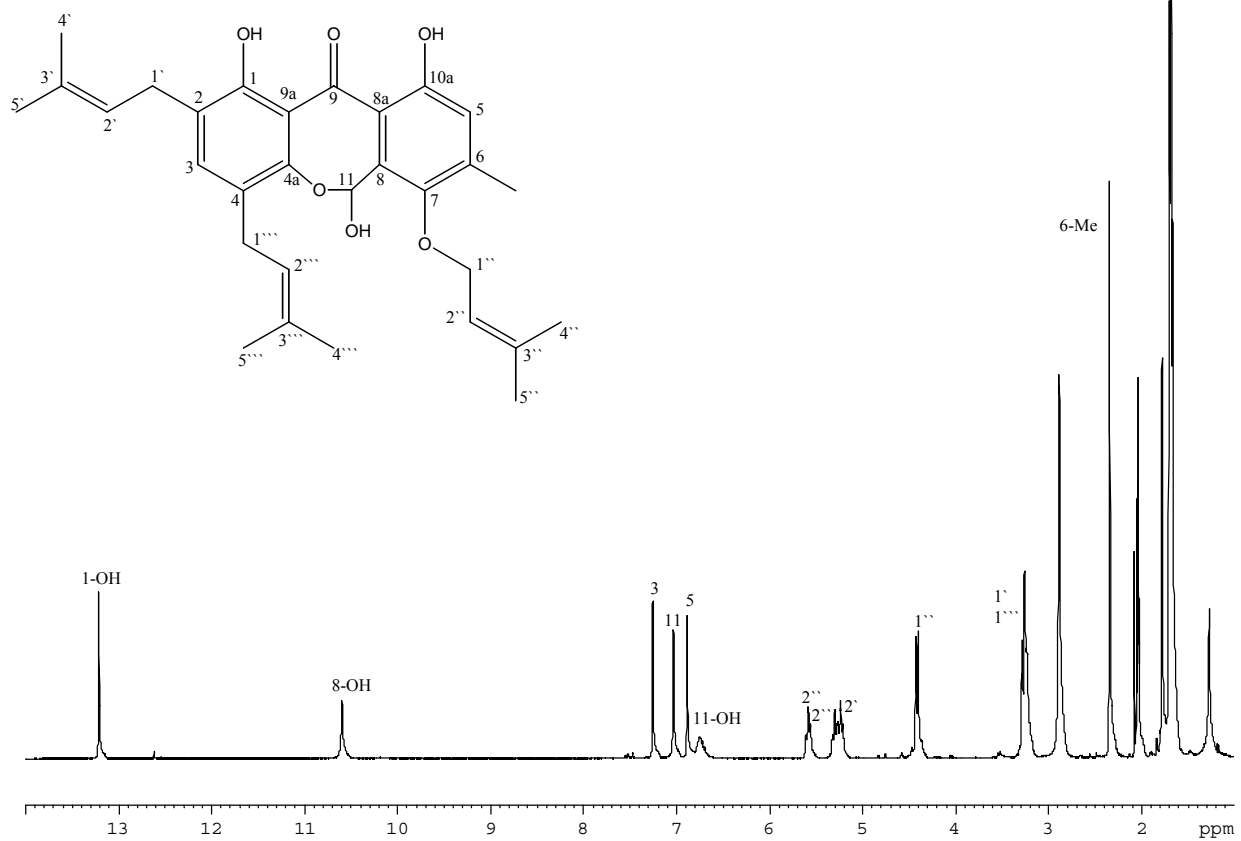
Samples were dissolved in methanol and tested against 36 tumor cell lines. Details are given in 3.9.2 chapter. Each test series was run in duplicate.

<sup>1)</sup> individual IC70 < 1/3 mean IC70; for example if mean IC70 = 2.1 µM the threshold for above average sensitivity was IC70 < 0.7 µM

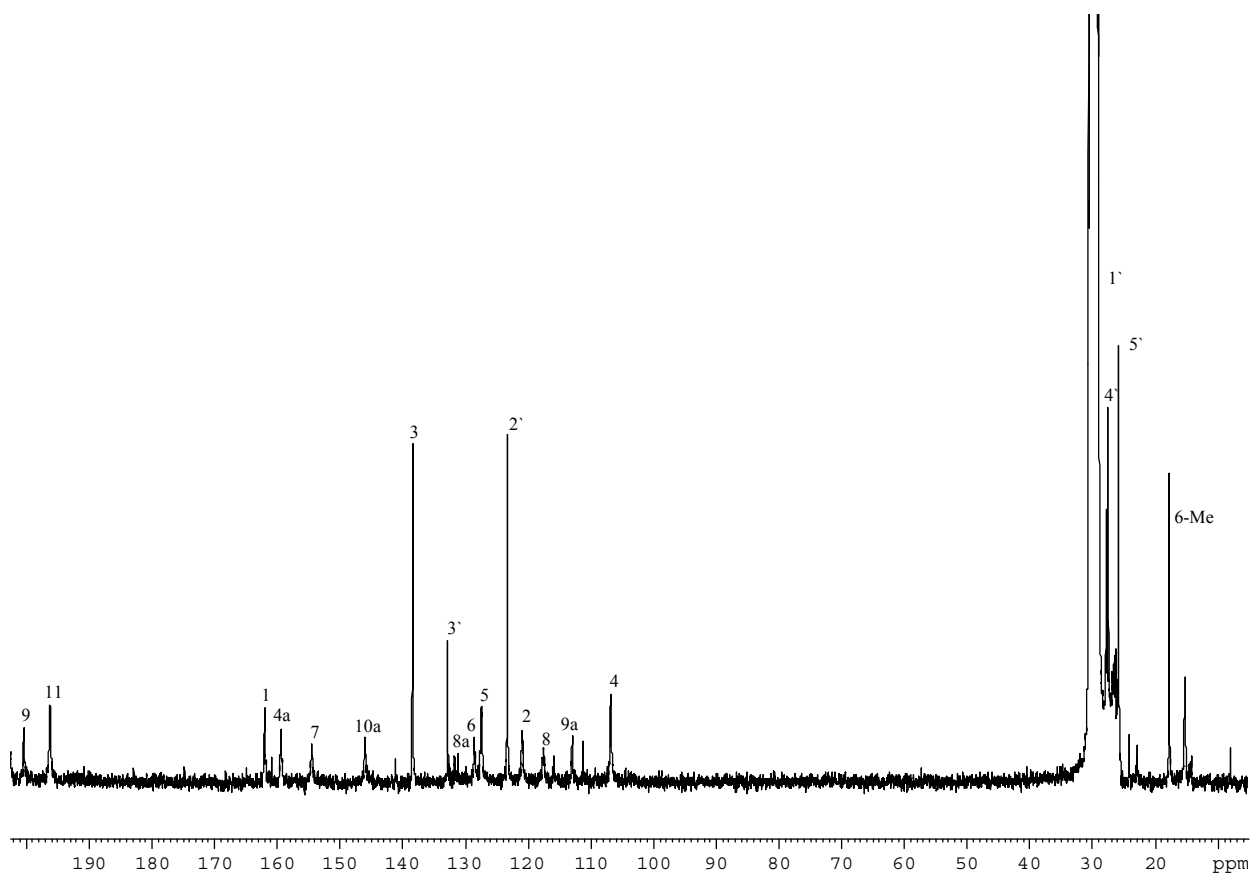
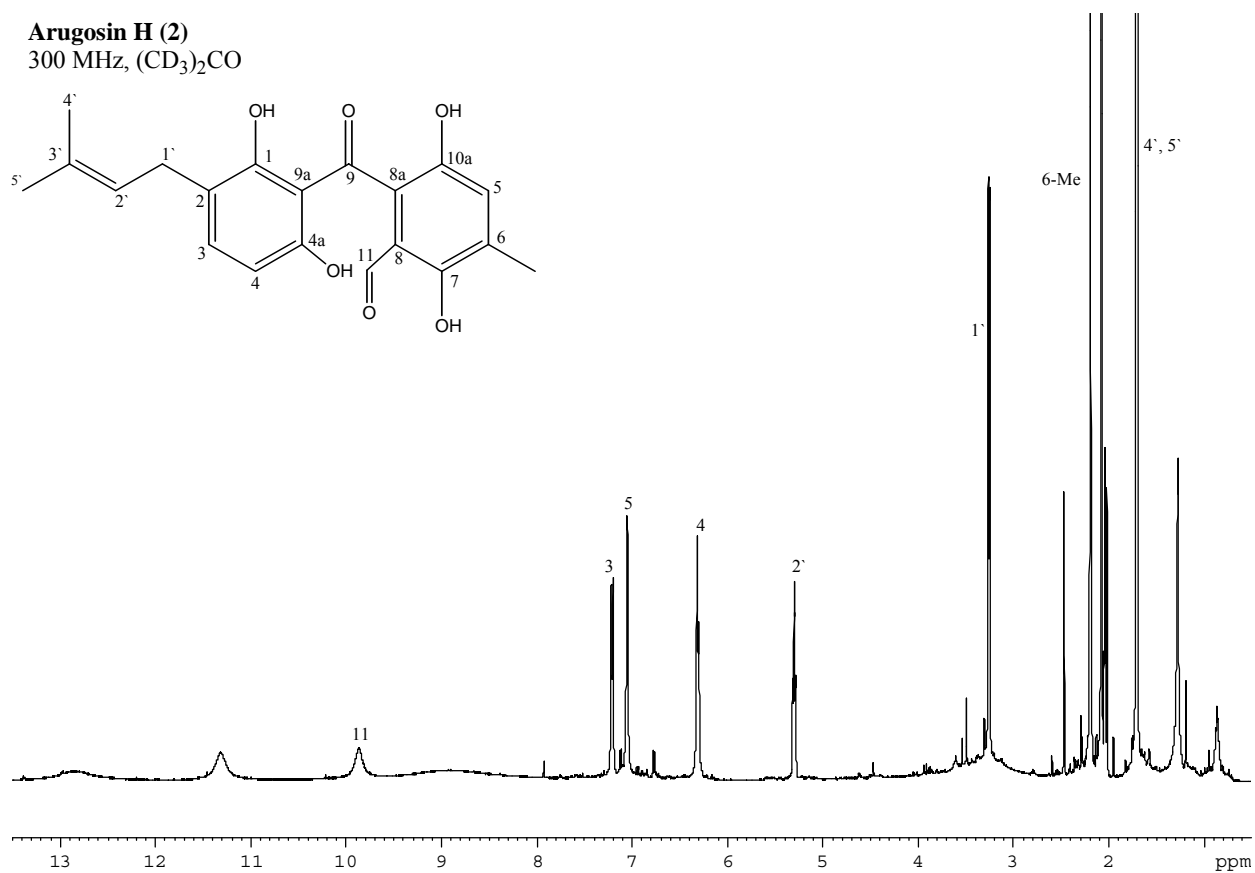
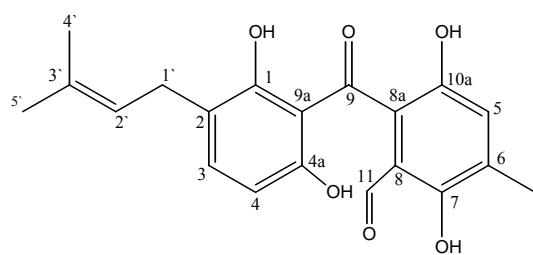
<sup>2)</sup> – (% selective = < 4 %); + (4 % > = 10 %); ++ (10 % > % selective >= 20 %); +++ (% selective > 20 %)

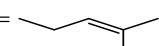
**8.2  $^1\text{H}$  and  $^{13}\text{C}$  NMR spectra of isolated compounds**

**Arugosin G (1)**  
300 MHz, (CD<sub>3</sub>)<sub>2</sub>CO



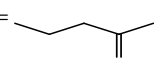
**Arugosin H (2)**  
300 MHz, (CD<sub>3</sub>)<sub>2</sub>CO



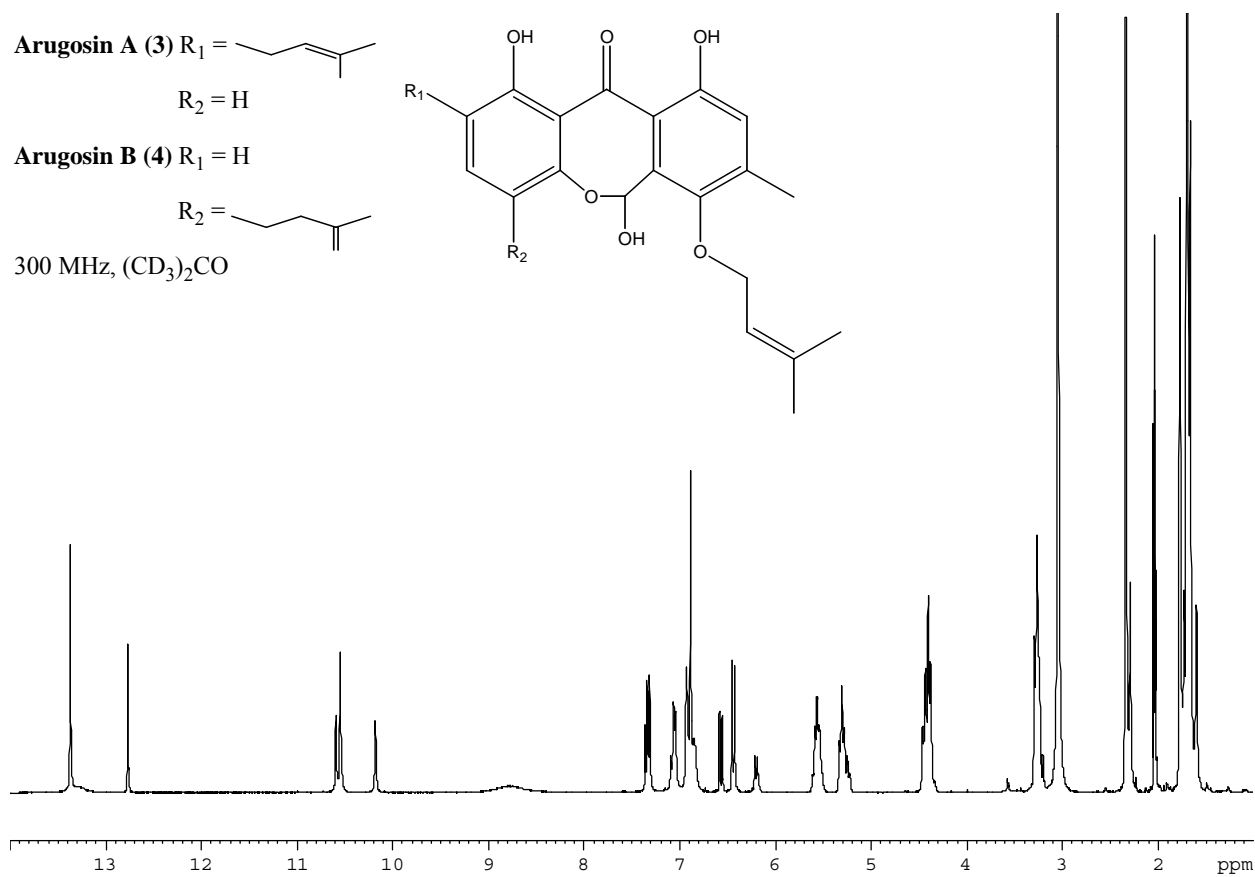
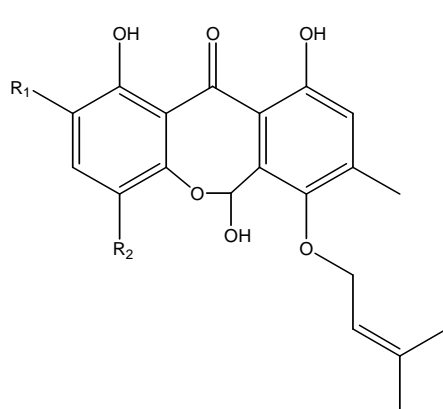
**Arugosin A (3)** R<sub>1</sub> = 

R<sub>2</sub> = H

**Arugosin B (4)** R<sub>1</sub> = H

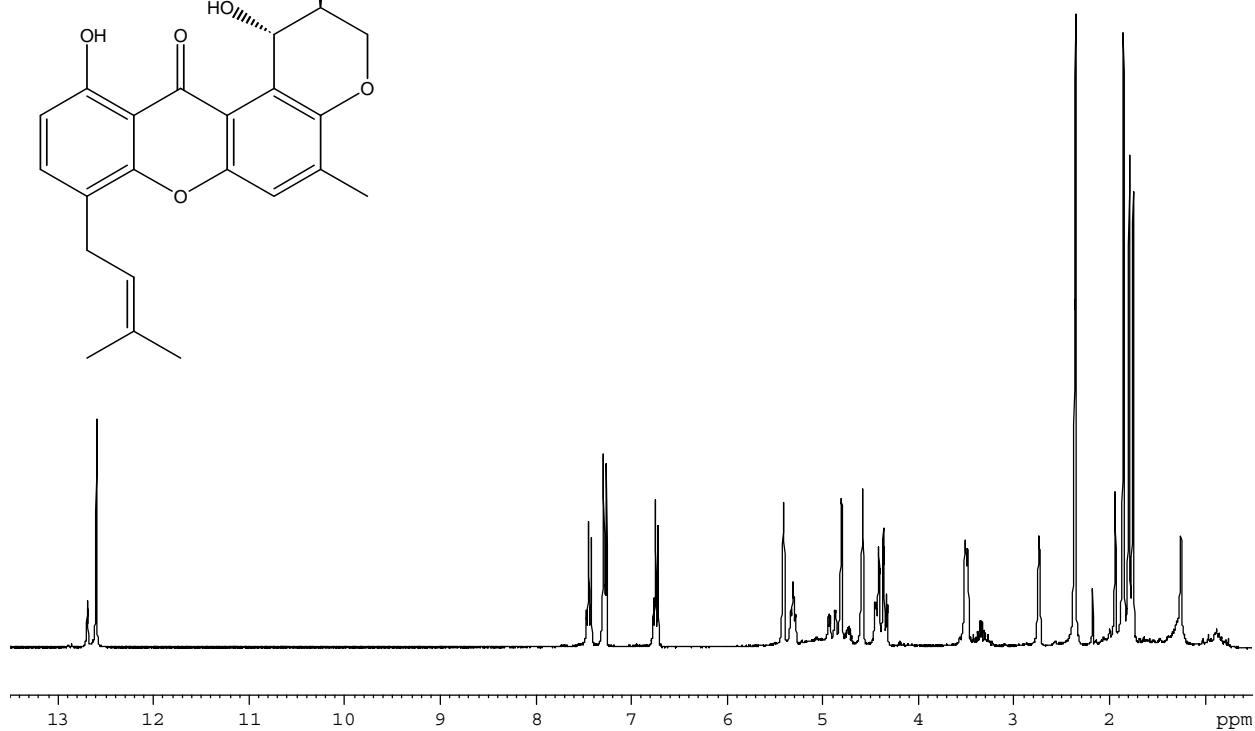
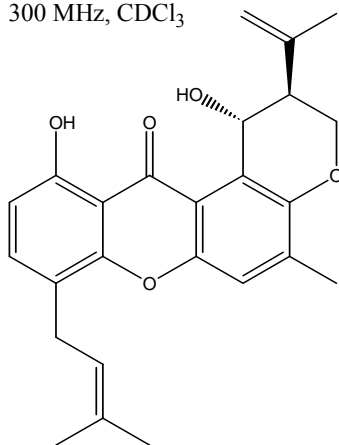
R<sub>2</sub> = 

300 MHz, (CD<sub>3</sub>)<sub>2</sub>CO

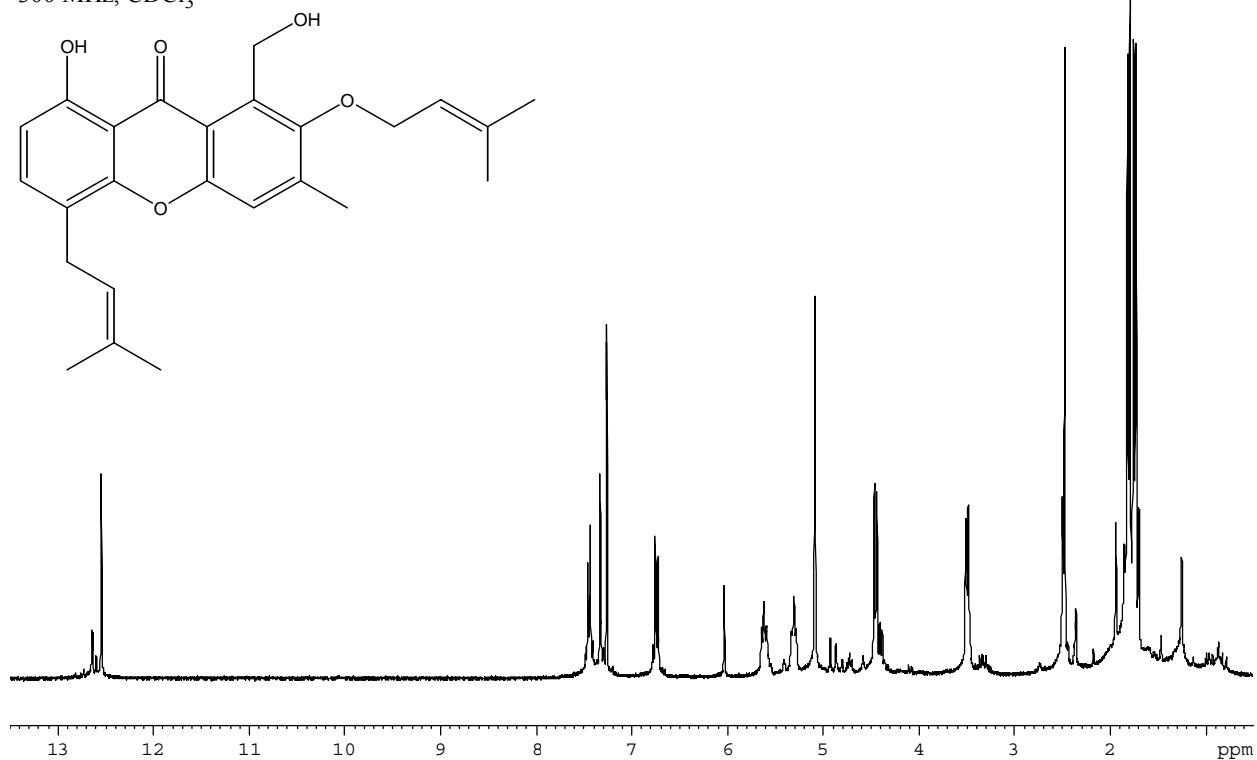


**Shamixanthone (5)**

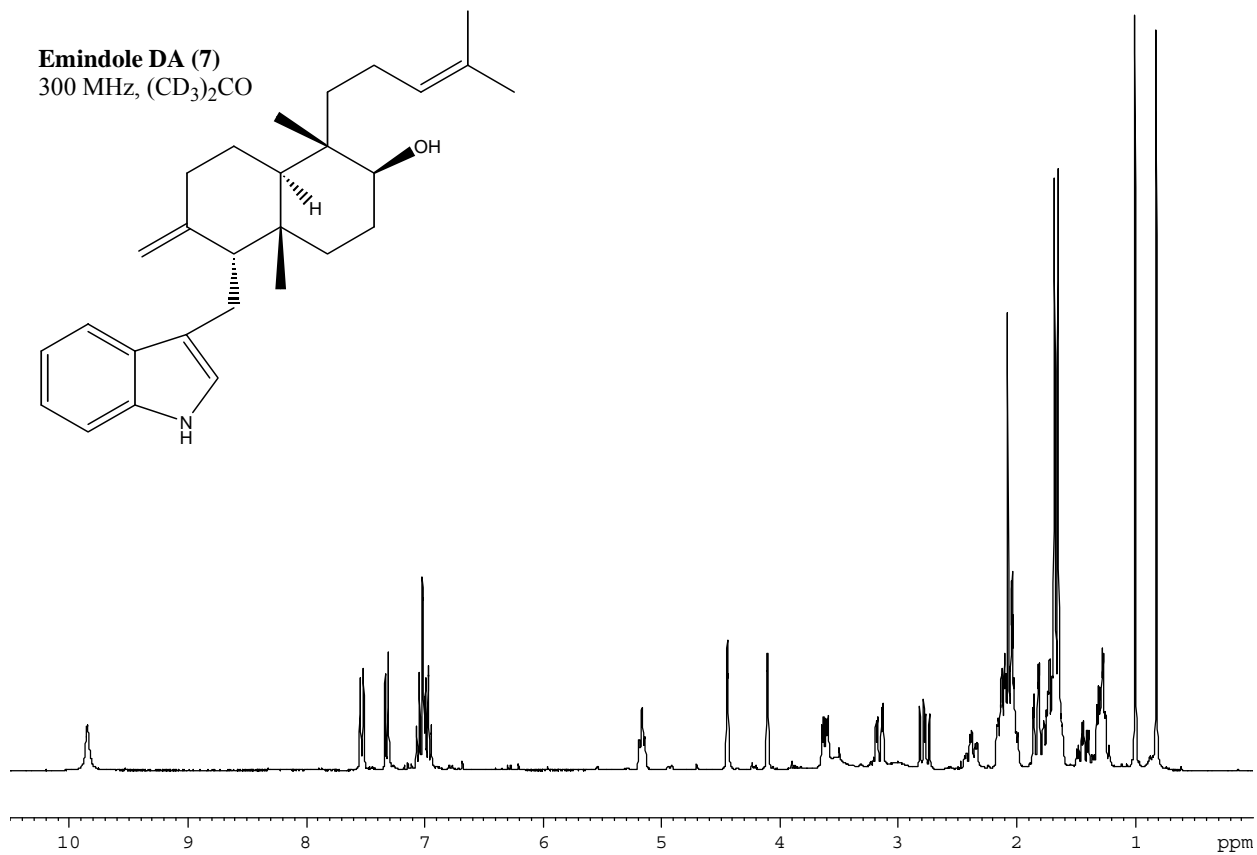
300 MHz, CDCl<sub>3</sub>

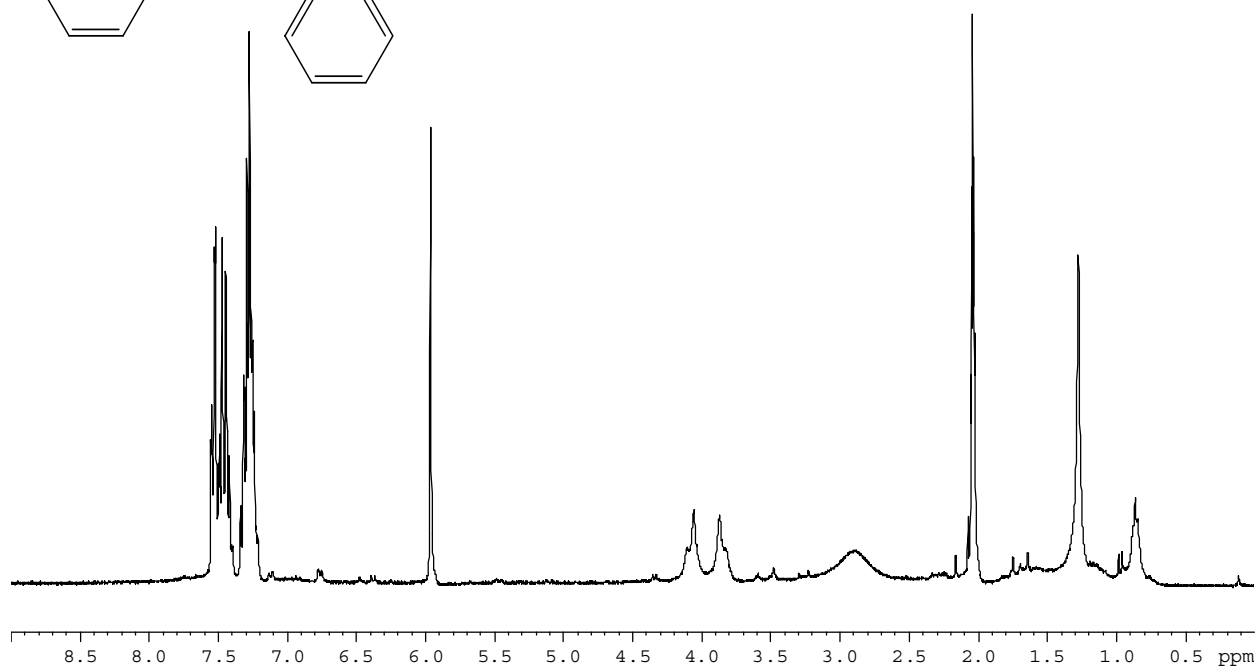
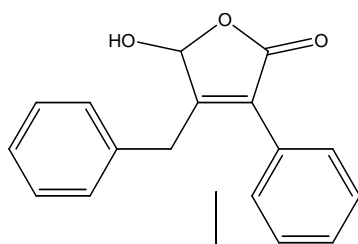
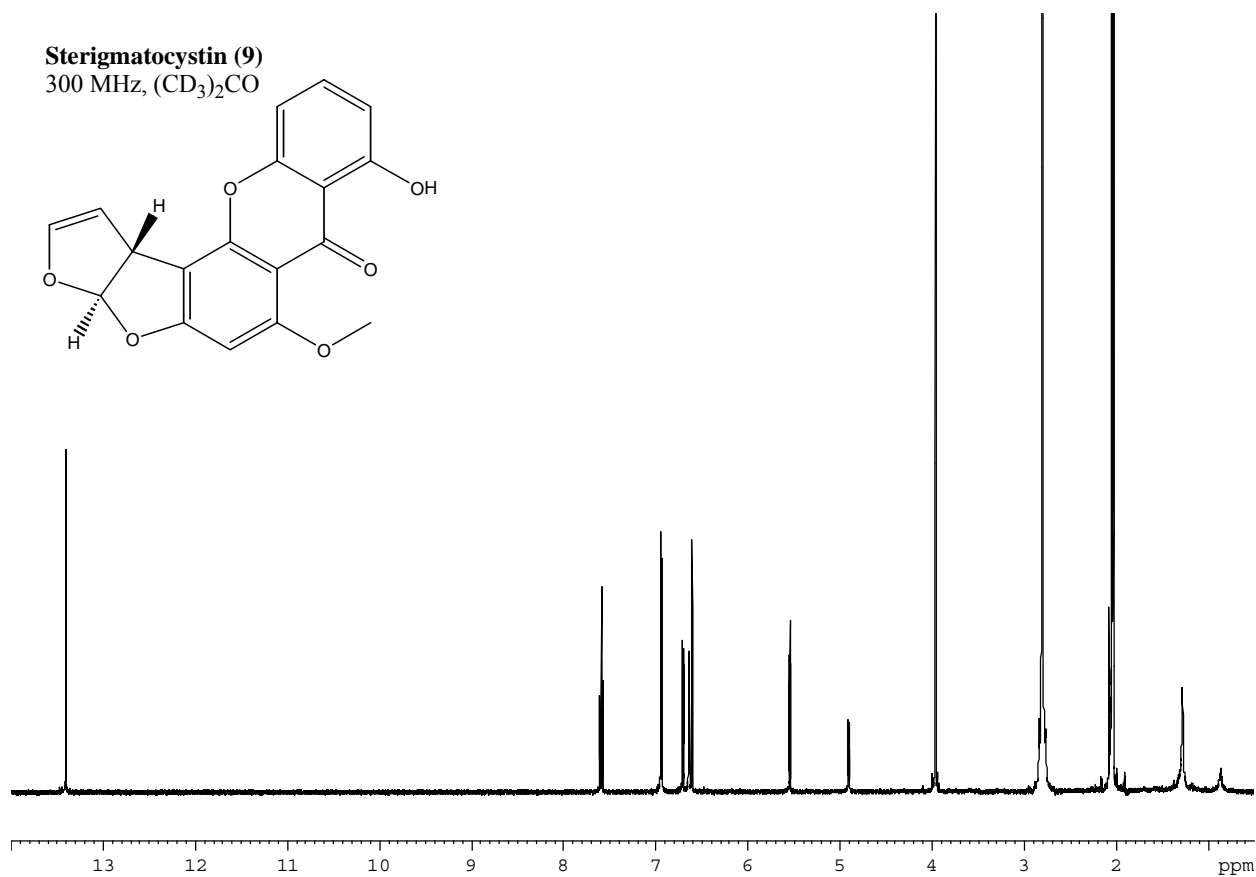
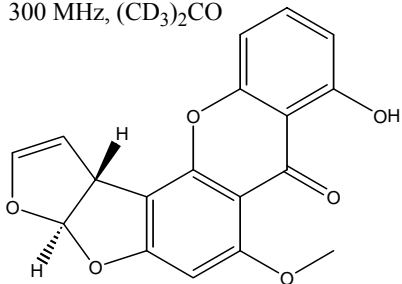


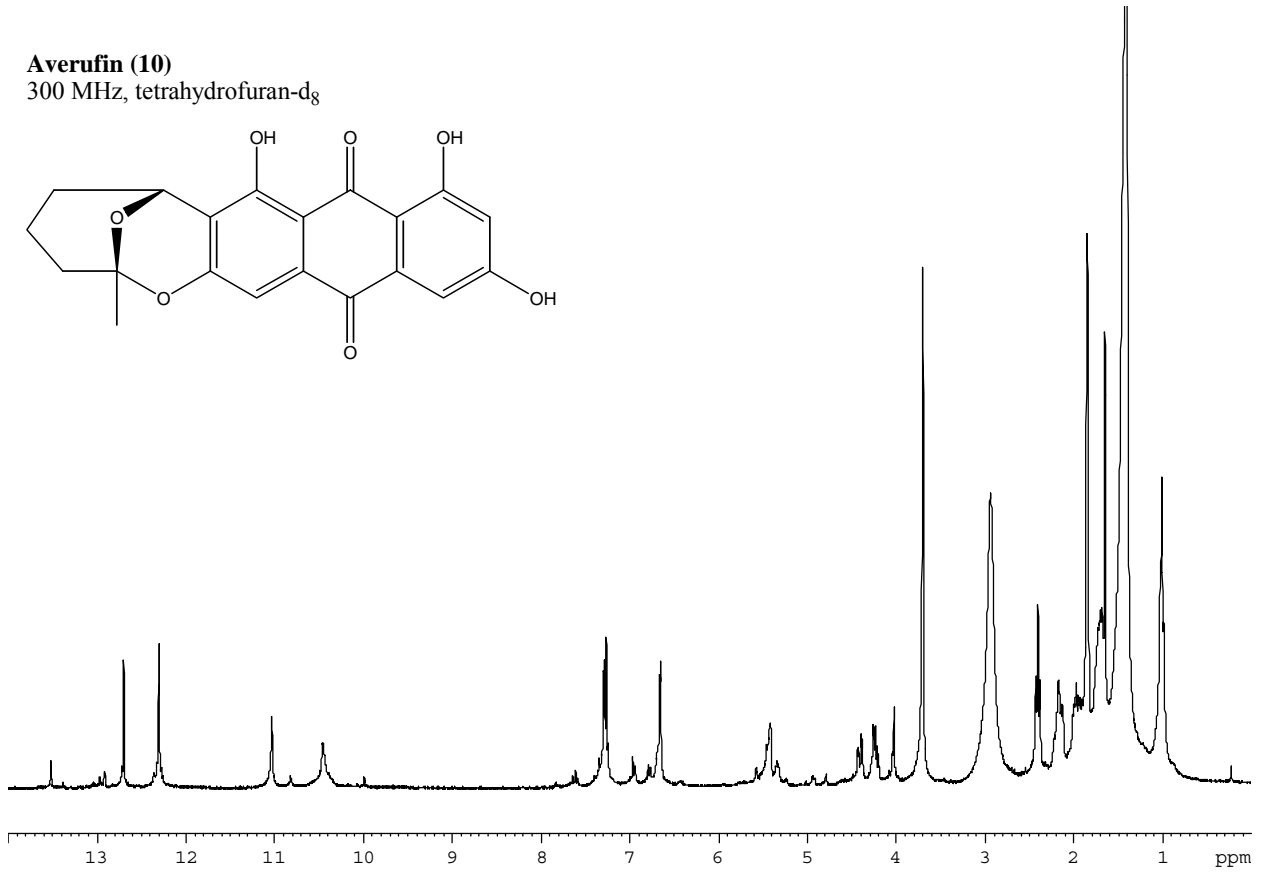
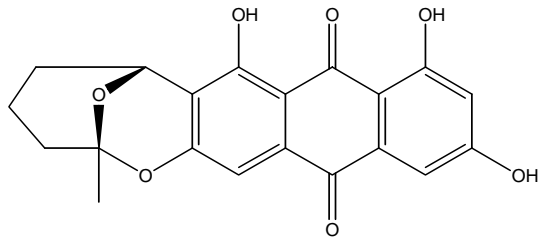
**Emericellin (6)**  
300 MHz, CDCl<sub>3</sub>



**Emindole DA (7)**  
300 MHz, (CD<sub>3</sub>)<sub>2</sub>CO

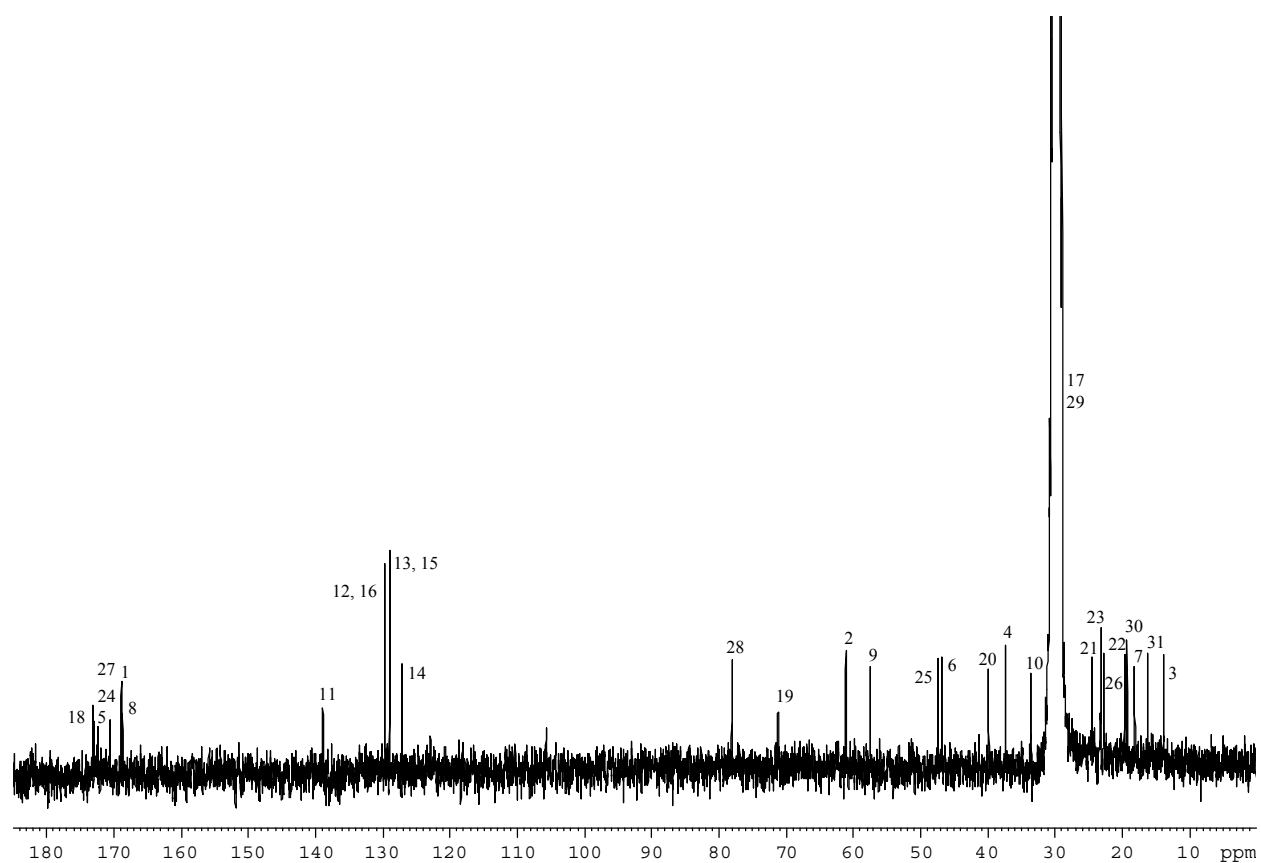
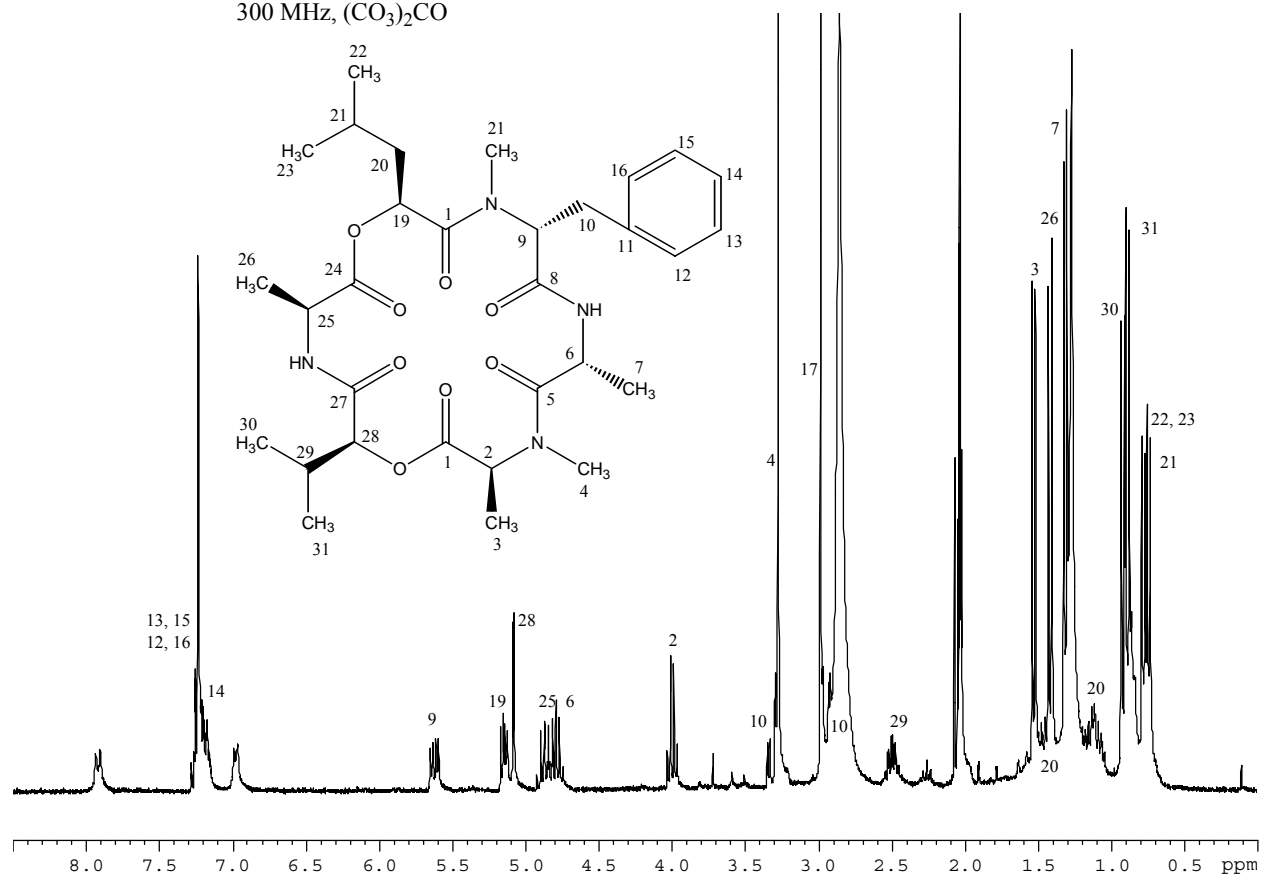


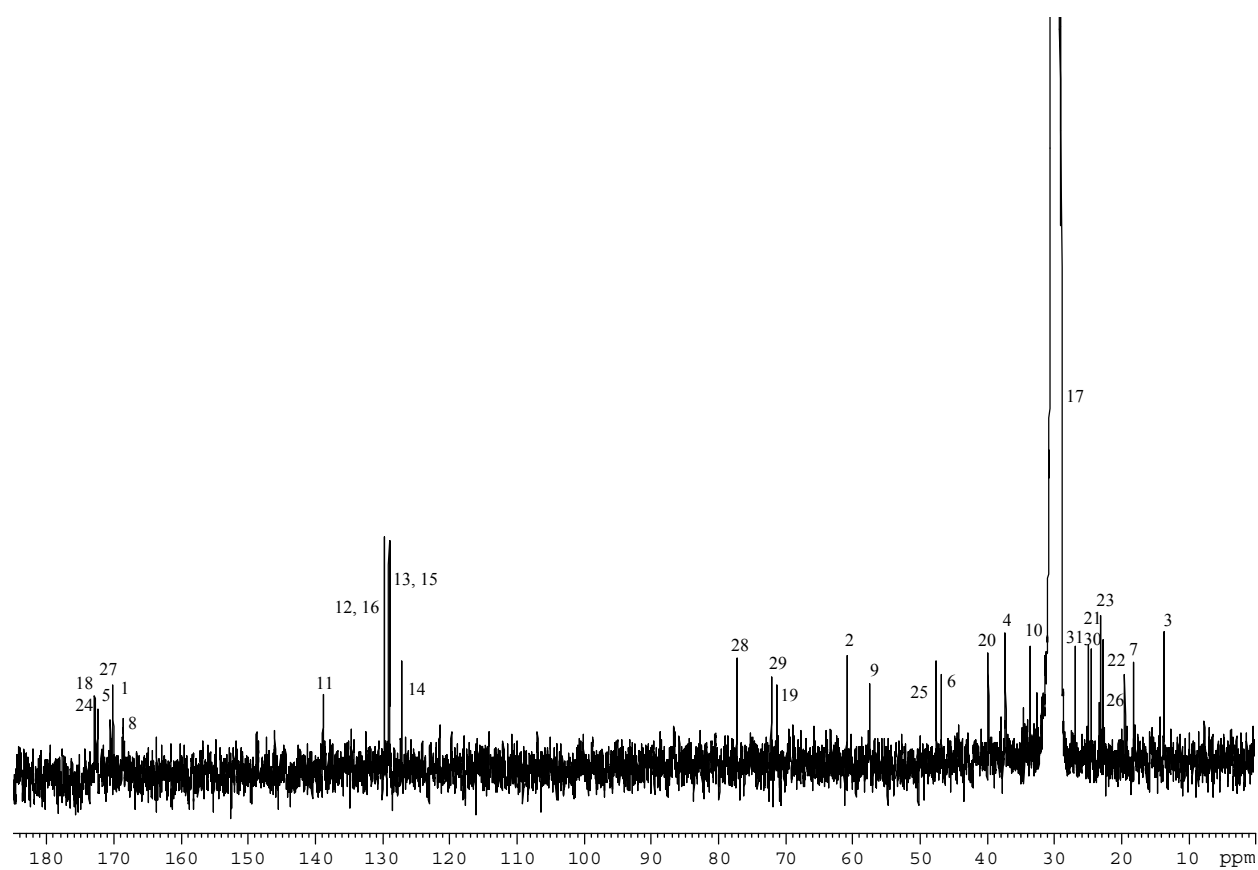
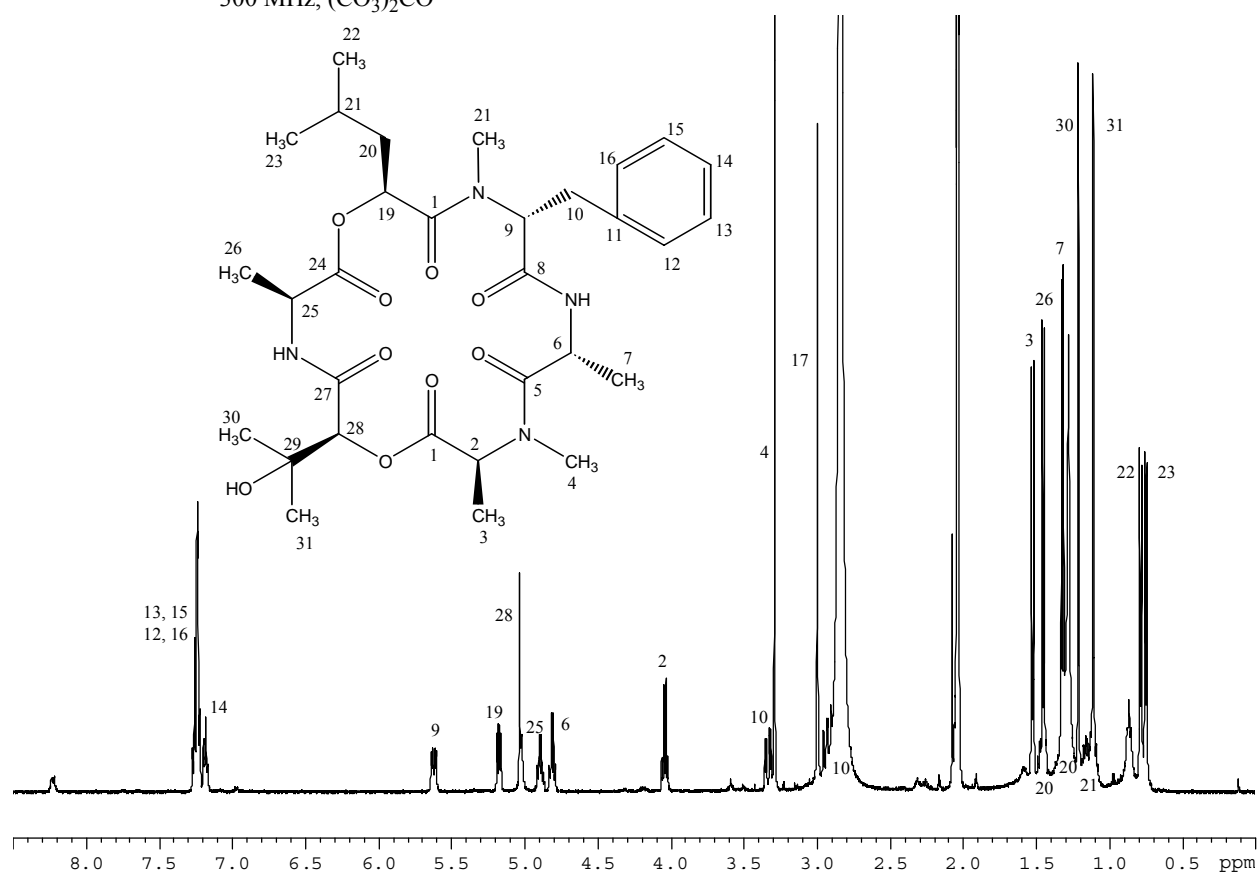
**Microperfuranone (8)**300 MHz, (CD<sub>3</sub>)<sub>2</sub>CO**Sterigmatocystin (9)**300 MHz, (CD<sub>3</sub>)<sub>2</sub>CO

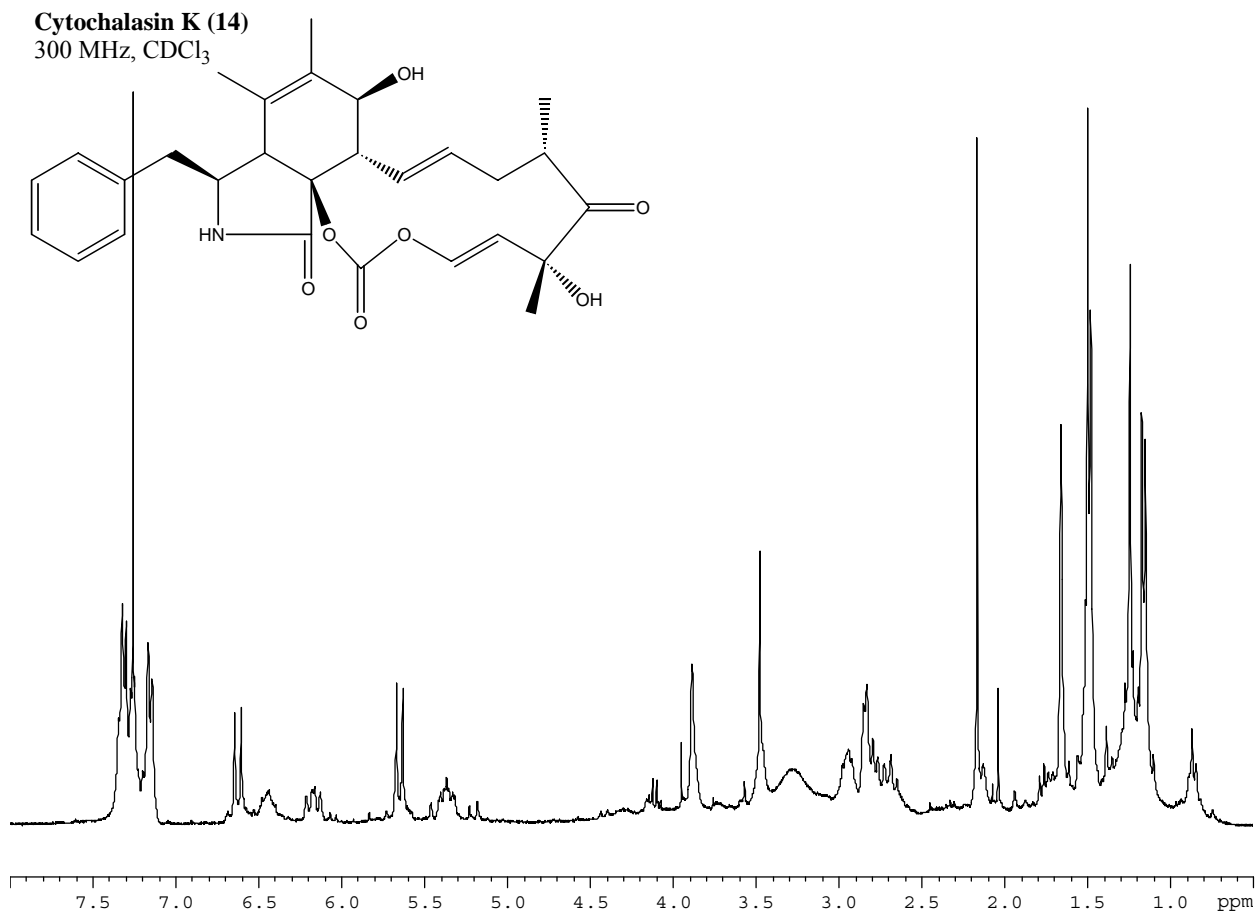
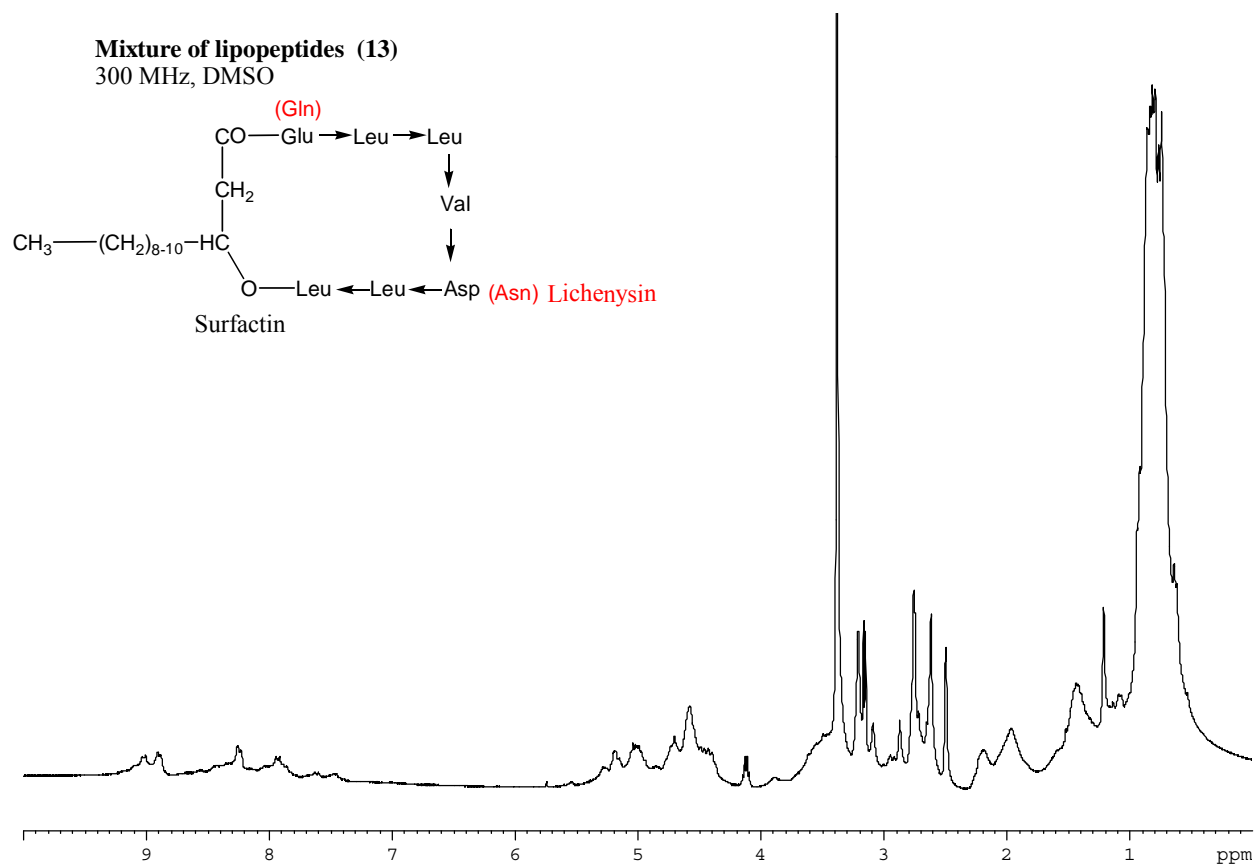
**Averufin (10)**300 MHz, tetrahydrofuran-d<sub>8</sub>

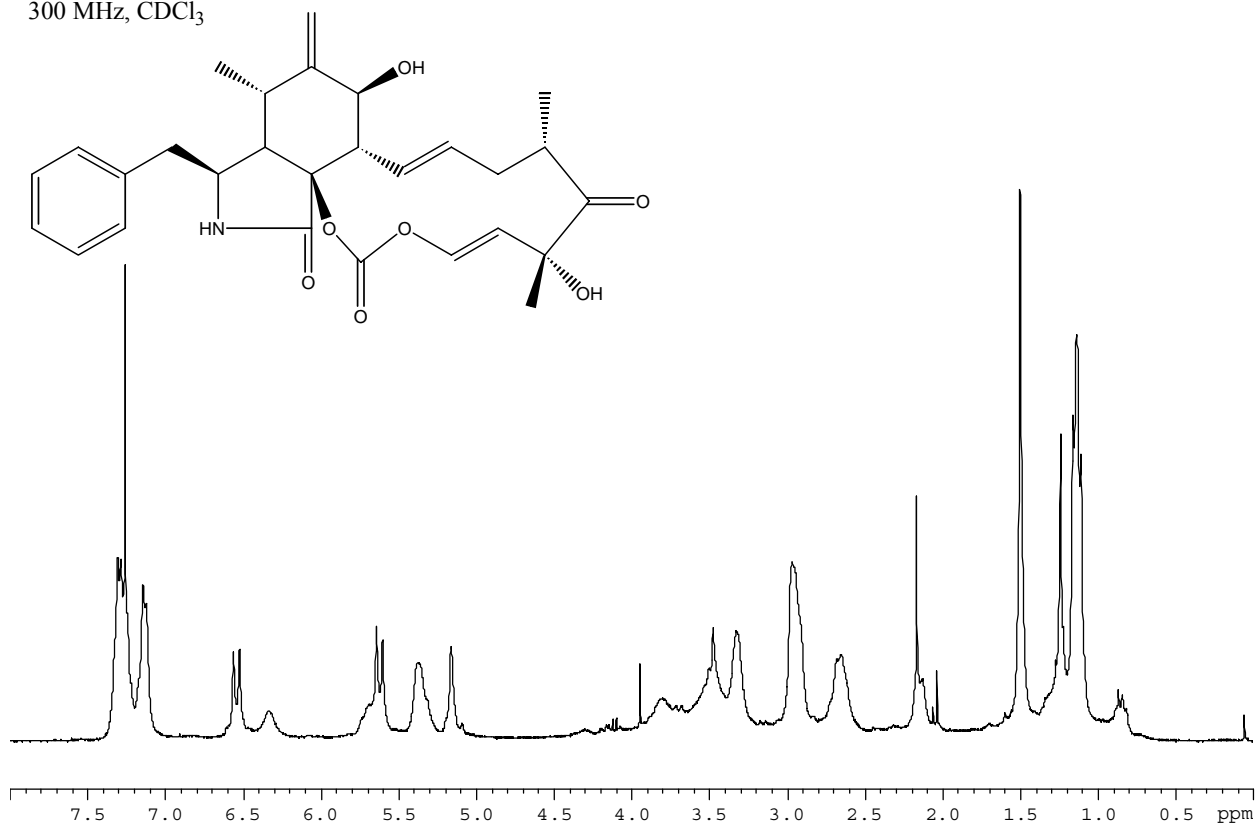
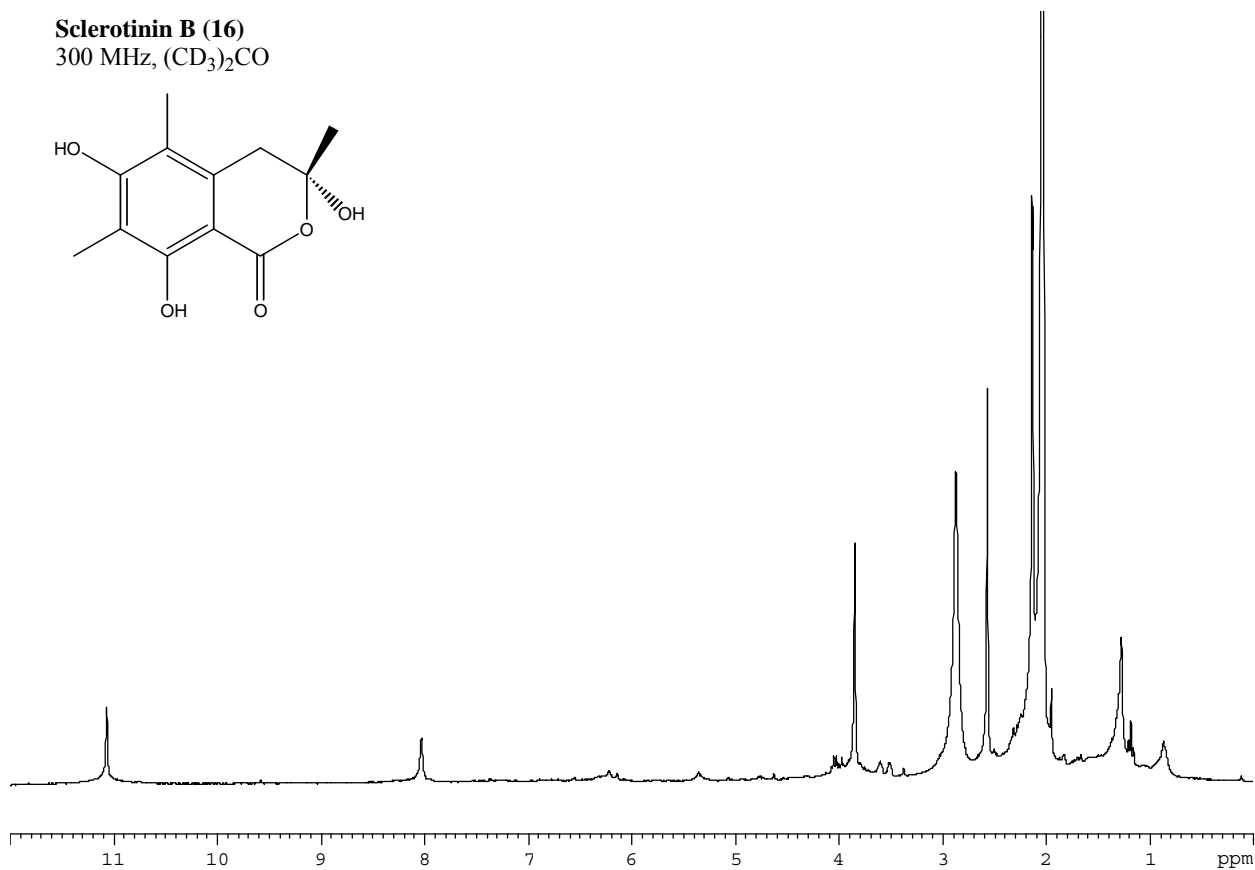


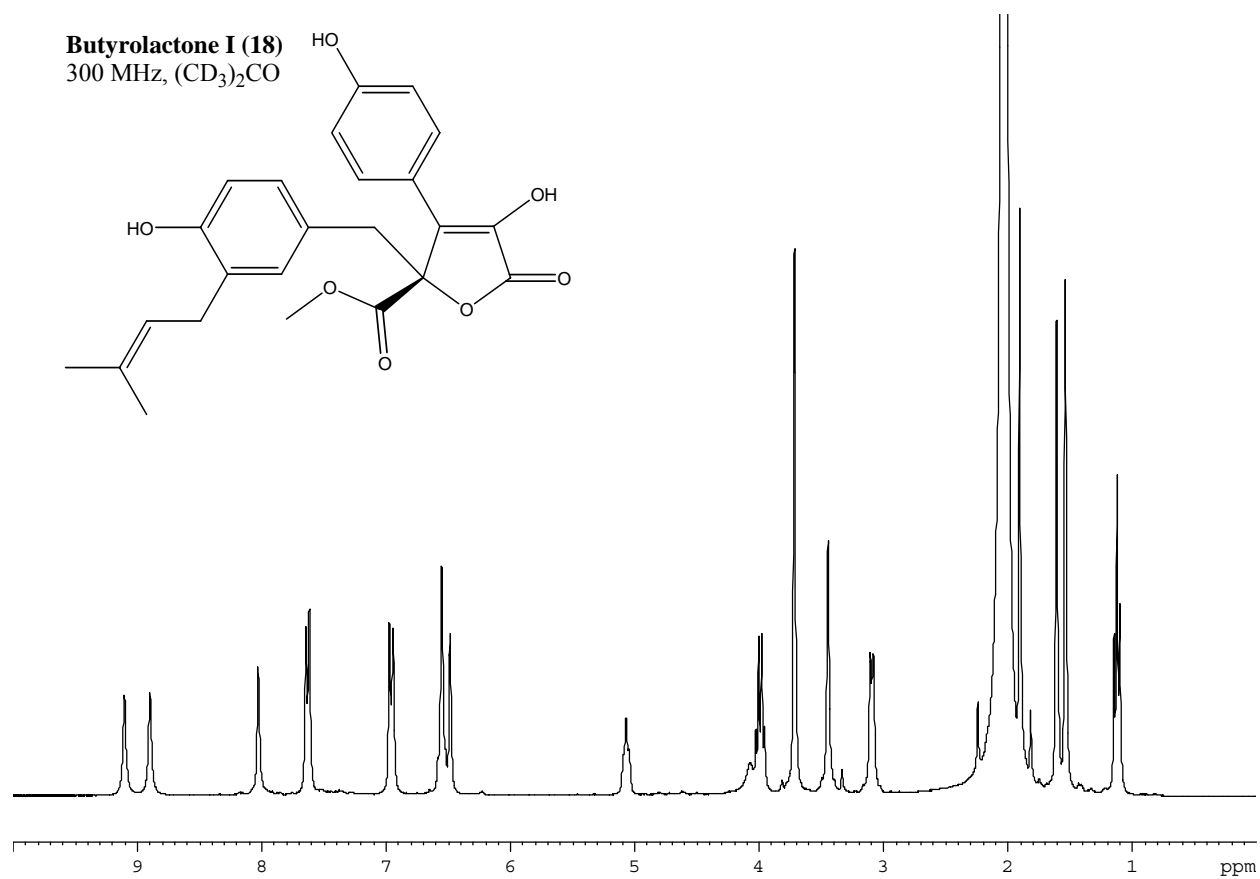
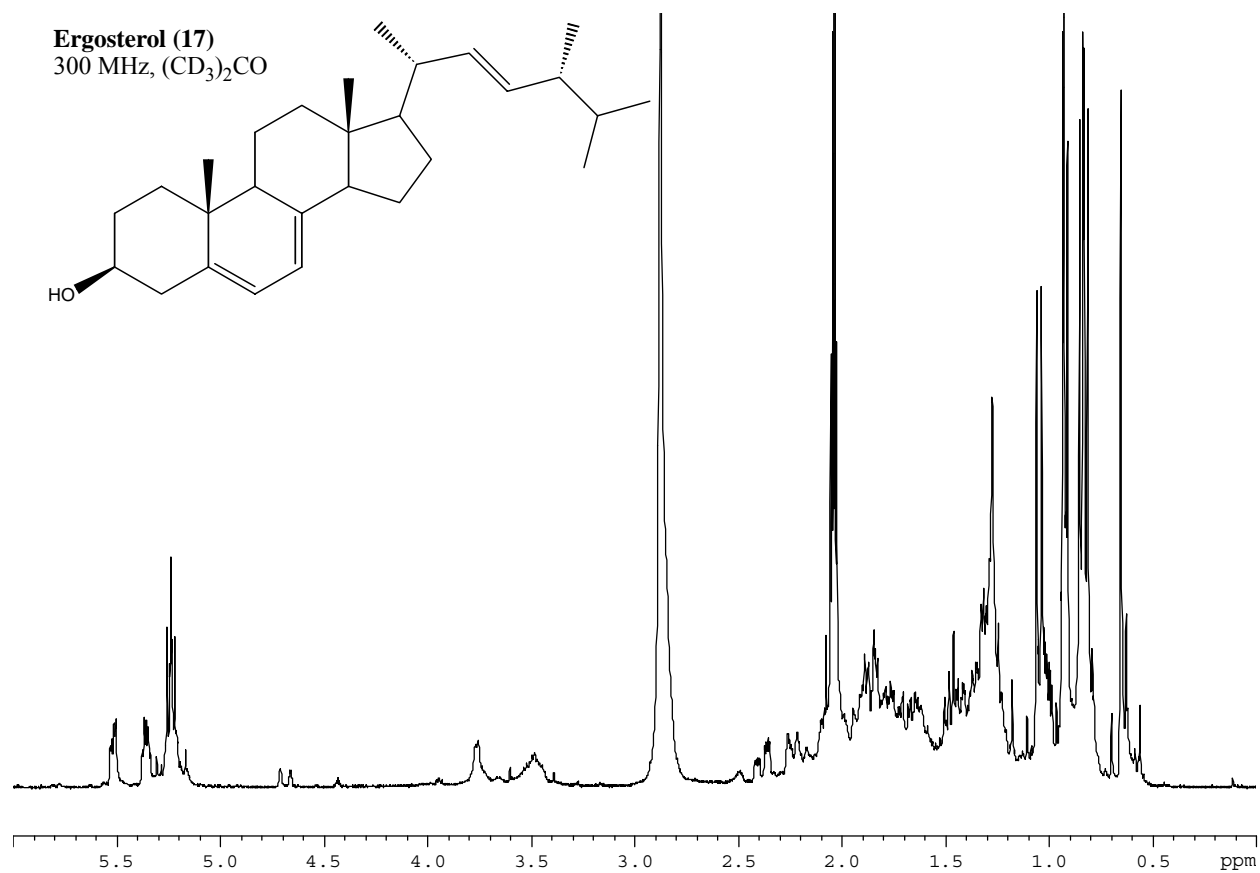
**Spicellamide A (11)**  
300 MHz, (CO<sub>3</sub>)<sub>2</sub>CO

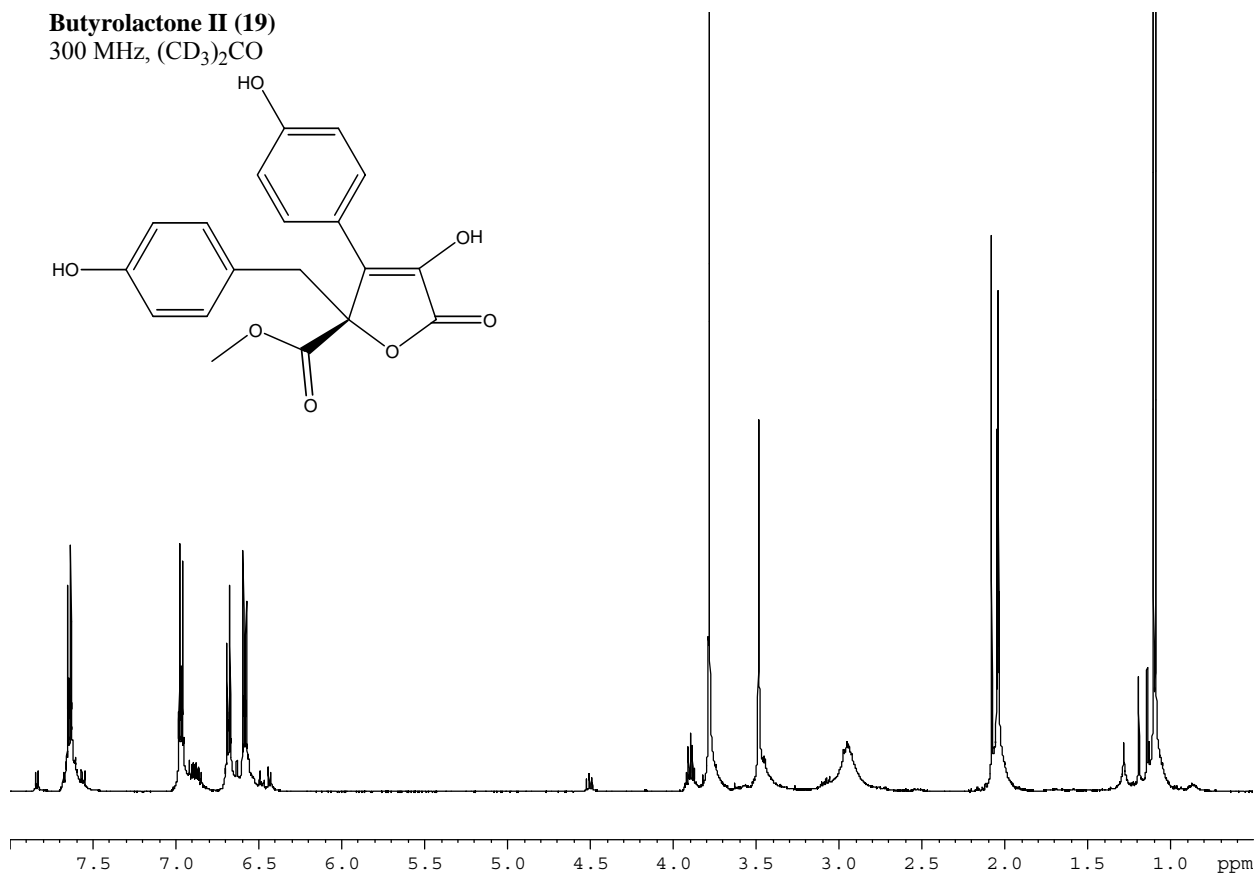
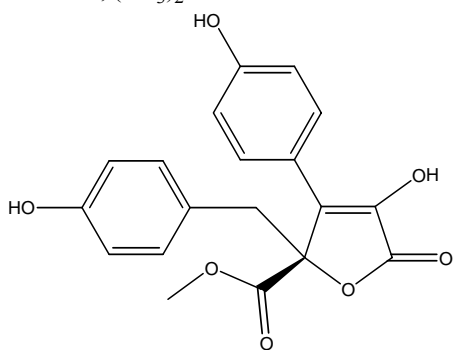
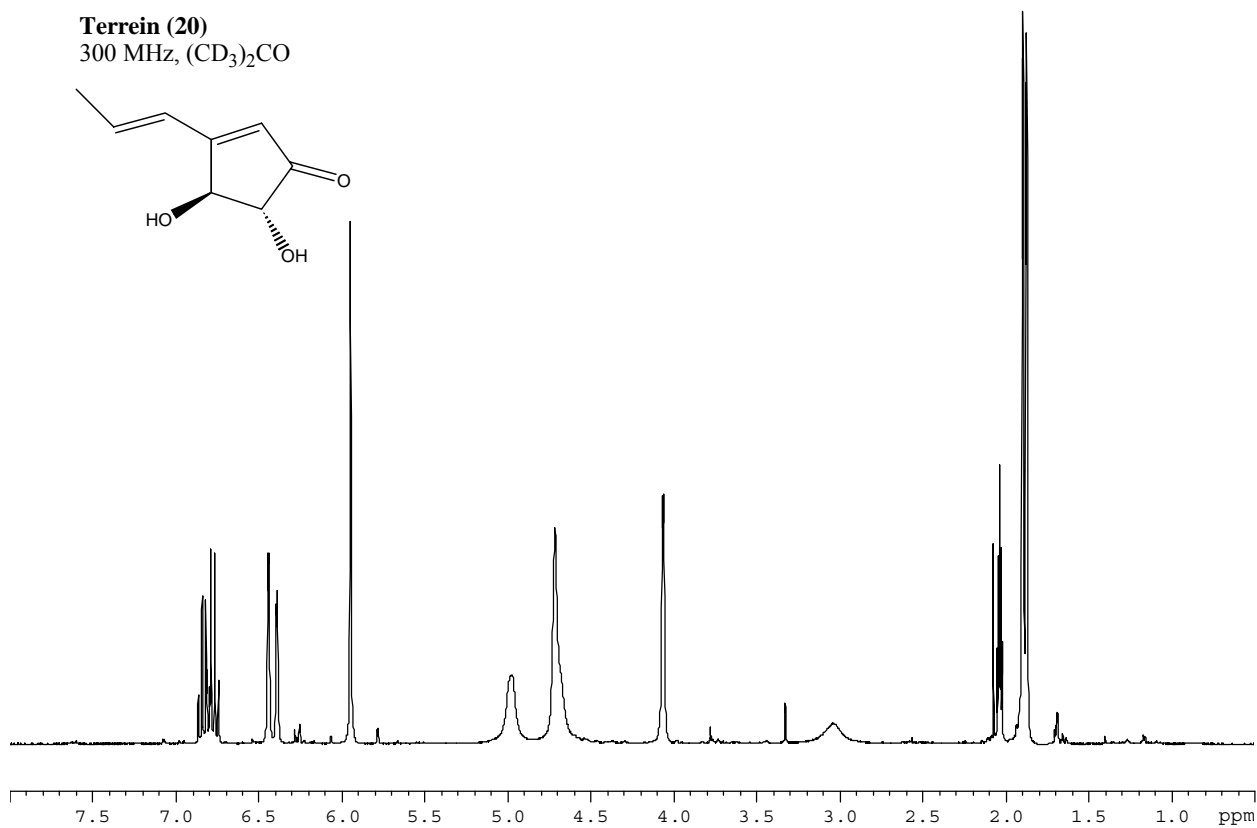
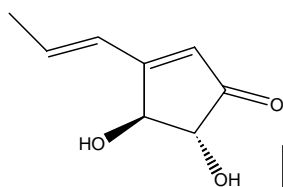


**Spicellamide B (12)**  
300 MHz, (CO<sub>3</sub>)<sub>2</sub>CO

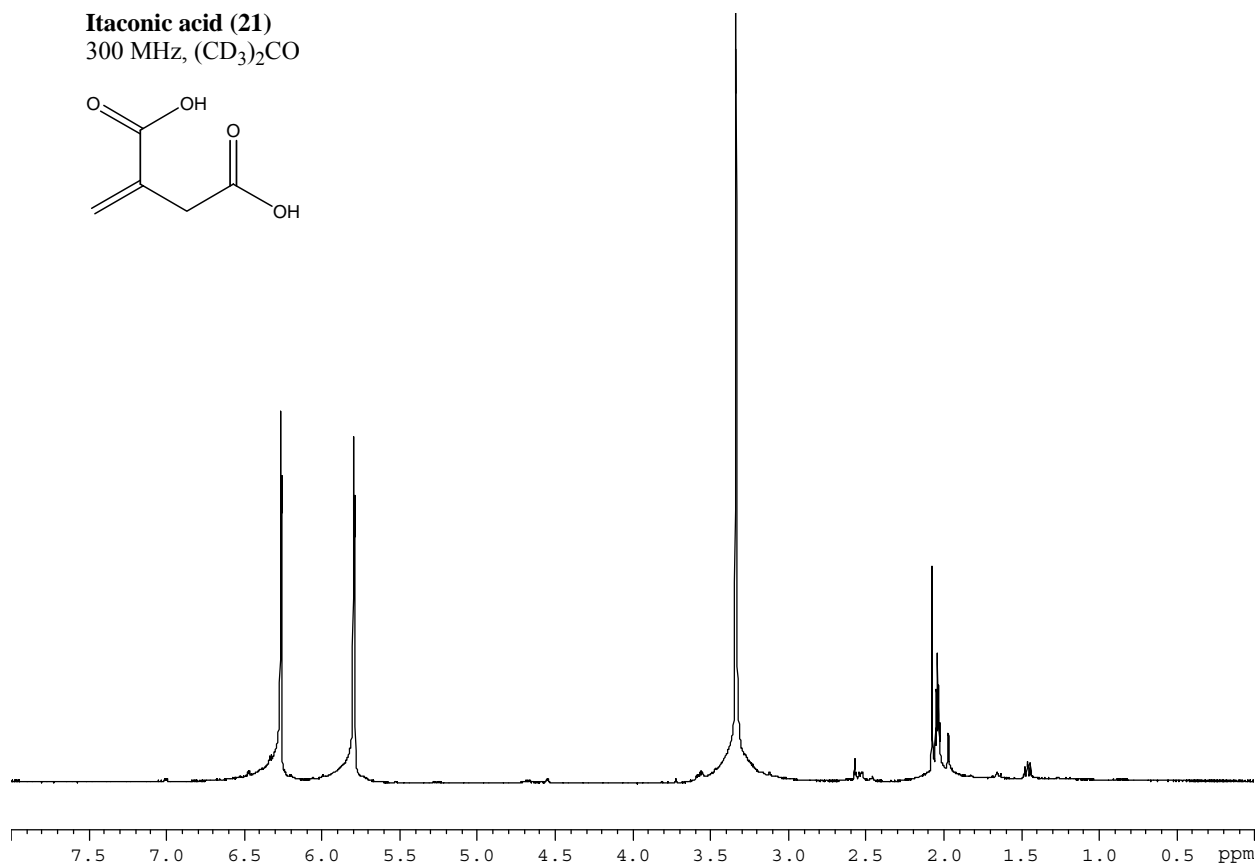
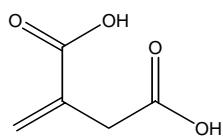


**6,12 isomer of Cytochalasin K (15)**300 MHz, CDCl<sub>3</sub>**Sclerotinin B (16)**300 MHz, (CD<sub>3</sub>)<sub>2</sub>CO

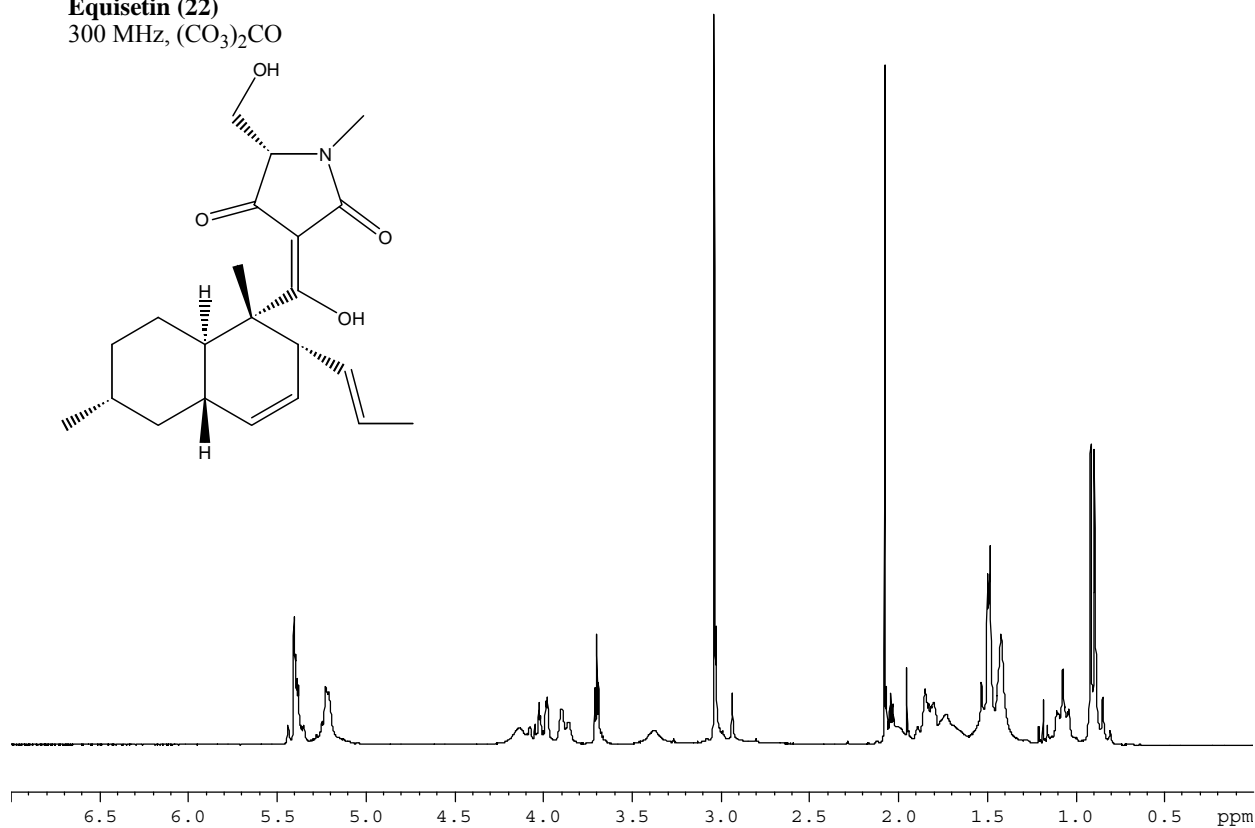
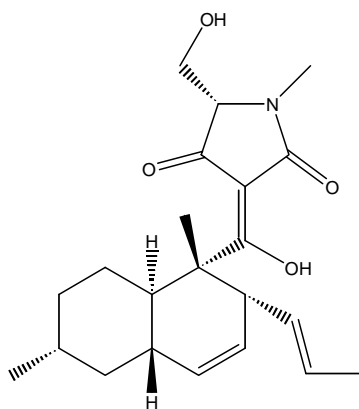


**Butyrolactone II (19)**300 MHz, (CD<sub>3</sub>)<sub>2</sub>CO**Terrein (20)**300 MHz, (CD<sub>3</sub>)<sub>2</sub>CO

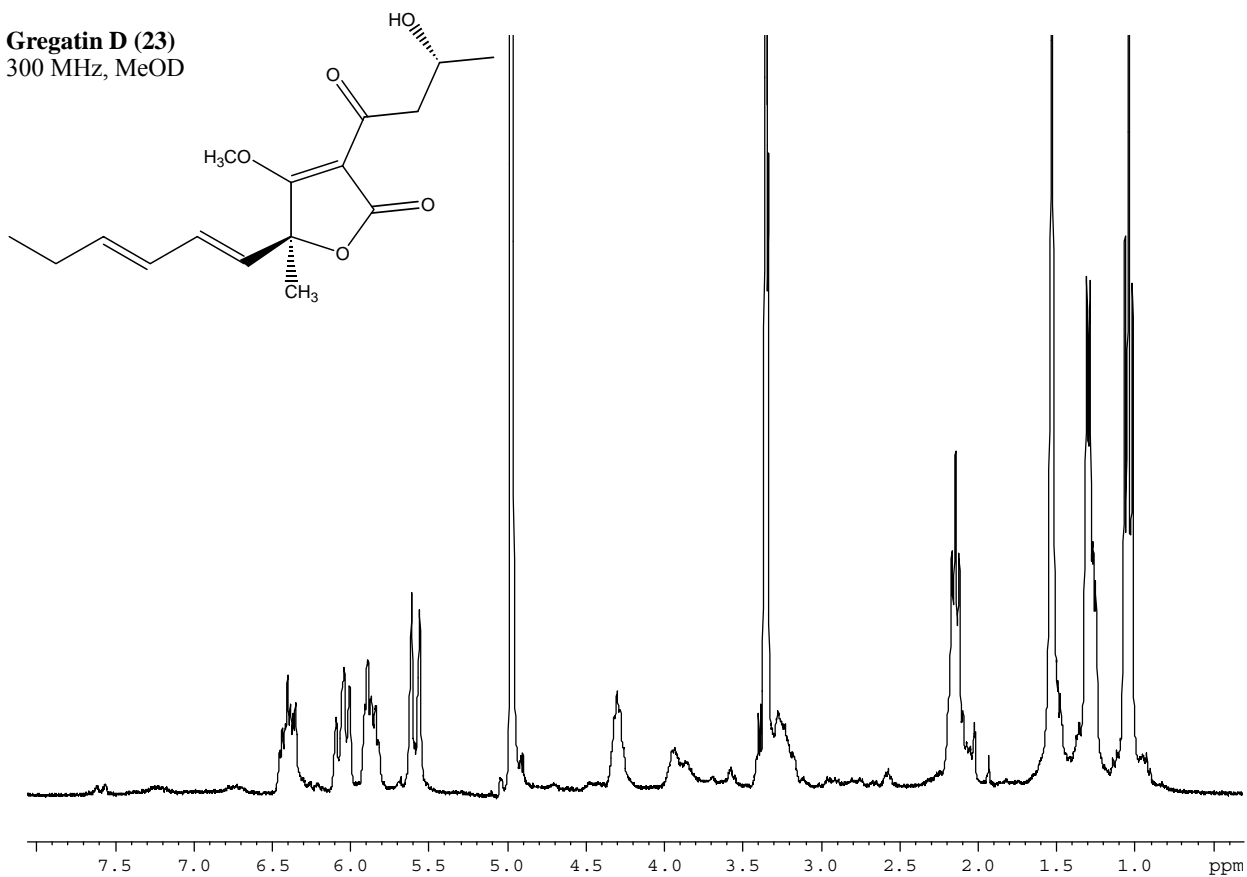
**Itaconic acid (21)**  
300 MHz, (CD<sub>3</sub>)<sub>2</sub>CO



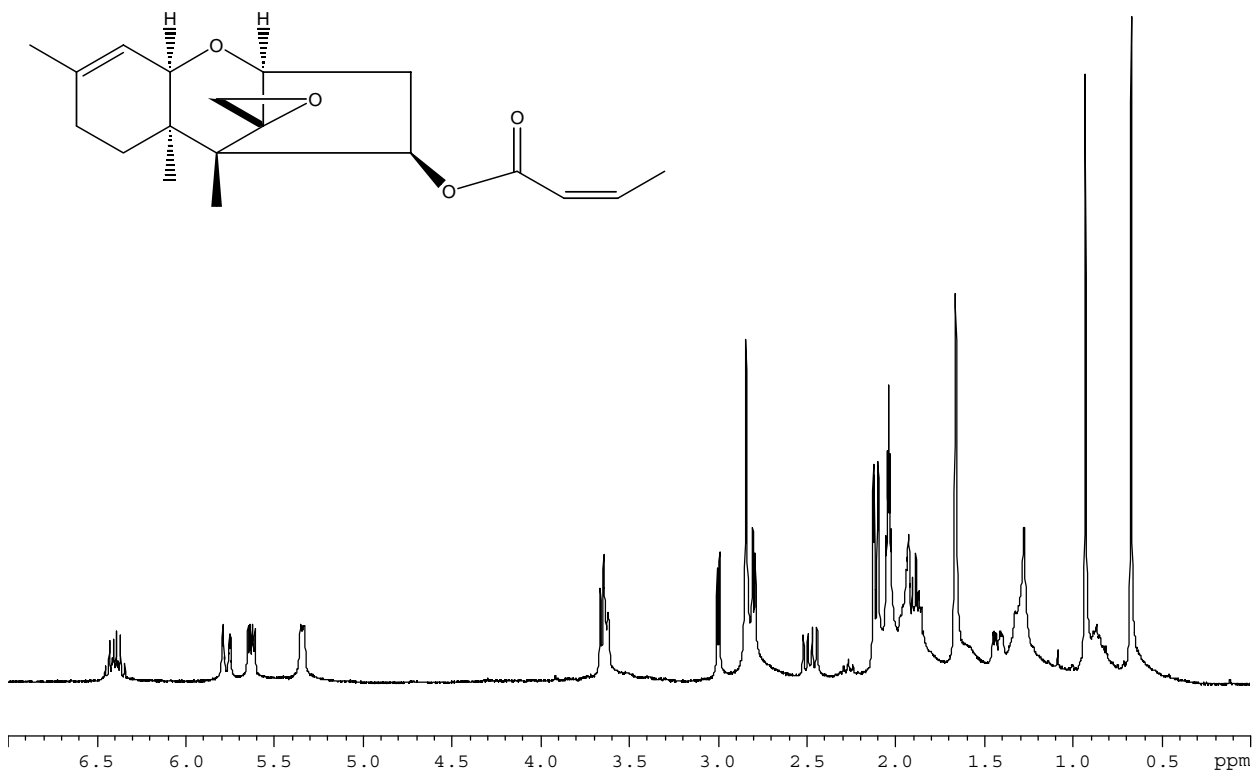
**Equisetin (22)**  
300 MHz, (CO<sub>3</sub>)<sub>2</sub>CO



**Gregatin D (23)**  
300 MHz, MeOD

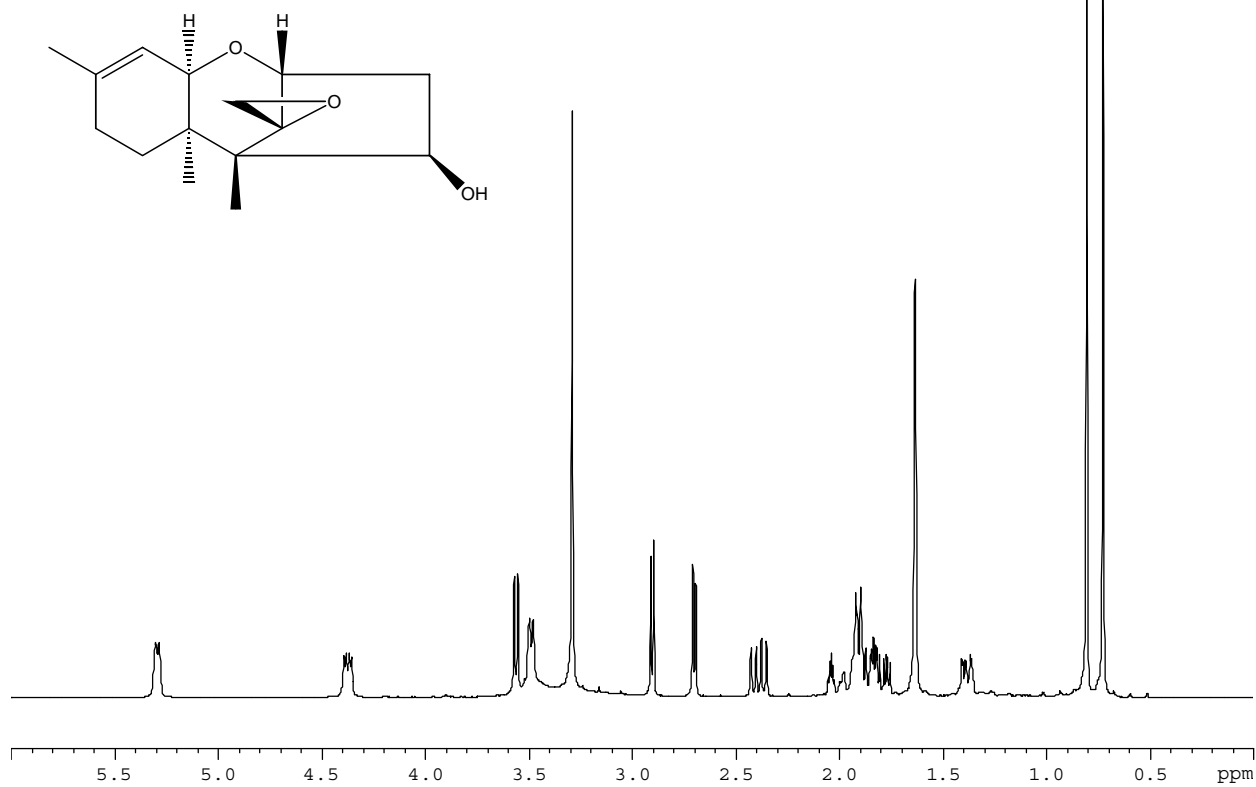


**8-Deoxy-trichothecin (24)**  
300 MHz, (CD<sub>3</sub>)<sub>2</sub>CO

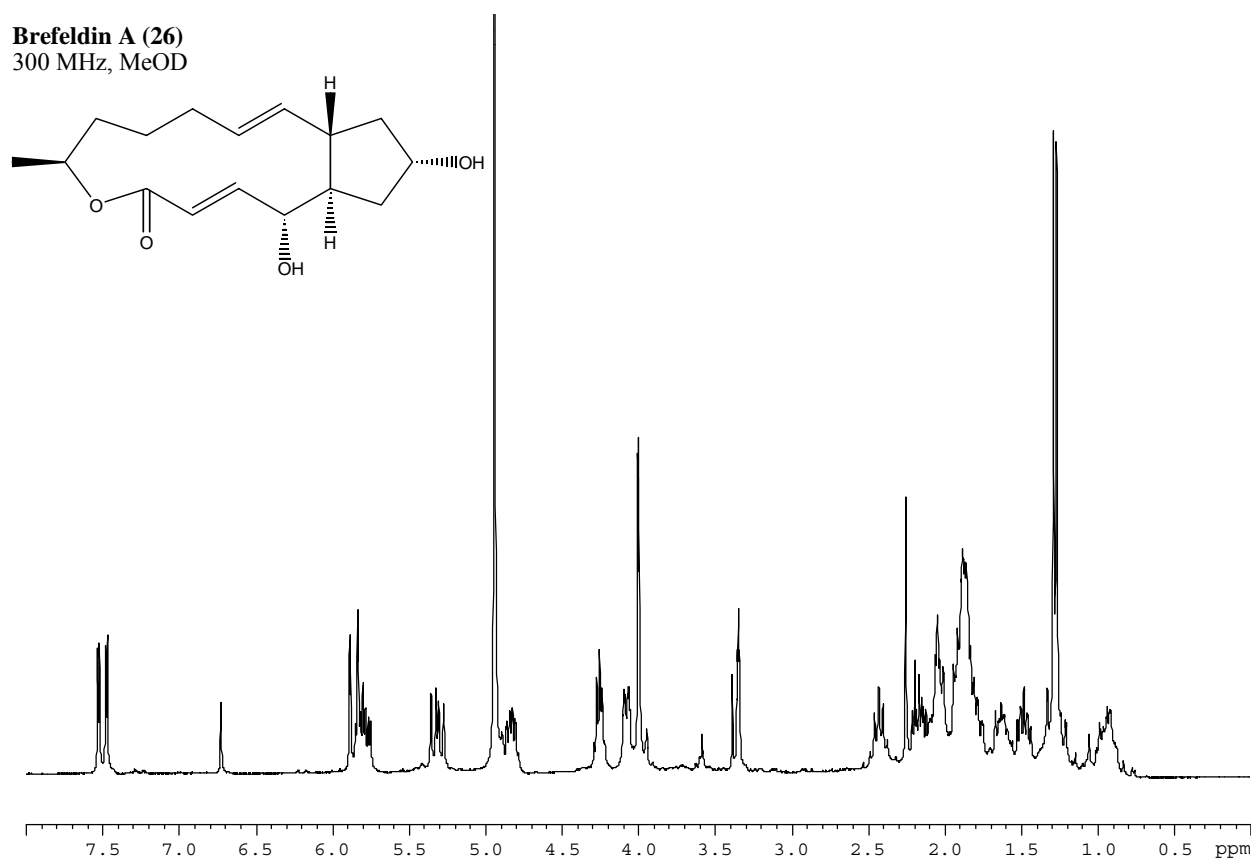


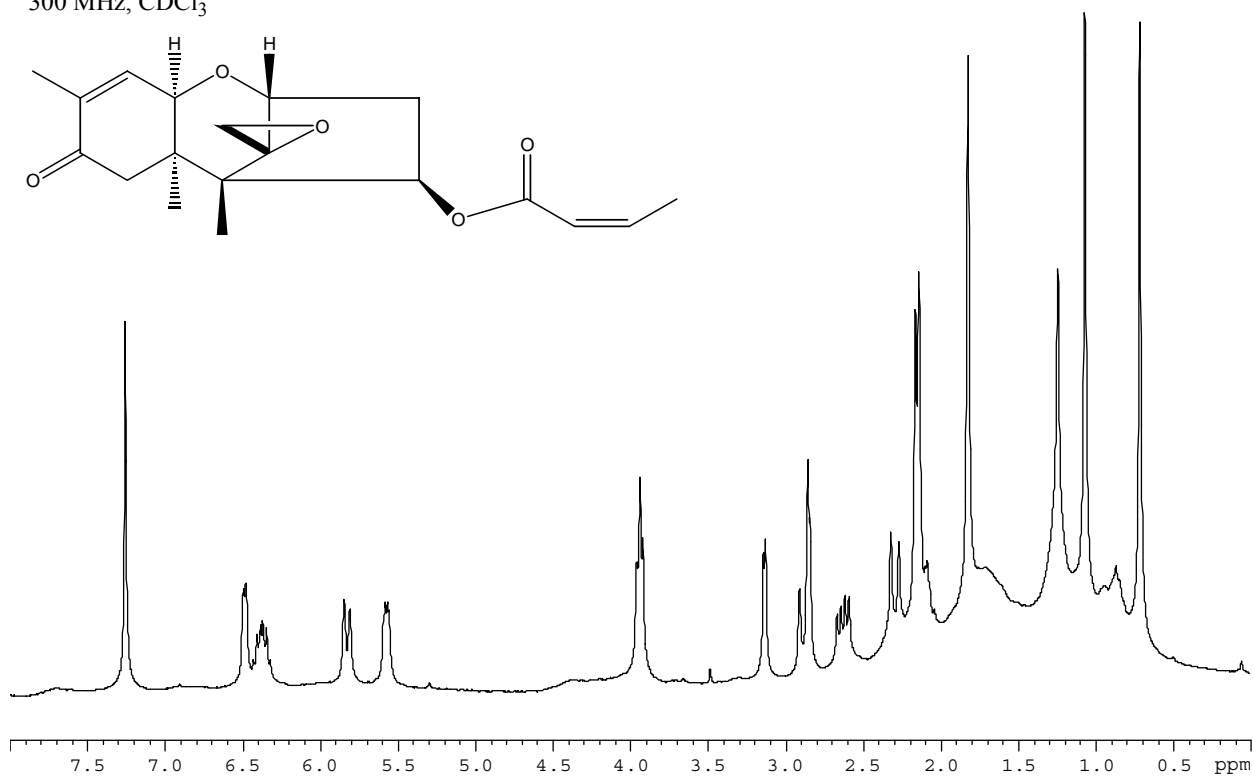
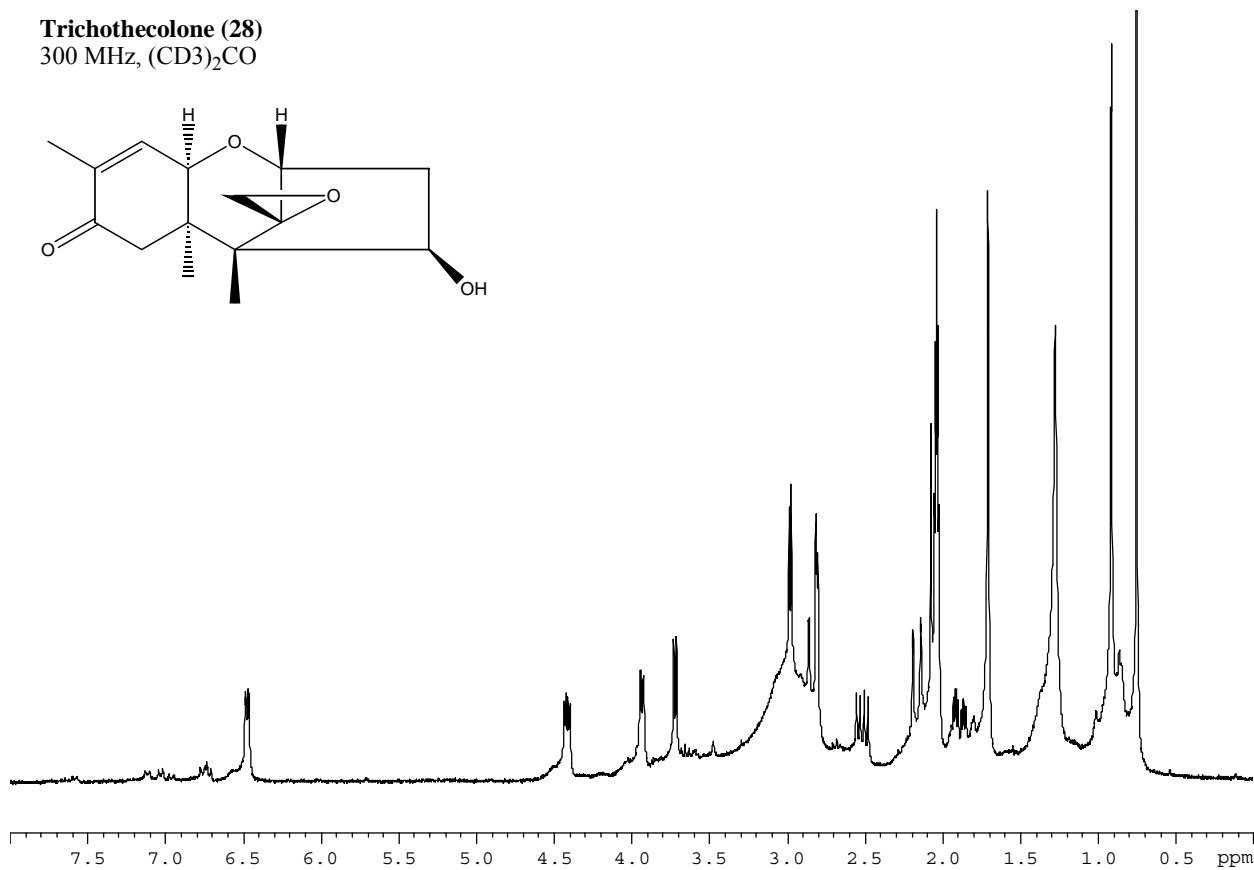


**Trichodermol (25)**  
300 MHz,  $(\text{CO}_3)_2\text{CO}$

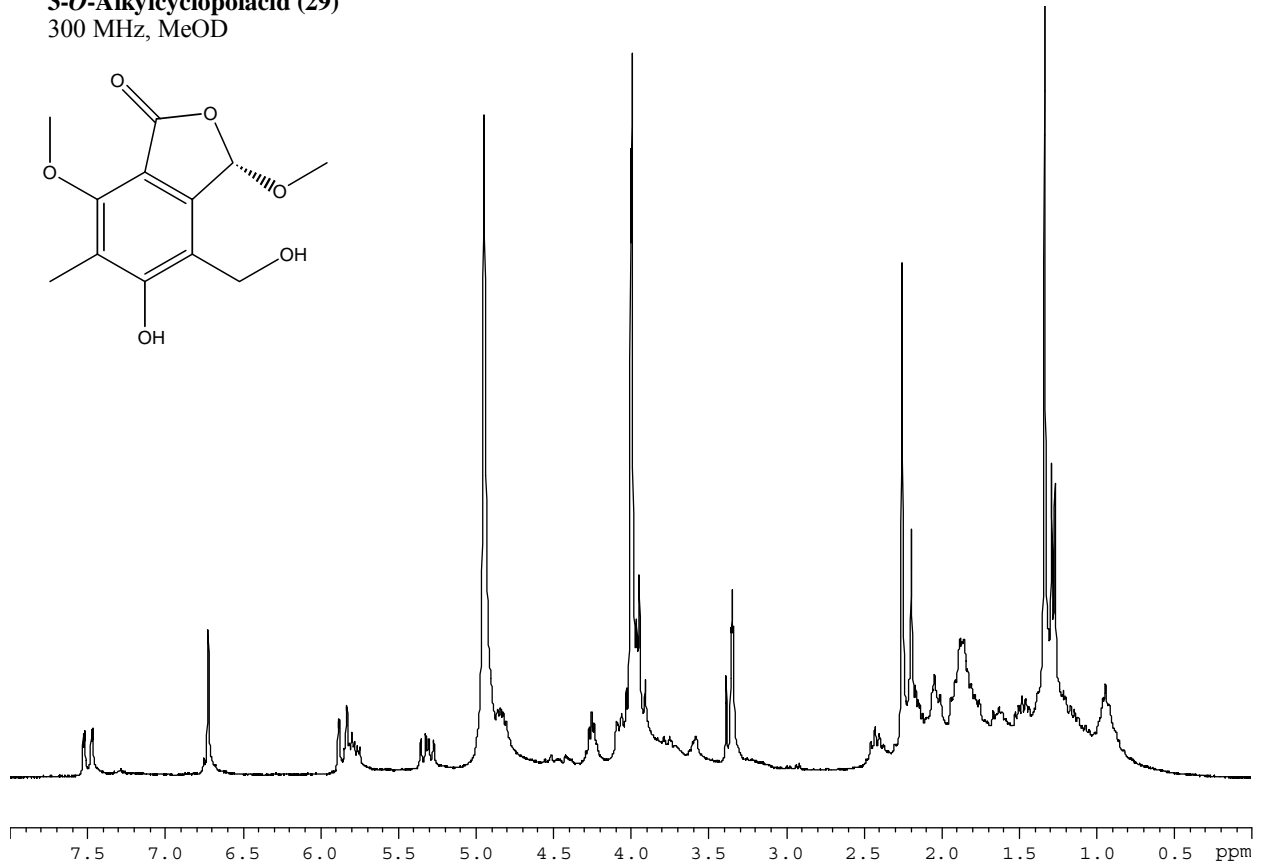
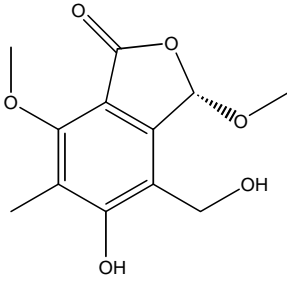


**Brefeldin A (26)**  
300 MHz, MeOD



**Trichothecin (27)**300 MHz, CDCl<sub>3</sub>**Trichothecolone (28)**300 MHz, (CD<sub>3</sub>)<sub>2</sub>CO

**3-O-Alkylcyclopolacid (29)**  
300 MHz, MeOD



## **Erklärung**

Hierhin versichere ich, die vorliegende Arbeit selbständig und unter ausschließlicher Verwendung der angegebenen Hilfsmittel verfasst zu haben, wobei ich die von mir verwendeten Quellen als solche gekennzeichnet habe.

Bonn, October 2007

-----  
Ana Kralj

## CURRICULUM VITAE

### *Personal Data*

Name, First Name	<b>KRALJ, ANA</b> (name of birth UREMOVIC)
Date of birth	April 8 <sup>th</sup> , 1980
Place of birth	Zagreb, Croatia
Family status	Married
Nationality	Croatian

### *Education*

12/2003 – 10/2007	Graduate Study of Pharmaceutical Sciences, Rheinische Friedrich-Wilhelms-Universität Bonn, Germany  PhD thesis: <i>“Isolation of secondary fungal metabolites and their influence on sphingolipid metabolism”</i>
10/1998 – 02/2003	University of Zagreb, Faculty of Pharmacy, Croatia  Diploma thesis: <i>“Action and usage of Borage and Evening primrose oils”</i> (original in Croatian; diploma thesis supervisor Prof. Dr. Zdenka Kalodjera, Department of Pharmacognosy)
09/1994-06/1998	High School – VII Gymnasium, Zagreb, Croatia
09/1986-06/1994	Primary School – Titus Brezovacki, Zagreb, Croatia